The Development and Application of Statistical Sampling Regime to Map out Hydrocarbons in Sediments

Abdulwaheed Suleiman Ahmed

A thesis submitted in partial fulfillment of the requirements of The Robert Gordon University Aberdeen for the degree of Doctor of Philosophy.

This research programme was carried out in collaboration with the Fisheries Research Services, Marine Laboratory, Aberdeen.

November, 2005

DECLARATION

I hereby declare that no portion of the work referred in this thesis has been submitted in support for an application for another degree or qualification of this or any other university or other institute of learning.

The thesis has been composed by me.

ACKNOWLEDGEMENT

I would like to thank Professor Pat Pollard of Centre for Research in Energy and Environment (CRE+E) at The Robert Gordon University, Aberdeen, for the opportunity to study and work under her as my director of studies. I would like to thank my other supervisory team Dr Colin Moffat, Dr Ian Davies and Dr Lynda Webster, all of Fisheries Research Services, Marine Laboratory, Aberdeen, for their advice and constructive criticisms, and also I would like to thank Professor Peter Robertson of CRE+E at The Robert Gordon University.

I would like to thank the government of Federal Republic of Nigeria, for the opportunity given to me by funding this PhD programmed through Petroleum Technology Development Fund (PTDF). I also would thank the management and staff of the PTDF, Abuja Nigeria, especially the Executive Secretary.

Special thanks goes to the management and staff of Fisheries Research Services, Marine Laboratory, Aberdeen, especially Dr Rob Fryer who finding time to go through all my statistical applications, all members of the Analytical group especially Dr Marie Russell and also all members of the Environmental Impact group. I must thank Gavin Grewar for his friendship and for sharing an office.

I would like to thank all my friends who are my sources of inspirations, especially Mustapha Dikko, Abdullahi Aliyu, Sageer Mahmoud, Abdulazeez Murtala, Hafsat Sambo, Lelia Bastos, kyari Yates, Yusuf Abdullahi, Adamu Abdullahi, Yahaya Bande and Atiku Koko.

Finally, I would like to thank my family, Dad, Mum, brothers and sisters who have supported me in everything I have done and have been a constant source of encouragement and love.

Thank You All

Abdulwaheed Suleiman Ahmed

TABLE OF CONTENTS

LIST OF FIGURES

LIST OF TABLES

Publications

The distribution and composition of hydrocarbons in sediments from the Fladen Ground, North Sea, an area of oil production. *Journal of Environmental Monitoring*. DOI:10.1039.

Hydrocarbons in sediments in the Fladen Ground: a comparison of grid and stratified random sampling regimes.
Submitted to *Journal of Environmental Science and Technology.*

Description and evaluation of a sampling system for monitoring of hydrocarbons in sediments.
Submitted to *Journal of Environmental Science and Technology.*

The development and application of a statistical sampling regime for determininig hydrocarbon distributions in marine sediments. Poster presented at the 22nd International meeting of organic geochemistry (IMOG) Seville, Spain. September 2005.

Distribution of hydrocarbon in the Fladen Ground. Poster presented at the International conference for exploration of the sea (ICES) Aberdeen, Scotland. September 2005.

GLOSSARY

Abbreviation	Term	Units
ANOVA	Analysis of Variance	
BCF	Bioconcentration Factor	
BCs	Background Concentrations	
B.L.U.E	Best Linear unbiased Estimator	
BRCs	Background reference Concentrations	
C/N	Carbon Nitrogen Ratio	
CHN	Carbon Hydrogen Nitrogen Analysis	
CI	Chemical Ionization	
CO_2	Carbon Dioxide	
CPI	Carbon Preference Index	
CPS_o	Oral cancer Slope Factor	
CRM	Certified reference Material	
CRS	Composite Random Sampling	
CV	Coefficient of Variance	
CYP1A	Cytochrome P1A	
DC	Direct Current	
DCM	Dichloro-Methane	
DNA	Deoxy nucleic Acid	
DQO	Data Quality Objectives	
DTI	Department of Trade and Industries	
EAC	Ecotoxicological Assessment Criteria	
EI	Electron Impact Ionization	
EPA	Environmental Protection Agency	
FI/Py	Fluoranthene/Pyrene Ratio	
FRS	Fisheries Research Services	
GC	Gas Chromatography	
GC-FID	Gas Chromatography-Flame Ionisation Detection	
GC-MS	Gas Chromatography-Mass Spectrometry	
GS	Grid Survey	
H_2	Helium Gas	

H_2O	Water
HCl	Hydrochloric Acid
HOMO	Highest Occupied Molecular Orbital
HPLC	High Performance Liquid Chromatography
K_{ow}	Octanol/water Partition coefficient
LCL	Lower Control Line
LRM	Laboratory Reference Material
LUMO	Lowest Unoccupied Molecular Orbital
LWL	Lower Warning Line
m/z	Mass to Charge Ratio
MFO	Mixed Function Oxidation
MLA SOP	Marine Laboratory Aberdeen Standard Operation Procedure
MLA	Marine Laboratory Aberdeen
MP/P	Methylphenanthrene/Phenanthrene Ratio
MS	Mass Spectrometer
MW	molecular Weight
N/A	Not Applicable
N/H	Nitrogen Hydrogen Ratio
N_2	Nitrogen Gas
Na_2SO_4	Anhydrous Sodium Sulphate
NOAA	National Oceanic and Atmospheric Administration
OSPAR	Oslo Paris Commission
P/A	Phenanthrene/Anthracene Ratio
PAHs	Polycyclic Aromatic hydrocarbons
PCA	Principal Component Analysis
PPM	Part Per Million
PSA	Particle Size Analysis
QUASIMEME	Quality Assurance of Information for Marine Environmental Monitoring in Europe
RBC	Risk Based Concentration
RDF	Probability Density Function
R_fD_o	Oral Reference Doses
RF	Radio Frequency
RS	Stratified Random Sampling

SCOT	Support Coated Open Tubular
SD	Standard Deviation
SE	Standard Error of the mean
SIM	Selected Ion Monitoring
SOP	Standard Operation Procedure
SRS	Simple Random Sampling
TOC	Total Organic Carbon
UCL	Upper Control Line
UCM	Unresolved Complex Mixtures
UKAS	United Kingdom Accreditation Services
UKOOA	United Kingdom Offshore Operators Association
UV	Ultra-Violet
UVF	Ultra-Violet Fluorescence
UWL	Upper Warning Line
WCOT	Wall Coated Open Tubular

EXECUTIVE SUMMARY

Polycyclic aromatic hydrocarbons (PAHs) are prevalent throughout the marine environment and represent toxicological hazard to marine inhabitants and the general habitant through the food chain. The aim of this research project was to design a robust spatial sampling strategy that will give representative information on hydrocarbon contamination in sediment. This thesis presents the results of investigations carried out into the effect of oil exploration and production activity in the Fladen Ground (northern North Sea) using two statistical sampling regimes; a conventional grid sampling regime and a new random stratified sampling design. Both sampling regimes were used to assess the spatial concentrations and composition of hydrocarbons in the chosen study area. Sixteen (16) Zones were constructed equally and the numbers of samples which had to be collected were allocated based upon the proportion of the far field area (areas > 5km from multiple oil wells and > 2km from a single well). The results from the stratified random sampling design were compared with those from the grid design. A field study was designed based on the outcome of the stratified random sampling design. A composite random sampling was designed to estimate a within–stratum mean value for each of the chosen measurement parameters with more thorough coverage (better representation), better precision and less variance at lower analytical cost in the near-shore environment.

The samples from the study area were analysed using a range of measurement methods to provide the data to assess the two sampling regimes. Two hundred and forty two (242) samples from the Fladen Ground, and twenty five (25) samples each from the Firth of Clyde and Firth of Forth sediments were analysed for particle size (PSA), total organic carbon (TOC), oil equivalents of Forties crude oil and diesel oil, total polycyclic aromatic hydrocarbon (PAH) concentration, total *n*-alkane concentration and geochemical biomarkers. Measurement techniques used included laser granulometry employing a Malvern Mastersizer E Particle Size Analyser (PSA), whilst TOC was determined using a Perkin Elmer CHN elementary analyser following acid treatment. Fluorescence analysis using ultraviolet visible absorption and fluorescence spectroscopy (UVF) was utilised for the oil equivalents of Forties crude oil and diesel oil. Gas

chromatography using mass spectroscopy (GC-MS) was utilised for PAHs and geochemical biomarkers and gas chromatography with flame ionisation detection (GC-FID) was used for the more general aliphatic hydrocarbon (including *n*-alkane) analysis. MINITAB 14 and SURFER 7 software's were used in the statistical and spatial analyses.

The data from the new stratified random sampling regime showed that the total PAH concentrations (2- to 6-ring parent and alkylated PAHs including the 16 US EPA PAHs) were highest in the Zones with more oil installations and/or muddy sediments with high organic carbon content. Low PAH concentrations were determined in sandy sediments and in Zones with limited oil activities. PAH profiles were similar across the Zones, with heavier, more persistent, 5- and 6-ring compounds dominating and with a high proportion of parent PAH. PAH concentration ratios were consistent with the main source of these compounds, in most Zones, being pyrolytic. Small, high boiling unresolved complex mixtures (UCMs) from the aliphatic profile were indicative of limited petrogenic input in some Zones. The geochemical biomarker (triterpane and sterane) profiles from the sediment contained a small bisnorhopane peak and a high proportion of norhopane, indicating that there was contamination from both Middle Eastern and North Sea crude oils.

The data obtained from the sediment samples collected using different sampling regimes were then compared. The stratified survey (2001) results were compared with the grid survey (2001) results. Also temporal trends were investigated by comparison with a 1989 grid survey. There were no significant differences in the overall mean for the oil equivalent of Forties crude and diesel oil and total PAH concentration between the grid and stratified surveys. However significant differences were observed in the overall mean of the total *n*-alkane concentrations and also within the mean of some Zones for diesel (Zone 10), Forties crude (Zone 11) and total PAH concentrations (Zone 11). The stratified random sampling design gave much more reliable mean concentrations for all the parameters, achieving a much lower variance than the grid sampling design. For the temporal trend there was a reduction in concentration for all the four parameters compared between the 2001 stratified, 2001 and 1989 grid surveys; this could be due to a cessation of discharges of cuttings in the late 1990s and tighter control of discharges of produced water and the amount of flaring at the flare-stacks.

Spatial structure analysis show the existence of a trend in the variogram, and the spatial pattern in the contour maps of the parameters measured, shows that the regionalized variable were non-stationarity and non-ergodic

The field study to investigate composite random sampling gave a mean value with less variance than the simple random sampling. The variations in the means of the composite random sampling are within the precision of the analytical methods for all the parameters.

Abstract

THE DEVELOPMENT AND APPLICATION OFA STATISTICAL SAMPLING REGIME TO MAP HYDROCARBON DISTRIBUTION IN SEDIMENT

A.S. AHMED

This thesis investigates and develops a stratified random sampling design for sediments in an offshore oil field environment. The sampling area was partitioned equally into 16 Zones, stratification were based on the near field and far field areas, and the number of samples in each Zone was chosen by *proportional allocation*, i.e. proportional to the available appropriate area (far field). Measurement techniques applied to the samples included laser granulometry, ultraviolet fluorescence, gas chromatography using mass selective detection or flame ionisation detection and elemental analysis.

The total PAH concentrations (2- to 6-ring parent and alkylated PAHs, including the 16 US EPA PAHs) in sediments were relatively low (< 100 μg kg^{-1} dry weight). The PAH concentrations, Forties crude oil equivalent and diesel oil equivalent concentrations were generally higher in sediment of fine grain size and higher organic carbon loading. PAH distributions and concentration ratios indicated a predominantly pyrolytic input, being dominated by the heavier, more persistent, 5- and 6-ring compounds, and with a high proportion of parent PAHs. The *n*-alkane profiles of a number of the sediments contained small, high boiling, UCMs, indicative of weathered oil arising from a limited petrogenic input. Spatial structure analysis shows the existence of a trend in the variogram, and also the spatial pattern in the contour maps of the parameters measured, shows that the regionalized variable exhibited non-stationarity and were non-ergodic.

The stratified random sampling scheme showed significant advantages over a classical grid sampling scheme when applied to the same area. Specifically, the stratified random sampling design gave much more reliable mean concentrations for all the parameters, achieving a much lower variance than the grid sampling.

A further composite random sampling scheme was designed for sediments in the near-shore. The aim is to estimate a within–stratum mean value for each of the chosen measurement parameters with more thorough coverage (better representation), better precision and less variance at lower analytical cost. This scheme was trialed in two near-shore environments, the Clyde Estuary and the Firth of Forth. The results show no significant differences between the mean and distribution profile of the individual samples and the composite samples for all the parameters measured.

This work utilised the best modern chemical analytical methods for the quantification of a range of hydrocarbon species, and utilised the results in a modern risk-based approach to environmental assessment. The new stratified random sampling design has been accepted for use in the national marine monitoring programme (NMMP) in the United Kingdom.

CHAPTER ONE

INTRODUCTION

1.1 BACKGROUND

Hydrocarbon is a mixture of organic compounds having simple to complex structures made up of combinations of carbon and hydrogen, and often occurring in petroleum, natural gas, coal and bitumen. The complex mixture of compounds may be classified according to similarity of properties, the classification can be done in a variety of ways. The compounds are generally classified into aromatic and non-aromatic (aliphatic) compounds. The aromatic compounds absorb ultra-violet light and re-emit it as visible light and are more water soluble than the aliphatic ones, on an equal molecular weight basis (Cretney *et al.*, 2003). The aliphatic compounds do not interact with the visible light. The classification is useful for toxicity of the compounds; the aliphatic compounds are not inherently toxic. The aromatic compounds can exhibit a variety of toxic modes that generally have distinct threshold concentrations. The thresholds form a hierarchy of concentrations in an organism, and some polycyclic aromatic compounds could have a "thresholds" of a single molecule (Gobas *et al.*, 2001). The aromatic and aliphatic compounds can be further subdivided according to their volatility, solubility or molecular weight of their respective constituents. In general, the three properties vary within each of these groups, such that the lower molecular weight compounds are more volatile and soluble than the high molecular weight compounds.

1.2 POLYCYCLIC AROMATIC HYDROCARBONS (PAHs)

Polycyclic aromatic hydrocarbons (PAHs) are ubiquitous organic contaminants that are present in coastal and marine sediments (LaFlamme and Hites, 1978; Gschwend and Hites, 1981; NOAA, 1988), and are listed on the OSPAR List of Chemicals for Priority Action (OSPAR Commission, 2002). Structures, number of rings and molecular weight of some of the polycyclic aromatic hydrocarbon are shown in Figure 1.1 and summarised in Table 1.1. The distribution and fate of PAHs in aquatic systems have received much attention due to the mutagenic and carcinogenic properties of some of the compounds (Grimmer, 1983; White, 1986; Harvey, 1991; Cerniglia, 1992; Law *et al.*, 2002; Gowland *et al.*, 2002). PAHs bioaccumulate in aquatic organisms, particularly invertebrates (Neff, 1979; Varanasi *et al.*, 1985; Long *et al.*, 1995).

Due to their hydrophobic and stable chemical properties, the PAHs are not very soluble in the water phase. Solubility (expressed as octanol:water partition coefficient, Log K_{ow}) decreases with increasing molecular weight and degree of alkylation's (Log K_{ow} = 4.7 and 7.66 for fluoranthene and indenopyrene, respectively) (Mackay *et al.*, 1992; Meador *et al.*, 1995; de Maagd *et al.*, 1998). Therefore PAHs sorbs rapidly onto particles (Karickhhoff *et al.*, 1979; Means *et al.*, 1980). Upon entering aquatic systems, PAHs distribute between different phases including truly dissolved, colloids, suspended particulate matter, surface sediments and biota (Readman *et al.*, 1987; Zhou *et al.*, 1998). The way in which PAHs are distributed between these different phases is controlled by their intrinsic physicochemical properties including solubility, vapour pressure and lipophilicity (Zhou *et al.*, 1998). Strong adsorption of PAHs onto sediment particles can reduce their bioavailability, subsequently slowing their biodegradation rates and aiding their preservation in sediments (McElroy *et al.*, 1989; McGroddy *et al.*, 1996). PAHs in sediments have the potential to transfer to biota

and biomagnification's of these toxic compounds may occur as they pass through the food chain (Neff, 2002), ultimately resulting in adverse biological effects.

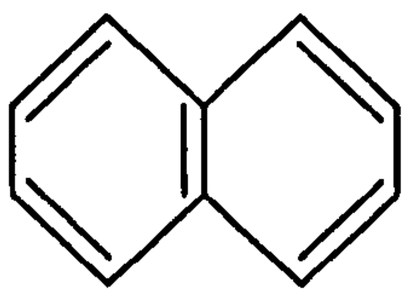

Naphthalene

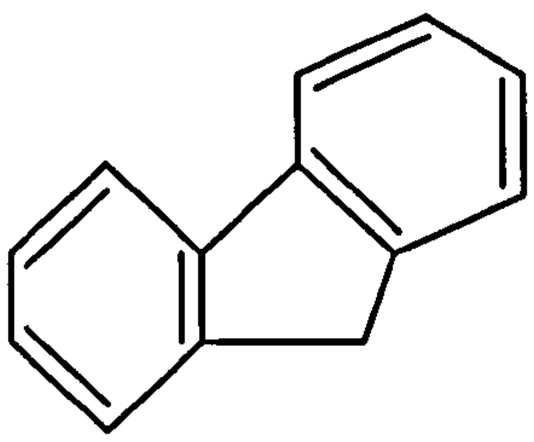

Fluorene

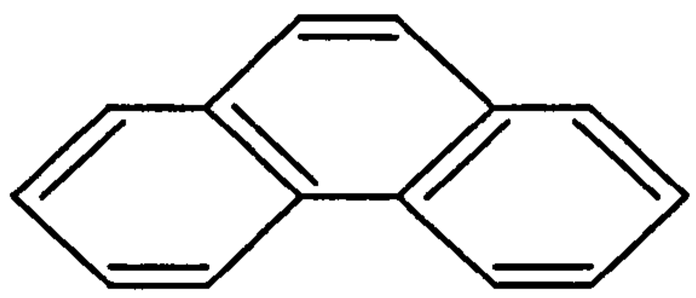

Phenanthrene

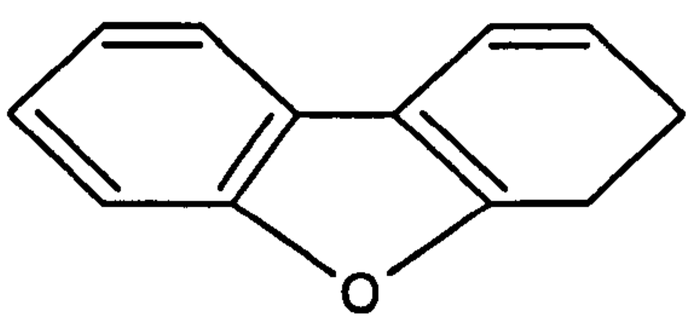

Dibenzofuran

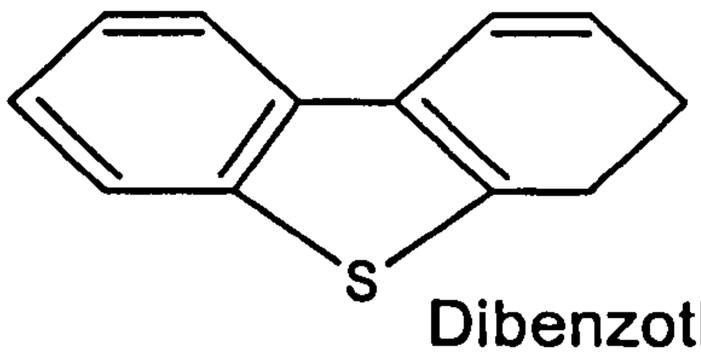

Dibenzothiophene

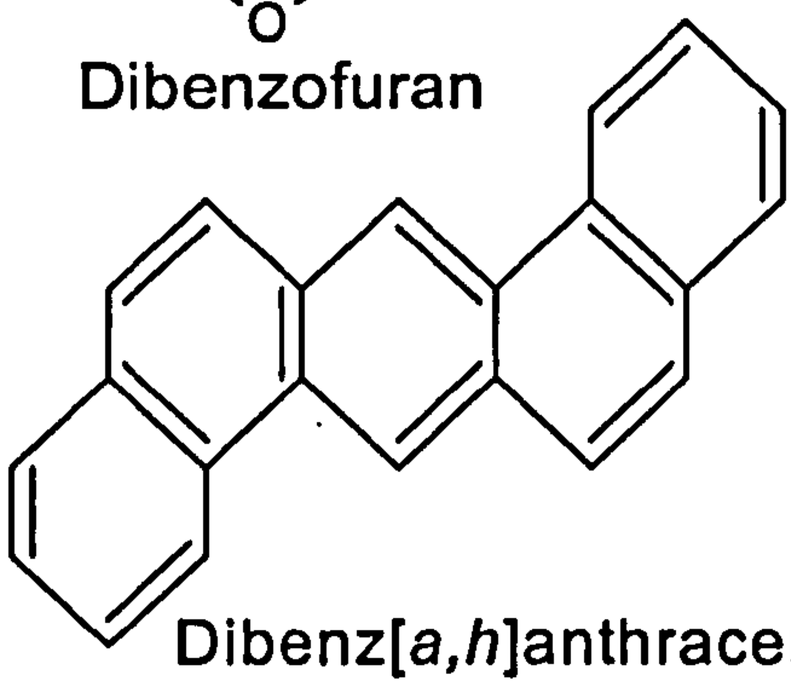

Dibenz[*a,h*]anthracene

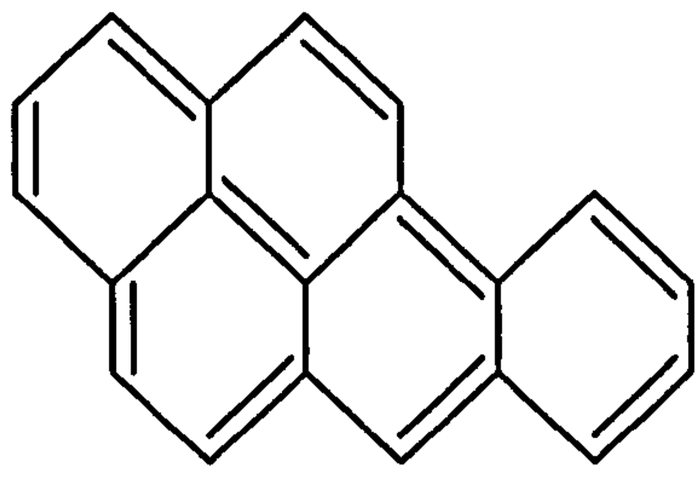

Benzo[*a*]pyrene

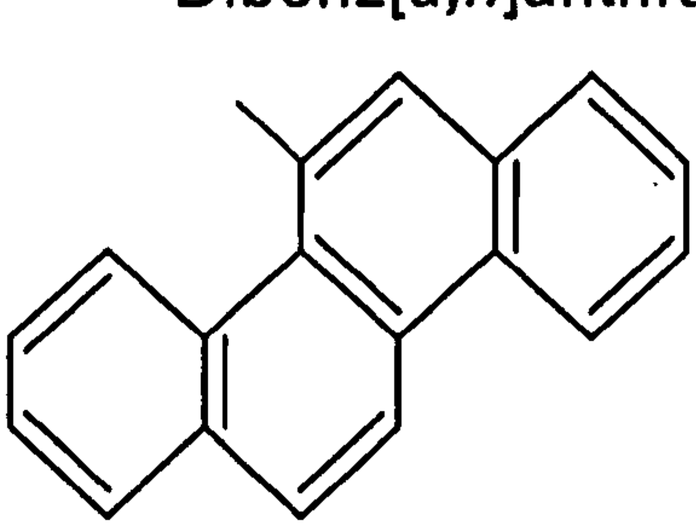

5 -Methylchrysene

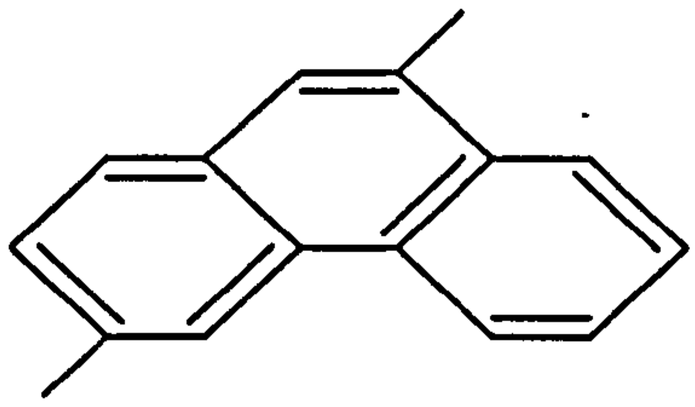

3,9 -Methylphenanthrene

Figure 1.1 Chemical structures of some polycyclic aromatic hydrocarbons. Alkylated PAHs are more abundant than the parent compounds in petroleum and produced water. The carcinogenic PAHs, such as benzo[*a*]pyrene, dibenz[*a,h*]anthracene, and 5-methylchrysene are present at low concentrations or are absent from the treated produced water. From Neff, (2002).

Table 1.1 Parent (C_0) and alkylated (C_1-C_4) PAH showing the molecular weight and number of rings. From Wang and Fingas (2003).

Compound	Number of Rings	Target Ions
Oil-characteristic parent and alkylated PAHs		
Naphthalenes		
C_0-naphthalene	2	128
C_1-naphthalene	2	142
C_2-naphthalene	2	156
C_3-naphthalene	2	170
C_4-naphthalene	2	184
Phenanthrenes		
C_0-phenanthrene	3	178
C_1-phenanthrene	3	192
C_2-phenanthrene	3	206
C_3-phenanthrene	3	220
Dibenzothiophenes		
C_0-dibenzothiophene	3	184
C_1-dibenzothiophene	3	198
C_2-dibenzothiophene	3	212
C_3-dibenzothiophene	3	226
Fluorenes		
C_0-fluorene	3	166
C_1-fluorene	3	180
C_2-fluorene	3	194
C_3-fluorene	3	208
Chrysenes		
C_0-chrysene	4	228
C_1-chrysene	4	242
C_2-chrysene	4	256
C_3-chrysene	4	270
Other OSPAR priority PAH pollutants		
Acenaphthylene	3	152
Acenaphthene	3	153
Anthracene	3	178
Fluoranthene	4	202
Pyrene	4	202
Benz[*a*]anthracene	4	228
Benzo[*a*]fluoranthene	5	252
Benzo[*k*]fluoranthene	5	252
Benzo[*e*]pyrene	5	252
Benzo[*a*]pyrene	5	252
Perylene	5	252
Indeno[1,2,3-*cd*]pyrene	6	276
Dibenz[*a,h*]anthracene	5	278
Benzo[*ghi*]perylene	6	276

1.3 SOURCES AND FORMATION OF PAHs

There are three primary sources of PAHs to the marine environment (Baumard *et al.*, 1998):

- Very rapid, high temperature incomplete combustion or pyrolysis of organic materials (pyrolytic PAHs).
- Very slow (millions of years) rearrangement and transformation of biogenic organic materials at moderate temperature (100 - 300^{0}C) to form fossil fuels (petrogenic PAHs).
- Direct biosynthesis by organisms (biogenic PAHs)

PAH from pyrolytic and petrogenic sources are introduced into the marine environment through effluent discharges, urban run-off, atmospheric transport, and spillage or disposal of oil and petroleum products (Cereceda-Balic *et al.*, 2002; Baumard *et al.*, 1998). Environmental behaviour and bioavailability of PAHs are source dependent (Gschwend and Hites, 1981). Studies have shown that PAHs from pyrolytic sources tend to be more strongly associated with sediment and soot particles and more resistant to microbial degradation than PAHs from petrogenic sources (McGroddy and Farrington, 1995; Gustafsson *et al.*, 1997).

1.3.a Petrogenic Source

Petroleum is a rich source of PAHs (Neff, 1990). Crude oil is derived from the thermal degradation and arrangement of organic polymers found in source rocks, often-sedimentary shales, in the subsurface (Tissot and Welte, 1984). The organic matter in the source rocks is usually derived primarily from sedimentation of dead plants and animals in freshwater

and marine environments. Most of the PAHs in crude oil are composed of two or three fused benzene rings e.g. naphthalenes and dibenzothiophenes (DBTs). The abundance of PAHs in petroleum usually decreases markedly with increasing molecular weight (Neff, 1990). Higher molecular weight 4- to 6-ring PAHs are much less abundant than 2- and 3-ring compounds in crude oils (Kerr *et al*, 2001). Tables 1.2 and 1.3 shows the ranges and percentage frequency of detection of PAHs found in crude oils.

Table 1.2 Concentration ranges of several parent PAHs in 60 crude oil samples from throughout the world (% detection is percentage above detection limit). Under lined PAHs are known or suspected mammalian carcinogens. Concentrations are mg/kg oil. From Neff (2002).

PAH	Number of rings	% Detection	Range (mg kg^{-1})	Mean (mg kg^{-1})
Naphthalene	2	100	1.2 – 3700	423
Acenaphthene	3	80	0-58	13.9
Anthracene	3	40	0-17	3.4
Phenanthrene	3	98	0-916	177
Fluorene	3	100	1.4-380	73.6
Fluoranthene	4	40	0-26	3.9
Pyrene	4	97	0-84	15.5
Benz[*a*]anthracene	4	67	0-38	5.5
Chrysene	4	100	4-120	28.5
Dibenz[*a*,*h*]anthracene	5	47	0-9.2	1.0
Benzo[*a*]pyrene	5	75	0-7.7	2.0
Benzo[*b*]fluoranthene	5	100	0-14	3.9
Benzo[*k*]fluoranthene	5	93	0-7	0.46
Indeno[1,2,3-*cd*]pyrene	6	7	0-1.7	0.06
Benzo[*ghi*]perylene	6	63	0-9.6	1.53

Table 1.3 Concentrations of individual alkylated PAH in crude oils. Concentrations are mg/kg. From Neff (2002).

PAH	Number of rings	Concentration (mg kg^{-1})
C_1-Naphthalene	2	3886
C_2-Naphthalene	2	4511
C_3-Naphthalene	2	2988
C_4-Naphthalene	2	1000
C_1-Fluorene	3	521
C_2-Fluorene	3	682
C_3-Fluorene	3	420
C_1-Phenanthrene/Anthracene	3	748
C_2-Phenanthrene/Anthracene	3	716
C_3-Phenanthrene/Anthracene	3	460
C_1-Dibenzothiopene	3	63
C_2-Dibenzothiopene	3	83
C_3-Dibenzothiopene	3	49
C_1-Chrysene	4	51
C_2-Chrysene	4	67
C_3-Chrysene	4	38

1.3.b Pyrolytic Sources

Combustion of organic matter is a major source of PAHs containing 3- or more rings to the environment (Neff, 1979). Pyrolysis generates a wide variety of PAHs ranging from naphthalene to complex PAH polymers, particularly if combustion takes place in an oxygen-deficient atmosphere. During combustion in an oxygen-deficient atmosphere, the organic matter is oxidised to low molecular weight organic molecules that condense as the combustion mixture cools to form complex, new molecular structures by a process called

pyrolysis or pyrosynthesis (Neff, 1979). The PAH yield depends on the composition of the organic matter, temperature, and the oxygen concentration.

1.3.c Biogenic PAHs

PAHs are synthesized by some organisms, particularly bacteria, fungi, higher plants and some insects (Mathey *et al.*, 1994; Silliman *et al.*, 1998; Jiang *et al.*, 2000). Direct biosynthesis is not a quantitatively important source of PAHs in the marine environment. Under anoxic or hypoxic conditions, quinones, phenols and related oxygenated aromatic compounds may be reduced to the parent PAH (Wakeham *et al.*, 1980; Hashimoto *et al.*, 1994). A five-ring PAH, perylene, is abundant in anoxic marine sediments, and its concentration tends to increase with depth in sediment cores (Wilcock and Northcott, 1995; Fernández *et al.*, 1996).

1.4 MECHANISMS FOR PAH SYNTHESIS

PAH are composed of two or more fused benzene rings (Neff, 1979). The formation of benzene can occur by the reaction of two propargyl (C_3H_3) radicals (Miller *et al.*, 1992) and by the reaction of C_4H_x with acetylene (Wang and Frenklach 1997; Walch, 1995). Three mechanisms have been proposed for the formation of additional rings. The first is due to Frenklach and co-workers (Wang & Frenklach 1994 & 1997, and Appel *et al.*, 2000), who postulate the successive loss of ring hydrogen atoms followed by acetylene additions to the ring and subsequent ring closure reactions (Figure 1.2). The second is the Bittner-Howard mechanism (Bittner & Howard, 1981), and this also involves acetylene additions, but in this mechanism the second acetylene adds to the first, which then reacts with the existing ring to form an additional ring (Figure 1.2). The third mechanism involves the reaction of two

C_5H_5 rings followed by rearrangement to form two fused benzene (C_6) rings (Moriarty *et al.*, 1999).

The mechanism of PAH formation in space could be very different from that in flame, as in space, reactions with oxygen atoms are much less likely to occur and also, depending on location, there might be much less thermal energy available to drive the reactions. Ultraviolet (UV) radiation is much more intense in space, and there is evidence that many of the PAH molecules in space are ionised due to the UV flux. However, PAH ions are common in flames as well (Weilműnster *et al.*, 1998).

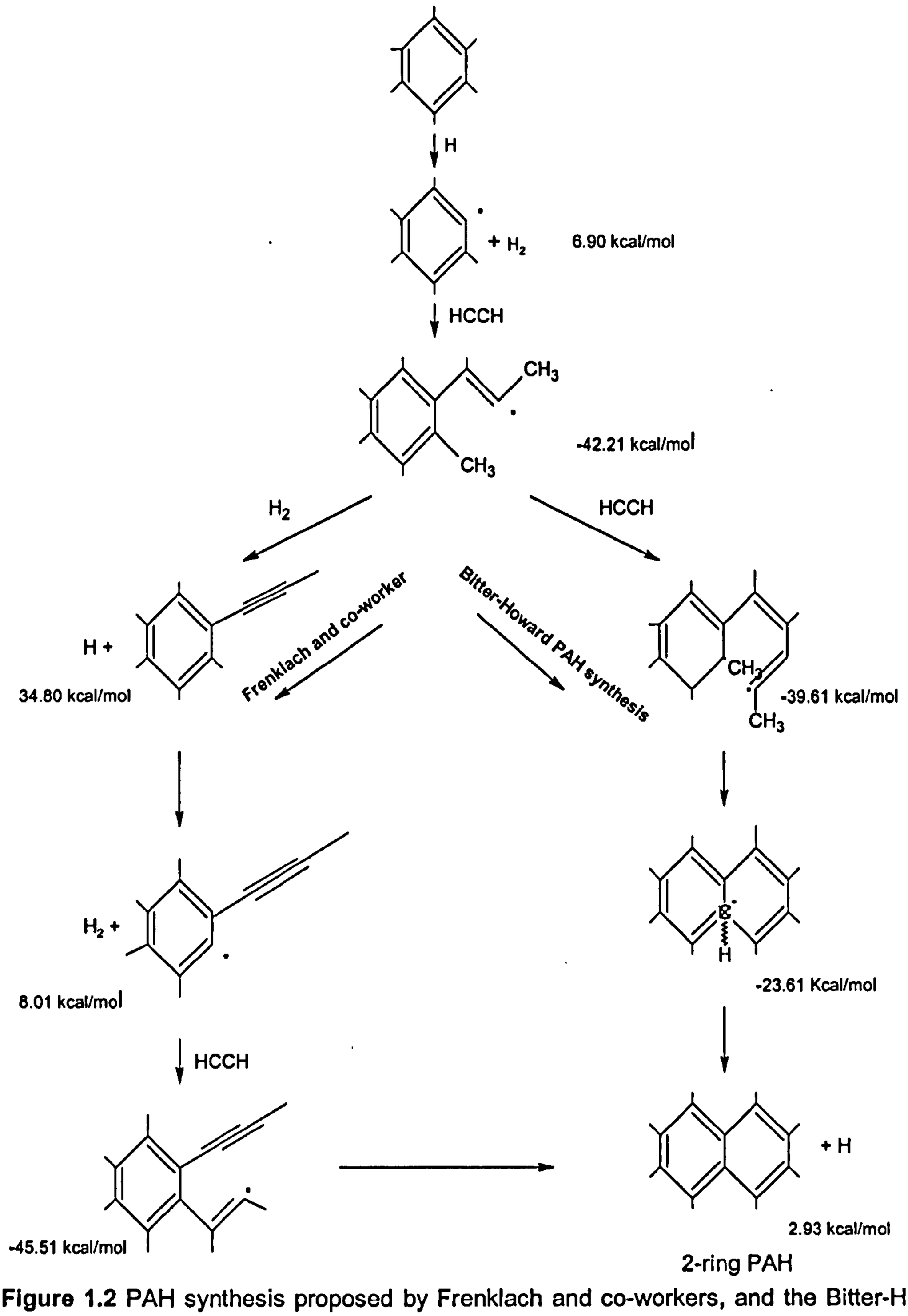

Figure 1.2 PAH synthesis proposed by Frenklach and co-workers, and the Bitter-Howard mechanism of PAHs. Source: Bauschlicher Jr. and Ricca (2000).

1.5 DEGRADATION OF POLYCYCLIC AROMATIC HYDROCARBONS

PAHs in water and sediments are not persistent, the 4- to 6- ringed PAHs are slowly degradable, and because of their low water solubility and their strong binding to organic matter, they often fail to be readily available for biodegradation. Biodegradation primarily occurs in 2 and 3- ringed PAHs, which also have the highest water solubility. PAHs are degraded by various natural processes to various polar organic chemicals, and ultimately to carbon dioxide and water. The most important degradative processes for PAHs in the marine environment are photooxidation and biodegradation (Bongiovanni *et al.*, 1989; Ehrhardt *et al.*, 1992).

1.5.a Photooxidation

Exposure of PAHs to solar radiation leads to several reactions that produce a variety of, mostly, more polar organic compounds. Recent studies of photooxidation in the sea surface and water column, shows that light Arabian crude oil was photoxidised at a rate of about 0.004% per day (Berthou and Vignier, 1986). Photooxidation substantially changes the physical and chemical properties of petroleum and its toxicity to marine organisms (Pelletier *et al.*, 1997).

The primary mechanism of photooxidation in PAHs is photo-oxygenation involving singlet oxygen (Thominette and Verdu, 1984; Syndes *et al.*, 1985). In the presence of ultraviolet radiation, energy transfer from electronic excited states (usually triplet) of the aromatic and polar components of the oil to molecular oxygen generates singlet oxygen (Gorman, 1992) that can then react with aromatic hydrocarbons and heterocyclic sulphur compounds by

addition (Nicodem *et al.*, 1997). The major photooxidation products are peroxides, aldehydes, ketones, alcohols, carbonyls, and fatty acids, all of which are more water-soluble than the parent compounds (Ehrhardt and Burns, 1990; Jacquot *et al.*, 1996). Dibenzothiophene (DBT) and its C_1- through C_3-alkyl homologues are photooxidised to their respective sulfoxides and sulfones under natural conditions (Berthou and Vignier, 1986).

Photodegradation rates of different PAHs vary widely. Degradation rates may depends on concentrations of PAHs and photosensitizers in the oil, and on the physical form of the PAH assemblage (Mill *et al.*, 1981; Valerio and Lazzarotto, 1985). PAHs bound to soot particles are less sensitive than dissolved PAHs to photooxidation (Kamens *et al.*, 1988). Naphthalene and its alkyl homologues and moderately weathered light Arabian crude oil are photooxidised rapidly in natural sunlight (Jacquot *et al.*, 1996; Dutta and Harayama 2000). Phenanthrene, DBTs and their alkyl homologues are more recalcitrant (Berthou and Vignier, 1986). DBTs and methyldibenzothiophenes in a weathered light Arabian crude oil were not photooxidised during a four-week exposure to artificial sunlight (Dutta and Harayama, 2000), although 16-91% of more highly alkylated DBTs are photooxidised. The efficiency of photoxidation of methylphenanthrenes and dimethylfluorenes also is low, different monomethyl and dimethyl- phenanthrene isomers are photoxidised at widely different rates (Jacquot *et al.*, 1996). Higher molecular weight, 4- through 6-ring, PAHs tend to be most sensitive to photooxidation (Mill *et al.*, 1981).

Direct photolysis increases with increasing molecular weight, for example the half-life of naphthalene (*MW* 128) in surface fresh water in sunlight equivalent to 40^0N latitude in mid-summer, is 61 hours, compared to half-life of 8 hours for phenanthrene (*MW* 178) and 0.54 hours for benzo[*a*]pyrene (*MW* 252). Most dissolved alkyl-PAHs are more sensitive to photolysis than the parent (unalkylated) PAHs (Ehrhardt *et al.*, 1992). Ultraviolet light

intensity decreases logarithmically with depth, so the rate of photolysis of PAHs also decreases with depth of water. Under intense sunlight, hydrocarbons in solution can be photooxidised to a depth of about 25 meters in clear seawater (Jacquot *et al.*, 1996). Sorption of PAHs to suspended matter, bottom sediments or colloids may decrease or increase photolysis rates. David and Boule (1993) showed that sorption to silica particles increase the rate of photolysis of anthracene, phenanthrene, and benz[*a*]anthracene. Ferric oxide, montmorillonite clay, and cellulose sorbents decrease photolysis rates.

Photooxidation may also lead to polymerisation reactions to producing high molecular weight compounds that are not soluble in either water or oil, resulting in a phase separation in the oil slick (Darling, 1988; Nicodem *et al.*, 1997). Studies of the Ekofisk crude oil in the North Sea in June when the daily solar radiation was at a maximum, showed that the high molecular weight resin/asphaltene fraction of oil reacted rapidly with oxygen. Lower molecular weight aromatic hydrocarbons, such as phenanthrene, were converted to polar oxidation products that tended to bind tightly, possibly covalently, to the resin/aspaltene fraction.

1.5.b Microbial Degradation

Nearly all-marine sediments contain populations of bacteria and fungi that are capable of biodegrading some PAHs. The rate of degradation depends on the physicochemical properties of the sediments and the hydrocarbon compound (Ahn *et al.*, 1999; Ravelet *et al.*, 2000). Low molecular weight *n*-alkanes with chain lengths of 10-22 carbons are metabolised most rapidly, followed by *iso*-alkanes and higher molecular weight *n*-alkanes, olefins, monocyclic aromatic hydrocarbons, PAHs, and finally, high condensed cycloalkanes, resins and asphaltenes. Degradation of DBT and its alkylated homologous

required mixed microbial assemblages and cosubstrates, that are usually present in oil contaminated sediments (Kropp *et al.*, 1994; Dyreborg *et al.*, 1996).

Some of the metabolic products produced as intermediates in the enzymatic degradation of PAHs by procaryotes (bacteria and blue-green algae) and eukaryotes (fungi, plant, and animals) are toxic, mutagenic or carcinogenic. PAHs that can be enzymatically activated to mutagens or carcinogens, such as the 4-, 5- and 6-ring PAHs like benz[*a*]anthracene, benzo[*a*]pyrene, and dibenz[*a,h*]anthrancene, react with trans-diol-epoxides, which interact with cellular DNA to induce cancer or mutation (Figure 1.3). The prokaryotic pathway does not produce these epoxide intermediates. Therefore, the products of bacterial degradation of PAHs are less mutagenic and carcinogenic than the products of PAH degradation by fungi and higher organisms (Figure 1.3).

1.5.c Prokaryotic Pathways

In prokaryotes (single organism without nucleus), PAH are degraded first to a *cis*-dihydrodiol by a dioxgenase enzyme. The enzyme incorporates the two atoms into aromatic substrate to form a dioxethane intermediate (Figure 1.3). The dioxethane is oxidized further to a *cis*-dihydrodiol and then to various dihydroxy products, the most common of which are catechols (Cerniglia, 1994; Wilson and Jones, 1993; Pothuluri and Cerniglia, 1994; Sutherland *et al.*, 1995). Sediment bacteria can also attack the alkyl side-group of alkyl-PAH, forming alcohols, aldehydes and carboxylic acids (Budzinski *et al.*, 2000).

1.5.d Eukaryotic Pathways

Most eukaryotes (organism with one or more cells with visible nuclei and organelles) use a mono-oxygenase system; the cytochrome P450 mixed function oxygenase system, to incorporate one oxygen atom into the aromatic substrate to form an arene oxide. The oxide either isomerizes spontaneously to form a phenol, or is hydrated by epoxide hydrase to form a trans-dihydrodiol or phenol (Cerniglia, 1993; Sutherland *et al.*, 1995) (Figure 1.3). As in procaryotes, the dihydrodiol could be oxidized to a dihydroxyl product, such as a catechol. Some fungi, such as white rot produce extracellular lignin peroxidases that can oxidise PAHs by a single electron transfer to form quinones (Sutherland, 1992; Cerniglia, 1993; Juhasz and Naidu, 2000).

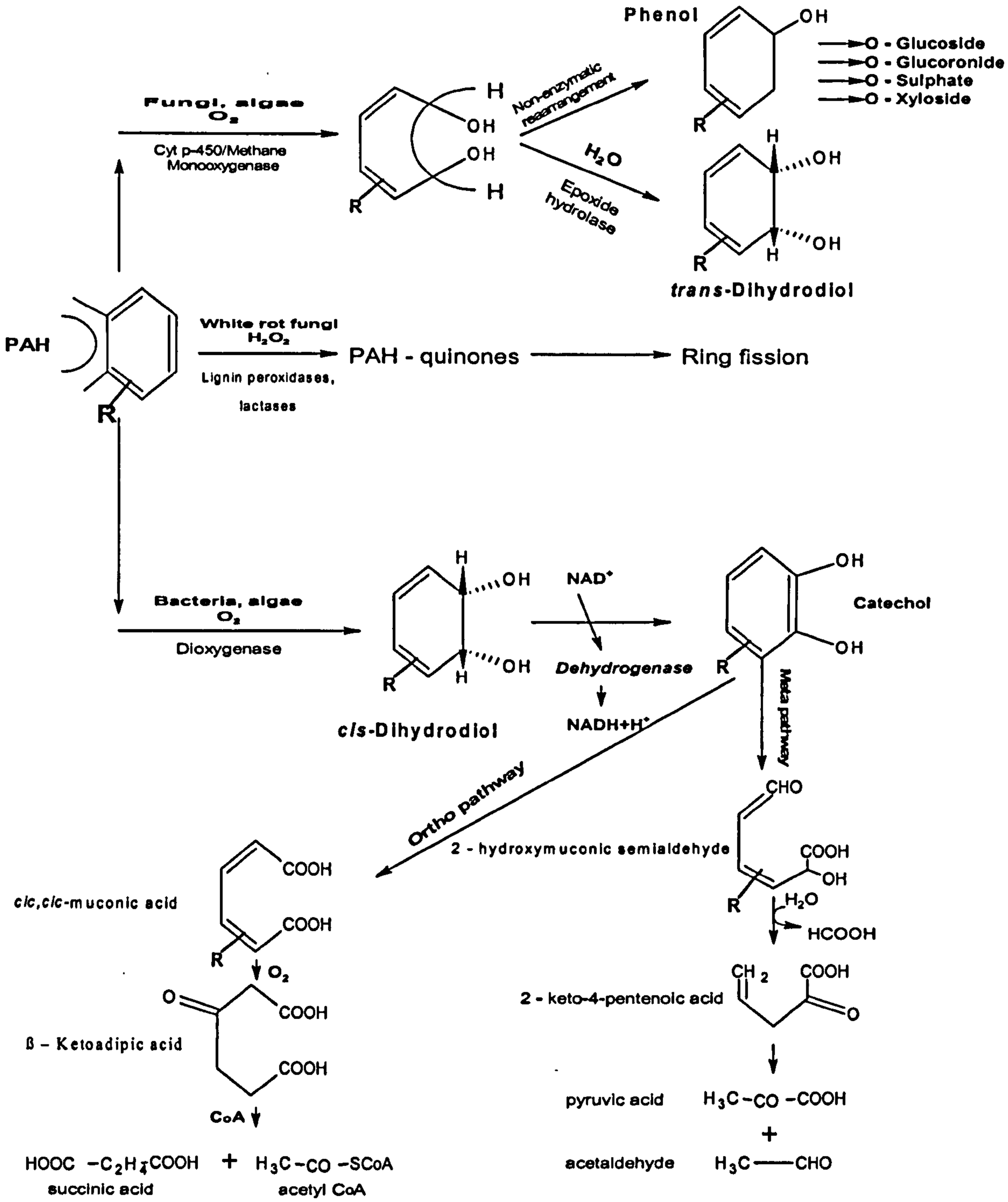

Figure 1.3 Biodegradation of PAHs by prokaryotes (bacteria) and eukaryotes (fungi, algae, plants, and animals). Trans-dihydrodiols of some higher molecular weight PAHs are carcinogenic. (Adapted from Cerniglia, 1993; Rochkind-Dubinsky *et al*., 1987).

1.6 BIOACCUMULATION OF PAHs BY MARINE ORGANISMS

Bioconcentration of PAHs from solution in water by marine organisms is directly proportional to their K_{ow}s (octanol/water partition coefficient). Bioaccumulation of PAHs from sediments and food is thought to involved an intermediate step in which the PAHs desorp or released into solution from the matrix and then partition into the lipid rich tissues of the marine organism. Thus, bioavailability of PAHs from sediments and food is less than that from solution in the water. Equilibrium bioconcentration factors (BCFs) which is the ratio of at equilibrium of concentration of a chemical in the tissues of the organism to the concentration of the chemical in solution in water to which the organism was exposed. There are many factors that affect the BCF/K_{ow} relationship. Biotic factors include active metabolism and excretion of the chemical, animal species, liquid content and distribution in the animal and feeding status, which usually varies depending on age, sex and stage of reproductive cycle (Meador *et al.*, 1995). Physical factors that affect the relationship between BCF and K_{ow} include temperature, salinity and the physical form of the chemical in the water of sediments.

Studies have shown that PAHs associated with soot and other organic rich particles (e.g. organic carbon) in sediments are not bioavailable. Because of the high affinity of dissolved and particulate organic mater for PAHs, there usually is an inverse relation between concentrations of total organic carbon (TOC) in sediments and the bioavailability of PAHs in the sediments to marine organism (Neff, 1984).

1.7 TOXICITY OF PAHs TO MARINE ORGANISMS

Some PAHs, accumulated into biota, have the ability to absorbed ultraviolet (UV) light energy. These photoactivated PAH can damage cellular membranes, resulting in biological impairment and death. PAH phototoxicity is caused by the transfer of UV (300-400nm) energy from a photoexcited PAH molecule to an oxygen molecule, creating oxygen radical that can disrupt cell membrane *via* lipid peroxidation (McDonald and Chapman, 2002). The excited PAH molecule may undergo two types of reactions, In the Type I reaction (photosensitization), the excited triplet state of the chromophore is reduced, leading to production of highly reactive free radicals that are capable of being oxidized to various photooxidation products or bind to biological molecules (Krylov *et al.*, 1997). In the Type II reaction (photomodification), the chromophore absorbs the UV energy to form the excited triplet state and then transfers the energy to dissolved oxygen, generating singlet oxygen or hydroxyl radicals.

Menkenyan *et al.* (1994) proposed that the relative phototoxicity of different photosensitive chemicals, such as PAHs, depends in the interaction of internal, structural factors (light absorption and compound stability) and external factors (UV exposure intensity and energy). They observed that the difference in the energies of the highest occupied molecular orbital (HOMO) and the lowest unoccupied molecular orbital (LUMO), the $E_{HOMO-LUMO}$ gap, is a good predictor of the photoxicity of PAHs to small aquatic animals such as *Daphnia magna*. The HOMO-LUMO gap defines the energy required to elevate an electron from the HOMO to LUMO. The phototoxicity is related to the size of the HOMO-LUMO gap, with a HOMO-LUMO gap between 6.7-7.5 eV having the greatest phototoxic potential, but compounds with a HOMO-LUMO gap greater than 7.5 eV are not phototoxic, because the short wavelength of UV light required to excite these molecules are not present in natural

sunlight (Menkenyan *et al.*, 1994; Veith *et al.*, 1995). Sediments contaminated with combustion derived PAHs (pyrolytic) are more phototoxic than the sediments contaminated with petroleum derived PAHs (petrogenic) (Boese *et al.*, 2000).

1.8 MUTAGENICITY AND CARCINOGENICITY OF PAHs

Some of higher molecular weight PAHs (4- to 7- ring) are carcinogenic when activated by the mixed function oxidation (MFO) system (Meek *et al.*, 1994; National Toxicology Program, 1998). The carcinogenicity of PAHs metabolites varies substantially, animal carcinogenicity PAHs depends on the two dimensional configuration of the PAH and presence and distribution of the alkyl carbons on the aromatic rings. Benzo(*a*)pyrene is highly carcinogenic, but its isomer, benzo(*e*)pyrene, is not carcinogenic. 5-Methylchrysene has a carcinogenic potency and mutagenicity similar to that of benzo(*a*)pyrene; however, other monomethylchrysenes have low/or not carcinogenic potency (Hecht et al., 1976). Most of the PAHs of the types found at highest concentrations in crude oil are, low molecular weight aromatic hydrocarbons, such as naphthalene, phenanthrene and anthracene, are not carcinogenic.

Fish have the metabolic ability to activate benzo(*a*)pyrene and some other carcinogenic PAHs to carcinogens (Stegeman and hahn, 1994). However, studies have shown that exposure to high concentrations (well above environmentally realistic levels) of the most potent higher animal carcinogens are required to induced cancers in fish in the laboratory (Neff, 1979). Chemicals that induce CYP1A in fish substantially increases the metabolism of the benzo(*a*)pyrene during exposure, fish produce PAH-DNA adducts in the liver and other tissues. DNA adducts produce genetic damage, sometimes leading to cancer. Hepatic microsomal preparations from a marine fish are able to produce mutagenic

metabolites of benzo(*a*)pyrene, dibenz(*a,h*)anthracene, and 7,12-dimethylbenzanthracene. However, there is no evidence that marine inverbrates can mobilize PAHs to mutagenic or carcinogenic products (Stegeman and Hahn, 1994).

1.9 HUMAN TOXICITY OF PAHS IN SEAFOODS

Risk-based concentrations (RBCs) based on oral cancer slope factors (CPSo) and oral reference doses (RfDo) for suspected carcinogens and non-carcinogens were established by the U.S EPA Region III (2000), and were estimated for carcinogens (Equation 1.1) and non-carcinogens (Equation 1.2).

$$RBC\left(mg/kg\right) = \frac{TR * BWa * ATc}{EFr * EDtot * \frac{IRF}{1000\frac{g}{kg}} * CPSo} \qquad \text{Equation 1.1}$$

$$RBC\left(mg/kg\right) = \frac{THQ * RfDo * BWa * ATn}{EFr * EDtot * \frac{IRF}{1000\frac{g}{kg}}} \qquad \text{Equation 1.2}$$

Where

TR = The target cancer risk.

BWa = The adult body mass.

ATc = The average time for carcinogenic effects.

EFr = The exposure frequency.

$EDtot$ = The exposure duration.

IFR = The fish ingestion rate.

CPSo = The carcinogenic slope factor particular carcinogen.

THQ = The target hazard quotient.

ATn = The average time for non-carcinogens.

RfDo = The reference oral dose for particular non-carcinogen.

Thus, the RBC concentrations in edible tissues of seafoods are unlikely to be harmful to the marine organisms themselves. The RBCs for suspected carcinogenic PAHs are intended to protect human consumers from their carcinogenic effects during long-term exposure in the food and are based in part on assumption of a high BCF and possible biomagnification's in food webs leading to man. However, most marine animals and terrestrial birds and mammals, including man, have the ability to rapidly metabolize and excrete high molecular weight PAHs ingested in food (Stegeman, 1981). The RBCs for non-carcinogenic PAHs are much higher than those for the carcinogens, reflecting their lower toxicity and low absorption efficiency from the human guts (Magee *et al.*, 1996).

1.10 AIMS OF THIS RESEARCH

From the literature review it can be observed that hydrocarbons (e.g. PAHs) are mixture of complex compound that are toxic and/or carcinogenic to the marine organisms. This demonstrate the need for the development a stratified random sampling regime to aid analysis of the risk presented by hydrocarbons in the environment to selected target resources, as risk indicators. This is the overall aim of the current research project. Also quantitative risk assessment can be used to describe and rank environmental risks from

different sources and scenarios, covering different seasons and activity plans. The ranking can also be used to identify high priority resources and geographic areas for contingency actions. The variability in presence and vulnerability of natural resources gives the possibility of adjusting activity plans according to the time window providing the lowest environmental risk.

1.10.a Objectives

⇒ *Design a robust spatial sampling strategy (stratified random sampling) that will give representative information on hydrocarbon contamination in an offshore oilfield*

⇒ *Determine analytical techniques to evaluate hydrocarbon contaminants in the sediments*

⇒ *Determine the correlation between the physical and chemical characteristics of the sediments and the hydrocarbon contaminants*

⇒ *Determine the statistical significance within the Zones of the hydrocarbons parameters*

⇒ *Describe the sources and spatial distribution of the hydrocarbon contaminant using the new stratified random sampling*

⇒ *Determine any risk/effect associated with the activities oil production to the marine organisms*

⇒ *Describe the spatial and temporal distribution of the hydrocarbon contaminant of the stratified random sampling design with the conventional grid sampling design and comparison of the statistical parameters.*

1.10.b Milestones:

- Investigation of statistical sampling regimes. (MPhil).

- Familiarisation with a range of analytical techniques; extraction of contaminant and analysis by gas chromatography with a flame ionisation detector (GC-FID) and gas chromatography using mass spectrometry (GC-MS) to be used to provide analytical results for sampling and temporal comparisons. (MPhil).

- Analysis of hydrocarbons in sediment samples from the North Sea (Fladen Ground) collected in 2001, using a random stratified sampling regime. (MPhil).

- Comparison of these analytical results with data obtained from samples collected in the same area at the same time using grid sampling. (MPhil).

- Interpretation of the data to evaluate and develop the statistical sampling regime. (MPhil).

- Investigate temporal trends in hydrocarbons from field samples from the North Sea collected in 1989, 1996, 1998 and 2001. (MPhil).

- Based on experience gained from the work in the North Sea, to design a field study to provide a statistical foundation for sampling regimes to map the dispersion of hydrocarbons in a marine/deltaic environment. (PhD).

- Carry out field studies, possibly in Nigeria, including use of fluorescent *in-situ* instrumentation, to measure hydrocarbon concentrations in the field, to test the proposed sampling regimes. To collect and analyse samples for validation purposes. (PhD).

- Analysis of field samples, after extraction of contaminant, by GC-FID, and GC-MS followed by interpretation of the data. (PhD).

CHAPTER TWO

DEVELOPMENT OF STATISTICAL SAMPLING REGIME

2.1 INTRODUCTION TO STATISTICAL SAMPLING REGIME

Sampling and monitoring to detect environmental impacts of human activities on the marine habitats in the oil and gas fields, require very careful thought. Much money, time and very substantial resources are often wasted because data are collected without carefully designing sampling so that statistical analyses and interpretation are valid and reliable. In the oil and gas production, large volume of produced water is discharged; the fundamental properties (Physical and chemical) of the produced water vary. The amount of produced water discharged from a single platform usually is less 1.5 million litres per day, whereas discharges from multiple oil wells may exceed 25 million litres per day (Neff, 2002). Following discharges to ocean, produced water undergoes a variety of changes (dilution, evaporation, adsorption/precipitation, biodegradation and photooxidation). The dispersion model studies of the produced water differ in specific details but all predict a rapid initial dilution factor of 30 – 100, within the ten metres of outfall, followed by a slower rate of dilution at greater distances (Strømgren *et al.*, 1995; Brandsma and Smith, 1996). Factors that affect rate of dilution includes discharge rate, ambient current rate, turbulent mixing regime, water column stratification, water depth, difference in density (as determined by temperature and total dissolved solids concentration) and chemical composition of the produced water and sea water.

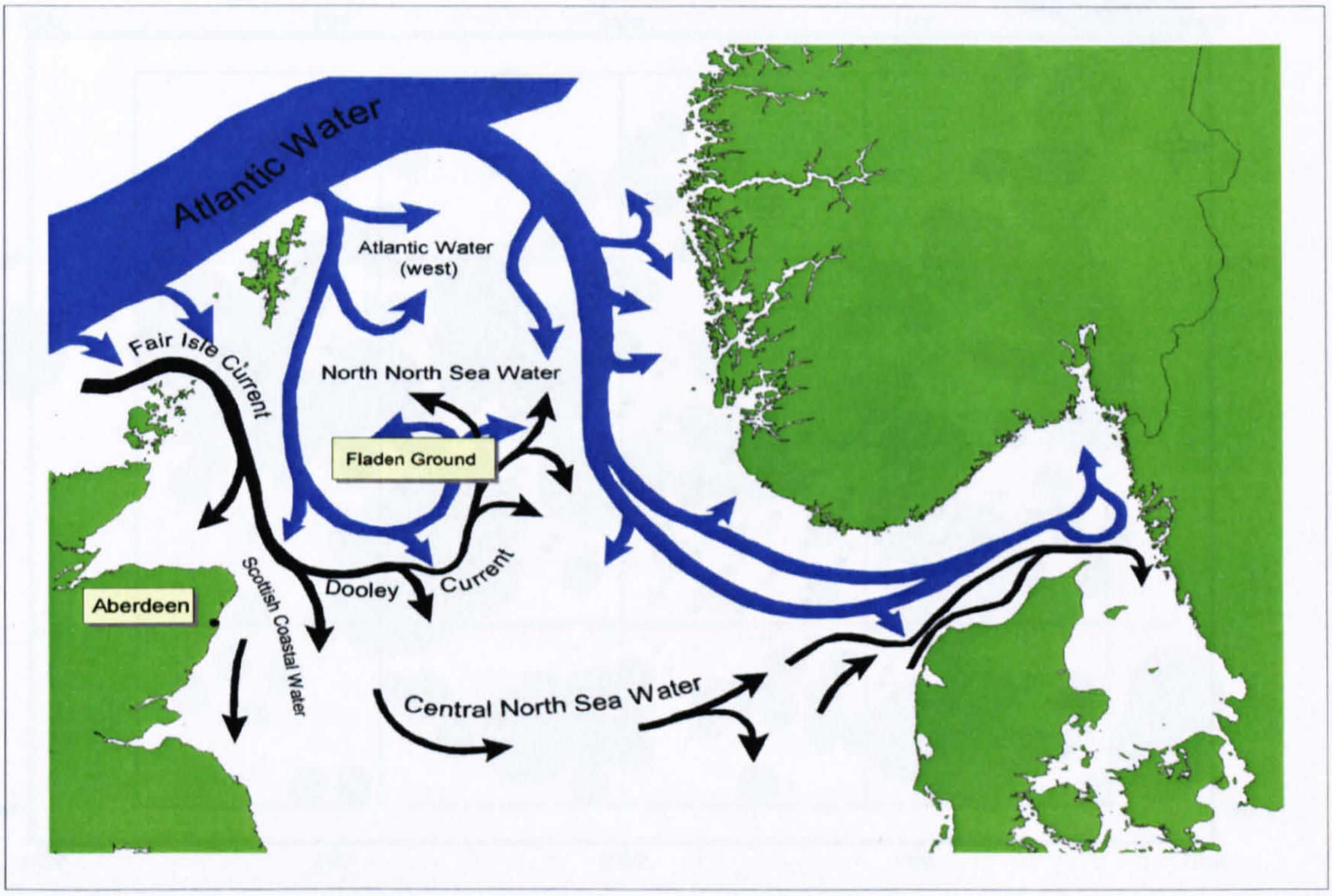

Figure 2.1 The generalised pattern of North Sea currents in relation to the Fladen Ground. Note the Fladen Ground is the centre of a semi-permanent cyclonic eddy, with currents sweeping round the outside.

The Fisheries Research Services (FRS) utilised the conventional grid-sampling regime in the Fladen Ground (Figure 2.1) in 1989 to monitor the impact of cuttings discharges (Walsham *et al.*, 2002). The survey was repeated in 2001 with the aim of assessing temporal changes in the hydrocarbon concentration and composition following the cessation of discharges of cuttings in late 1990s. Sediments were collected at 3km intervals along five transects, spaced 5km apart (Figure 2.2). The aim of this chapter is to develop a new robust sampling strategy that will accommodate the various changes that undergoes during sedimentation.

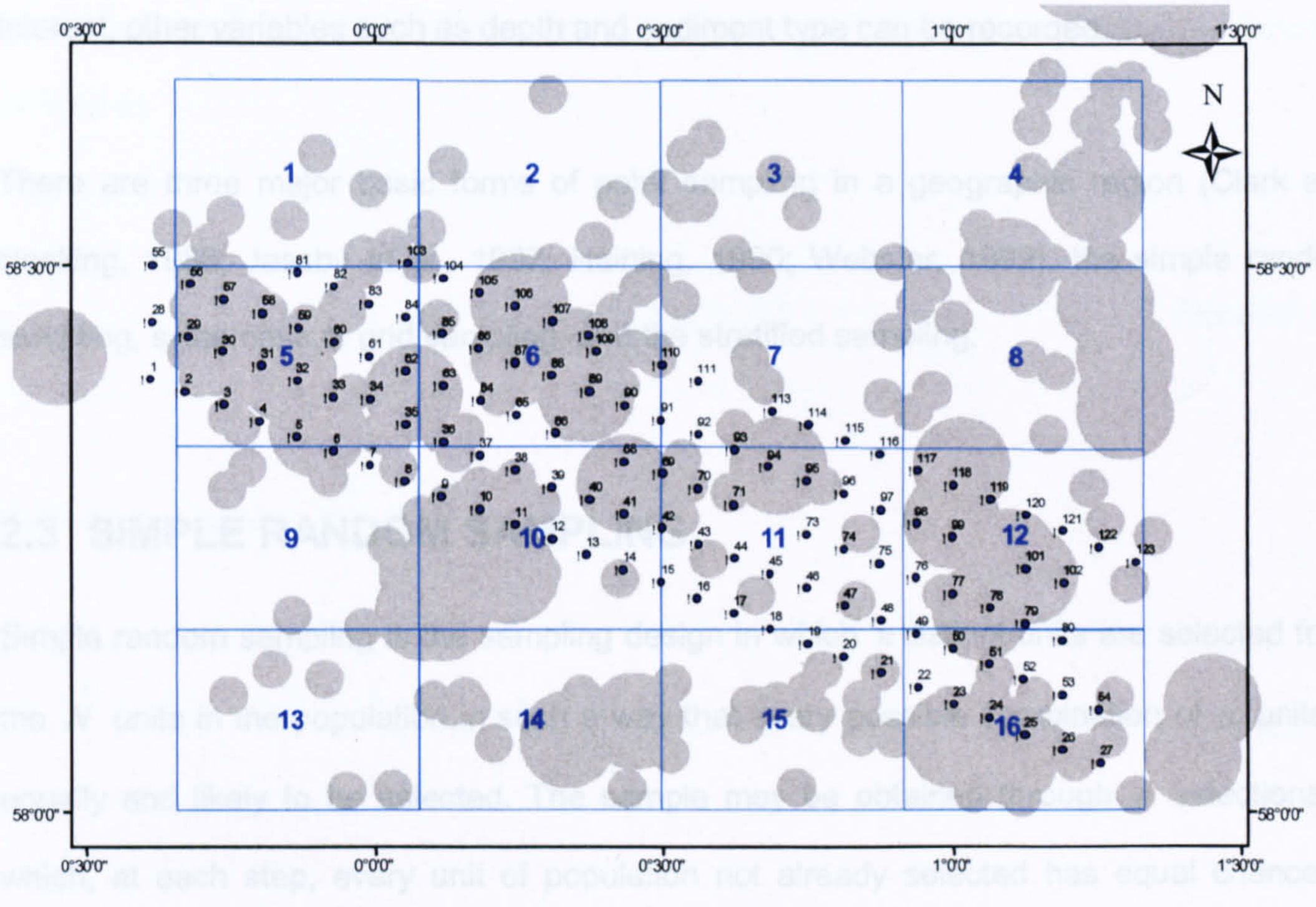

Figure 2.2 Location of common site of the 1989 and 2001 grid sampling (GS), indicating the Zones and oil platforms. Large grey circles are < 5km radius of multiple oil wells and small grey circles are < 2km radius of a single oil well. Black dots are grid samples site with labelled number.

2.2 SAMPLING AND STATISTIC PROCEDURES

Sampling consists of selecting some part of a population to observe so that one may estimate something about the whole population. The procedure by which the sample of units is selected from the population is known as the sampling design. In the basic sampling set-up, the population consists of a known, finite number N of units such as plots of ground (e.g. Fladen Ground). With each unit is associated a value of a variable interest, referred to as y-value of that unit. The data collected consist of the y-value for each unit

in the sample, together with the location of the sediment. In addition to the variable of interest, other variables such as depth and sediment type can be recorded.

There are three major basic forms of point sampling in a geographic region (Clark and Hosking, 1986; Jassby *et al.*, 1997; Haining, 1990; Webster, 1999), the simple random sampling, systematic or grid sampling, and the stratified sampling.

2.3 SIMPLE RANDOM SAMPLING

Simple random sampling is the sampling design in which n distinct units are selected from the N units in the population in such a way that every possible combination of n units is equally and likely to be selected. The sample may be obtained through n selections in which, at each step, every unit of population not already selected has equal chance of selection.

Estimating the population mean; the sample mean $\bar{y}$ is an unbiased estimator of the population mean μ. The population mean μ is the average of the y-values in the whole population:

$$\mu = \frac{1}{N}\sum_{i=1}^{N} y_i \qquad \text{Equation 2.1}$$

The sample mean $\bar{y}$ is the average of the y-values in the sample:

$$\bar{y} = \frac{1}{n}\sum_{i=1}^{n} y_i \qquad \text{Equation 2.1}$$

Also with simple random sampling, the standard deviation *s, and* the sample variance s^2 is an unbiased estimator of the *finite population variance* σ^2. The finite population variance is defined as

$$\sigma^2 = \frac{1}{N-1}\sum_{i=1}^{N}(y_i - \mu)^2 \qquad \text{Equation 2.2}$$

The sample variance is defined as

$$s^2 = \frac{1}{n-1}\sum_{i=1}^{n}(y_i - \bar{y})^2 \qquad \text{Equation 2.3}$$

The variance of the estimator $\bar{y}$ with simple random sampling is

$$\text{var}(\bar{y}) = \left(\frac{N-n}{N}\right)\frac{\sigma^2}{n} \qquad \text{Equation 2.4}$$

An unbiased estimator of this variance is

$$\hat{\text{v}}\text{ar}(\bar{y}) = \left(\frac{N-n}{N}\right)\frac{s^2}{n} \qquad \text{Equation 2.5}$$

The square root of the variance or the estimator is its standard deviation; the estimated standard error (ε) is in general not an unbiased estimator of the actual standard error.

$$\varepsilon = \frac{s^2}{n}$$ Equation 2.7

The quantity $\left(\frac{N-n}{N}\right)$, or alternatively written as $\left(1-\frac{n}{N}\right)$, is termed the finite population correction factor. If the population is large relative to the sample size, so that the finite population correction factor will be close to one, and the variance of the mean $\bar{y}$ will be approximately equal to $\frac{\sigma^2}{r}$.

To estimate the population total τ, where

$$\tau = N\mu = \sum_{i=1}^{N} y_i$$ Equation 2.8

The sample mean μ is multiplied by N. An unbiased estimator of the population total is

$$\hat{\tau} = N\bar{y} = \frac{N}{n}\sum_{i=1}^{n} y_i$$ Equation 2.9

Since the estimator $\hat{\tau}$ is N times the estimator $\bar{y}$, the variance of $\hat{\tau}$ is N^2 times the variance of $\bar{y}$. Thus,

$$\text{var}(\hat{\tau}) = N^2 \text{ var}(\bar{y}) = N(N-n)\frac{\sigma^2}{n}$$ Equation 2.10

An unbiased estimator of this variance is

$$\hat{\text{var}}(\hat{\tau}) = N^2\,\hat{\text{var}}(\bar{y}) = N(N-n)\frac{s^2}{n} \qquad \text{Equation 2.11}$$

2.3.a Benefits

The primary benefit of simple random sampling is that it protects against bias selection, by guaranteeing selection of a sample that is representative of the sampling frame, provided that the sample size is not extremely small. Moreover, the procedures needed to select a simple random sample are relatively simple.

Other benefit of random sampling includes:

- Statistical analysis of data is relatively straightforward because most common statistical analysis procedures assume that the data were obtained using a simple random design.
- Explicit formulae, as well as tables and charts in reference books, are available for estimating the minimum sample size needed to support many statistical analyses.

2.3.b Limitations

Simple random sampling has two primary limitations:

- Because all possible samples are equally and likely selected, by definition, the sample points could, by random chance, not be uniformly dispersed in space and/or

time. The importance of this limitation decreases as the size increases, but it remains a consideration, even with a large number of samples.

- Simple random sampling design ignores all prior information, or professional knowledge, regarding the site or process being sampled, except for the expected variable of the site or process of measurement.

2.4 GRID SAMPLING

Grid sampling, also called systematic sampling consists of collecting samples at locations or over time in a specified pattern. Grid sampling is used to ensure that the target population is fully and uniformly represented in the set of *n* samples collected. A probability-based design is made and an initial sampling location is chosen at random. Then the remaining (*n* -1) sampling locations are chosen so that all *n* are spaced according to some pattern.

There are two major applications for systematic sampling:

- Spatial designs. Samples are collected in one, two, or three dimensions if the population characteristic of interest has a spatial component. Sampling along a line of transect (one dimension), sampling every node on a grid laid over an area of interest (two dimension).
- Temporal designs. Samples are selected to represent a target population that changes over time, samples collected will use a one dimension, where every n^{th} unit sample is collected at specific point in time.

Grid sampling is suitable when there is no information about a population and the objective is to determine if there is pattern or correlation among units and estimate the shape or

strength of the correlation pattern. In grid sampling there is bias in the spatial pattern in the population. Therefore formulae for random samples may not be applicable, unless some assumptions are made.

Assumptions

- No spatial or temporal trends in the variable
- No natural strata
- No correlations among individual samples.

Given these assumptions, a grid sample will, on average, estimate the true mean with the same precision as a simple random or a stratified random sample of the same size.

2.4.a Benefits

The grid sampling has the following benefits:

- Provides the maximum spatial coverage of an area for a given number of samples.
- The design and implementation is relatively straightforward and has intuitive appeal.
- Regularly spaced or timed samples allow for spatial and temporal correlations to be calculated.
- The design can be implemented with little or no prior information about a site.

2.4.b Limitations

Grid sampling may not be as efficient as other designs if prior information is available about the population. Such information could be used as a basis for stratification or identifying areas of higher likelihood of finding population properties of interest. If the population

properties of interest are aligned with the grid, the sampling raises the possibility of an overestimation or underestimation (bias) of a population characteristic. Another limitation of grid in the marine environment especially in the oil and gas production environment is that missing stations that arises from the buffer region (near field site) or bad weather at sea can make if difficult to accommodate. Also Number of samples can never be optimised the number of samples. Grid sampling cannot be used to get a completely valid estimate of the standard error of the mean, i.e., variance of the mean, without some assumptions about the population. This could result in an inaccurate calculation for the confidence interval of the mean.

2.5 STRATIFIED SAMPLING

Stratified sampling is a sampling design in which prior information about the population is used to determine groups called strata/zones that are sampled independently. Each possible sampling unit or population member belongs to only one stratum/zone. Because the selections in different strata/zones are made independently, the variances of the estimators for individual strata/zones can be added together to obtain variances of the estimators for the whole population. Since only the within-stratum/zone variances enter into the variances of the estimators, the principle of stratification is to partition the population in such a way that units in each stratum/zone are as similar as possible. When the strata/zones are constructed to be relatively homogenous with respect to the variables being estimated, a stratified sampling design can produce estimates of the overall parameters with greater precision than estimates obtained from simple random sampling.

Let N_h represent the number of units in stratum/zone h and n_h the number of units in the sample from that stratum/zone.

The total number of units in that population is:

$$N = \sum_{h=1}^{L} N_h \qquad \text{Equation 2.6}$$

And the total size is

$$n = \sum_{h=1}^{L} n_h \qquad \text{Equation 2.7}$$

The total of the y-values in stratum/zone h is:

$$\tau_h = \sum_{i=1}^{N_h} y_{hi} \qquad \text{Equation 2.8}$$

Whilst the mean for that stratum/zone is:

$$\mu_h = \frac{\tau_h}{N_h} \qquad \text{Equation 2.9}$$

The overall population mean is:

$$\mu = \frac{\tau}{N} \qquad \textbf{Equation 2.10}$$

Estimating the population total

With any stratified design

The unbiased estimator of the population total τ is obtained by adding together the stratum/zone estimators.

$$\hat{\tau}_{st} = \sum_{h=1}^{L} \hat{\tau}_h \qquad \text{Equation 2.11}$$

The variance of the stratified estimator, because of the independence of the selections in different strata, is the sum of the individual stratum/zone variances:

$$\text{var}(\hat{\tau}_{st}) = \sum_{h=1}^{L} \text{var}(\hat{\tau}_h) \qquad \text{Equation 2.12}$$

An unbiased estimator of that variance is the sum of individual stratum/zone estimators;

$$\widehat{\text{var}}(\hat{\tau}_{st}) = \sum_{h=1}^{L} \widehat{\text{var}}(\hat{\tau}_h) \qquad \text{Equation 2.13}$$

With stratified random sampling

If the sample is selected by simple random sampling without replacement in each stratum/zone, then

$$\hat{\tau}_h = N_h \bar{y}_h \qquad \text{Equation 2.20}$$

Is an unbiased estimator of τ_h, where

$$\bar{y}_h = \frac{1}{n_h}\sum_{i=1}^{n_h} y_{hi} \qquad \text{Equation 2.14}$$

Is the sample mean for stratum/zone h.

An unbiased estimator for the population total τ is

$$\hat{\tau}_{st} = \sum_{h=1}^{L} N_h \bar{y}_h \qquad \text{Equation 2.15}$$

Having variance

$$\text{var}(\hat{\tau}_{st}) = \sum_{h=1}^{L} N_h (N_h - n_h)\frac{\sigma_h^2}{n_h} \qquad \text{Equation 2.16}$$

Where

$$\sigma_h^2 = \frac{1}{N_h - 1}\sum_{i=1}^{N_h} (y_{hi} - \mu_h)^2 \qquad \text{Equation 2.17}$$

Is the finite population variance from stratum/zone h.

An unbiased estimator of the variance of $\hat{\tau}_{st}$ is

$$\hat{\text{var}}(\hat{\tau}_{st}) = \sum_{h=1}^{L} N_h (N_h - n_h) \frac{s_h^2}{n_h} \qquad \text{Equation 2.18}$$

Where

$$s_h^2 = \frac{1}{n_h - 1} \sum_{i=1}^{n_h} (y_{hi} - \bar{y}_h)^2 \qquad \text{Equation 2.19}$$

Is the sample variance from stratum/zone h.

Estimating the population mean

With any stratified design

Since $\mu = \frac{\tau}{N}$, the stratified estimator for μ is

$$\hat{\mu}_{st} = \frac{\hat{\tau}_{st}}{N} \qquad \text{Equation 2.20}$$

Assuming that the selections in different strata have been made independently, the variance of the estimator is

$$\hat{\text{var}}(\hat{\mu}_{st}) = \frac{1}{N^2} \text{var}(\hat{\tau}_{st}) \qquad \text{Equation 2.21}$$

With unbiased estimator of variance

$$\hat{\text{var}}(\hat{\mu}_{st}) = \frac{1}{N^2}\hat{\text{var}}(\hat{\tau}_{st}) \qquad \text{Equation 2.22}$$

With stratified random sampling

With stratified random sampling, unbiased estimator of the population mean μ is the stratified sample mean (overall mean):

$$\bar{y}_{st} = \frac{1}{N}\sum_{h=1}^{L} N_h \bar{y}_h \qquad \text{Equation 2.30}$$

Its variance is

$$\text{var}(\bar{y}_{st}) = \sum_{h=1}^{L}\left(\frac{N_h}{N}\right)^2\left(\frac{N_h - n_h}{N_h}\right)\frac{\sigma_h^2}{n_h} \qquad \text{Equation 2.23}$$

An unbiased estimator of this variance is

$$\hat{\text{var}}(\bar{y}_{st}) = \sum_{h=1}^{L}\left(\frac{N_h}{N}\right)^2\left(\frac{N_h - n_h}{N_h}\right)\frac{s_h^2}{n_h} \qquad \text{Equation 2.24}$$

Standard error (ε_{st}) of the overall mean

$$\varepsilon_{st} = \sqrt{\sum_{h=1}^{L} \rho_h^2 \frac{S^2}{n_h}} = \sqrt{\frac{\sum_{h=1}^{L} A_h^2 \varepsilon_h^2}{A^2}} \qquad \text{Equation 2.25}$$

Where

$\rho_h = \frac{A_h}{A}$ = The proportion of the h^{th} stratum/zone

A = The total far field area

A_h = The far field area in the h^{th} stratum/zone.

ε_h = The standard error in the h^{th} stratum/zone.

2.5.a Benefits

The primary benefit of stratification is that it is cost and time effective and produces estimates with increased precision compared to other sampling designs. The stratified random sampling allowed the accommodation of missing stations that arise because of the near field site in the oil and gas environment. Also the stratified random sampling allowed the allocation of optimum number of samples in stratum/zone, which gives estimates with the lowest variance for a fixed total sample size.

2.5.b Limitation

Stratified sampling needs reliable prior knowledge of the population in order to effectively define the strata and allocate the sample sizes. The gains in the precision, or reductions in cost, depend on the quality of the information used to set up the design. Any possible increases in precision are particularly dependent on the strength of the correlation of the auxiliary, stratification variable with the variable observed in the study.

2.6 STRATIFIED RANDOM SAMPLING DESIGN

It is Environmental Protection Agency (US EPA) policy (EPA, 2000) that all EPA organisations use a systematic planning process to develop acceptance of performance criteria for collection, evaluation, or use of environmental data. Systematic planning identifies the expected outcome of the study; the data quality objectives (DQO) process (Figure 2.3) is the agency's recommended planning process for decision-making or determining compliance with a standard.

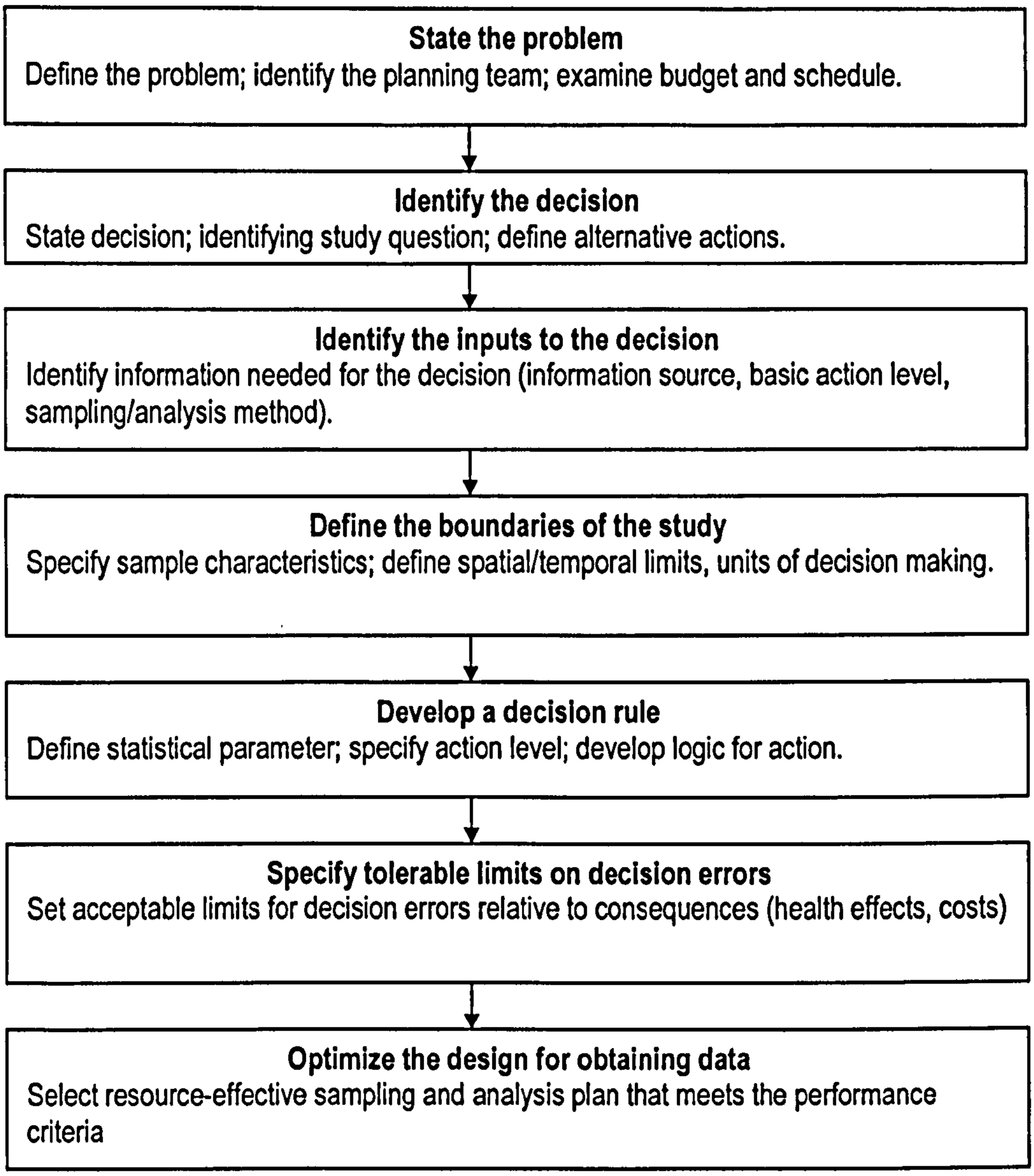

Figure 2.3 The Data Quality Objectives (DQO) Process.

In the development of the new stratified random design for the monitoring of the impacts of oil and gas production in the Fladen Ground, many factors determine the choice of the stratified random design (Figure 2.4).

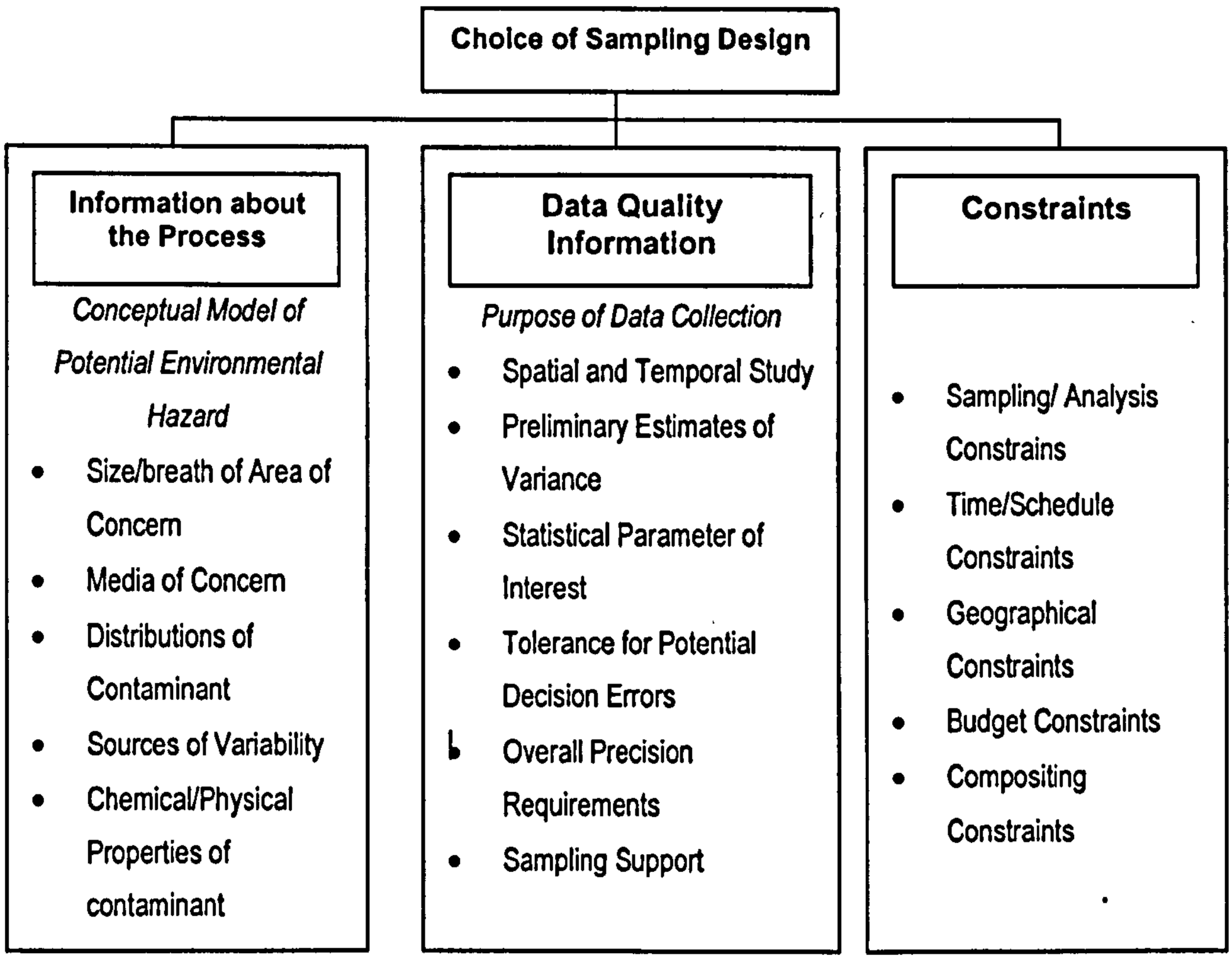

Figure 2.4 Factors in selecting a sampling design.

Using the nature of the sampling area and behaviour of the variables, two areas are defined, near and far field areas. The near field are area within 5 km from a multiple oil wells and 2 km from single oil well, whilst the far field are areas above 5 km from a multiple oil wells and 2 km from single oil well (Figure 2.5).

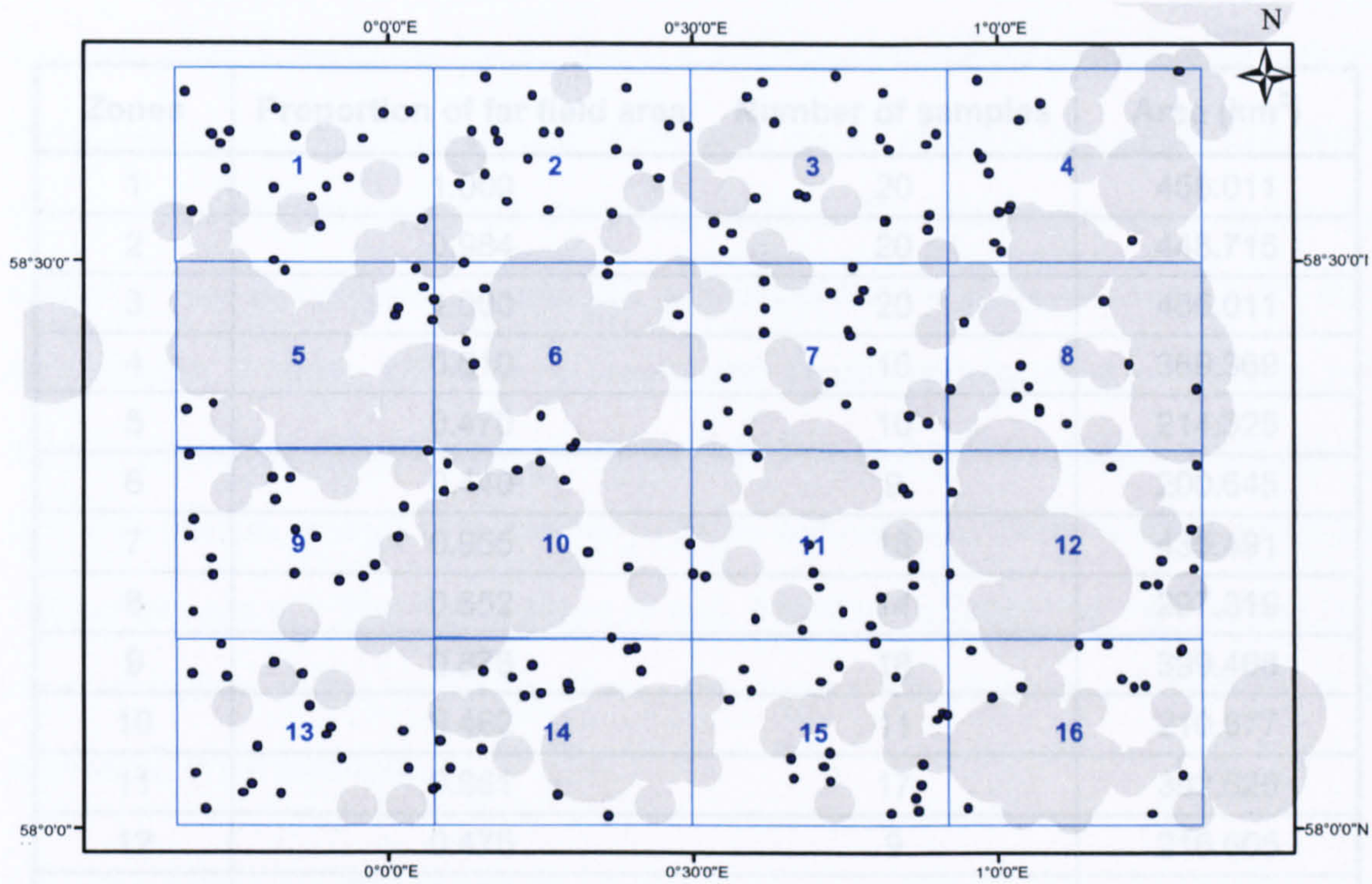

Figure 2.5 Location of the stratified random sampling site, indicating the Zones and oil platforms. Grey circles are near field sites (big circle are multiple oil wells and small circles are single well).

The near field area act as a buffer region, which accommodates the varieties of changes of the discharges, since the major sources of the contaminant in the oil field are the discharges of produced water, cuttings (stopped in the late 1990s), oil spillage and flaring of gases. The sampling area was partitioned equally into 16 Zones (Figure 2.5), these Zones are classified as Zones with multiple oil wells or single oil, Five Zones are classified single oil Zones and nine Zones are classified multiple oil Zones having at least one multiple oil wells. The number of samples in each Zone was chosen by *proportional allocation*, with the number of samples proportional to the available far field area (Table 2.1).

Table 2.1 Zones showing number of samples, proportion and area of the far fields.

Zones	Proportion of far field area	Number of samples	Area (km^2)
1	1.000	20	456.011
2	0.984	20	448.715
3	1.000	20	456.011
4	0.810	16	369.369
5	0.470	10	214.325
6	0.440	9	200.645
7	0.955	18	435.491
8	0.652	14	297.319
9	0.876	18	399.466
10	0.462	11	210.677
11	0.861	17	392.626
12	0.475	9	216.605
13	0.977	20	445.523
14	0.668	14	304.615
15	0.975	20	444.611
16	0.653	13	297.775
Overall	N/A	242	5589.784

N/A = Not Applicable.

Total number of samples was calculated based on the sum of the proportion of the far field area by taking the nearest whole number. Sampling unit was calculated based on the dimension of the Day grab (30cm by 30cm). Therefore, sampling unit equals to the area of Day grab ($0.09m^2$), the total far field area and total sampling units were $5589.78km^2$ and 6.21×10^{10} units, respectively. Two hundred and forty two samples were collected with a range of 9-20 samples per Zone, and samples were collected randomly and independently.

2.7 CONCLUSIONS

The aim of this current work was to design a robust spatial sampling strategy that will give representative information on contamination since one-off sampling can clearly give results that are unrepresentative of the site being studied. The stratified random design was chosen to assess the spatial composition and concentrations of hydrocarbons in the study area (Fladen Ground). Zones were constructed equally and numbers of samples were allocated based on the proportion of the far field area in the Zone. Near field are areas < 5km from multiple oil wells or < 2km from a single well, whilst far field are areas > 5km from multiple oil wells or > 2km from a single oil well. A total of 16 Zones was then defined using prior information on the spatial variation in the physical and chemical characteristic of the sediments, in the field area.

CHAPTER THREE

THEORY AND INSTRUMENTAL TECHNIQUES

3.1 INTRODUCTION

The determination of hydrocarbons in sediments is frequently performed in the oil and gas exploration and production environment. Given the wide variety of hydrocarbon contaminants that are found in sediment, there is a need for methods that satisfactory separate and quantify these compounds. In this thesis, a modern risk-based assessment and quantification of a range of hydrocarbon species is presented. A range of analytical instruments has been used to measure the data required, namely the polycyclic aromatic hydrocarbon determined by gas chromatography-mass spectrometry (GC-MS), the oil equivalents as determined by ultraviolet (UV) fluorescence techniques and the sum of individual *n*-alkanes determined by the gas chromatography with flame ionization detection (GC-FID) to determine the concentrations of the hydrocarbons in field samples. The theory of each technique is presented in this chapter.

3.2 FLUORESCENCE

Fluorescence is an analytically important emission process in which atoms or molecules are first excited by absorption of a beam of ultraviolet radiation, and then loose some energy by non radiative relation before relax to the ground state, giving up their excess energy as photons. As some energy has already been lost in non radiative decay fluorescent emission is always at lower energy (i.e. longer wavelength) compared to the excitation process. Absorption and emission occurs at specific wavelengths characteristic of the compound, or group of compounds, being measured.

This gives information on molecular configurations, electronic transitions and energy levels within the molecules. The information can be used to characterise particular compounds, possibly leading to identification and, with suitable calibration, can be used to determine the quantity present. Fluorescence with ultraviolet light source was used in determining the oil equivalent concentrations of the diesel oil and Forties crude oil. The oils are mixtures which often contain compounds that fluoresce; these compounds usually are aromatic rings or extended conjugated double bonds. The oil equivalent of the oil is quantified by UVF against standard dilution of the Forties crude and diesel oils.

3.2.a Theory of Molecular Fluorescence

In a partial energy diagram (Figure 3.1) for a hypothetical molecular species, three electronic energy states are shown S_0, S_1 and S_2, where S_0 is the ground state and S_1 and S_2 are the electronic excited states. Each electronic state is shown as having four excited vibration states. Irradiation of this species with a band of radiation made up of wavelengths λ_1 to λ_4 results in momentary population of the four vibrational levels of the first excited electron state S_1. Similarly, when the molecules are irradiated with a more energetic band of radiation made up of shorter wavelengths, the four vibrational levels of the higher electronic state S_2 become briefly populated.

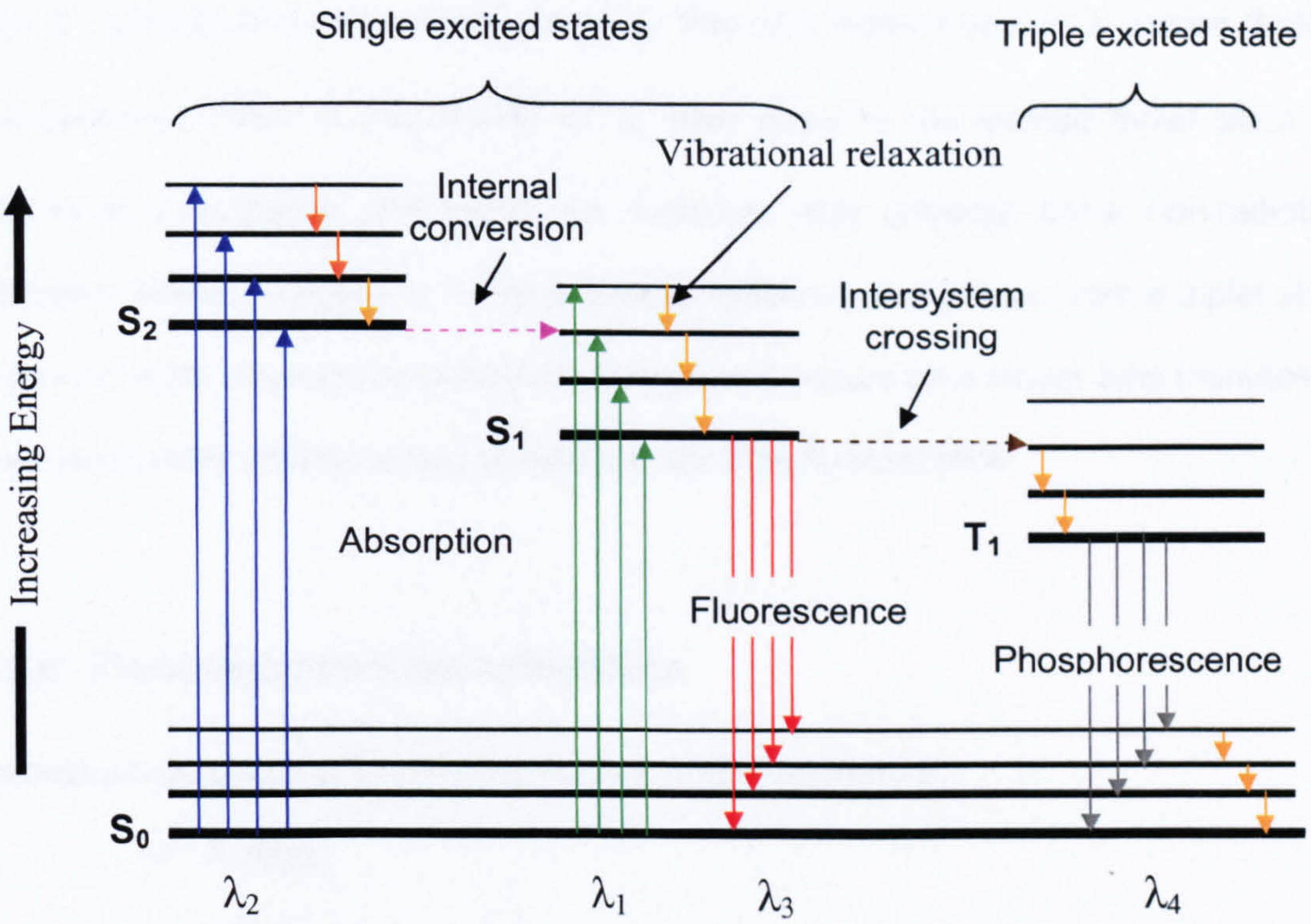

Figure 3.1 Energy level diagram showing absorption, fluorescence and phosphorescence (Skoog *et al.*, 1997).

The lifetime of an excited species is brief, and the excess energy released as the species returns to its ground state can be lost by non-radiative relaxation and/or radiative relaxation. The non-radiative relaxations (i.e. *vibrational* relaxation and *internal* conversion) occur during collision between excited molecules and molecules of the solvent; the excess *vibrational* energy is transferred to solvent molecules in a series of steps (Figure 3.1). The gain in *vibrational* energy of the solvent is reflected in a slight increase in the temperature of the medium. The lifetime of an excited vibrational state is only about 10^{-15} s, whilst for internal conversion is between 10^{-6} and 10^{-9} s. The mechanism by which *internal* conversion occurs is not fully understood.

If radiative relaxation from any of the vibrational levels of the ground state takes place, giving a band of emitted wavelength λ_3, all these lines are lower in energy, or longer

in wavelength, than the excitation lines. The phenomenon whereby a photon is emitted from a molecule at a lower energy level S_1 than the incident photon is named Stokes fluorescence. Some of the energy in S_1 may cross to the excited triplet state T_1 (*intersystem crossing*), and again the molecule may undergo some non-radiative relaxation before a photon is emitted. Energy released as a photon from a triplet state to ground state is known as phosphorescence and occurs on a longer time (minutes or even hours after irradiation has ceased) scale than fluorescence.

3.2.b Fluorescence Characteristics

Fluorescence can be characterised by four main parameters:

- Energy
- Lifetime
- Quantum yield
- Polarisation

The energy during a transition can be calculated from the emission spectrum using the following equation:

$$E = h\nu = \frac{hc}{\lambda} \qquad \text{Equation 3.1}$$

Where

E = Energy of photon (J)

h = Plank's constant (6.63×10^{-34} Js)

ν = Frequency of radiation (s)

c = Speed of light in vacuum (2.99×10^{8} ms^{-1})

λ = Wavelength of radiation (m).

Fluorescence lifetimes have in general been shown to follow first order exponential decay rate laws (Campbell and Dwek, 1984). This gives a general expression relating the fluorescence intensity, I, with the fluorescence lifetime, τ, of:

$$I = I_0 e^{-t/\tau} \qquad \text{Equation 3.2}$$

Where

I = The fluorescence intensity at any time

I_0 = The maximum fluorescence intensity during excitation

t = The time after the excitation source has been removed

τ = The average lifetime of the excitation.

The quantum yield $(\Phi)$of a system is defined as the number of quanta emitted for every quantum absorbed. This is effectively a measurement of the efficiency of the photo-system and can be represented as:

$$\Phi = \frac{number\ \ of\ \ fluorescence\ \ quanta\ \ emitted}{number\ \ of\ \ absorbed\ \ quanta} \qquad \text{Equation 3.3}$$

The polarisation of the emitted photon can be described by polarisation (Γ) and anisotropy $(\forall)$and given by the equations:

$$\Gamma = \frac{I_{\parallel} - I_{\perp}}{I_{\parallel} + I_{\perp}} \qquad \text{Equation 3.4}$$

$$\forall = \frac{I_{\shortparallel} - I_{\perp}}{I_{\shortparallel} + 2I_{\perp}} \qquad \text{Equation 3.5}$$

Where

$I_{\shortparallel}$ = The fluorescence intensity parallel to the excitation UV light

$I_{\perp}$ = The fluorescence intensity perpendicular to the excitation UV light.

Compounds containing aromatic rings give intense and analytically useful molecular fluorescence emissions. They fluoresce in solution, with the quantum efficiency increasing with the number of rings and their degree of condensation. In most molecules, the efficiency of fluorescence decreases with increasing temperature because of the increased frequency of collision at elevated temperatures.

3.2.c Effect of Concentration on Fluorescence Intensity

The power of fluorescence radiation F is proportional to the radiant power of the excitation beam absorbed by the system:

$$F = K''(P_0 - P) \qquad \text{Equation 3.6}$$

Where

P_0 = the power of the beam incident on the solution

P = the power after it traverses a length b of a medium

K'' = constant depending on the quantum efficiency of the florescence.

In order to relate F to the concentration c of the fluorescing particle, we write Beer Lambert's Law in the form.

$$\frac{P}{P_0} = 10^{-\varepsilon bc} \qquad \text{Equation 3.7}$$

Where

ε = the molar absorptivity of the fluorescing species.

But

$$\varepsilon bc = A \qquad \text{Equation 3.8}$$

Where

A = Absorbance

By substituting Equation 3.6 into Equation 3.7, we obtain.

$$F = K'' P_0 \left(1 - 10^{-\varepsilon bc}\right) \qquad \text{Equation 3.9}$$

Expanding Equation 3.9 exponential term as a series

$$F = K'' P_0 \left[2.3\varepsilon bc - \frac{(2.3\varepsilon bc)^2}{2!} + \frac{(2.3\varepsilon bc)^2}{3!} \ldots\ldots\right] \qquad \text{Equation 3.10}$$

Provided $\varepsilon bc = A < 0.05$, all of the subsequent terms in Equation 3.10, all of the subsequent terms in the brackets become small with respect to the first; under these conditions,

$$F = 2.3K''\varepsilon bcP_0 \qquad \text{Equation 3.11}$$

And, at constant P_0.

$$F = Kc \qquad \text{Equation 3.12}$$

3.3 APPLICATION OF THE UVF ANALYSIS

UVF analysis was used to measure the oil equivalents concentration of the diesel and Forties crude oil. Fluorescence methods are generally one to three orders of magnitude more sensitive than methods based upon absorption, because increasing the power or amplification of the detector signal affects the two measured quantities in an identical way and leads to no improvement. Fluorescence instruments (Figure 3.2) are usually double-beam in design in order to compensate for fluctuations in the power of the source. The beam to the samples first passes through a primary filter or a monochromator, which transmits radiation that excites fluorescence but exclude or limits radiation that corresponds to fluorescence wavelengths. The emitted radiation reaches a photoelectric detector after passing through the secondary filter, which isolates a fluorescence peak for measurement. The reference beam passes through an attenuator to decrease its power to approximately that of the fluorescence radiation. The signals from the reference and sample phototubes are then processed by a difference amplifier whose output is displayed on a meter or recorder.

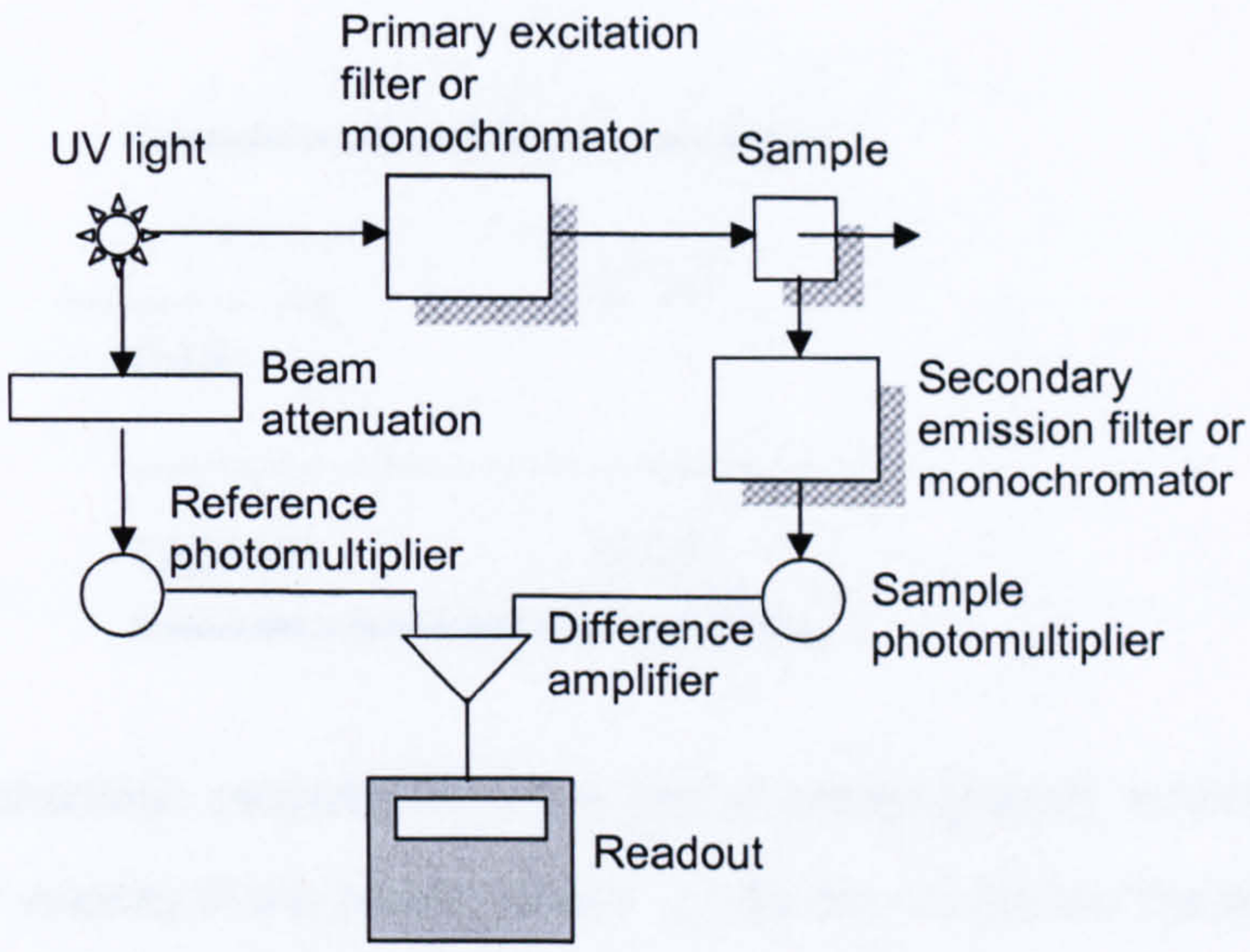

Figure 3.2 Schematic of a spectrofluorometer (Skoog *et al.*, 1997).

3.4 CHROMATOGRAPHY

Chromatography is widely used for separation, identification, and determination of the chemical components of complex mixtures. No other separation method is as powerful and generally applicable as is chromatography. Chromatography is defined as a technique in which the components of a mixture are separated based on the rates at which they are carried through a stationary phase by a gaseous or liquid mobile phase. The stationary phase is fixed in place either in a column or on a planar surface. The mobile phase moves over or through the stationary phase, carrying the analytes with it.

3.4.a Theory of Gas Chromatography

In gas chromatography the analytes are distributed between a liquid stationary phase and ideal gas as the mobile phase as schematically shown in Figure 3.3.

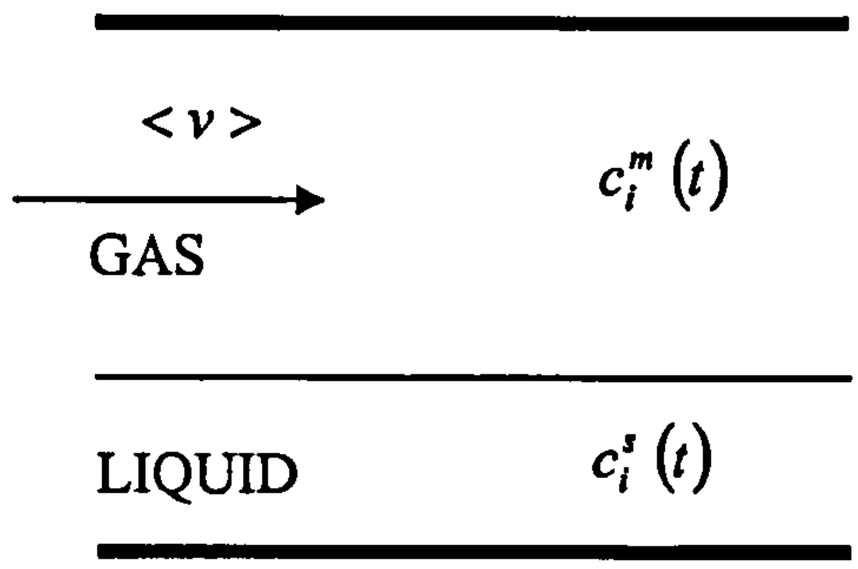

Figure 3.3 Schematic presentation of a gas chromatographic system. $< v >$ is the average linear velocity of the mobile phase. $c_i^m(t)$ and $c_i^s(t)$ are the concentrations of the analyte, i, in the mobile (m) and stationary (s) phase, respectively. Both are functions of time.

The distribution of the analytes (K_i) between the mobile and stationary phases is determined by the partition constant, given as usual by.

$$K_i = \frac{c_i^l}{c_i^m} \qquad \text{Equation 3.13}$$

For the concentration in the liquid, the vapour pressure of the solute, i, over the binary mixture consisting of the liquid phase and analytes follows Henry's Law.

$$p_i = \alpha_H p_i^\circ = \gamma_i^\circ x_i^l p_i^\circ \qquad \text{Equation 3.14}$$

Where

α_H = the Henry constant,

x_i^l = the mole fraction of analyte, i , in the liquid phase,

γ_i^o = the activity coefficient (at finite dilution),

p^o = the vapour pressure of the analyte (as pure compound) at given temperature.

The partial pressure, p_i, of the analyte in the ideal gas phase is given by Dalton's Law.

$$p_i = \frac{n_i^g}{V^g} RT \qquad \text{Equation 3.15}$$

T = the absolute temperature

R = the gas constant

V^g = the volume in the gas phase

n_i^g = the number of moles of analyte, i , in the gas phase.

Substituting the volume concentration in Equation 3.15 (for the finite dilution) gives the expression for the partition constant

$$K_i^o = \frac{RT}{p_i^o \gamma_i^o V_{s,mol}} \qquad \text{Equation 3.16}$$

Where

$V_{s,mol}$ = the mean molar volume of the stationary phase.

p_i^o = the vapour pressure of analyte as pure compound at temperature T

γ_i^o = the activity coefficient of the analyte in stationary liquid (at infinite dilution).

Separation selectivity of two consecutively eluting components, i and j, is defined in chromatography by the selectivity factor, α_{ji},

$$\alpha_{ji} = \frac{K_j}{K_i} \qquad \text{Equation 3.17}$$

Where

K_i = the partition coefficient of the less retained species

K_j = the partition coefficient of more retained species

The capacity factor, k', describe as the migration rate of the elutes on column is defined as:

$$k_i' = \frac{K_i V_s}{V_m} \qquad \text{Equation 3.18}$$

Where

V_m = the volume of the mobile phase

Substitution of equation 3.17 and analogous equation for eluting component j into equation 3.18 provides a relationship between the selectivity factor for the i and j components and their capacity factors:

$$\alpha_{ji} = \frac{k_j'}{k_i'} \qquad \text{Equation 3.19}$$

The selectivity coefficient using Equation 3.16 is thus

$$\alpha_{ji} = \frac{p_i^o \gamma_i^o}{p_j^o \gamma_j^o} \qquad \text{Equation 3.20}$$

Therefore, the selectivity in GC is determined by ratios;

- The ratio of the vapour pressures of the analytes as pure compounds (at working temperature).
- The ratio of the activity coefficients the in stationary phase (at infinite dilution).

Whereas the temperature only influences the first ratio, the second ratio reflects the difference in the chemical interactions of the two components with the stationary liquid.

3.4.b Temperature Dependence of Distribution Constant

In contrary to Equation 3.14 the distribution constant (K), and the capacity factor (k') as well, decreases with increasing temperature, because the linear dependence of K on T is more than overcompensated by the exponential increase of the vapour pressure, p_i^o, with temperature, according to the *Clausius-Claperon* equation.

$$\frac{d \quad In \quad p}{dT} = \frac{\Delta H_{vap}}{RT^2} \qquad \text{Equation 3.21}$$

Therefore the following linear approximation can be found:

$$\log K_i^o \quad resp. \quad \log k_i' \quad \propto \quad \frac{1}{T} \qquad \text{Equation 3.22}$$

3.4.c Retention Index I_R

In gas chromatography, the retention index provides a useful and generally accepted parameter for the identification of analytes. This parameter is based on the finding that $\log k'$ values of the members of a homologous series of organic compounds are commonly linearly dependent on the number of carbon atoms, n, in the molecules. Applied to the homologous series of *n*-alkenes this means that,

$$\log k'_n = A + B.n \qquad \text{Equation 3.23}$$

A pair of *n*-alkanes exists for each analyte i with a certain capacity factor, between which the analyte is eluted in the chromatogram. This analyte is considered as a fictive *n*-alkene with a hypothetical number of carbon atoms. This number, multiplied by 100, is the Kovats retention index. The retention index of analyte i is normally determined as shown below, with higher accuracy than would be possible by graphical interpolation:

$$I_{Ri} = 100z\frac{\log k'_i - \log k'_n}{\log'_{n+1} - \log'_n} + 100n \qquad \text{Equation 3.24}$$

Substitution of the capacity factors by the net retention times

$$t^N_{Ri} = t_{Ri} - t_{Ro} \qquad \text{Equation 3.25}$$

$$I_{Ri} = 100z \frac{\log t^{N}_{Ri} / t^{N}_{Rn}}{\log t^{N}_{r(n+z)} / t^{N}_{Rn}} + 100n \qquad \text{Equation 3.26}$$

n = the numbers of carbon atoms of *n*-alkanes eluting before the analyte.

$(n+z)$ = the numbers of carbon atoms of *n*-alkanes eluting after the analyte.

Z = Ion charges

Therefore, the retention index is independent of certain varying experimental parameters:

- Velocity of the mobile phase
- Phase ratio
- Length of the column.

It depends on:

- The nature of the stationary phase
- Column temperature.

3.4.d Dispersion in capillary GC

As the two components travel through the chromatographic capillary column (capillary column are open tubes made from metal or glass; discussed in section 3.5.b), the distance between the band centres increases, and the bands broaden out. *Resolution* is defined as:

$$R_s = \frac{t_{R2} - t_{r1}}{\frac{1}{2}(W_1 + W_2)}$$ Equation 3.27

Where

t_{R1} = the retention time of peak 1

t_{R2} = the retention time of peak 2

W_1 = the basal peak widths of 1

W_2 = the basal peak widths of 2.

The larger the value of R_s, the better the separation.

Gas chromatographic efficiency is affected by the amount of band broadening; the rate theorem of chromatography describes the shape and breadths of the elution peaks in quantitative terms based on a random-walk mechanism for the migration of molecules through a column. A detail discussion of the rate theory is beyond the scope of these studies. Two related terms are used as quantitative measures of the efficiency of the chromatographic columns, the plate height (H) and the number of theoretical plates (N). The two are related by the equation below:

$$N = \frac{L}{H}$$ Equation 3.28

Where

L = the length of column (usually in centimetres).

The plate height can be describe as the length of column that contains a fraction of the analytes, because the area under a normal error curve bounded by $\pm\ \sigma$ is about 68%

of the total area, the plate height, as defined (the variance per unit length of column), contains (34%) of the analyte, and is used as a measure of column efficiency;

$$H = \frac{\sigma^2}{L} \qquad \text{Equation 3.29}$$

Where

σ^2 = the variance of a Gaussian curve.

The number of theoretical plates N and plate height widely used as measured of column performance can be determined from a chromatogram as:

$$N = 5.54\left(\frac{t_R}{W_{1/2}}\right)^2 \qquad \text{Equation 3.30}$$

Where

t_R = the retention time

$W_{1/2}$ = the peak width at half its height.

The breadth of peaks in capillary GC separations is described by the model of the theoretical plate height, H. Four processes were found to contribute to the total plate height in chromatography.

⇒ H_{diff} describes the contribution from longitudinal diffusion

⇒ H_{conv} that from convective mixture

⇒ $H_{ex,m}$ that stemming from kinetics of mass exchange from the mobile phase to the interface between mobile and stationary phase

⇒ $H_{ex,s}$ that from the kinetics of mass exchange from the stationary phase.

Consequently the total plate height is the sum of the four contributions:

$$H = H_{diff} + H_{conv} + H_{ex,m} + H_{ex,s} \qquad \text{Equation 3.31}$$

The H_{diff}, that in direction of zone migration is caused by the concentration gradient occurring between the sample and its surroundings in this direction. According to the Einstein equation, the resulting peak variance in the space domain is given by,

$$\alpha_z^2 = 2D_{m,i}t \qquad \text{Equation 3.32}$$

Where

$D_{m,i}$ = diffusion coefficient.

The equivalent expression for the relation between plate height and variance is

$$\alpha_z^2 = Hz \qquad \text{Equation 3.33}$$

The contribution is more pronounced the larger the diffusion coefficient of the analyte in the mobile phase, and the longer the period that is available for diffusion. This increment increases with decreasing velocity of the mobile phase, and is proportional to $1/v$. It follows that the plate height contribution due to longitudinal diffusion is,

$$H_{diff} = \frac{2D_{m,l}}{v} \qquad \text{Equation 3.34}$$

Longitudinal diffusion in the stationary phase does not significantly contribute to peak broadening.

The radial velocity profile of the mobile phase through the column introduces an effect to peak broadening due to convective mixing. The flow profile can be analytically described as parabolic shape with zero velocity at the capillary wall, and maximum velocity at the centre of the tube with radius r_c. For a non-retained component, the contribution to the plate height is described by the Taylor dispersion equation.

$$H_{conv} = \frac{r_c^2}{24D_{m,l}} \qquad \text{Equation 3.35}$$

The amount of analyte exchanged between stationary and mobile phases has a finite rate of mass transport from the inner part of the mobile or stationary phase, respectively, to the interface between these two phases. A higher concentration than equilibrium concentration exists at the front of the peak in the mobile phase, and the reverse is the case at the rear side. For these kinetic reasons, peak dispersion occurs, which increases with increasing velocity of the mobile phase. The effect in the mobile phase is related to the flow characteristics. Therefore, the contribution of the finite mass transfer rate in the mobile phase is combined with that stemming from the flow profile, and the combination of both effects leads to,

$$H_{conv-ex,m} = \frac{\left(1+6k_i'+11k_i'^2\right)}{\left(1+k_i'\right)^2}\frac{r_c^2}{24D_{m,i}} \qquad \text{Equation 3.36}$$

The term which stems from the kinetics of mass transport in the stationary phase is given by,

$$H_{ex,s} = \frac{2}{3}\frac{k_i'}{\left(1+k_i'\right)^2}\frac{d_f^2}{D_{s,i}} \qquad \text{Equation 3.37}$$

Where

d_f = the thickness of the stationary phase layer

$D_{s,i}$ = the diffusion coefficient in the stationary phase.

The Golay equation described the total height, given by the sum of the particular increments that contribute to peak dispersion:

$$H = \frac{2D_{m,i}}{v} + \frac{\left(1+6k_i'+11k_i'^2\right)}{\left(1+k_i'\right)^2} + \frac{r_c^2}{24D_{m,i}}v + \frac{2}{3}\frac{k'}{\left(1+k_i'\right)^2}\frac{d_f^2}{D_{s,i}} \qquad \text{Equation 3.38}$$

3.5 APPLICATION OF THE GAS CHROMATOGRAPHY

A gas chromatograph consists of several parts, which are schematically shown in Figure 3.4. The main elements of a GC system are the carrier gas supply, the sample inlet, the column (positioned in a column oven), the detector(s) and a device for data collection, acquisition and processing.

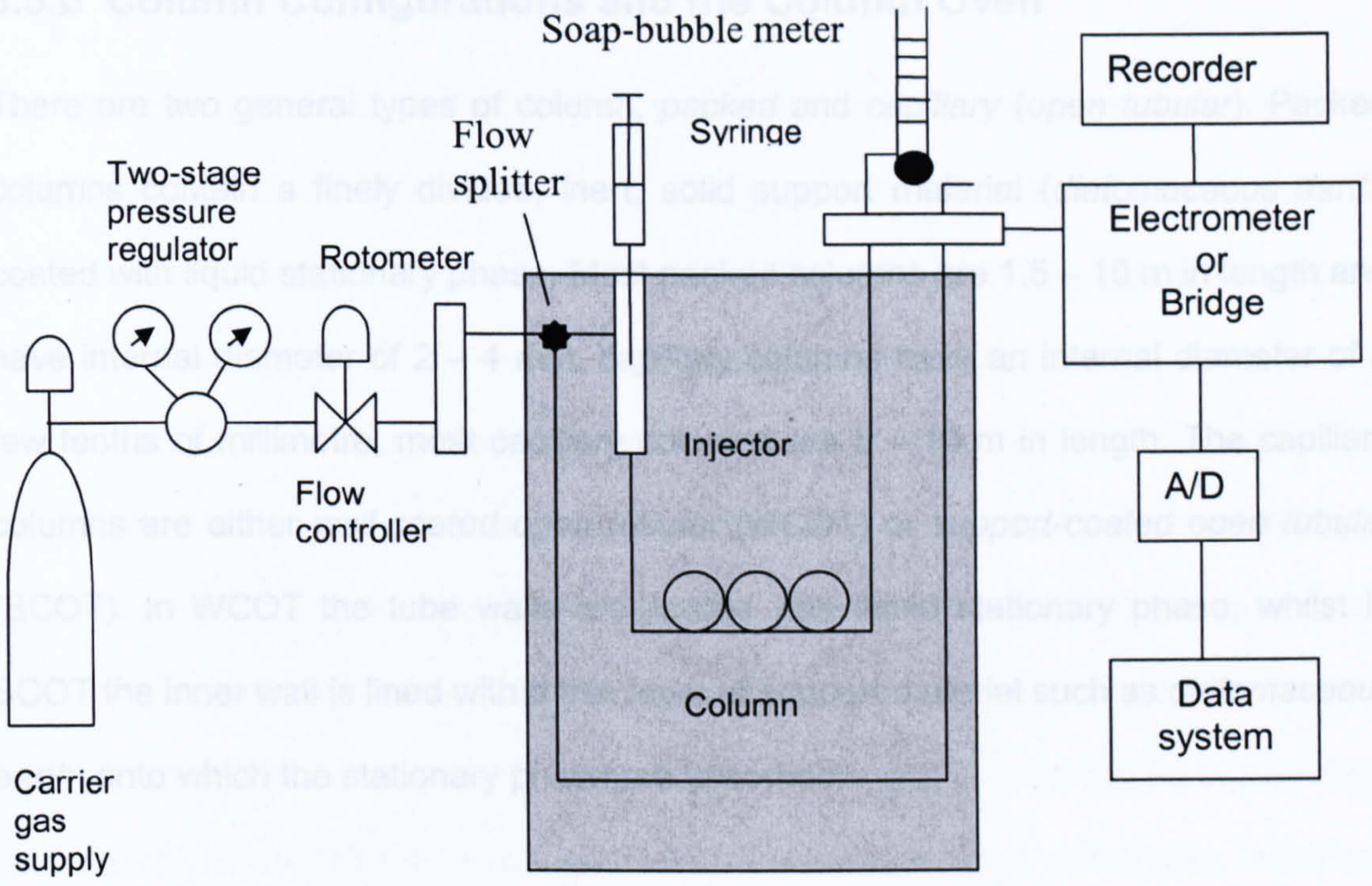

Figure 3.4 Schematic of a gas chromatograph instrument (Skoog *et al.*, 1997).

3.5.a Carrier Gas Supply

Carrier gases must be chemically inert, and the most common carrier gases include helium, nitrogen and hydrogen. Associated with the gas supply are pressure regulators, gauges, and flow meters. In addition, the carrier gas system often contains molecular sieves to remove water or other impurities. The choice of the carrier gas depends on several demands, e.g. the appropriate operation of detector (He for combination with mass spectrometry), on separation efficiency and speed, on safety reasons (H_2 is explosive), or on price (N_2 is the cheapest). He gas was used for the analyses in this study for GC-MS, nitrogen for analysis by GC-FID.

3.5.b Column Configurations and the Column Oven

There are two general types of column, *packed* and *capillary* (*open tubular*). Packed columns contain a finely divided, inert, solid support material (*diatomaceous earth*) coated with liquid stationary phase. Most packed columns are 1.5 – 10 m in length and have internal diameter of 2 – 4 mm. capillary columns have an internal diameter of a few tenths of millimetre, most capillary columns are 5 – 10 m in length. The capillary columns are either *wall-coated open tubular* (WCOT) or *support-coated open tubular* (SCOT). In WCOT the tube walls are coated with liquid stationary phase, whilst in SCOT the inner wall is lined with a thin layer of support material such as *diatomaceous earth*, onto which the stationary phase are absorbed.

Packed columns are rarely used now, and have generally been replaced by the faster capillary columns for most applications. The capillary column has the advantages of physical strength, flexibility and much lower reactivity towards sample components (avoiding adsorption interactions between analytes and adsorption centre leading to tailing peaks). Zebron column with a 5% phenyl polysiloxane film, 30 m length, 0.25 mm internal diameter and 0.25 μm film thickness was used for the analyses in this study.

For precise work, column temperature must be controlled to within tenths of a degree. The optimum column temperature is dependent upon the boiling point of the sample. A temperature slightly above the average boiling point of the sample results in an elution time of 2 – 30 min. Lower temperatures gives good resolution, but increase elution times. Temperature programming is essential if the analytes cover a wide range of boiling points; the column temperature can be increased either continuously or in steps as separation proceeds.

3.5.c Sample Injection System

For optimum column efficiency, the sample should not be too large, and should be introduced onto the column as a "plug" of vapour – slow injection of large samples causes peak broadening and loss of resolution. The most common injection method is by a micro-syringe, which is used to inject the sample through a rubber septum into a flash vapouriser port at the head of the column. For packed columns, the sample size ranges from tenths of a μL up to 20 μl. Capillary column requires much less sample, typically around 1μl. The injection can be used in one or two modes; split or splitless. The injector contains a heated chamber containing a glass liner into which the sample is injected through the septum. The carrier gas enters the chamber and leave by three routes (split mode). The sample vaporises to form a mixture of carrier gas, vaporised solvent and vaporised solutes. In this study, on-column injection was used; on-column injection has the advantages of avoiding mass discrimination effects, and its enables quantitative insertion of sample into the column (trace analysis) and labile components are not stressed thermally. With on-column technique the sample solution is directly inserted into the column with the aid of a syringe with a long, narrow needle, whereby the injector is maintained at low temperature. The capillary for the retention gap is mounted in the column oven, whose temperature must be adjusted to the boiling point of the solvent. If the temperature is below the boiling point, solvent trapping occurs. If it is selected slightly above the boiling point, cold trapping of the sample components occurs. In both cases the chromatogram must be developed with an adequate temperature program of the column, which is an essential step when using this injection type.

3.5.d Detectors

The ideal detector for GC has the following characteristics:

- Adequate sensitivity (10^{-8} – 10^{-15} g/s)
- Good stability and reproducibility
- Linear response to solute extending over several orders of magnitude
- Temperature range from room temperature to at least 400 °C
- Quick response time, independent of flow rate
- High reliability
- Similarity in response towards all solutes
- Non-destructive of sample.

3.5.d.i Flame Ionization Detectors (FID)

The flame ionization detector (FID) is the most widely used and generally applicable detector for a GC, with schematic diagram shown in Figure 3.5. The effluent from column is mixed with hydrogen and air and then ignited electrically. The FID couple with GC was used in the determination of the aliphatic hydrocarbons because of it high sensitivity for compounds containing carbon. Most organic compounds, when pyrolyzed at room temperature by a hydrogen/air flame, produce ions and electrons that can conduct electricity through the flame. A potential of a few hundred volts is applied across the burner tip and a collector electrode located above the flame. The resulting current (~10^{-12} A) is then directed into a high-impedance operational amplifier for measurement.

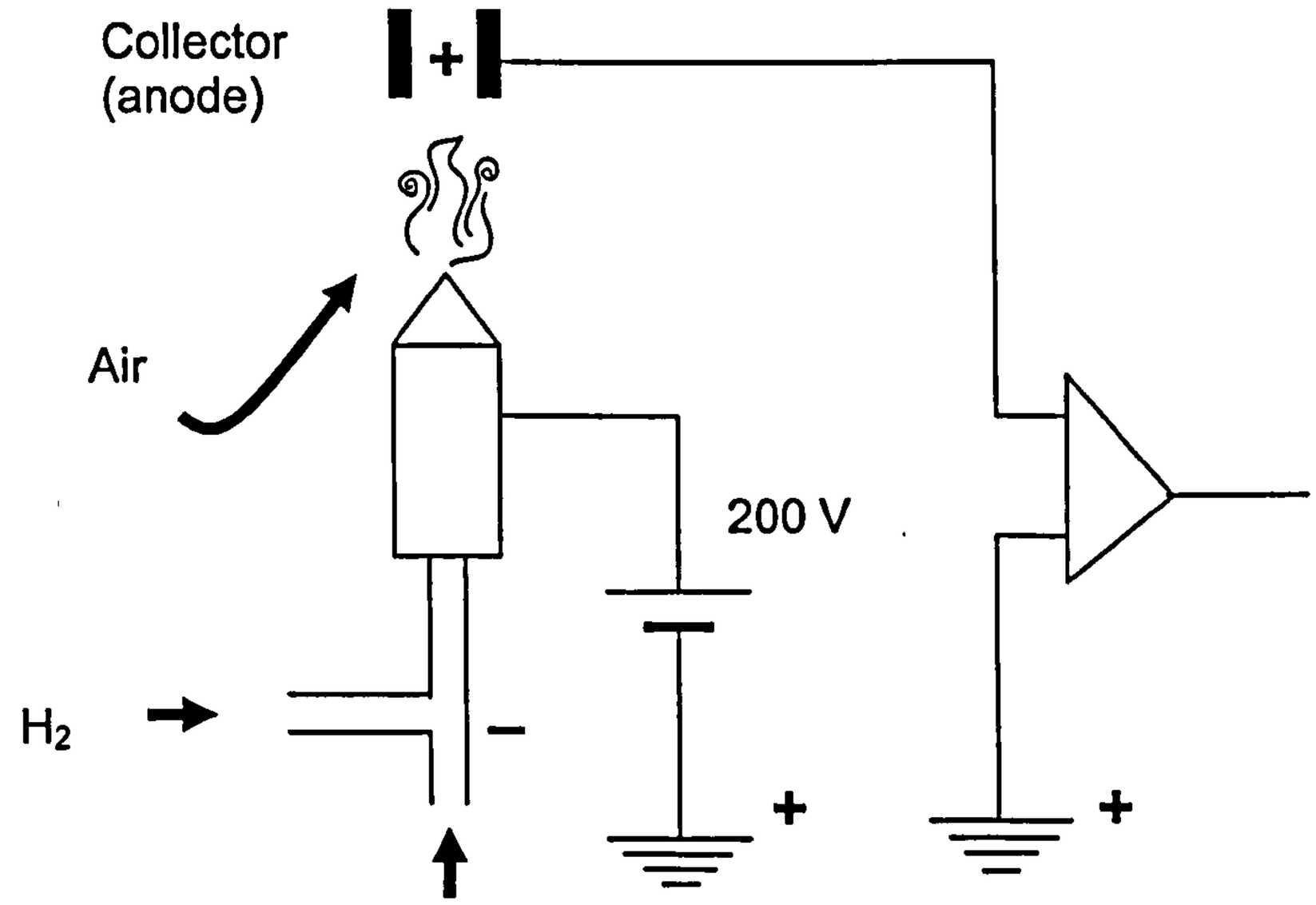

Figure 3.5 Schematic drawing of a flame ionization detector (FID) (Skoog *et al.*, 1997).

3.5.d.ii Mass Spectrometer

A mass spectrometer creates charged particles (ions) from molecules. It then analyzes those ions to provide information about the molecular weight of the compound and its chemical structure. There are many types of mass spectrometers and sample introduction techniques which allow a wide range of analyses. This discussion will focus on mass spectrometry as it's used in the powerful and widely used method of coupling Gas Chromatography (GC) with Mass Spectrometry (MS). The GC-MS was used in determination of PAHs and the geochemical biomarker analysis (sterane and triterpane). All mass spectrometers consist of three distinct regions:

⇒ Ionizer

⇒ Ion Analyzer

⇒ Detector

Ionizer

In the GC-MS, the charged particles (ions) required for mass analysis are formed by Electron Impact (EI) Ionization. The advantage of EI over chemical ionization (CI) is molecular and fragment ions are created in EI, whilst in CI no structural information is obtained due to lack of fragment ions. The gas molecules exiting the GC are bombarded by a high-energy electron beam (70 eV). An electron which strikes a molecule may impart enough energy to remove another electron from that molecule. EI Ionization usually produces singly charged ions containing one unpaired electron. A charged molecule which remains intact is called the molecular ion. Energy imparted by the electron impact and, more importantly, instability in a molecular ion can cause that ion to break into smaller pieces (fragments). The molecule ion may fragment in various ways, with one fragment carrying the charge and one fragment remaining uncharged.

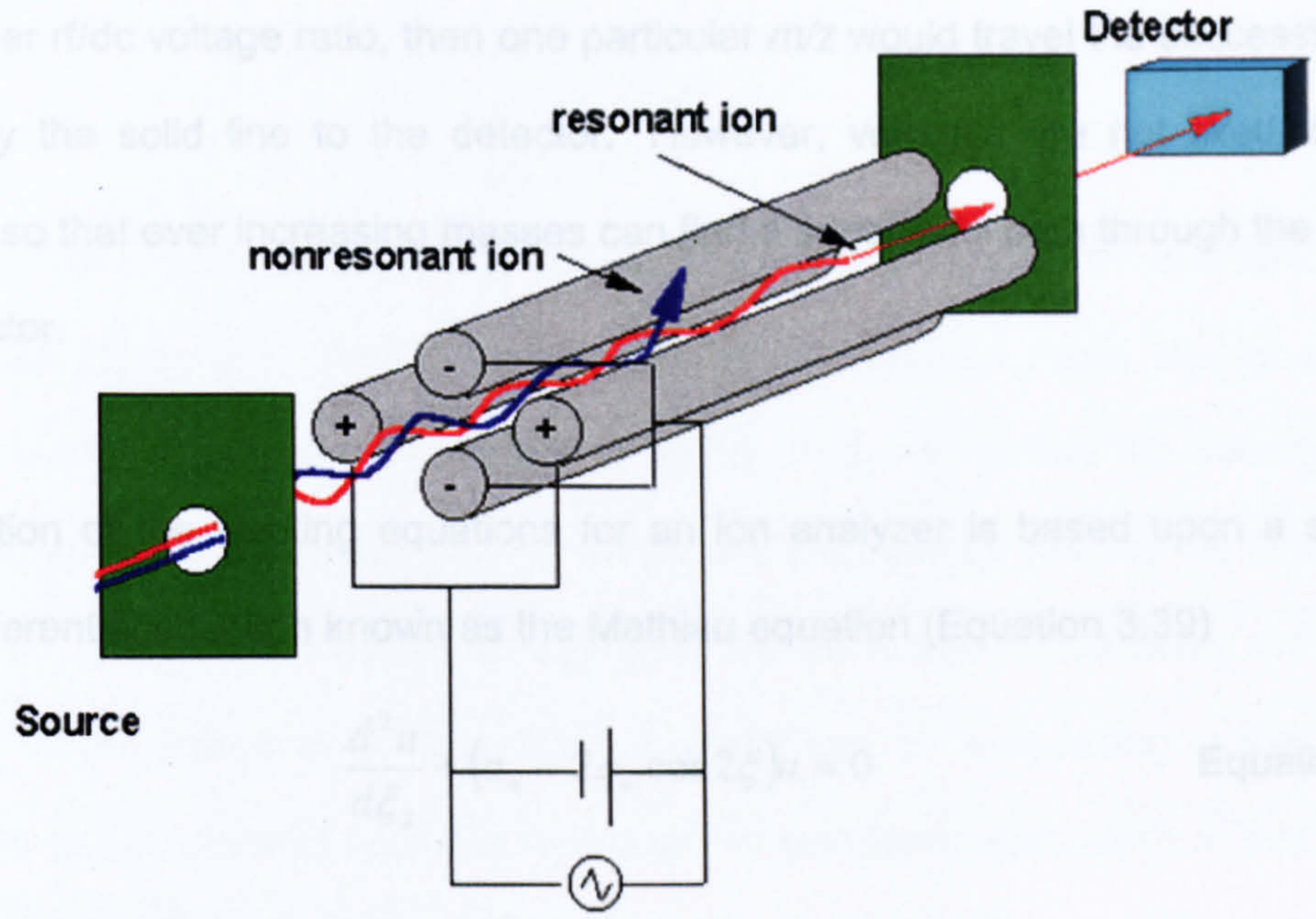

Figure 3.6 A schematic diagram of a quadrupole mass filter from Frauhofer-Institute for process engineering and packaging IVV.

Ion Analyzer

Molecular ions and fragment ions are accelerated by manipulation of the charged particles through the mass spectrometer. Uncharged molecules and fragments are pumped away. The quadrupole mass analyzer (Figure 3.6) used in this study, uses positive (+) and negative (-) voltages to control the path of the ions. The quadropole mass filter can be operated in a scan or select ion monitoring (SIM) modes. In SIM, the mass filter is set to pass one selected mass to charge ratio (*m/z)*, this provides the greatest sensitivity and is used for quantitative application, whilst the mass filter in the scan mode is set to sequentially pass a range of masses, and it has lower sensitivity because most of the ions strike the rods during scan. In this study EI using SIM modes was used. Ions travel down the path based on their *m/z*. EI ionization produces singly

charged particles, so the charge (z) is one. Therefore an ion's path will depend on its mass. If the (+) and (-) rods shown in the mass spectrometer schematic were 'fixed' at a particular rf/dc voltage ratio, then one particular *m/z* would travel the successful path shown by the solid line to the detector. However, voltages are not fixed, but are scanned so that ever increasing masses can find a successful path through the rods to the detector.

A derivation of the working equations for an ion analyzer is based upon a second-order differential equation known as the Mathieu equation (Equation 3.39)

$$\frac{d^2u}{d\xi_2} + \left(a_u - 2q_u \cos 2\xi\right)u = 0 \qquad \text{Equation 3.39}$$

And

$$a_u = \frac{8eU}{mr_0^2\Omega^2} \qquad \text{Equation 3.40}$$

$$q_u = \frac{4eV}{mr_0^2\Omega^2} \qquad \text{Equation 3.41}$$

Where

u	=	position of the coordinate axes (x or y)
ξ	=	parameter representing $\Omega t/2$
t	=	time
e	=	charge on electron
U	=	the applied DC voltage
V	=	the applied zero-to-peak radio frequency (RF) voltage
m	=	the mass of the ion
r	=	effective radius between electrodes

Ω = the applied RF frequency.

Detector

There are many types of detectors, but most work by producing an electronic signal when struck by an ion. Timing mechanisms which integrate those signals with the scanning voltages allow the instrument to report which *m/z* strikes the detector. The mass analyzer sorts the ions according to m/z and the detector records the abundance of each m/z. Regular calibration (or tuning) of the m/z scale is necessary to maintain accuracy in the instrument. Calibration is performed by introducing a well known compound (six deuterated aromatic hydrocarbon standards were used in this studies d_8-naphthalene, d_{10}-biphenyl, d_8-dibenzothiophene, d_{10}-anthracene, d_{10}-pyrene and d_{12}-benzo[*a*]pyrene) into the instrument and "tweaking" the circuits so that the compound's molecular ion and fragment ions are reported accurately.

3.6 CONCLUSIONS

UVF analysis was used in determination of the oil equivalent concentrations of the Forties crude oil and diesel oil, the GC-FID used in determination of the aliphatic hydrocarbon concentrations and the GC-MS used in the determination of the PAHs concentrations and identifications of the geochemical biomarker analysis. The choice of these techniques is important to determine the characteristics of the hydrocarbons in sediments. The concentrations are used in assessing and evaluating the sources and effects of the hydrocarbon contamination in the sediments to the marine and wider environment.

The GC-FID method utilized separation properties of the GC with the identification ability of the FID, because the FID responds only to oxidizable carbon atoms, fully

oxidized carbon compounds (*e.g.*, CO_2) and non-oxidizable compounds (e.g., polysulfides or S_8) are not detected. Furthermore, the fact that the compounds are detected following the flame ionization means that while detector response is proportional to the amount of oxidizable material that was ionized, it is not impacted by the chemical nature of the compound itself. Thus, while the FID response can vary as a function of the amount of material being ionized in the flame, it does not vary significantly as a function of the chemistry of the compound; a C_6 alkane (hexane) will exhibit an FID detector response similar to that of a C_6 aromatic (benzene). Additionally, FID response has been shown to be linear over nearly 6 orders of magnitude differences in compound concentration. For these and other reasons (high sensitivity, great reliability, etc.) the GC-FID was chosen for the determination of the aliphatic fraction of the hydrocarbon.

In marked contrast to the GC-FID, detection using a GC-MS can be significantly affected by both the amount and the chemical nature of the compound. This is due, in part to the ionization potential of the specific compound. It is this attribute which makes the MS such a useful tool in characterizing specific compounds.

Because of the significant differences in detector response as a function of the chemistry, quantification using mass spectrometry is usually done only when there is a specific standard for the compound of interest, and six deuterated aromatic standards (d_8-naphthalene, d_{10}—biphenyl, d_8-dibenzothiopene, d_{10}-antracene,d_{10}-pyrene and d_{12}-benzo[*a*]pyrene) were used in this studies.

CHAPTER FOUR

METHODOLOGY

4.1 INTRODUCTION

In order to evaluate the effects of hydrocarbon pollution to the ecosystem, it is essential to analyse the individual characteristics of the sediment. To compare sample sites, the origin and amount of contaminants has to be investigated. The analytical methods and the quality control procedures are described in this Chapter.

4.2 MATERIALS

Dichloromethane (DCM), *iso*-hexane, methanol and acetone were purchased from Rathburn Chemicals Ltd. (Walkerburn, Scotland). Anhydrous sodium sulphate (Na_2SO_4) was of analytical grade from Fisher Chemicals (Loughborough, UK).

4.3 SAMPLE COLLECTION

Sediment samples were collected by Day Grab. The top 2 cm layer of sediment was scraped off each sample and the sediment was mixed before transferring (~200 g) to a solvent washed aluminium can which was labelled and stored at -20 ± 5°C until required for analysis. All sediments collected were analysed for ultra-violet fluorescence (UVF) oil equivalent concentrations, PAHs and *n*-alkanes while selected samples were analysed for steranes and triterpanes.

4.4 FREEZE-DRYING

Freeze-drying is a process of separation of liquid water from a wet solid product, solution or dispersion of given concentration in a form of solid phase, ice, and its subsequent removal by vacuum sublimation, leaving the solute or substrates in their anhydrous, or almost anhydrous state. At low pressures and temperatures water in the form of ice can be converted directly into water vapour. By avoiding the liquid phase of water, boiling is inhibited, and the sample remains intact.

4.4.a Freeze Drying of Sediments

The freeze-drying of the sediment sample was performed on a Lyotrap Ultra LF/LYO/03/1 (serial-No L6831) (MLA SOP 0110) freeze drier. It is essential that **the samples were frozen** before being placed in the freeze drier. The samples need to be unsealed to allow the water vapour generated from the sublimation of the ice to escape. The samples were freeze-dried for 36 ± 4 hrs below -30^{0}C.

4.5 PARTICLE SIZE ANALYSIS (PSA)

The particle size analysis (PSA) is a method used to determine the particle size distributions of the sediments in the range 0.1-2000 microns. Two instruments were used

4.5.a Principle of PSA

The principle is based on the scattering of laser radiation by particles in a flow cell and the measurement of the intensities of the scattered light concentric circles at the focal length point of the optical detection system. The results were given as a histogram of the distribution and as the percentage of particles with diameter < 20 µm and < 63 µm.

4.5.b Analysis

PSA was first performed on a Mastersizer/E, Malvern (Serial-No 7271), later a new Malvern instrument Mastersizer 2000 Compiles with 21CFR 1040 10 and 1040 11 version 5.22 (Serial-No MAL 100570) was used for the rest of the samples. The freeze-dried sediment sample was sieved through a 500 and 2000 µm sieve for the old and new instrument, respectively, into the mixing cell and sonicated until a particle size reading was obtained before recording the measurement (MLA SOP 840). The particle size distributions were calculated by the Mastersizer computer (Powermate 425-PM – 1222-2431). In the old instruments Mastersizer/E, Malvern (Serial-No 7271), manual sieving was used to calculate particle sizes above 500 µm.

4.6 ANALYSIS OF CARBON, HYDROGEN AND NITROGEN (CHN)

The CHN analysis is a method used to determine the organic carbon and nitrogen content of sediments in the range of 0.06-55.6 mg and 0.005-6.07 mg per sample for carbon and nitrogen, respectively.

4.6.a Principle of the CHN analysis

Sediment samples were acidified with HCl in silver cups, prior to analysis to remove the inorganic carbon fraction. The CHN analyser uses a combustion method to convert the sample elements into simple gases (CO_2, H_2O and N_2) the sample is first oxidised in a pure oxygen environment; the resulting gases are then controlled at exact conditions of pressure, temperature and volume. Finally, the product gases are separated. Then, under steady state conditions, the gases are measured as a function of thermal

conductivity, and expressed as percentage of the whole sample and as C/N and N/H ratios. Acetanilide is used to calibrate the machine on start-up. Mess -2 and Tibet soil are used as system suitability checks for C and N respectively. "Clean" homogenised sediment from Raasay Sound is used as a laboratory reference material (LRM).

4.6.b Analysis

A freeze-dried sample of 10-20 mg of finely ground material was weighed on a Sartorious MC2106 Auto balance, into 12 mm silver capsules. The samples then underwent acidification (MLA SOP 170), by adding an initial 20 µl of HCl (15% v/v) and allowed to evaporate in a Teflon tray on a hotplate at 70^{0}C. Another three portions at 15 minutes intervals were added then follow by 4 additions at 15 minutes intervals of 30 µl of HCl (15% v/v). The samples were then transferred to an aluminium tray and left for an hour to remove excess HCl which may interfere with the CHN analyser when the sample is analysed. Nitrogen and the total organic carbon (TOC) content were determined using a Thermo Quest FlashEA 1112 elemental analyser (MLA SOP 885).

4.7 PREPARATION OF GLASSWARE AND SODIUM SULPHATE

All glassware were washed and dried in a GW 4000-glassware washer (Camlab Ltd., Cambridge, UK). Prior to use, all glassware was rinsed twice with DCM and then twice with *iso*-hexane, the latter being allowed to evaporate before proceeding. Anhydrous sodium sulphate, used for drying the organic extracts, was washed ultrasonically with DCM (2 x 500 ml) followed by *iso*-hexane (2 x 500 ml) and dried overnight at 150 °C.

4.8 EXTRACTION OF SEDIMENTS FOR FLUORESCENCE AND HYDROCARBON ANALYSIS

This method describes the extraction of sediments for the determination of total hydrocarbons by fluorescence, aliphatic hydrocarbons by gas chromatography with flame ionisation detection (GC-FID) and PAHs by gas chromatography - mass spectroscopy (GC-MS).

4.8.a Principle of the Method

The hydrocarbons are extracted using a polar solvent mixture with sonication. The chlorinated solvent is isolated from the methanol by partitioning with water. The chlorinated solvent is dried and then diluted to a standard volume from which small aliquot is removed for fluorescence determination. The remaining solution is solvent exchanged to *iso*-hexane and the hydrocarbons fractionated into aliphatic and aromatic fractions by normal phase high performance liquid chromatography (HPLC). The final concentration is quoted on the basic of dry weight of sediment.

4.8.b Hydrocarbon Extraction

20 ± 0.5 g of the sediment sample was weighed into a centrifuge tube, and 200 ± 3 µl of the aliphatic hydrocarbon internal standards (heptamethylnonane and squalane) (MLA SOP 1605) and 100 ± 1 µl of the six deuterated aromatic hydrocarbon standards (d_8-naphthalene, d_{10}-biphenyl, d_8-dibenzothiophene, d_{10}-anthracene, d_{10}-pyrene and d_{12}-benzo[*a*]pyrene) (MLA SOP 1605) were added. The hydrocarbons were extracted twice using 20 ± 2 ml dichloromethane/methanol with sonication and centrifugation, the halogenated solvent isolated and dried over Na_2SO_4. The DCM fraction was made to a known volume (100 ml) and an aliquot (10 ml) removed for UVF analysis. The remaining

extract was solvent exchanged to *iso*-hexane and the extract reduced in volume by rotary evaporation prior to concentration to a small volume (~500 μl) under a scrubbed nitrogen stream (MLA SOP 1600).

4.8.c Sample Fractionation

The aliphatic and aromatic hydrocarbons were separated by isocratic high performance liquid chromatography (HPLC). An aliquot (150 μl) of the *iso*-hexane extract was injected on to a previously calibrated Genesis SIL 4 μm HPLC column (25 x 4.6 cm id; Jones Chromatography, Mid Glamorgan, UK) and eluted with *iso*-hexane at a flow rate of 2 ml min^{-1}. The two fractions collected were concentrated (~ 50 μl) prior to chromatographic analysis. The extracts were analysed by gas chromatography with flame ionisation detection (GC-FID) for aliphatic hydrocarbon analysis and gas chromatography – mass spectroscopy (GC-MS) for PAHs and biomarkers (MLA SOP 1600).

4.9 ULTRA-VIOLET FLUORESCENCE (UVF) ANALYSIS

This method described the determination of oil equivalents in sediments using ultraviolet UV radiation as source of excitation. Calibration standards were prepared for reference diesel fuel oil and reference Forties crude oil; these were analysed with each batch of samples. A stock solution of oil, each was prepared (~ 100 μg ml^{-1}). From this, aliquots were removed and dilutions prepared covering the concentration range 0.02 - 5 μg ml^{-1}. The samples were introduced, *via* a cuvette, into a Perkin Elmer LS 5 spectrophotometer (Perkin Elmer, Beconsfield, UK).

4.9.a Principle of the Method

The principle of fluorescence was described in Chapter 3. The oil equivalent of the oil is quantified by UVF against standard dilution of the Forties crude and diesel oils.

4.9.b Analysis

The optimum excitation and emission wavelengths were determined for both Forties crude oil and diesel fuel. Diesel calibration standards were read with the spectrometer set with an excitation of 270 nm and an emission of 330 nm, while Forties calibration standards were read with an excitation of 310 nm and an emission of 360 nm. Samples were read against the wavelength settings for both diesel fuel oil and Forties crude oil. The instrument was set with a fixed scale of 1 and a slit width of 5 nm. Fluorescence analyses at high concentrations are susceptible to self-quenching. Self-quenching results from the collisions of excited molecules, it increases with concentration due to the increased probability of collisions. To account for any self-quenching samples were measured at each wavelength and then diluted (50%) in dichloromethane and re-read. This step was repeated until readings were almost half that of the previous reading.

4.10 ANALYSIS OF ALIPHATIC HYDROCARBONS

This method describes the quantitative determination of aliphatic hydrocarbons, specifically *n*-alkanes, from sediment samples by gas chromatography with flame ionisation detection (GC-FID).

4.10.a Principle of the Method

The principle is base on separation of volatile and semi-volatile compound by the GC column, and subsequent burning of the compound in small hydrogen flame (chapter 3).

Ionic fragments and free electrons formed in the combustion are collected via an electrostatic field surrounding the flame, and an electronic current proportional to the amount of sample entering the flame is created.

4.10.b Analysis

The *n*-alkane distribution was determined by Gas Chromatography with Flame Ionisation Detection (GC-FID) using an HP 5890 Series II gas chromatograph (Hewlett Packard Ltd, Stockport, England), equipped with an HP 7673 automated, cool on-column injector and fitted with a non-polar, Ultra 1 column (25 m x 0.2 mm id, film thickness 0.33 μm; Agilent Ltd, Stockport, England). The carrier gas was ECD grade nitrogen (16 psi). Injections were made at 60°C and the oven temperature held at this for 3 minutes. Thereafter the temperature was raised at 4°C min^{-1} up to 280°C and held at this temperature until the end of the run. The detector was maintained at 300°C throughout. Data were collected using a PE Nelson 600 series link box and processed using Turbochrom Navigator software (Perkin-Elmer Ltd, Beaconsfield, England) (MLA SOP 1610).

4.11 ANALYSIS OF GEOCHEMICAL BIOMARKERS (STERANES AND TRITERPANES)

This method described the qualitative analysis of steranes and triterpanes in sediment samples; the geochemical biomarker profile can be used to identify oil contamination from weathered or bacterial oxidised oil.

4.11.a Principle of the Method

The principle is based on separation of volatile and semi-volatile compounds on the GC column, and subsequent identifications of the sterene and triterpane of the crude oil (aliphatic fraction) unaffected by weathering, by the MS (Chapter 3).

4.11.b Analysis

The sterane and triterpane compositions were determined by GC-MS using an HP6890 Series gas chromatograph interfaced with an HP5973 MS and fitted with a cool on-column injector. A Zebron column with a 5% phenyl polysiloxane film was used for the analyses (ZB5, 30 m x 0.25 mm id, 0.25 μm film thickness: Phenomenex, Cheshire, UK). Injections were made at 60°C and the oven temperature held constant for 0.5 min after which it was increased at 40°C min^{-1} up to 150°C. This was followed by a slower ramp of 5°C min^{-1} up to a final temperature of 300°C and held at this temperature for 22 min. The carrier gas was helium set at a constant flow of 0.7 ml min^{-1}. Geochemical biomarker analysis was carried out using the selective ion monitoring mode (SIM) to enhance sensitivity according to UNEP/IOC/IAEA (1992). Triterpanes were monitored using *m/z* 177 and 191 and steranes monitored using *m/z* 217 and 218 with a dwell time of 80 msec and a delay of 10 msec.

4.12 ANALYSIS OF POLYCYCLIC AROMATIC HYDROCARBONS (PAHs)

This method describes the determination of polycyclic aromatic hydrocarbons (PAHs) in sediments by the gas chromatography - mass spectroscopy (GC-MS). The analysis incorporates two- to six-ring, parent and branched PAHs. This does not cover all of the

many PAH compounds that exist. The concentration range of the method is from the limit of detection to 10 g kg^{-1}.

4.12.a Principle of the Method

The principle is based on separation of the volatile and semi-volatile compounds on the GC column and subsequent identification by MS (Chapter 3). Deuterated PAH standards (D_8-naphthalene, D_{10}-biphenyl, D_8-dibenzothiophene, D_{10}-anthracene, D_{10}-pyrene and D_{12}-benzo[*a*]pyrene) are used as internal standards, and are added to the sediment before the extraction. The GC-MS is calibrated using seven different concentrations of a solution containing 33 PAHs.

4.12.b Analysis

The concentration and composition of the PAHs were determined by GC-MS using an HP6890 Series gas chromatograph interfaced with an HP5973 MS and fitted with a cool on-column injector. A Zebron column with a 5% phenyl polysiloxane film was used for the analyses (ZB5, 30 m x 0.25 mm id, 0.25 μm film thickness: Phenomenex, Cheshire, UK). The carrier gas was helium set at a constant flow of 0.7 ml min^{-1}. Injections were made at 50°C and the oven temperature held at this for 3 minutes. Thereafter the temperature was raised at 20°C min^{-1} up to 100°C. This was followed by a ramp of 4°C min^{-1} up to a final temperature of 270°C. The MS was set for selective ion monitoring (SIM) with a dwell time of 50 ms. A total of 29 ions plus the six internal standard ions were measured over the period of the analysis. Thus the analysis incorporated 2- to 6-ring, parent and branched PAHs (Table 3.1) (Webster *et al.*, 1997a; Topping *et al.*, 1997; Whittle *et al.*, 1997; Moffat *et al.*, 1998). The limit of detection was found to be less than 0.1 µg kg^{-1} for benzo[*b*]fluoranthene and less than 0.2 µg kg^{-1} for

benzo[*a*]pyrene. Recoveries of greater than 70% were achieved for sediments spiked to give a concentration of 1 μg kg^{-1} dry weight of individual PAHs (MLA SOP 1625).

Table 4.1. List of ions determined by GC-MS.

Polycyclic Aromatic Hydrocarbon (PAH)	**Molecular Weight/Da**				
	Parent PAH	Alkylated PAH			
		C_1	C_2	C_3	C_4
Naphthalene	128	142	156	170	184
Phenanthrene/Anthracene	178	192	206	220	
Dibenzothiophene	184	198	212	226	
Fluoranthene/pyrene	202	216	230	244	
Benzo[*c*]phenanthrene/Benz[*a*]anthracene/ Benz[*b*]anthracene Chrysene+Triphenylene	228	242	256		
Benzofluoranthene/benzo[*e*]pyrene/ benzo[*a*]pyrene Perylene	252	266	280		
Benzoperylene/Indenopyrene	276	290	304		
Acenaphthylene	152				
Acenaphthene	154				
Fluorene	166				
Dibenz[*a*,*h*]anthracene	278				

4.13 QUALITY ASSURANCE AND METHOD VALIDATION

The assessment of environmental impacts to the aquatic system by the oil and gas production is dependent on good quality analytical data, especially where detection levels are at very low concentrations, usually parts per billion (ppb). At these concentrations, the potential for contamination and adsorption losses are magnified and special care is required in all aspects of the handling and analysis. In order to support the PAH, total organic carbon and particle size analysis methods were accredited by the United Kingdom Accreditation Services (UKAS). As part of the procedures, items such as balances are calibrated against a known "check" weight and recorded before use to prove the accuracy of the balance (MLA SOP 240). Similarly all samples are stored at appropriate temperatures and deviations in these temperatures monitored automatically. In addition, all operation of instruments is recorded, allowing cleaning and maintenance to be carried out at the scheduled time.

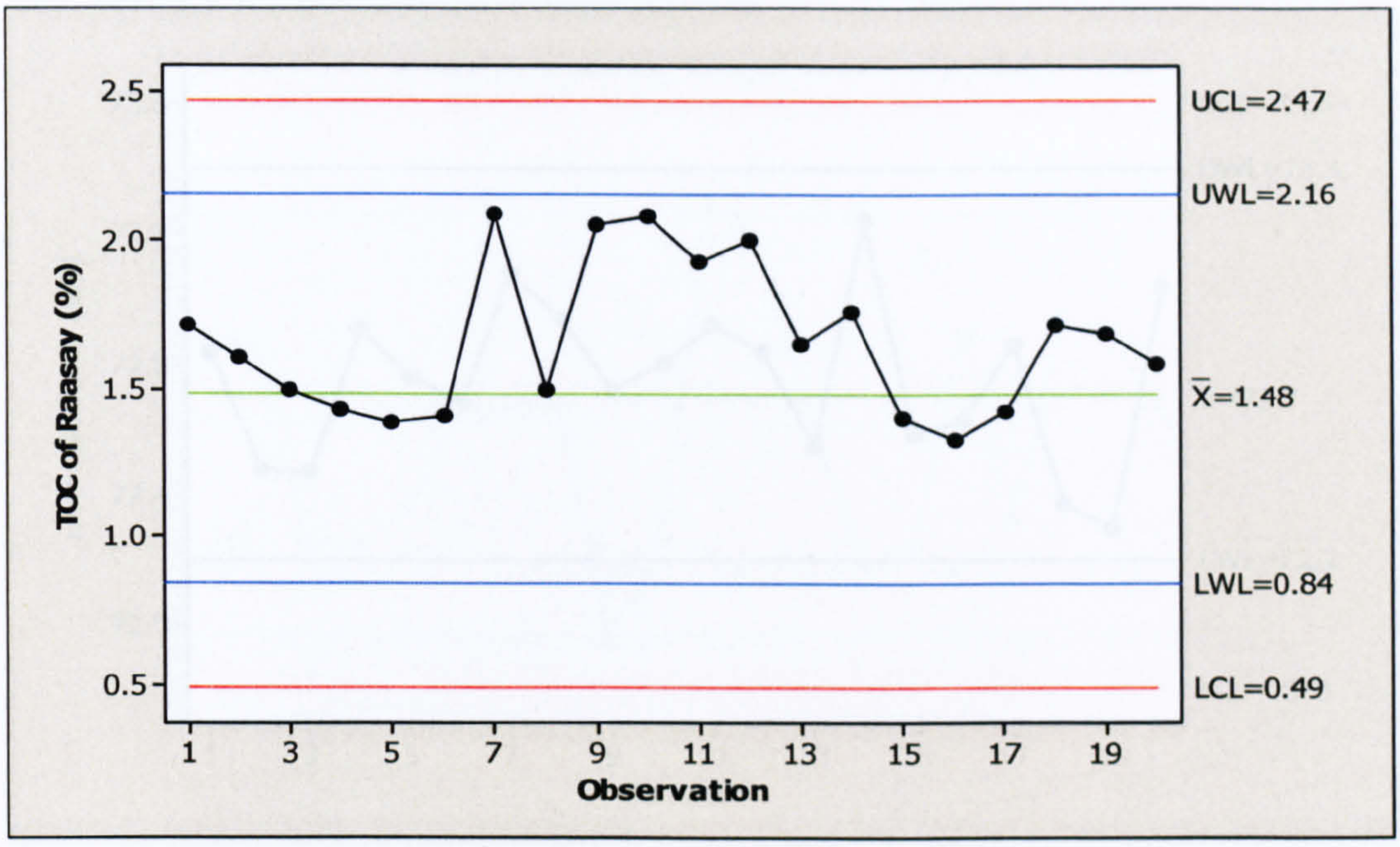

Figure 4.1 Shewhart charts of the LRM (Raasay) for the CHN analysis.

$\bar{x}$ = mean, LWL = lower warning line, UWL = upper warning line; LCL = lower control line; UCL = upper control line.

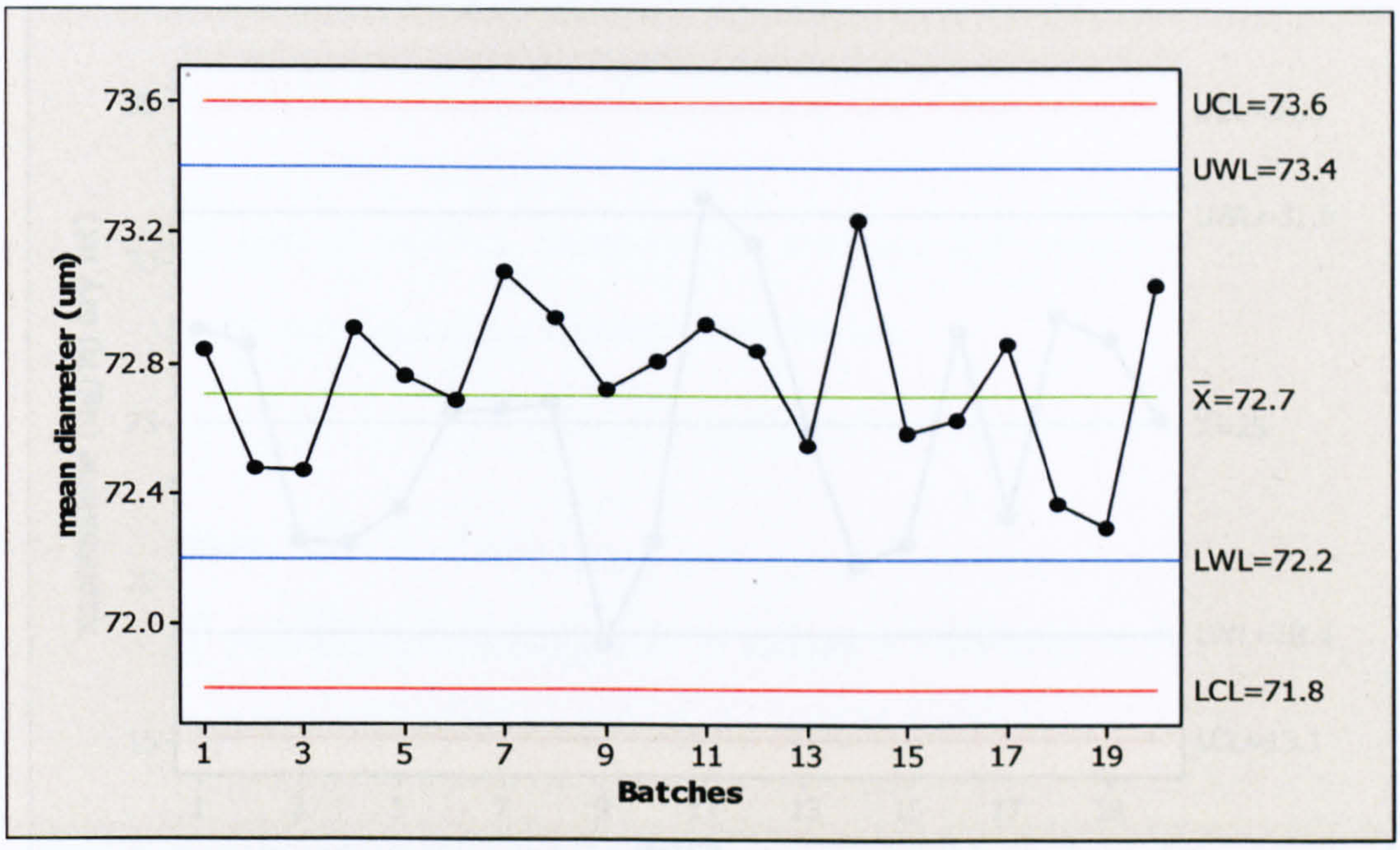

Figure 4.2 Shewhart charts of the LRM for the PSA,

$\bar{x}$ = mean, LWL = lower warning line, UWL = upper warning line; LCL = lower control line; UCL = upper control line.

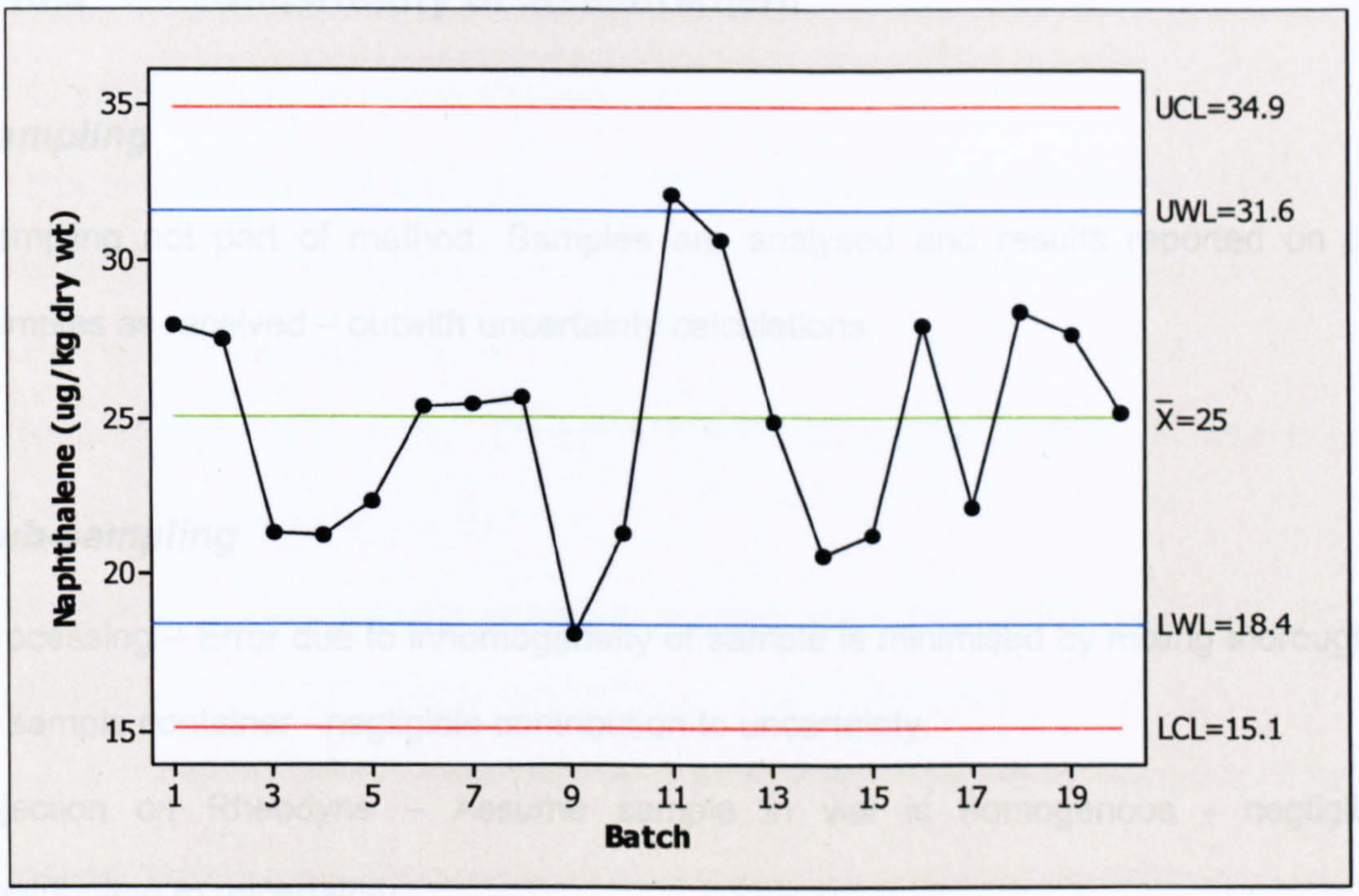

Figure 4.3 Shewhart charts of the LRM (142) for one of the compounds (Naphthalene) of PAHs,

$\bar{x}$ = mean, LWL = lower warning line, UWL = upper warning line; LCL = lower control line; UCL = upper control line.

Internal quality control procedures include the use of laboratory reference materials (LRM) and certified reference materials (CRMs) in each batch of samples. Procedural blanks were also analysed with each batch, and the concentrations adjusted accordingly. The data obtained from the LRM and CRMs were transferred onto NWA (Northwest Analytical) Quality Analyst and Shewhart charts produced with warning and action limits at ± 2 X and ± 3 X the standard deviation of the mean (Figures 4.1, 4.2 and 4.3). Data are used only if it passes the quality control values. Further quality control was assured through successful participation in the QUASIMEME (Quality Assurance of Information for Marine Environmental Monitoring in Europe) Laboratory Performance Studies (MLA SOP 1310).

4.13.a Uncertainty of Measurement

Sampling

Sampling not part of method. Samples are analysed and results reported on the samples as received – outwith uncertainty calculations.

Sub-sampling

Processing – Error due to inhomogeneity of sample is minimised by mixing thoroughly in sample container - negligible contribution to uncertainty.

Injection on Rheodyne – Assume sample in vial is homogenous - negligible contribution to uncertainty.

Injection on GC-MS – Assume sample in vial is homogenous – negligible contribution to uncertainty.

Storage

Samples are stored deep frozen to minimise degradation.

Reagent purity

All solvents are from Rathburn Chemicals and of at least HPLC Grade, considered sufficient – uncertainty accounted for in validation data.

Other chemicals are at least Analar quality, considered sufficient – uncertainty accounted for in validation data.

Chemical standards used in the preparation of calibration solutions are of the highest purity available at time of purchase. Final concentrations of the calibration solutions have been corrected for purity- uncertainty accounted for in the validation data.

Instrument effects

All syringes are solvent washed between samples.

Weight – Tolerance of balance – balances check weight tolerances 0.05% and 0.002%, 2, 3 and 4 decimal places used, sufficient for accuracy required. Uncertainty accounted for in validation data.

Volume – Pipettes used for calibration standards calibrated to < 1%. Uncertainty accounted for in validation data.

Temperature – Thermometer to measure rotary evaporator water bath temperature calibrated to < 1°C. Uncertainty accounted for in validation data.

Timer – Timer for HPLC flow calibrated to < 2 sec. Uncertainty accounted for in validation data.

Environmental conditions

Contamination is minimised by the use of dedicated accommodation, equipment and glassware for organic analysis. Glassware is also separated during cleaning – uncertainty accounted for in validation data.

Computational Effects

Integration of peaks by means of instrument software. Concentrations calculated by means of internal standard using instrument integrations. Manual checks of peak integrations are made for each sample, negligible contribution.

Blank Correction

A procedural blank is analysed with each batch of samples. No contribution to uncertainty.

Operator Effects

Only trained personnel may perform method unsupervised. Variations between operators are accounted for by control chart data. Uncertainty accounted for in validation data.

Random Effects

These will be accounted for by validation data.

4.13.b Precision of the Methods

The precision of an analytical method is the amount of scatter in the results obtained from multiple analyses of a homogeneous sample. The precision study was performed using the exact sample and standard preparation procedures. Two types of precisions were performed, the first type of precision studies comprise much of what historically has been called ruggedness. Intermediate precision (UKAS analytical precision) was the precision obtained when the assay is performed by multiple analysts, using multiple instruments, on multiple batches. Different sources of reagents and multiple lots of columns should also be included in this study. Intermediate precision results are used to identify which of the above factors contribute significant variability to the final result. The second type is repeatability or intra-assay precision. Intra-assay precision (calculated precision) data are obtained by repeatedly analysing, on one batch,

aliquots of a homogeneous sample, each of which has been independently prepared according to the method procedure.

The intermediate precision (UKAS analytical precision) was performed using the LRM samples; whilst the intra-assay (calculated precision) was performed using 4 replicates the sediment samples. The precisions were calculated using the coefficients of variance between the samples. Table 4.2 shows the results of the two precision types, UVF analysis (Forties crude and diesel oil) and aliphatic analysis (*n*-alkanes) are not UKAS accredited, therefore are not included in the intermediate precisions. The result shows that there was more precision in the intra-assay precision than the intermediate precision.

Table 4.2 Precisions of the UKAS accredited analyses and calculated analyses.

Analytical Method	UKAS Analytical Precision (%)	Calculated Precision (%)
CHN	2.5	0.8
PSA	2.5	1.6
Diesel oil	N/A	8.6
Forties crude oil	N/A	10.4
PAHs	20.0	9.8
n-alkanes	N/A	10.6

N/A = Not applicable.

CHAPTER FIVE

EFFECTS OF OIL EXPLORATION AND PRODUCTION IN THE FLADEN GROUND USING STRATIFIED RANDOM SAMPLING REGIME

5.1 BACKGROUND

The North Sea has been the focus of offshore oil and gas production over the past 30-40 years, with estimated reserves of ca 1267 million tonnes (9886 million barrels) of oil and condensate (DTI Brown Book, 2004). As a result of these activities, hydrocarbons have historically been discharged to the area during drilling, production and flaring operations. Since the amount of produced water increases as a field matures, present regulatory attention in the Convention for the Protection of the Marine Environment of the North-East Atlantic (OSPAR) is being directed towards a tighter control of this discharge, with permitted oil in water level < 40 mg/kg (ppm) (Wills and Sakhalina, 2000). In 2003, the industry average total oil in produced water in the North Sea was 20 mg/kg (DTI Brown Book, 2004a), Table 5.1 summarises the average amount of oil in produced water discharged "between" 1991 to 2003. One source of PAHs in the Fladen area of the North Sea, and indeed any other oil and gas exploration or production environment, is the flaring of unwanted gases. The incomplete combustion of these gases at the flarestacks on production platforms produces high temperature, pyrolytic polycyclic aromatic hydrocarbons (PAHs). Atmospheric discharges of hydrocarbons via fall out from inefficient flaring are difficult to assess. However, they are thought to be a relatively small proportion of the combined oil and gas inputs and indeed comprise only a small proportion of overall atmospheric input compared to other sources in UK (Van

den Hout, 1993; OSPAR, 2002). Figure 5.1 shows the volume of gas flaring "between" 1977 to 2002 in cubic meter per tonne of oil produced in the North Sea; an average of 14.135 cubic meters per tonne of oil produced was flared at offshore installations in 2002. The proportion of the gas flared to oil production fell during the mid 1980s. The rise thereafter was consequence of the Piper Alpha and subsequence safety work, it fell steeply in 1985, and continue to decline since then. The current low level of the gas flared reflects the increasing utilization of the gas produced as part of the oil production over the years, (DTI Brown Book, 2004b).

Table 5.1 Oil Discharged with Produced Water 1991 – 2003 (DTI Brown Book, 2004a). This data was last updated on: July 2004 and is due to be updated on: may 2005.

	1991	1992	1993	994	1995	1996	1997	1998	1999	2000	2001	2002	2003
Total Oil Discharged (tonnes)	5490	4850	4232	4418	5855	5706	5767	5692	5641	5395	5613	5590	5190
Total Water Discharged (million tonnes)	153	135	148	147	192	210	234	253	261	244	261	272	266
Number of Installations Permitted to Discharge Oil	39	43	46	52	55	60	64	64	73	68	74	74	85
Average Oil in Water Content (mg/kg)	35	36	28	30	30	27	25	22	21.5	21.5	21	21	20

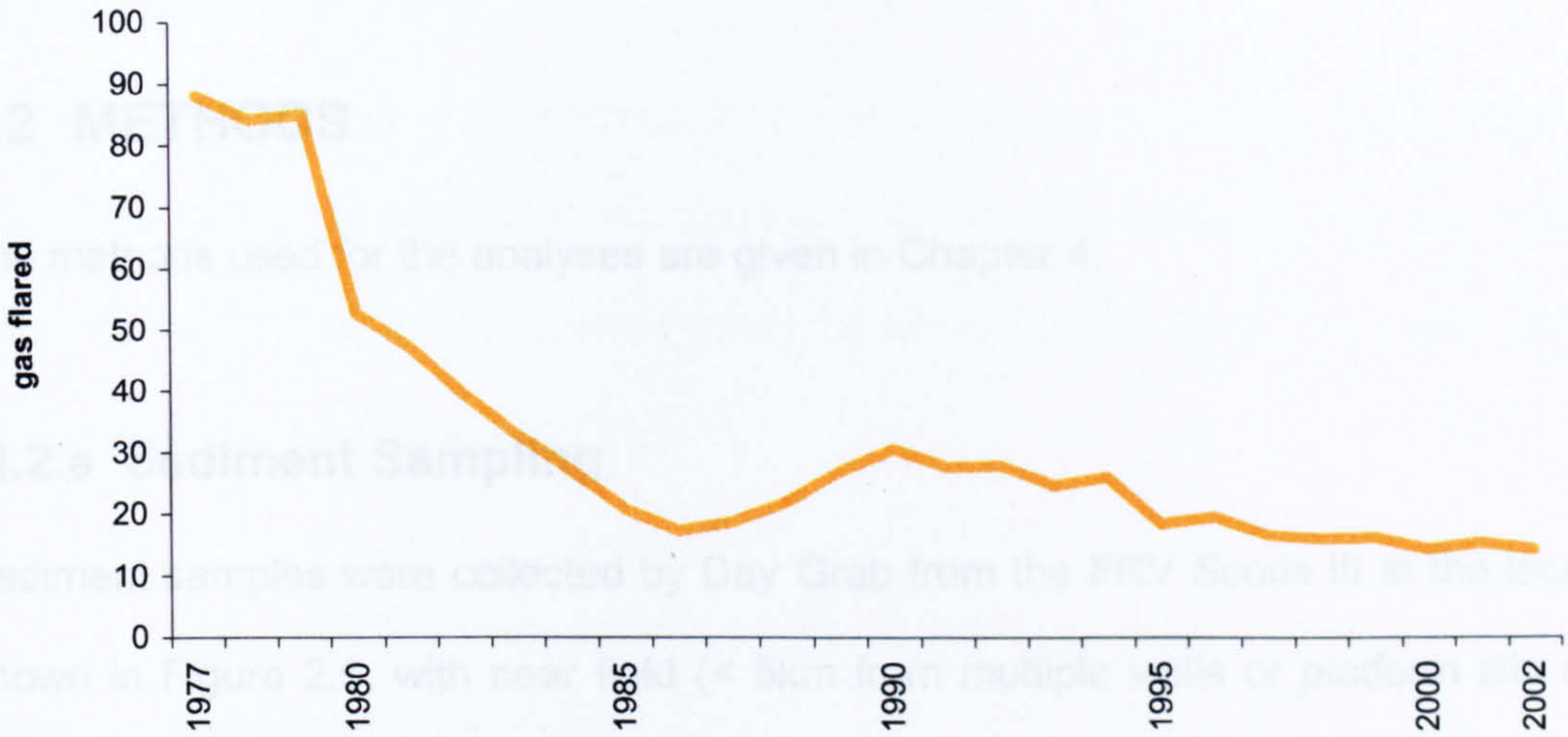

Figure 5.1 Gas Flaring relative to oil production, 1977 - 2002 in cubic metre per tonne of gas produced. Source: DTI Brown Book, 2004b

The Fladen Ground is situated approximately 160 kilometres north east of Aberdeen, Scotland in the northern part of the North Sea (Figure 2.1). It is an area of relatively deep water (120 – 150 metres) and is characterised by fine muds and high sediment organic carbon levels of between 0.5 and 1.8% (Bailey *et al.,* 1993). This results in generally increased levels of benthic productivity (Basford and Eleftheriou, 1989) that serve as the base of the food chain, culminating in abundant commercial fish and shellfish stocks. As a consequence, the Fladen Ground is one of the most intensively fished areas of the North Sea (Walsham *et al*., 2002; Russell *et al*., 2004).

There are three principal routes of water inflow to the northern North Sea; eastwards through the Fair Isle passage, southwards along east Coast of Shetland and southwards along western edge of the Norwegian Trench. The circulation pattern of the northern North Sea is influenced by the Atlantic inflow east of Shetland and the Fair Isle/Dooley current system and includes a semi-permanent cyclonic eddy over the Fladen Ground (Figure 2.1). The aim of this study is to assess the effects of oil

exploration and production in the Fladen Ground on sea bed sediments and to identify any areas of environmental concern using the developed stratified random design.

5.2 METHODS

The methods used for the analyses are given in Chapter 4.

5.2.a Sediment Sampling

Sediment samples were collected by Day Grab from the FRV *Scotia* III at the locations shown in Figure 2.5, with near field (< 5km from multiple wells or platform site and < 2km from a single well) and far field (> 5km from multiple wells or platform site and > 2km from a single well). All the samples were collected in the far-field area (5589.78km^2) out of total sampling area of 7295.59km^2 using the developed stratified random sampling regime. Two hundred and forty two (242) samples were collected in sixteen different Zones. The top 2 cm layer of sediment was scraped off each sample and the sediment was mixed before transferring (~200 g) to a solvent washed aluminium can which was labelled and stored at -20 ± 5°C until required for analysis. All sediments collected were analysed for ultra-violet fluorescence (UVF) oil equivalent concentrations, PAHs and *n*-alkanes while selected samples were analysed for steranes and triterpanes. Full details of the sampling locations are given in Appendix 1.

5.2.b Statistical Analyses

Data were analysed using the MINITAB® software version 14. Analysis of variance (ANOVA) at significance level of 5% was used to detect significant differences among the means of percentage of TOC, and PSA, and the oil equivalents of the Forties crude and diesel, PAHs and *n*-alkanes concentrations of the Zones. Spearman' Rank correlation was used to determine linear relationships among the parameters measured.

5.3 RESULTS AND DISCUSSION

5.3.a Data Summary

The data are tabulated in Appendices 2 - 7 and summarised in Tables 5.2, 5.3, 5.5 – 5.7 and 5.10 – 5.12. In particular, the summary tables give mean values with standard errors for the far-field in each Zone and for the whole far-field area. The mean value y_{st} for the whole far-field is estimated by

$$y_{st} = \frac{1}{A}\sum_{h=1}^{L} A_h y_h \qquad \text{Equation 5.1}$$

With the standard error $SE(y_{st})$

$$SE(y_{st}) = \frac{1}{A}\sqrt{\sum_{h=1}^{L}(A_h SE(y_h))^2} \qquad \text{Equation 5.2}$$

Where, y_h is the mean far-field value in Zone h, and $SE(y_h)$ is the standard error of the mean in Zone h, A_h is the far-field area in Zone h and A is the total far-field area.

5.3.b Physical and Chemical Characteristics of the Sediments

Physical characteristics of the sediment samples are tabulated in Appendix 2, summarised in Tables 5.1 and 5.2, and shown spatially in Figure 5.2. Percentage of the individual total organic carbon (TOC) varied between samples from 0.09 to 1.89%; mean TOC varied between Zones from 0.62 to 1.31%; and the mean TOC for the whole far-field was 0.91% (SE = 0.01%).

Table 5.2 Summary of percentage total organic carbon in dry weight sediments.

Zones	No of samples	Min	Mean	Med	Max	SD	CV	Var	S E
1	20	0.29	0.64	0.60	0.98	0.18	29.03	0.03	0.04
2	20	0.09	0.90	0.94	1.27	0.10	14.80	0.02	0.03
3	20	0.62	0.98	1.00	1.43	0.22	22.19	0.05	0.05
4	13	0.41	0.97	1.09	1.61	0.38	38.64	0.14	0.10
5	10	0.43	0.71	0.81	0.92	0.21	29.81	0.05	0.07
6	9	0.54	0.89	0.89	1.17	0.18	20.54	0.03	0.06
7	18	0.89	1.10	1.04	1.47	0.17	15.58	0.03	0.04
8	10	0.52	0.80	0.86	1.05	0.17	21.06	0.03	0.05
9	18	0.41	0.62	0.63	1.01	0.16	25.44	0.03	0.04
10	11	0.42	0.93	1.02	1.28	0.29	31.73	0.09	0.09
11	17	0.91	1.31	1.24	1.89	0.26	19.62	0.07	0.06
12	9	0.54	0.76	0.71	1.06	0.16	20.99	0.03	0.05
13	20	0.51	0.69	0.68	0.89	0.12	17.02	0.01	0.03
14	14	0.83	0.98	0.96	1.22	0.11	11.28	0.01	0.03
15	20	0.97	1.19	1.19	1.47	0.13	10.94	0.02	0.03
16	13	0.67	0.91	0.89	1.21	0.21	23.43	0.05	0.06
Total	242	0.09	0.91	N/A	1.89	0.20	23.35	0.04	0.01

Min = Minimum; Med = Median; Max = Maximum; SD = Standard Deviation;
CV = Coefficient of Variance; Var = Sample Variance; SE = Standard Error of the mean.

Since small size fractions contain mainly silt and clay minerals, and organic matter associated with these fractions are mainly humic substances absorbed onto mineral surfaces (Mayer, 1999). Using the particle size data, sediment samples were classified as coarse silts, sandy medium-coarse silts and fine sands. The percentage of the individual < 63 μm particle size (PSA) varied between samples from 25.1 to 89.0%; mean PSA varied between Zones from 48.9 to 85.7%; and the mean PSA for the whole far-field was 67.6% (SE = 0.8%).

Table 5.3 Summary of percentage < 63 µm fraction particle size (dry weight).

Zones	No of samples	Min	Mean	Med	Max	SD	CV	Var	SE
1	20	25.1	48.9	46.4	75.8	11.5	23.6	133.2	2.6
2	20	46.1	73.1	76.1	84.2	9.8	13.4	96.1	2.2
3	20	36.1	68.6	69.0	85.0	13.5	19.7	182.0	3.0
4	13	29.1	63.2	77.7	83.6	22.3	35.3	495.8	5.7
5	10	38.9	64.1	68.6	75.0	13.3	20.8	177.7	4.2
6	9	46.4	73.9	77.1	85.0	10.9	14.8	119.1	3.6
7	18	69.6	79.6	79.4	86.7	5.3	6.7	28.1	1.2
8	10	34.1	59.3	61.9	80.8	14.5	24.5	210.5	4.6
9	18	32.9	51.4	49.1	73.7	13.7	26.7	188.5	3.2
10	11	28.7	64.8	77.5	86.6	25.0	38.6	626.3	7.5
11	17	82.5	85.7	85.4	89.0	1.6	1.8	2.5	0.4
12	9	42.9	67.9	71.7	85.6	15.6	23.0	243.5	5.2
13	20	45.0	58.0	57.5	68.9	6.8	11.8	46.9	1.5
14	14	56.2	75.5	77.9	83.7	8.6	11.4	74.8	2.3
15	20	75.6	82.3	82.8	88.6	3.8	4.6	14.1	0.8
16	13	52.0	65.5	64.2	82.9	10.8	16.5	116.1	3.0
Total	242	25.1	67.6	N/A	89.0	10.9	17.3	152.5	0.8

Min = Minimum; Med = Median; Max = Maximum; SD = Standard Deviation;
CV = Coefficient of Variance; Var = Sample Variance; SE = Standard Error of the mean.

TOC and PSA were generally lowest in the west of the survey area (Zones 1, 5, 9, 13) and highest in the centre-east of the survey area (Zones 3, 7, 11, 15) (Figure 5.2).

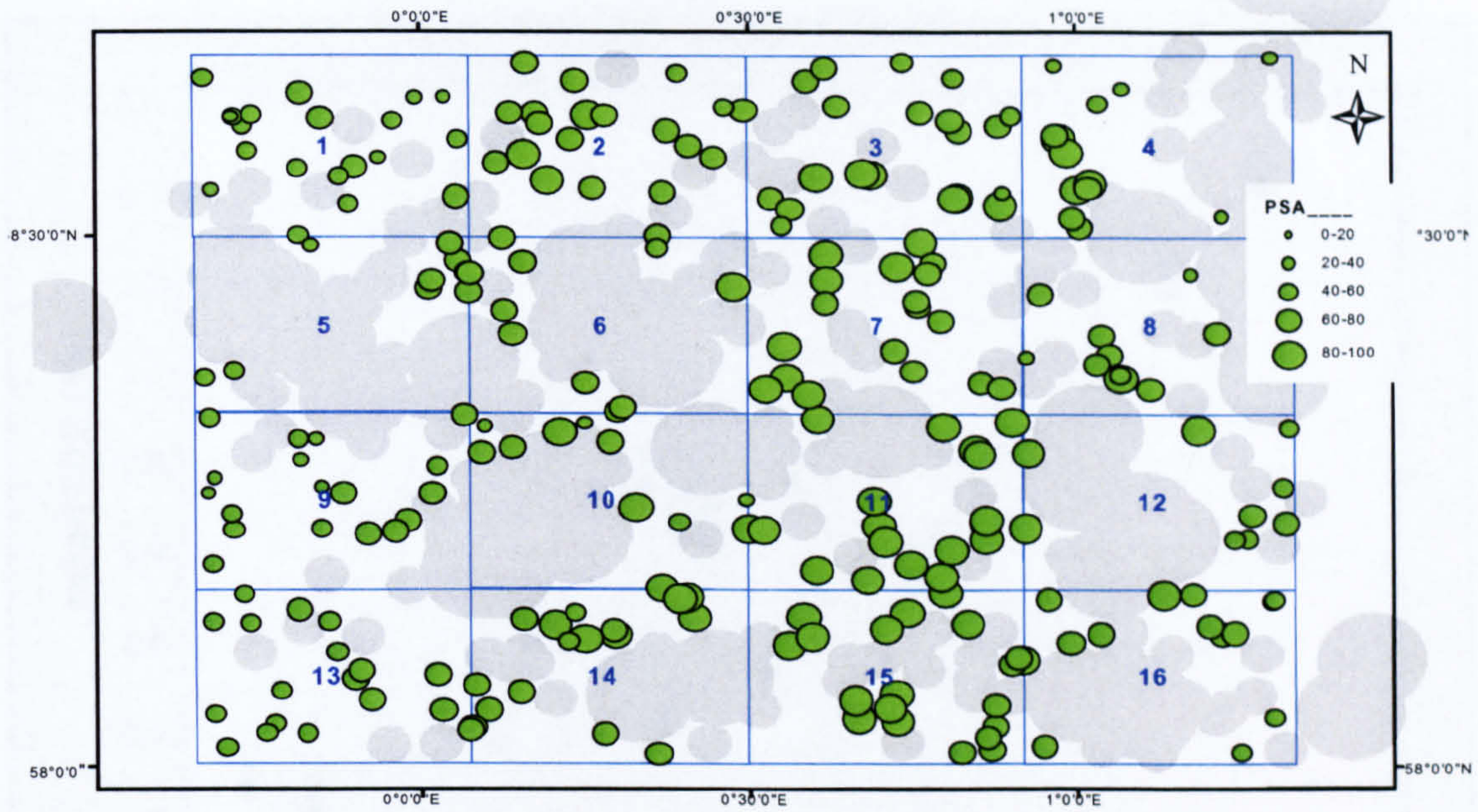

(a)

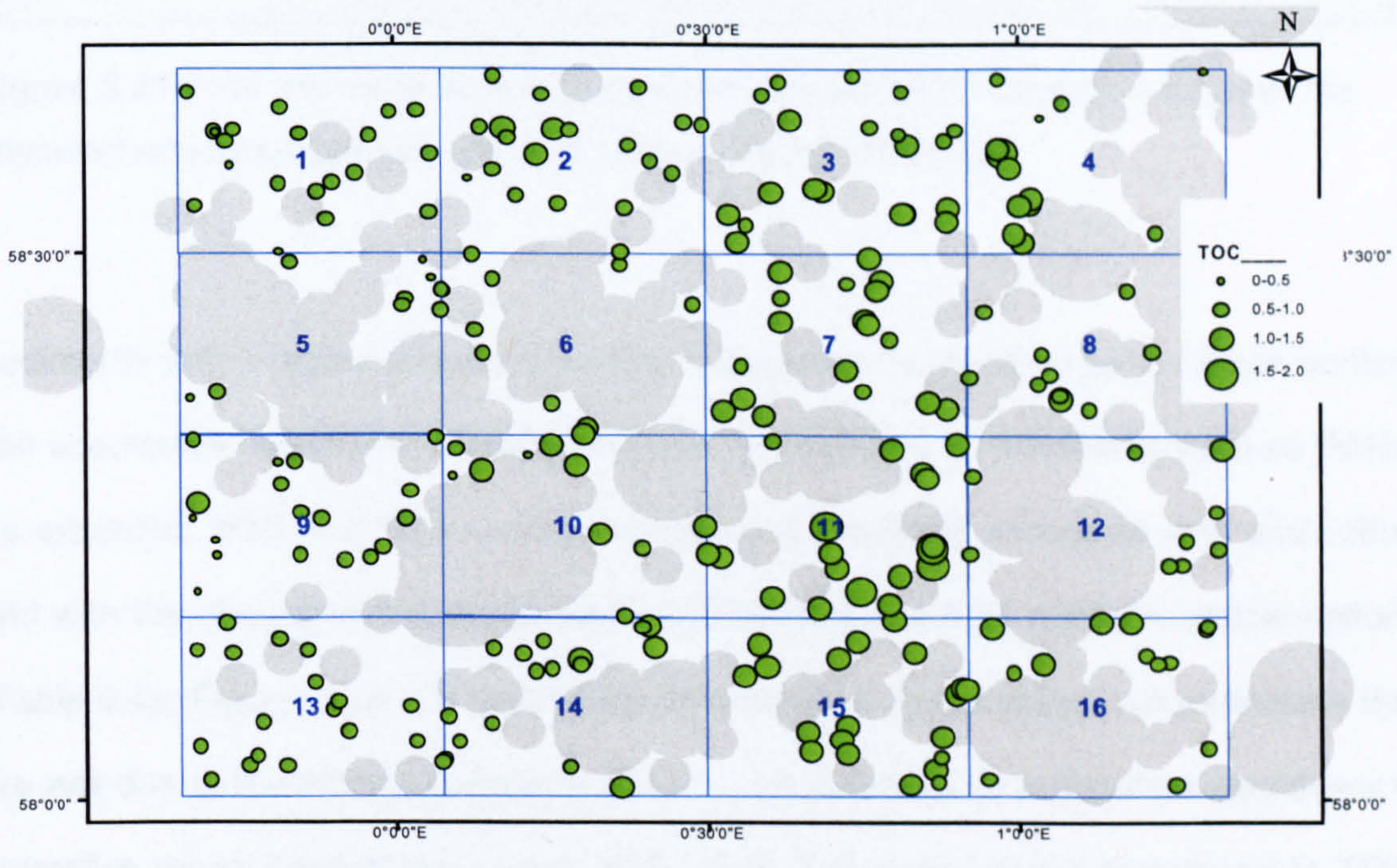

(b)

Figure 5.2 Spatial distribution of (a) particle size (< 63 μm [%]) and (b) total organic carbon (%). Large grey circles are < 5km radius of multiple oil wells and small grey circles are < 2km radius of a single oil well. Green circles are proportional to percentage content of particle size and TOC. Note the relationship between PSA & TOC especially the second column Zones from the right.

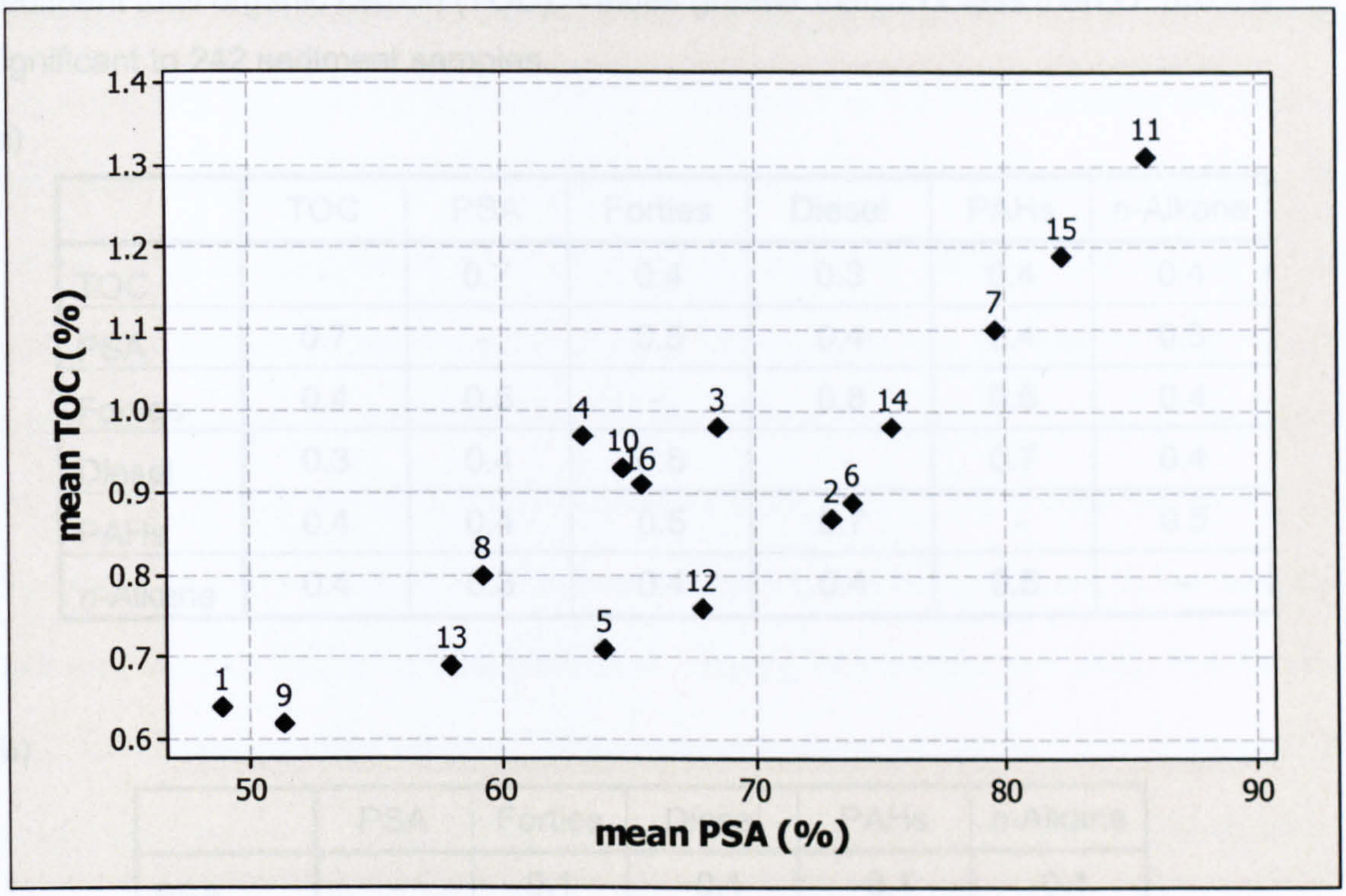

Figure 5.3 Plot of the mean zonal values showing significant correlation between the physicochemical properties, where numbers symbolised Zones.

Sediments with a higher proportion of fine material and a higher organic carbon content can accumulate significant concentrations of hydrophobic contaminants such as PAHs. As expected, TOC and PSA measurements were positively correlated with each other and with the corresponding oil equivalent, total PAH and total *n*-alkane concentrations (Table 5.4a, Figures 5.3). To investigate differences in hydrocarbon concentrations that are **not** due to the physical characteristics of the sediment, it is therefore necessary to normalise the concentrations to e.g. TOC. Note that, even having normalised to TOC, the oil equivalent, total PAH and total *n*-alkane concentrations are still positively correlated (Table 5.4b). This just means that, even having accounted for the physical characteristics of the sediment, samples with higher oil equivalent concentrations also tended to have higher total PAH and total *n*-alkane concentrations.

Table 5.4 Spearman' Rank correlation coefficient (a) Real data, (b) Normalised data to sediment total organic carbon (TOC). Values greater than 1 or less than -1 are 5% significant to 242 sediment samples.

(a)

	TOC	PSA	Forties	Diesel	PAHs	*n*-Alkane
TOC	-	0.7	0.4	0.3	0.4	0.4
PSA	0.7	-	0.5	0.4	0.4	0.3
Forties	0.4	0.5	-	0.8	0.5	0.4
Diesel	0.3	0.4	0.8	-	0.7	0.4
PAHs	0.4	0.4	0.5	0.7	-	0.5
n-Alkane	0.4	0.3	0.4	0.4	0.5	-

(b)

	PSA	Forties	Diesel	PAHs	*n*-Alkane
PSA	-	0.1	-0.1	-0.1	-0.1
Forties	0.1	-	0.7	0.5	0.4
Diesel	-0.1	0.7	-	0.7	0.5
PAHs	-0.1	0.5	0.7	-	0.5
n-Alkane	-0.1	0.4	0.5	0.5	-

5.3.c Ultra-Violet Fluorescence (UVF) Analysis

Ultraviolet fluorescence (UVF) determination is a rapid, low cost method for screening large numbers of samples. Estimates of 'total hydrocarbon' concentrations are expressed as 'oil' equivalents of crude (Forties crude) or diesel oil and can be used to select samples for more detailed analysis by GC-MS. Forties crude oil equivalents of around 50 μg g^{-1} dry weight are typical of muddy sediments (Walsham *et al.*, 2002; Russell *et al.*, 2004) in areas remote from oil and gas activity. Concentrations in offshore sediments above this background value are generally associated with offshore oil exploration and production activity.

All the sediments were screened for total hydrocarbons, using this method. The total hydrocarbons, measured as Forties crude oil equivalents and diesel oil equivalent concentrations are reported in Appendix 2. Tables 5.5 and 5.6 summarises the mean of the Forties crude and diesel oil equivalent concentrations in each of the Zones. The Forties crude oil equivalents were all below 'background' varying from 4.0 μg g^{-1} dry weight in a sample in Zone 4 to 41.2 μg g^{-1} dry weight in a sample in Zone 10. The mean Forties crude oil equivalent across the Zones ranged from 7.4 μg g^{-1} dry weight (SE = 0.4 μg g^{-1} dry weight, n = 20) in Zone 13 to 22.2 μg g^{-1} dry weight (SE = 1.7 μg g^{-1} dry weight, n = 17) in Zone 11. The mean Forties crude oil equivalent for the whole far field area was 13.8 μg g^{-1} dry weight (SE = 1.2 μg g^{-1} dry weight, n = 242). The diesel oil equivalents ranged from 1.6 μg g^{-1} dry weight in a sample in Zone 13 to 14.4 μg g^{-1} dry weight in a sample in Zone 8. The mean diesel oil equivalent across the Zones ranged from 2.2 μg g^{-1} dry weight (SE = 2.8 μg g^{-1} dry weight, n = 20) in Zone 13 to 7.0 μg g^{-1} dry weight in Zones 4 and 5 (SE = 0.2 and 0.6 μg g^{-1} dry weight, n = 13 and 10, respectively). The mean diesel for the whole far field area was 5.1 μg g^{-1} dry weight (SE = 0.4 μg g^{-1} dry weight, n = 242).

Table 5.5 Summary of UVF oil equivalent concentrations of Forties crude (μg g^{-1} dry weight).

Zones	Number of samples	Forties crude oil								Forties crude oil normalised to TOC							
		Min	Mean	Med	Max	SD	CV	Var	SE	Min	Mean	Med	Max	SD	CV	Var	SE
1	20	5.9	9.7	8.3	20.1	3.7	38.6	13.9	0.8	8.2	16.0	14.7	39.1	6.8	42.7	46.4	1.5
2	20	6.1	12.1	10.9	22.6	4.6	38.1	21.1	1.0	7.5	19.0	12.3	128.8	26.2	138.3	687.1	5.9
3	20	5.0	8.7	9.0	14.1	2.6	29.6	6.6	0.6	5.1	9.0	8.7	15.6	2.4	26.8	5.8	0.5
4	13	4.0	13.1	12.6	24.3	6.2	47.5	38.9	1.7	8.5	13.6	13.6	25.9	4.6	34.1	21.4	1.3
5	10	9.8	14.5	14.4	20.5	3.7	25.2	13.3	1.2	11.2	21.6	21.4	34.2	6.5	29.9	41.8	2.0
6	9	12.2	18.2	17.4	22.9	4.1	22.5	16.8	1.4	10.9	21.9	20.8	39.8	8.8	40.4	78.1	2.9
7	18	10.2	19.5	18.8	37.4	6.1	31.5	37.6	1.4	9.2	18.2	15.8	36.6	6.8	37.3	45.9	1.6
8	10	6.9	12.4	10.2	30.6	7.5	60.0	55.7	2.4	8.1	15.2	12.8	33.9	7.4	49.0	55.3	2.4
9	18	4.6	10.2	10.7	17.5	3.5	34.4	12.2	0.8	6.8	16.9	16.7	27.5	5.3	31.5	28.2	1.3
10	11	8.7	21.0	18.8	41.2	9.1	43.5	83.1	2.7	8.2	27.6	19.8	97.9	27.5	99.8	756.8	8.3
11	17	16.5	22.2	22.7	36.2	5.3	23.9	28.0	1.3	9.6	17.7	15.8	31.8	5.8	33.1	34.2	1.4
12	9	10.8	17.0	15.0	24.0	4.9	28.8	24.1	1.6	17.0	23.4	19.2	43.3	9.0	38.3	80.1	3.0
13	20	5.0	7.4	7.2	11.8	1.7	23.3	3.0	0.4	6.4	11.2	10.4	20.5	3.6	32.3	13.1	0.8
14	14	9.1	14.0	12.5	26.2	4.4	31.5	19.4	1.2	9.5	14.5	14.1	27.6	5.0	34.6	25.3	1.3
15	20	6.9	13.0	11.9	21.9	4.2	32.1	17.4	0.9	5.5	11.2	10.2	20.9	4.1	37.1	17.2	0.9
16	13	10.6	17.5	17.7	34.4	6.2	35.2	37.8	1.7	12.8	19.5	17.9	31.0	5.9	30.2	34.9	1.6
Total	242	4.0	13.8	N/A	41.2	4.6	34.1	24.5	0.3	5.5	16.3	N/A	128.8	8.03	45.9	113.4	0.7

Min = Minimum; Med = Median; Max = Maximum; SD = Standard Deviation; CV = Coefficient of Variance; Var = Sample Variance; SE = Standard Error of the mean.

Table 5.6 Summary of UVF oil equivalent concentrations of diesel (µg g^{-1} dry weight).

Zones	Number of samples	Diesel oil								Diesel oil normalised to TOC							
		Min	Mean	Med	Max	SD	CV	Var	SE	Min	Mean	Med	Max	SD	CV	Var	SE
1	20	3.1	5.0	4.6	10.7	1.8	37.0	3.4	0.4	4.3	8.2	7.7	19.4	3.4	41.5	11.7	0.8
2	20	3.0	6.2	5.8	10.6	2.2	35.0	4.7	0.5	4.0	9.7	6.3	65.2	13.2	136.7	174.8	3.0
3	20	3.1	4.5	4.6	7.1	1.1	23.5	1.1	0.2	2.9	4.7	5.0	7.6	1.2	25.5	1.5	0.3
4	13	2.4	7.0	6.7	12.7	3.0	42.9	9.0	0.8	4.7	7.4	7.1	13.5	2.4	32.1	5.7	0.7
5	10	4.2	7.0	7.1	9.4	1.8	26.0	3.3	0.6	5.0	10.4	10.2	15.4	3.2	30.3	10.0	1.0
6	9	3.3	5.2	4.8	6.5	1.2	22.3	1.4	0.4	3.4	6.3	6.1	12.0	2.7	42.5	7.2	0.9
7	18	3.4	5.8	5.6	7.9	1.2	19.9	1.3	0.3	3.3	5.4	5.1	7.9	1.5	27.7	2.3	0.4
8	10	4.4	6.6	5.6	14.4	3.0	44.9	8.7	0.9	5.1	8.0	7.2	16.0	3.1	38.8	9.7	1.0
9	18	1.7	3.3	3.3	5.2	1.0	29.9	1.0	0.2	2.7	5.5	5.4	8.2	1.4	26.4	2.1	0.3
10	11	3.0	6.1	5.9	12.2	2.6	42.2	6.7	0.8	2.8	8.4	6.0	29.0	8.1	96.1	65.0	2.4
11	17	4.8	6.5	6.6	10.2	1.4	21.2	1.9	0.3	3.5	5.2	4.6	9.0	1.6	30.9	2.6	0.4
12	9	3.7	5.0	4.7	6.7	1.2	23.2	1.4	0.4	4.7	6.9	5.9	12.4	2.4	35.1	5.9	0.8
13	20	1.6	2.2	2.2	3.2	0.4	19.8	0.2	0.1	2.0	3.4	3.2	5.5	1.0	30.5	1.1	0.2
14	14	2.7	4.6	4.6	7.0	1.2	25.8	1.4	0.3	2.8	4.7	4.8	7.4	1.2	26.3	1.5	0.3
15	20	1.9	4.0	3.9	6.1	1.0	24.9	1.0	0.2	1.5	3.4	3.1	5.7	1.0	30.2	1.1	0.2
16	13	2.9	5.3	5.2	10.0	1.7	30.9	2.7	0.5	3.9	6.0	5.4	9.0	1.7	27.6	2.8	0.5
Total	242	1.6	5.1	N/A	14.4	1.5	29.0	2.9	0.1	1.5	6.3	N/A	65.2	3.0	42.2	20.2	0.3

Min = Minimum; Med = Median; Max = Maximum; SD = Standard Deviation; CV = Coefficient of Variance; Var = sample Variance; SE = Standard Error of the mean.

(a)

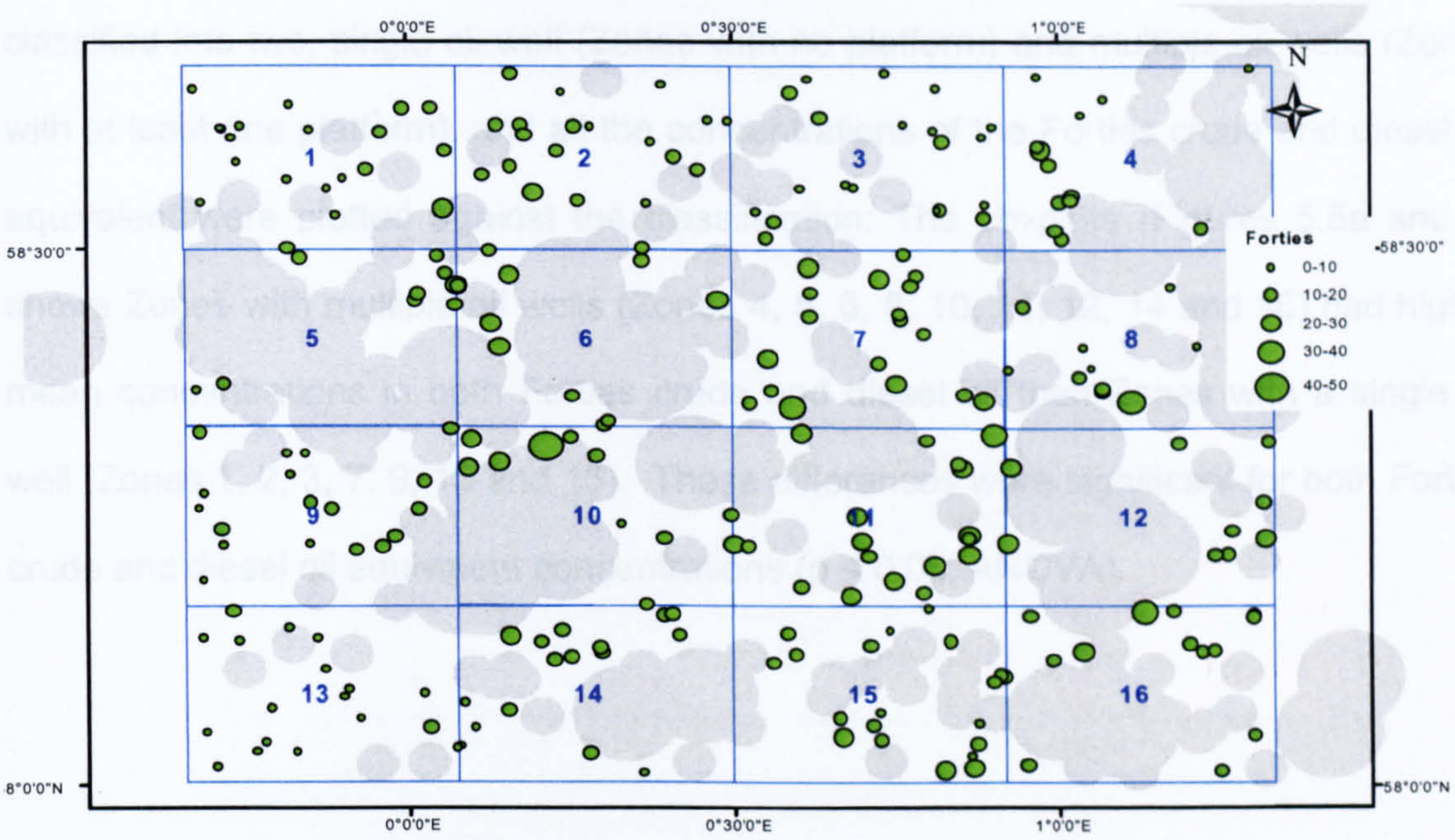

(b)

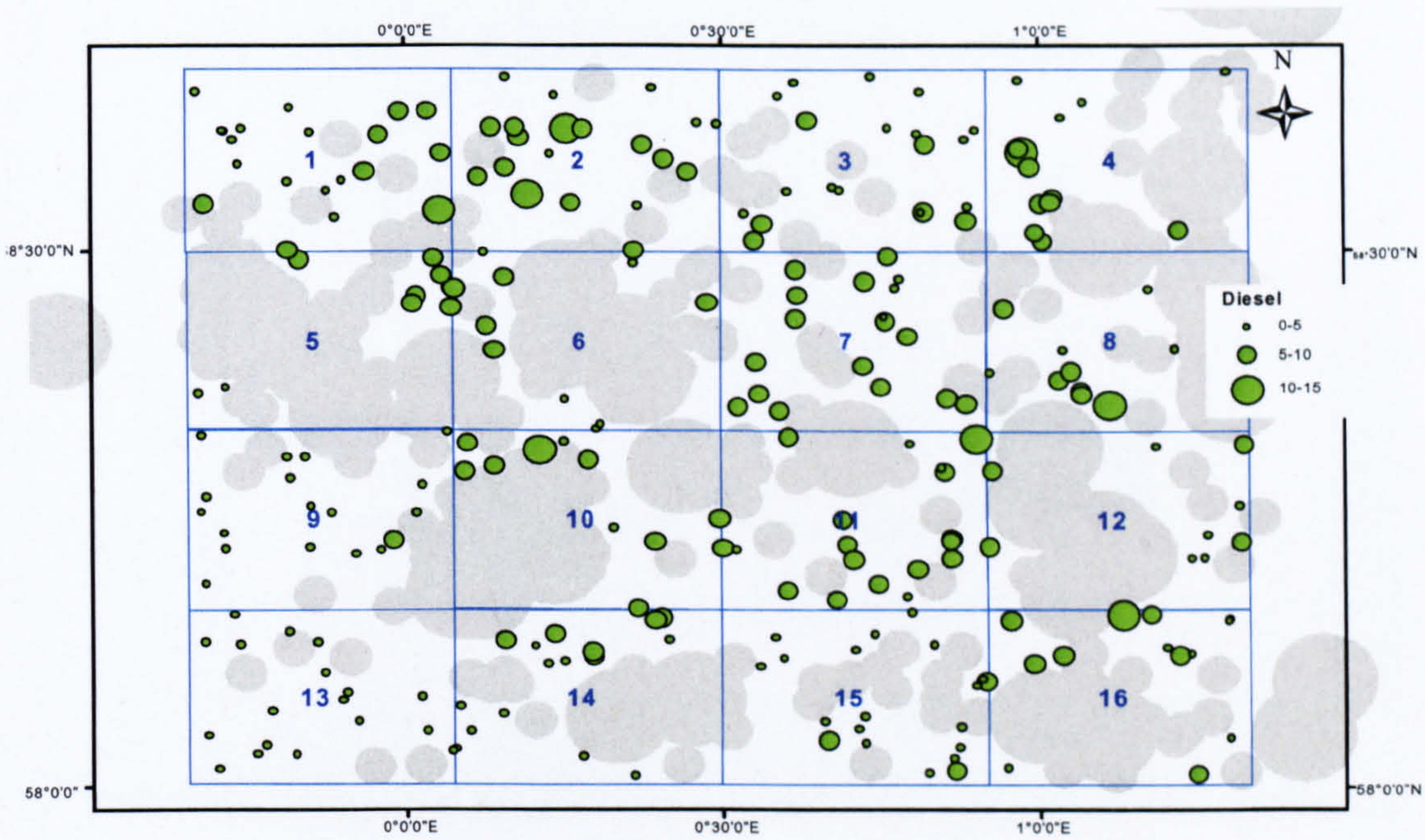

Figure 5.4 Spatial distribution of (a) Forties oil equivalent concentrations (μg g^{-1} dry weight) and (b) Diesel oil equivalent concentrations (μg g^{-1} dry weight). Large grey circles are < 5km radius of multiple oil wells and small grey circles are < 2km radius of a single well. Green circles are proportional to concentrations of Forties or diesel oil equivalents.

Higher Forties crude and diesel oil equivalent were found in Zones with fine sediment material and high organic carbon content (Figures 5.4a and b). The Zones are further classified into two, single oil well (Zones with no platform) and multiple oil wells (Zones with at least one platform), and all the concentrations of the Forties crude and diesel oil equivalent were plotted against the classification. The boxplots (Figures 5.5a and b) shows Zones with multiple oil wells (Zones 4, 5, 6, 8, 10, 11, 12, 14 and 16) had higher mean concentrations in both Forties crude and diesel oil than Zones with a single oil well (Zones 1, 2, 3, 7, 9, 13 and 15). These differences were significant for both Forties crude and diesel oil equivalent concentrations ($p < 0.05$; ANOVA).

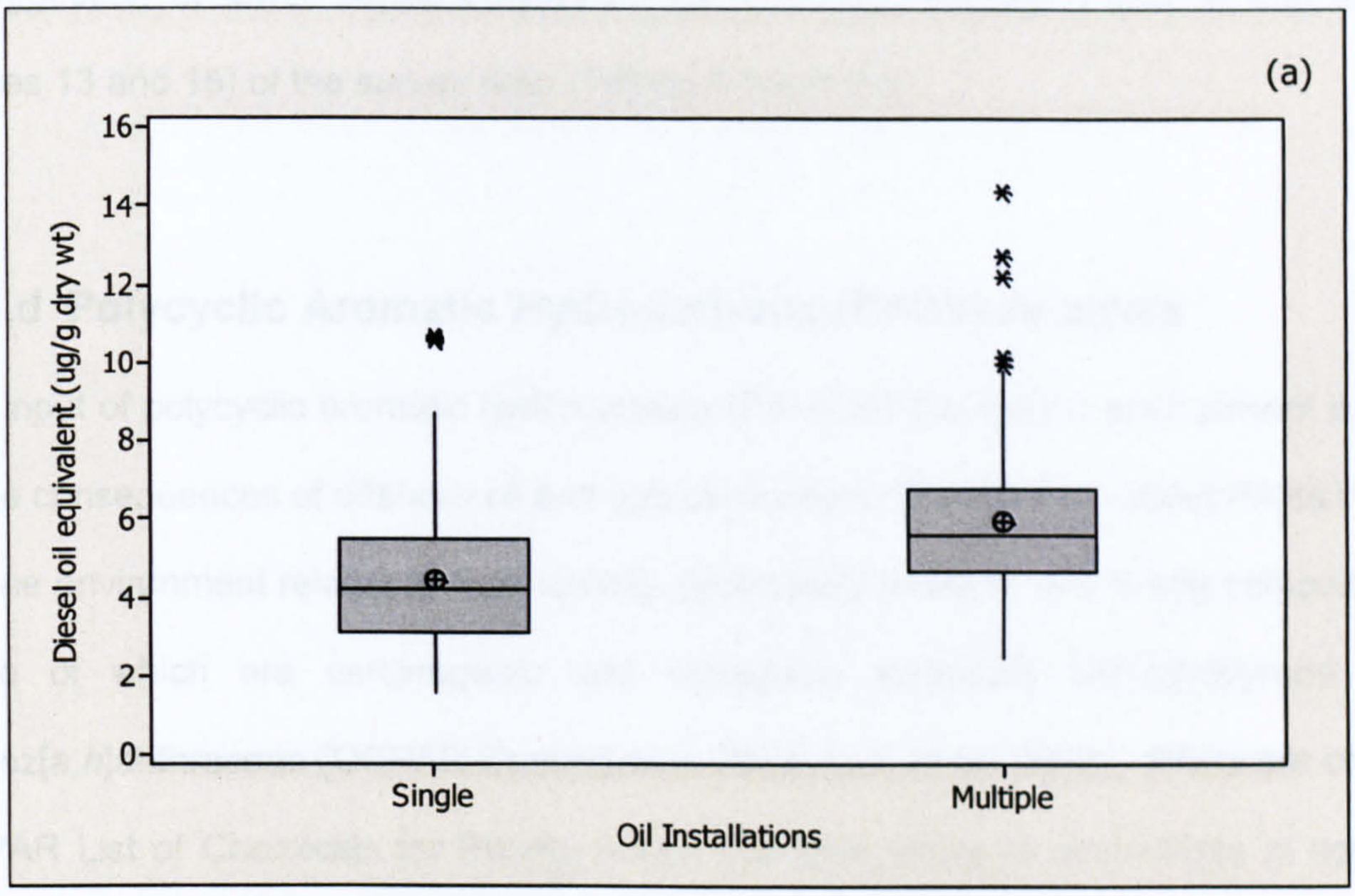

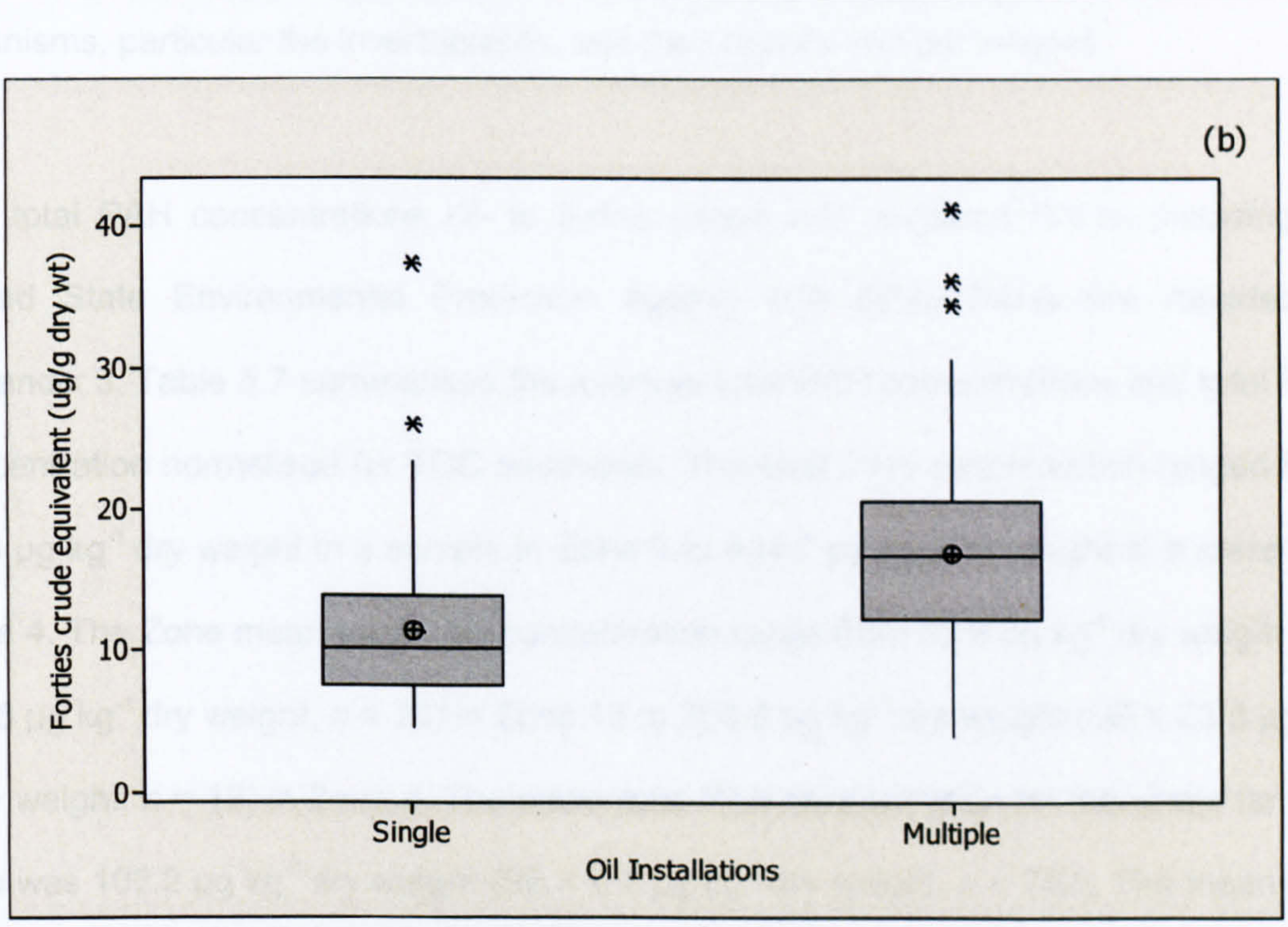

Figure 5.5 Boxplots showing oil equivalent (μg g^{-1} dry weight) for, (a) diesel oil and (b) Forties crude oil. The line within the box denotes the median and the symbol is the mean, the asterisk shows extreme values. Note Zones with multiple oil wells or platforms had mean Forties and diesel oil equivalents higher than Zones with single wells.

The oil equivalents, normalised for TOC, show no clear spatial pattern, although there is a suggestion of lower concentrations in the north-east (Zones 3 and 4) and south (Zones 13 and 15) of the survey area (Tables 5.5 and 5.6).

5.3.d Polycyclic Aromatic Hydrocarbons (PAHs) Analysis

The input of polycyclic aromatic hydrocarbons (PAHs) to the marine environment is one of the consequences of offshore oil and gas production. The concern about PAHs in the marine environment relates to their toxicity, particularly of the 5- and 6-ring compounds, some of which are carcinogenic and mutagenic especially benzo[*a*]pyrene and dibenz[*a,h*]anthracene (OSPAR Commission, 2002; Law *et al.*, 2002). PAHs are on the OSPAR List of Chemicals for Priority Action due their ability to accumulate in aquatic organisms, particular the invertebrates, and their toxicity and persistence.

The total PAH concentrations (2- to 6-ring parent and alkylated PAHs) including 16 United State Environmental Protection Agency (US EPA) PAHs are reported in Appendix 3. Table 5.7 summarises the average total PAH concentrations and total PAH concentration normalised for TOC sediments. The total PAH concentration ranged from 29.0 µg kg^{-1} dry weight in a sample in Zone 9 to 404.7 µg kg^{-1} dry weight in a sample in Zone 4. The Zone mean total PAH concentration range from 53.9 µg kg^{-1} dry weight (SE = 2.8 µg kg^{-1} dry weight, n = 20) in Zone 13 to 206.6 µg kg^{-1} dry weight (SE = 23.0 µg kg^{-1} dry weight, n = 13) in Zone 4. The mean total PAH concentration for the whole far field area was 108.2 µg kg^{-1} dry weight (SE = 9.2 µg kg^{-1} dry weight, n = 242). The mean total PAH concentrations varied widely between Zones; most of the PAHs were detected with only acenaphthylene, acenaphthene and fluorene being not detected in a few samples.

Table 5.7 Summary of the total PAHs concentrations in µg kg^{-1} dry weight (2- to 6-ring, parent and alkylated PAHs including 16 EPA). Total

Zones	Number of samples	Total PAH concentration								Total PAH concentration normalised to TOC							
		Min	Mean	Med	Max	SD	CV	Var	SE	Min	Mean	Med	Max	SD	CV	Var	SE
1	20	68.5	95.9	97.9	133.2	18.7	19.5	350.5	4.2	97.2	164.2	140.6	404.4	68.8	41.9	4730.9	15.4
2	20	52.0	94.6	93.3	161.3	30.3	32.0	917.6	6.8	63.7	135.4	102.5	700.1	136.1	100.5	18517.3	30.4
3	20	55.9	104.0	102.7	221.0	38.2	36.7	1460.8	8.5	67.4	106.9	95.5	167.5	31.4	29.4	985.4	7.0
4	13	96.1	206.6	214.1	404.7	83.0	40.2	6896.5	23.0	138.1	228.0	190.1	545.3	104.2	45.7	10849.8	28.9
5	10	84.1	133.9	122.6	269.2	52.5	39.2	2754.0	16.6	93.4	220.1	170.6	617.8	156.8	71.3	24595.0	49.6
6	9	55.4	89.1	79.0	128.5	23.4	26.2	546.2	7.8	47.2	108.3	98.0	238.9	53.7	49.6	2880.9	17.9
7	18	80.5	154.6	141.1	256.9	47.3	30.6	2233.1	11.1	79.2	144.5	138.8	264.4	45.8	31.7	2096.2	10.8
8	10	79.3	147.1	119.7	328.9	75.2	51.1	5655.2	23.8	129.3	180.2	151.8	364.6	74.7	41.4	5578.2	23.6
9	18	29.0	61.7	63.9	95.9	18.0	29.2	324.5	4.2	40.6	104.4	100.3	179.9	35.3	33.8	1243.5	8.3
10	11	53.0	107.0	102.5	146.2	27.0	25.3	731.1	8.2	50.2	125.7	108.0	347.4	84.6	67.3	7154.0	25.5
11	17	94.8	137.2	132.2	184.5	23.8	17.4	568.6	5.8	70.1	108.7	104.0	168.7	29.3	26.9	857.7	7.1
12	9	44.5	87.0	86.8	147.8	31.5	36.2	993.1	10.5	70.0	116.7	103.8	176.2	40.1	34.4	1609.4	13.4
13	20	32.6	53.9	54.9	82.0	12.7	23.5	160.5	2.8	42.9	81.9	78.6	141.9	27.4	33.5	751.0	6.1
14	14	55.5	81.6	71.5	180.6	32.5	39.8	1055.7	8.7	50.6	84.5	76.0	189.8	35.2	41.7	1240.2	9.4
15	20	60.1	95.5	90.2	142.1	22.4	23.5	503.7	5.0	55.7	80.8	73.2	118.8	19.8	24.5	392.5	4.4
16	13	47.9	88.1	76.0	169.7	38.5	43.7	1481.3	10.7	48.1	100.4	95.8	245.9	50.6	50.4	2562.3	14.0
Total	242	29.0	108.2	N/A	404.7	34.9	31.3	1595.6	2.7	40.6	128.5	N/A	700.1	59.2	43.8	4952.3	4.6

PAH = Sum of (total naphthalene + total 178 + total DBTs + total 202 + total 228 + total 252 + total 276 + acenaphthylene + acenaphthene + fluorene + dibenz[a,h]anthracene). Numbers represents ions monitored for that group of compounds (see appendix 5). Min = Minimum; Med = Median; Max = Maximum; SD = Standard Deviation; CV = Coefficient of Variance; Var = Sample Variance; SE = Standard Error of the mean.

The sample with the highest total PAH concentration, also contained higher total *n*-alkane concentration (314.3 µg kg^{-1} dry weight), Forties crude oil equivalent (24.3 µg g^{-1} dry weight) and diesel oil equivalent concentrations (12.7 µg g^{-1} dry weight). This sample was situated in a Zone with multiple wells (Zone 4) and was characterised with fine sediment (83.6% of the < 63 µm fraction) and high organic carbon content (1.61%). The sample with the lowest concentration was situated in a Zone with a single well (Zone 9). This sample had lower total *n*-alkane concentrations (44.2 µg kg^{-1} dry weight), Forties crude oil equivalent (4.6 µg g^{-1} dry weight) and diesel oil equivalent (1.9 µg g^{-1} dry weight), and was characterised as sandy sediment (44.2% of the < 63 µm fraction) with low organic content (0.48%).

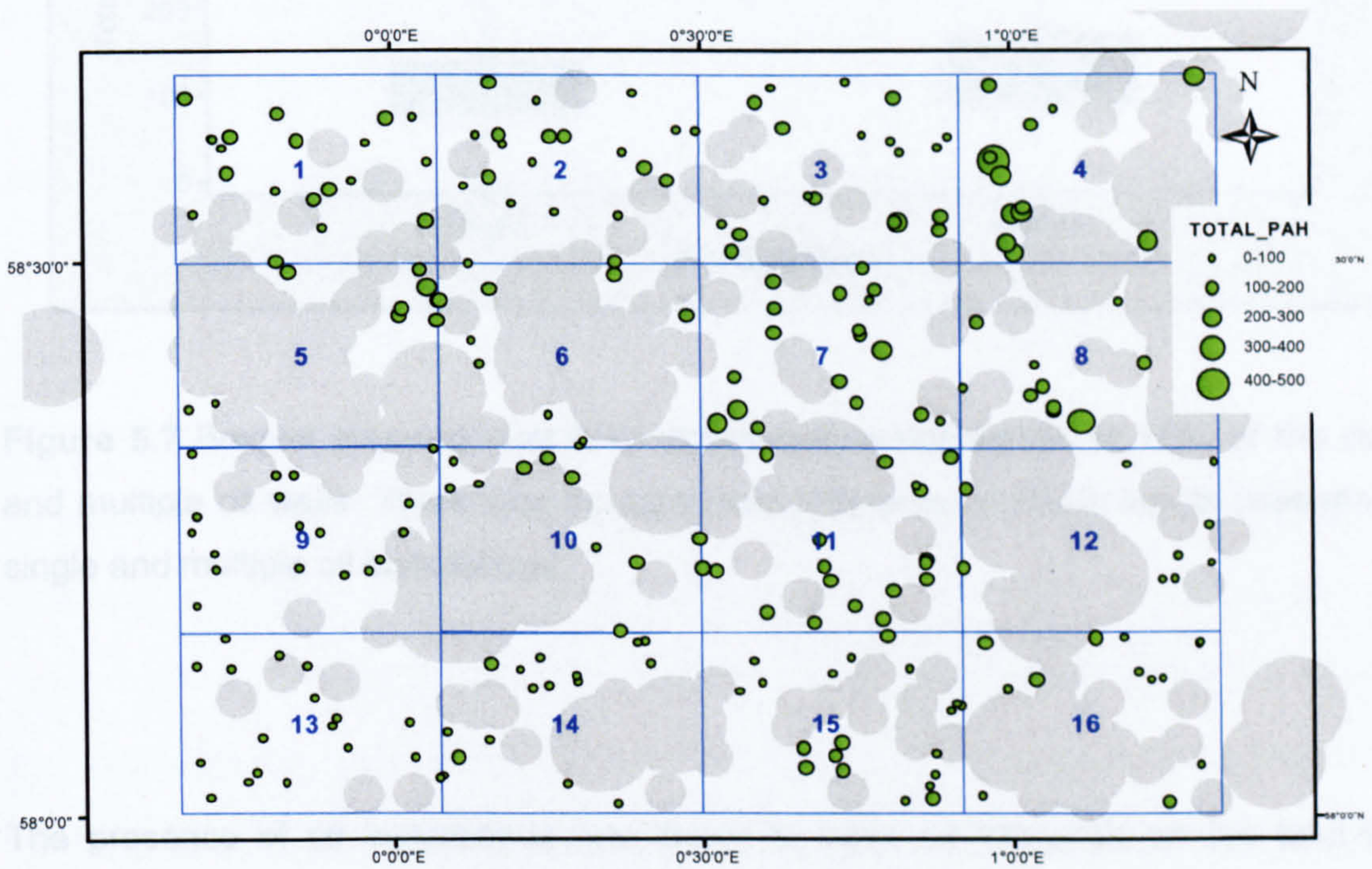

Figure 5.6 Spatial distribution of PAHs (µg kg^{-1} dry weight), showing higher total PAH concentrations in Zones with higher organic carbon and proportion of the < 63 µm particle size. Also samples close to oil platform have high total PAHs concentration value. Large grey circles are < 5km radius of multiple oil wells and small grey circles are < 2km radius of a single oil well. Green circles are proportional to concentrations.

Significantly higher mean total PAH concentrations (> 100 µg kg^{-1} dry weight) were found in sediments in Zones with multiple oil wells ($p < 0.05$; ANOVA) (Figure 5.6) and/or more muddy character with a high organic content (> 0.98%). However, there was no significant difference in the boxplot of the normalised data with TOC between the overall single and multiple oil installations (Figure 5.7).

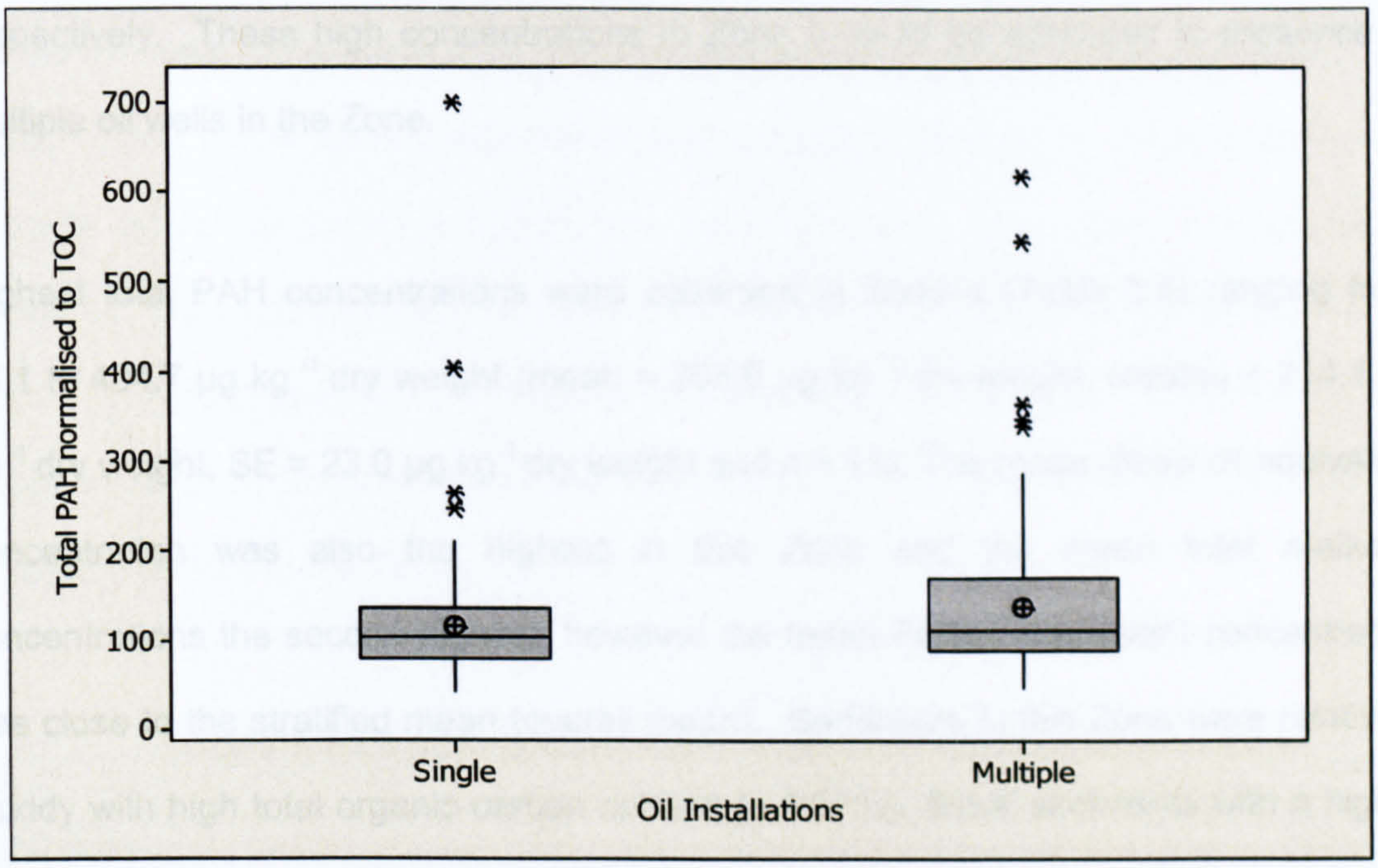

Figure 5.7 Boxplot showing total PAH concentration normalised to TOC of the single and multiple oil wells. There was no significant difference in PAHs inputs between the single and multiple oil installations.

The presence of oil installations was found to have an influence on the total PAH concentrations observed in the eastern Zones of the Fladen Ground (Zones 1, 5, 9 and 13). Also similar results were observed in both Forties crude and diesel oil equivalent concentrations in those vertical Zones. These Zones had similar lower values of both percentage fraction size (48.9 – 64.1%) and organic carbon content (0.62 - 0.71%) (Figures 5.2a and b). However, the mean total PAH concentration (133.9 µg kg^{-1} dry

weight), Forties crude (14.5 μg g^{-1} dry weight) and diesel oil equivalent (7.0 μg g^{-1} dry weight) in Zone 5 were higher than their overall means (stratified mean) (Tables 5.4, 5.5 and 5.6). Also the means were significantly different from the rest of the Zones ($p < 0.05$; ANOVA). As Zones 1, 9 and 13 all had single oil well installation, and all had mean values less than 100 μg kg^{-1} dry weight for total PAH concentrations, 10.5 μg g^{-1} dry weight for Forties crude and 5.1 μg g^{-1} dry weight for diesel oil equivalents, respectively. These high concentrations in Zone 5 could be attributed to presence of multiple oil wells in the Zone.

Highest total PAH concentrations were observed in Zone 4 (Table 5.5) ranging from 96.1 to 404.7 μg kg^{-1} dry weight (mean = 206.6 μg kg^{-1} dry weight, median = 214.1 μg kg^{-1} dry weight, SE = 23.0 μg kg^{-1} dry weight and n = 13). The mean diesel oil equivalent concentration was also the highest in this Zone and the mean total *n*-alkane concentrations the second highest, however the mean Forties equivalent concentration was close to the stratified mean (overall mean). Sediments in this Zone were relatively muddy with high total organic carbon content (> 0.97%). Since sediments with a higher proportion of fine material and a higher organic carbon content have the potential to accumulate significant concentrations of hydrophobic contaminants such as PAHs. Difference in PAH concentrations between Zones were investigated by a mixture of graphical and multivariate techniques. Throughout, total PAH concentration were normalised by the TOC content, to account for the increased accumulation of PAHs by the sediments with high carbon content. The mean total PAH concentration (normalised for TOC) at each Zone, together with the 95% confidence limits on the mean, is shown in Figure 5.8. Significant difference is declared for each of Zone, if and only if their intervals do not lap. The results of the normalised data shows that Zone 4 remained the highest in the Fladen ground with a range of 138.1 to 545.3 μg kg^{-1} dry weight normalised to TOC (mean = 228.0 μg kg^{-1} dry weight normalised to TOC, median =

190.1 µg kg $^{-1}$ dry weight normalised to TOC, SE = 28.9 and *n* = 13; Table 4.7). There are clearly significant differences in total PAH concentration between the north-east Zones (Zones 4 and 8) and the Zones in the south of the Fladen Ground (Zones 13-16) ($p > 0.05$; ANOVA). However, there were no significant differences in the upper top of the survey area (Figure 5.8). The PAHs input were generally higher in the north of the survey area, and lower in the south of the survey area, in particularly, southern end of the survey area. The graph also had shown a diagonal relationship in the mean PAH concentration of the Zones, with mean concentrations decreasing down easterly and westerly except for Zones 2 and 5, and Zones 3 and 8, were mean concentrations increases. These differences can readily be attributed to the circulation pattern in the Fladen Ground (Figure 2.1). Therefore, the accumulation of PAHs may be due to a higher input of hydrocarbon, and the sediment type, and generally, influence by the circulation pattern in the Fladen Ground.

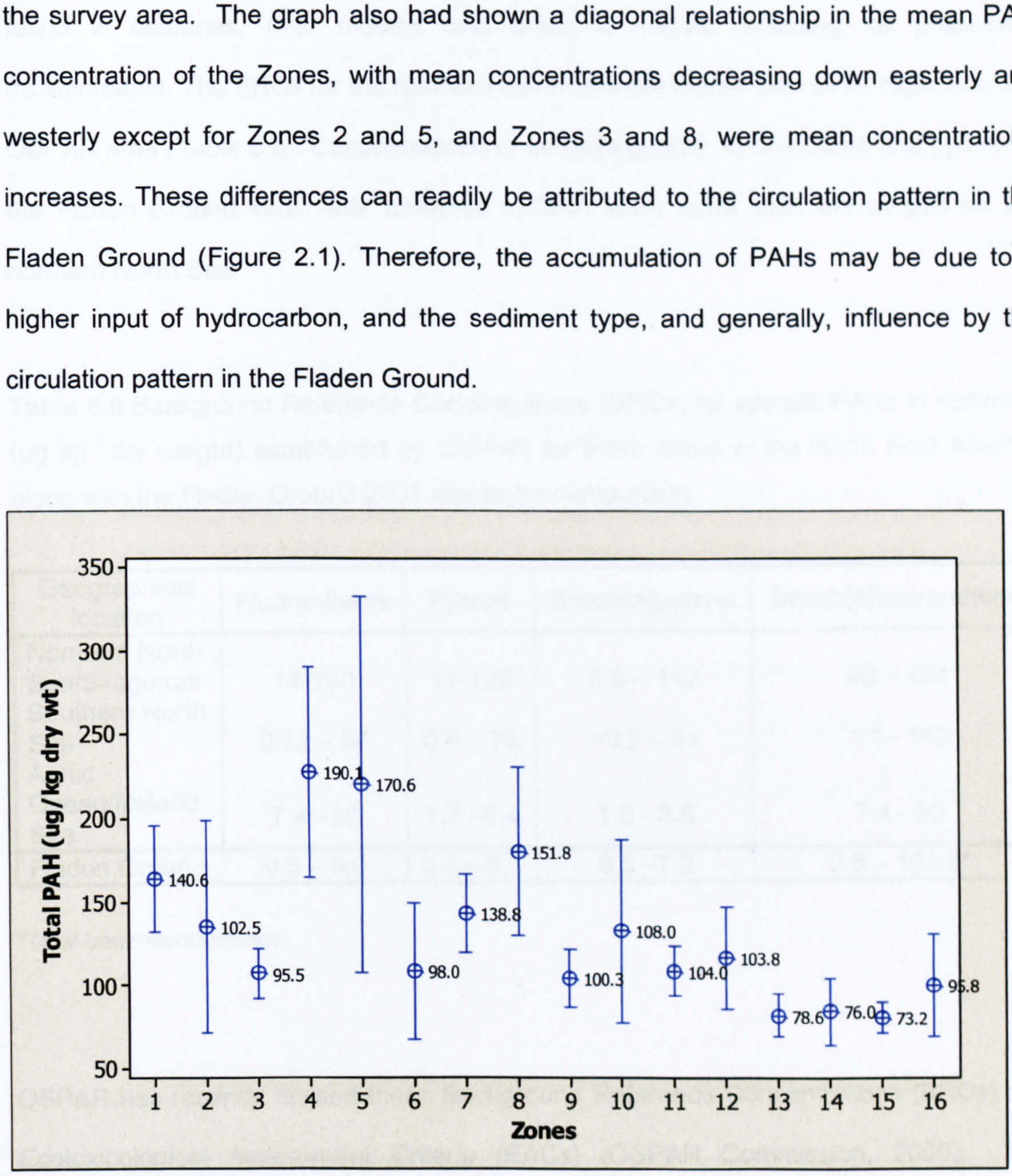

Figure 5.8 The mean total PAH concentration (normalised for TOC) at each Zone, together with 95% confidence limits on the mean.

5.3.e Comparison to Background Reference Concentrations (BRCs)

The Oslo and Paris Commission (OSPAR) previously established Background Reference Concentrations (BRCs) and Ecotoxicological Assessment Criteria (EACs) to assess chemical monitoring data and identify areas of environmental concern (OSPAR Commission, 2000). BRCs are the typical range of concentrations found in OSPAR area (north-east Atlantic). The highest PAH concentrations in sediments are normally found in estuaries, river mouths and areas of regular shipping, oil production transportation. The BRCs for the northern North Sea are higher than other regions in the OSPAR area (Table 5.8). Concentrations of benzo[*a*]pyrene, fluoranthene and pyrene in the Fladen Ground sediments collected in 2001 were lower than the ranges for the northern North Sea.

Table 5.8 Background Reference Concentrations (BRCs) for specific PAHs in sediment (μg kg^{-1} dry weight) established by OSPAR for three areas in the North East Atlantic, along with the Fladen Ground 2001 values for comparison.

Geographical location	Fluoranthene	Pyrene	Benzo[*a*]pyrene	Benzo[*b*]fluoranthene
Northern North Sea/Skagerrak	14-160	11-128	8.8 – 112	46 – 434
Southern North Sea	0.72 – 97	0.6 – 78	<0.2 – 51	1.1– 142
Arctic Ocean/Iceland Sea	7.4 –30	1.7 –6.4	1.0 - 3.8	7.4 - 30
Fladen Ground	0.5 – 9.0	0.3 – 6.1	0.5 –7.2	2.8 – 101.9*

*Total benzofluoranthene

OSPAR has recently revised these Background Reference Concentrations (BRCs) and Ecotoxicological Assessment Criteria (EACs) (OSPAR Commission, 2005). The terminology for BRCs has been changed to Background Concentrations (BCs) and

EACs have been changed to Environmental Assessment Criteria. For naturally occurring substances, such as PAHs, BCs are the typical ranges of concentrations found in uncontaminated waters in the OSPAR area (North-East Atlantic). To assess whether concentrations are near background or close to zero a statistical method using Background Assessment Criteria (BACs) was developed. OSPAR has established provisional BACs for PAHs in sediment, normalised to 2.5% organic carbon to determine whether concentrations in a particular area are close to background (Table 5.9). To enable this comparison, individual PAH concentrations in the Fladen Ground were normalised to 2.5% organic carbon and the mean and 95% confidence limits $(\bar{y}_h \pm 1.645SE)$ calculated, where $\bar{y}_h$ is mean for h^{th} Zone and SE is the standard error. The upper bound concentration for the overall Fladen Ground for the ten PAH, for which BACs have been established (naphthalene, phenanthrene, anthracene, fluoranthene, pyrene, benz[*a*]anthracene, chrysene, benzo[*a*]pyrene, indenopyrene and benzoperylene), were below the provisional BACs in the Fladen area (Table 5.9). Along the Zones, Zone 1 had the highest naphthalene mean and upper bound limit value (8.4 and 10.7 µg kg^{-1} dry weight, normalised to 2.5% organic carbon) higher than the BAC naphthalene value, also Zone 8 had chrysene/triphenylene close to provisional BAC chrysene value. The Provision BAC established were generally lowest in the north of the survey area (the Fladen Ground), in particular Zones 13, 14, 15 and 16. The highest were in Zones 4, 5 and 8, and this is in consistent with the amount of hydrocarbon observed in the Forties crude and diesel oil equivalent concentrations.

Table 5.9 Provisional Background Assessment Criteria (BACs) for specific PAHs in sediment (μg kg^{-1} dry weight) normalised to 2.5% organic carbon established by OSPAR. The mean PAH concentration ranges (normalised to 2.5% organic carbon) for the Fladen Ground has been included for comparison. The figures in brackets are the 95% upper confidence bound.

	Nap	Phe	An	Fl	Py	B[*a*]An	Chr	B[*a*]Py	Bper	Ind
BC	5	17	3	20	13	9	11	15	45	50
Provisional BAC	8	32	5	39	24	16	20	30	80	103
Zone 1	8.4 (10.3)	6.3 (6.4)	0.9 (1.1)	7.9 (8.5)	5.5 (5.9)	3.9 (4.2)	7.8^ (8.3^)	7.2 (7.6)	48.3 (51.1)	51.3 (54.2)
Zone 2	1.7 (1.9)	5.3 (5.9)	0.4 (0.5)	6.9 (7.7)	4.7 (5.4)	3.7 (4.2)	6.7^ (7.5^)	6.3 (7.1)	40.9 (47.6)	45.7 (52.9)
Zone 3	1.7 (1.8)	3.6 (3.8)	0.5 (0.5)	3.6 (4.0)	3.4 (3.6)	3.5 (3.6)	5.2^ (5.4^)	4.9 (5.1)	28.4 (29.5)	37.6 (39.0)
Zone 4	3.1 (3.6)	9.2 (10.4)	1.1 (1.4)	13.5 (15.4)	8.3 (9.1)	8.0 (9.0)	12.1^ (13.6^)	9.7 (10.8)	56.8 (60.1)	79.0 (84.0)
Zone 5	4.5 (5.4)	8.6 (9.8)	1.0 (1.1)	9.6 (11.0)	6.9 (7.9)	4.9 (5.6)	10.2^ (11.7^)	9.4 (10.5)	68.0 (78.6)	72.0 (83.2)
Zone 6	1.4 (1.6)	3.8 (4.3)	0.5 (0.6)	4.6 (5.1)	3.2 (3.5)	2.4 (2.7)	4.8^ (5.3^)	5.5 (7.1)	33.8 (37.3)	38.3 (42.3)
Zone 7	1.2 (1.3)	4.1 (4.4)	0.4 (0.4)	4.4 (4.7)	3.1 (3.4)	2.3 (2.5)	4.4^ (4.7^)	7.8 (8.3)	52.6 (55.9)	55.4 (58.3)
Zone 8	2.5 (2.8)	7.3 (7.9)	0.7 (0.8)	8.8 (9.8)	6.0 (6.6)	5.1 (5.8)	15.0^ (19.3^)	9.3 (10.0)	46.8 (51.2)	66.2 (74.2)
Zone 9	1.3 (1.4)	3.7 (4.0)	0.5 (0.5)	4.9 (5.2)	3.2 (3.4)	2.2 (2.3)	4.6^ (4.9^)	6.0 (7.1)	34.3 (36.1)	35.4 (37.2)
Zone 10	1.5 (1.7)	5.8 (6.6)	0.8 (1.0)	7.0 (7.9)	5.2 (6.0)	3.0 (3.4)	6.4^ (7.1^)	7.1 (7.8)	40.1 (43.5)	44.5 (50.3)
Zone 11	1.3 (1.4)	4.2 (4.4)	0.5 (0.5)	5.2 (5.5)	3.7 (3.9)	2.7 (2.8)	5.3^ (5.6^)	5.7 (6.1)	34.5 (36.0)	35.5 (37.0)
Zone 12	1.6 1.8)	4.8 (5.1)	0.6 (0.6)	5.8 (6.2)	4.1 (4.4)	3.1 (3.4)	5.9^ (6.4^)	6.1 (6.5)	36.1 (39.0)	37.4 (40.4)
Zone 13	1.1 (1.2)	3.3 (3.6)	0.5 (0.5)	4.3 (4.6)	3.0 (3.1)	2.4 (2.5)	4.1^ (4.3^)	4.3 (4.3)	24.9 (26.1)	25.1 (26.3)
Zone 14	0.9 (1.0)	3.3 (3.5)	0.3 (0.4)	7.3 (9.5)	2.8 (3.0)	2.1 (2.4)	4.1^ (4.4^)	3.9 (4.2)	26.5 (28.4)	27.4 (29.3)
Zone 15	1.3 (1.4)	3.2 (3.4)	0.4 (0.5)	4.1 (4.4)	3.0 (3.2)	2.3 (2.4)	3.9^ (4.1^)	4.0 (4.2)	25.3 (26.1)	25.9 (26.8)
Zone 16	1.4 (1.5)	3.7 (3.9)	0.5 (0.6)	4.7 (5.0)	3.4 (3.6)	2.5 (2.6)	4.7^ (4.9^)	4.3 (4.6)	27.6 (29.4)	28.4 (30.2)
Total Fladen Ground	2.2 (2.6)	4.9 (5.3)	0.6 (0.7)	6.3 (6.9)	4.2 (4.6)	3.4 (3.6)	6.4^ (7.1^)	6.2 (6.7)	38.4 (41.3)	43.3 (46.8)

Nap = Naphthalene; Phe = Phenanthrene; An = Anthracene; Fl = Fluoranthene;
Py = Pyrene; B[a]An = Benzo[a]Anthracene; Chr = Chrysene; B[a]Py = Benzo[a]Pyrene;
^ Chrysene/Triphenylene.

5.3.f Sources of the PAH

Kinetic and/or thermodynamic criteria and the nature of organic matter govern the PAHs distribution in the environment. PAHs have different distribution patterns according to their production sources; difficulties exist in identifying their origins in sedimentary medium, owing to the possible co-existence of several sources (various pyrolytic sources, petrogenic contaminant, and biogenic). In addition, physical-chemical properties of some PAHs, like chemical reactivity (photooxidation and oxidation), can contribute to modify the original distribution pattern of the emission sources (Butler and Crossley, 1981). In the marine ecosystem, PAHs can undergo degradation by photooxidation on the surface water layer (Mill *et al.*, 1981), solubilization, evaporation (Hunt, 1996), and by microbial activities into the sediment (Cerniglia and Heitkamp, 1989). However, PAHs ubiquity in the sediments indicates that accumulation phenomena dominate degradation processes in sedimentary matrices (Readman *et al.*, 1984; Smith and Levy, 1990); therefore, some PAHs could exhibit comparable evolution kinetics.

Molecular indices based on PAH physical-chemical behaviour co-variability were developed to assess the various origins of these pollutants (Soclo, 1986; Baumard *et al.*, 1998). With simultaneous association of various molecular indices, it is possible to determine which process generated such hydrocarbons in the studied matrices (Lake et *al.*, 1979; Neff, 1979; Budzinski *et al.*, 1997). Study of PAH distributions and PAH concentration ratios can be used to distinguish PAHs of petrogenic and pyrolytic origin (Fernandes *et al.*, 1997; Baumard *et al.*, 1998a, 1998b and 1999; Webster *et al.*, 2001 and 2003). Petrogenic sources yield mainly alkylated 2- and 3-ring compounds and thermodynamically favoured isomers (naphthalene and phenanthrene) whereas PAHs from pyrolytic sources are mainly the 4- to 6-ring parent compounds.

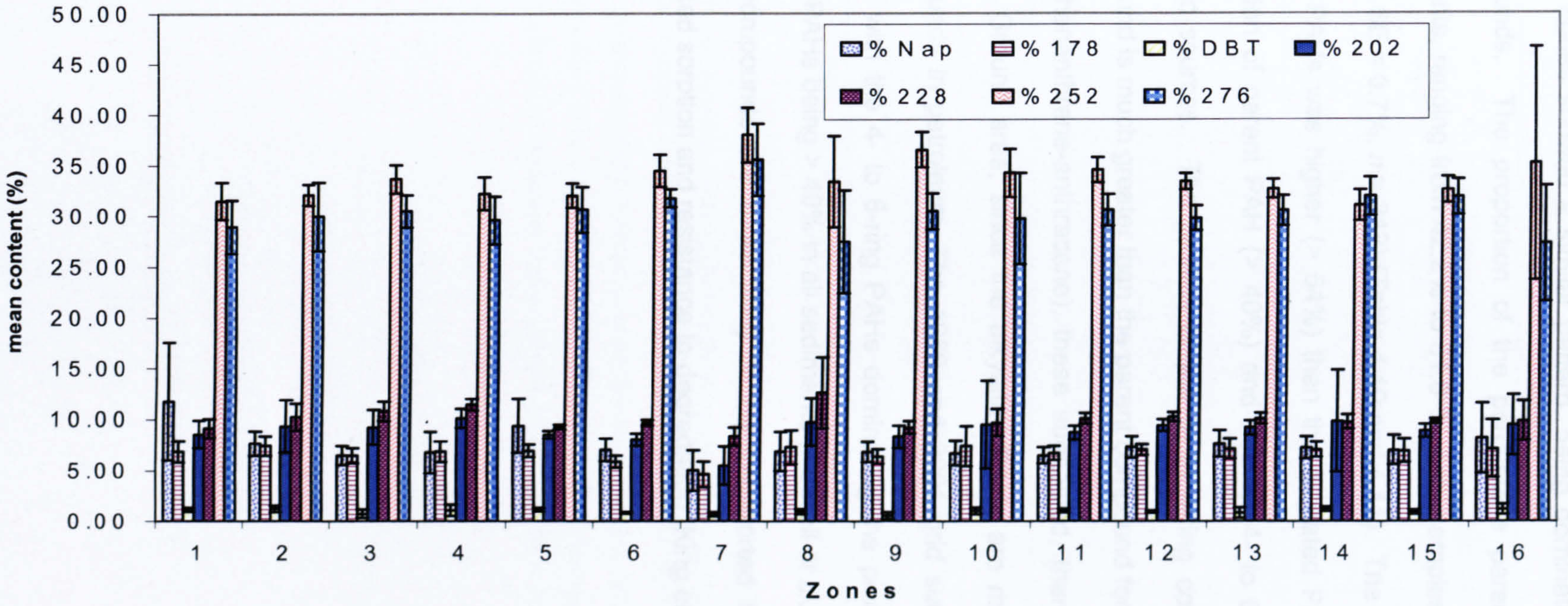

Figure 5.9 PAH profile for the stratified sampling survey by Zone. Note the predominance of the 4- to 6-ring (%202 - %276) PAHs, which indicates a more pyrolytic input.

% 128, naphthalenes (parent and C_1-C_4); %178, phenanthrene/anthracene (parent and C_1-C_3); %DBT, dibenzothiophenes (parent and C_1-C_3); %202, fluoranthene/pyrene (parent and C_1-C_3); %228, benzanthracene/benzophenthrenes/chrysene/triphenylenes (parent and C_1-C_2); %252, benzofluoranthene/benzopyrene/perylene and %276, indenopyrene/benzoperylene (parent and C_1-C_2).

Figure 5.9 shows the PAH distributions by Zone. The mean PAH percentage profile for the 16 Zones showed a similar pattern, being dominated by the heavier 4- to 6-ring compounds. The proportion of the percentage parent PAHs was high in all the sediments, ranging from 42.2% to 81.0 %, both samples in Zone 16 (stratified mean = 56.6%, SE = 0.7%, *n* = 242) (Table 4.10 and 4.11). The mean proportion of percentage parent PAHs was higher (> 54%) than the alkylated PAHs in all the Zones. A high proportion of parent PAH (> 40%) and heavier 4- to 6-ring PAH profile is typical of pyrolytic sources. The profiles of the 3- to 4-ring compounds shows the alkylated compound is much greater than the parent compound for the total naphthalene and total 178 (phenanthrene-anthracene), these suggested, there was petrogenic input in the Fladen Ground area, since the alkylated PAHs are more abundant than the parent compounds in petroleum. The 1989 and 2001 grid survey sediments gave a similar pattern with the 4- to 6-ring PAHs dominating the profiles and the proportion of the parent PAHs being > 40% in all sediments (Russell *et al.*, 2004). Generally the heavier PAH compounds are more likely to be transported to sediment bed due to their increased sorption and resistance to degradation (King *et al.*, 2003).

Table 5.10 Summary of the total parent PAH concentrations in µg kg^{-1} dry weight (2- to 6-ring PAHs including 16 EPA).

Zones	No of Samples	Min	Mean	Med	Max	SD	CV	Var	SE
1	20	37.5	53.6	52.8	74.9	10.3	19.2	105.6	2.3
2	20	28.9	52.9	51.9	89.7	17.1	32.3	292.9	3.8
3	20	29.6	56.2	54.4	115.0	20.0	35.6	399.9	4.5
4	13	55.0	112.9	116.1	218.8	44.7	39.6	2002.5	12.4
5	10	46.2	73.3	66.4	151.4	29.7	40.5	880.6	9.4
6	9	31.4	50.7	45.2	71.6	13.4	26.5	180.0	4.5
7	18	49.9	94.7	86.0	160.4	29.1	30.7	847.0	6.9
8	10	43.6	85.9	65.9	191.8	46.4	54.0	2150.0	14.7
9	18	18.0	36.3	38.1	56.4	10.3	28.3	105.9	2.4
10	11	31.7	61.4	61.2	85.0	16.2	26.4	263.2	4.9
11	17	54.6	78.3	77.1	102.9	12.8	16.3	163.2	3.1
12	9	24.5	8.1	46.4	86.0	17.9	219.9	319.0	6.0
13	20	18.8	30.2	30.1	43.1	6.6	21.7	43.0	1.5
14	14	31.5	45.4	38.6	97.5	17.7	39.1	314.0	4.7
15	20	34.5	53.2	49.9	77.7	12.1	22.7	145.8	2.7
16	13	20.2	52.3	42.2	137.5	30.8	58.9	948.7	8.5
Total	242	18.0	61.4	N/A	218.8	20.2	38.9	541.6	1.6

Parent PAHs = sum of naphthalene, phenanthrcene, anthracene, dibenzothiohene (DBT), fluoranthene, pyrene, benzo[*c*]phenanthrene, benz[*a*]anthracene, chrysene/tripheylene, benz[*b*]anthracene, benzofluoranthenes, benzo[*e*]pyrene, pyrelene, indonopyrelene, benzopyrelene, acenaphthylene, acenaphthene, fluorene, dibenz[*a,h*]anthracene.
Min = Minimum; Med = Median; Max = Maximum; SD = Standard Deviation;
CV = Coefficient of Variance; Var = Sample Variance; SE = Standard Error of the mean.

Table 5.11 Summary of the percentage total parent PAHs concentration (2- to 6-ring PAHs including 16 EPA) in dry weight.

Zones	No of Samples	Min	Mean	Med	Max	SD	CV	Var	SE
1	20	52.5	55.9	55.8	60.8	2.0	3.5	3.8	0.4
2	20	51.2	55.9	55.9	61.9	2.3	4.2	5.5	0.5
3	20	48.1	54.2	54.9	56.4	2.1	3.8	4.3	0.5
4	13	51.4	54.8	54.9	57.2	1.6	2.9	2.5	0.4
5	10	52.2	54.7	54.7	57.8	1.6	3.0	2.6	0.5
6	9	54.5	56.9	56.7	59.7	1.6	2.8	2.5	0.5
7	18	55.8	60.4	61.9	65.2	2.9	4.8	8.2	0.7
8	10	53.3	57.6	55.5	69.5	5.2	9.0	26.9	1.6
9	18	52.0	59.2	58.7	63.3	2.6	4.5	6.9	0.6
10	11	55.2	58.3	58.0	61.5	2.2	3.8	4.9	0.7
11	17	55.0	57.2	57.2	62.6	1.9	3.4	3.7	0.5
12	9	53.5	55.4	55.0	58.2	1.5	2.7	2.2	0.5
13	20	52.6	56.3	56.1	65.4	2.8	5.1	8.1	0.6
14	14	53.3	55.7	55.4	65.1	2.9	5.3	8.6	0.8
15	20	54.4	55.9	55.3	59.6	1.5	2.8	2.4	0.3
16	13	42.2	57.1	55.6	81.0	8.3	14.5	68.9	2.3
Total	242	42.2	56.6	N/A	81.0	2.6	4.7	9.5	0.2

$$Parent \quad PAHs \quad (\%) = \frac{Parent \quad concentration}{Total \quad PAH \quad concentration} * 100$$

Min = Minimum; Med = Median; Max = Maximum; SD = Standard Deviation;

CV = Coefficient of Variance; Var = Sample Variance; SE = Standard Error of the mean.

Plotting PAH concentration ratios can aid sources identification (Webster *et al.*, 2003). Plotting the fluoranthene/pyrene (Fl/Py) ratio against the phenanthrene/anthracene (P/A) ratio or methylphenanthrene/phenanthrene (MP/P) ratio, pyrolytic or petrogenic zones can be identified. The zones defined by high Fl/Py ratios and low P/A or MP/P are characteristic of pyrolytic PAHs (top left quadrant), and low Fl/Py ratios and high P/A or MP/P are characteristic of petrogenic PAH (bottom right quadrant). The other two quadrants may be indicative of a mixed source of PAHs (Figures 5.10a and b).

A plot of the ratios showed most of the samples falling within the pyrolytic zone (Figures 5.10a and b). The Fl/Py against MP/P ratios plot (Figure 5.10a) shows nearly all samples clustered in the pyrolytic zone, with only one sample from Zone 9 in the mixed zone, having MP/P ratios > 2. The Fl/Py against P/A ratios is more dispersed, 21 samples about 23% of samples with measurable anthracene, fell in the mixed zone due to the P/A ratios being greater than 10. The remaining samples were in the pyrolytic zone (Figure 5.10b); the high P/A ratios suggest a possible petrogenic source of PAHs, however, a low proportion of anthracene can often be found at remote sites if the main source is atmospheric deposition as a result of photooxidation during atmospheric transportation (Li *et al.*, 1998). The majorities of samples in this mixed zone were from Zones 4, 7 and 8 and also had the highest mean total PAH concentrations. All these Zones, except Zone 7 had oil platforms or multiple wells and are situated close to each other in the top right hand corner of the Fladen Ground (Figure 2.5). In addition the current flow (Figure 2.1) in the Fladen Ground could result in the accumulation of hydrocarbons in this area. High boiling unresolved complex mixtures (UCM) characteristic of petrogenic contamination, were also observed in the GC-FID chromatograms of samples from these Zones (4, 7 and 8). Furthermore, the geochemical biomarker analysis showed evidence of low levels of crude oil contamination from their triterpane profiles (see sections 5.2g and h).

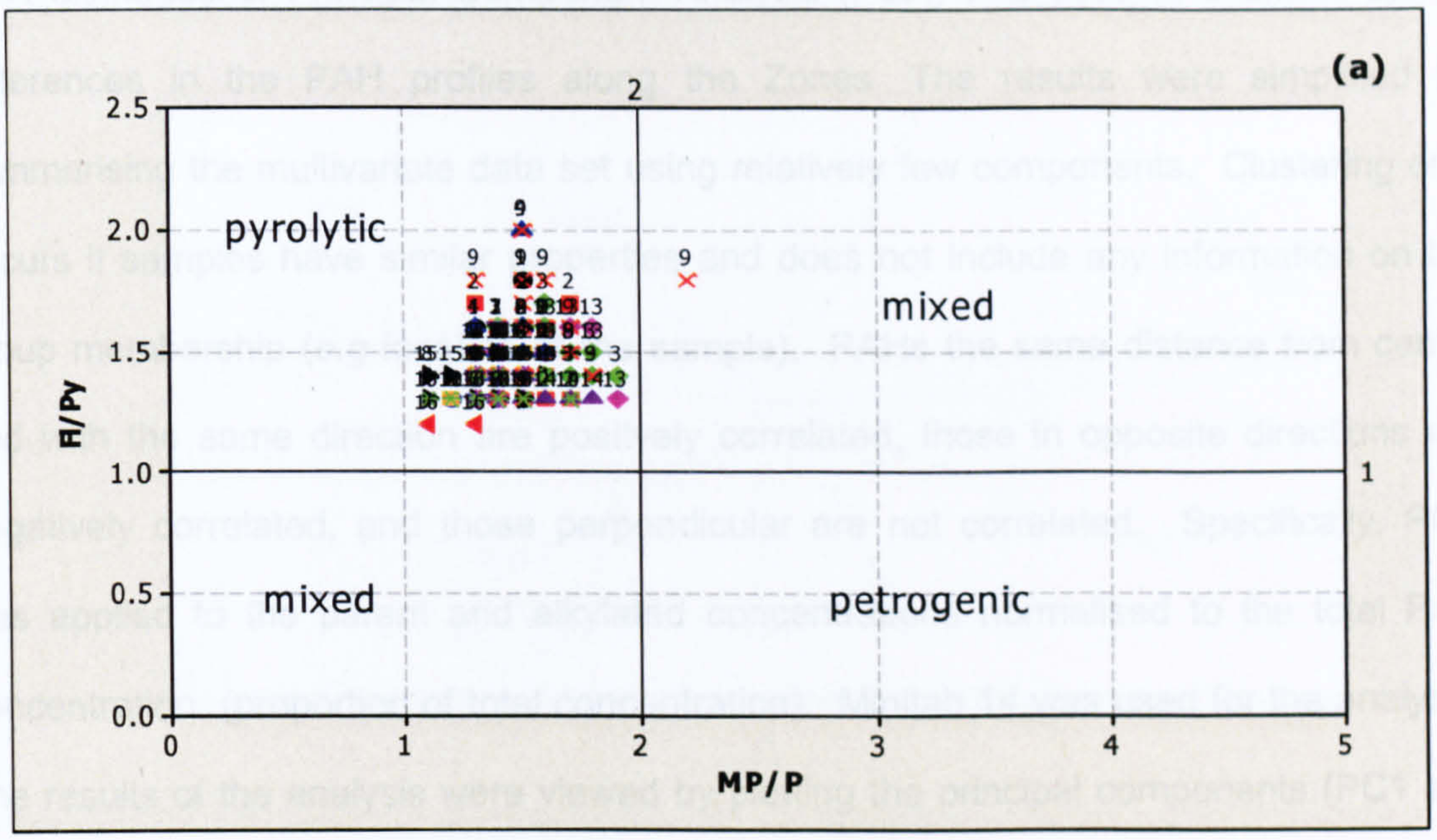

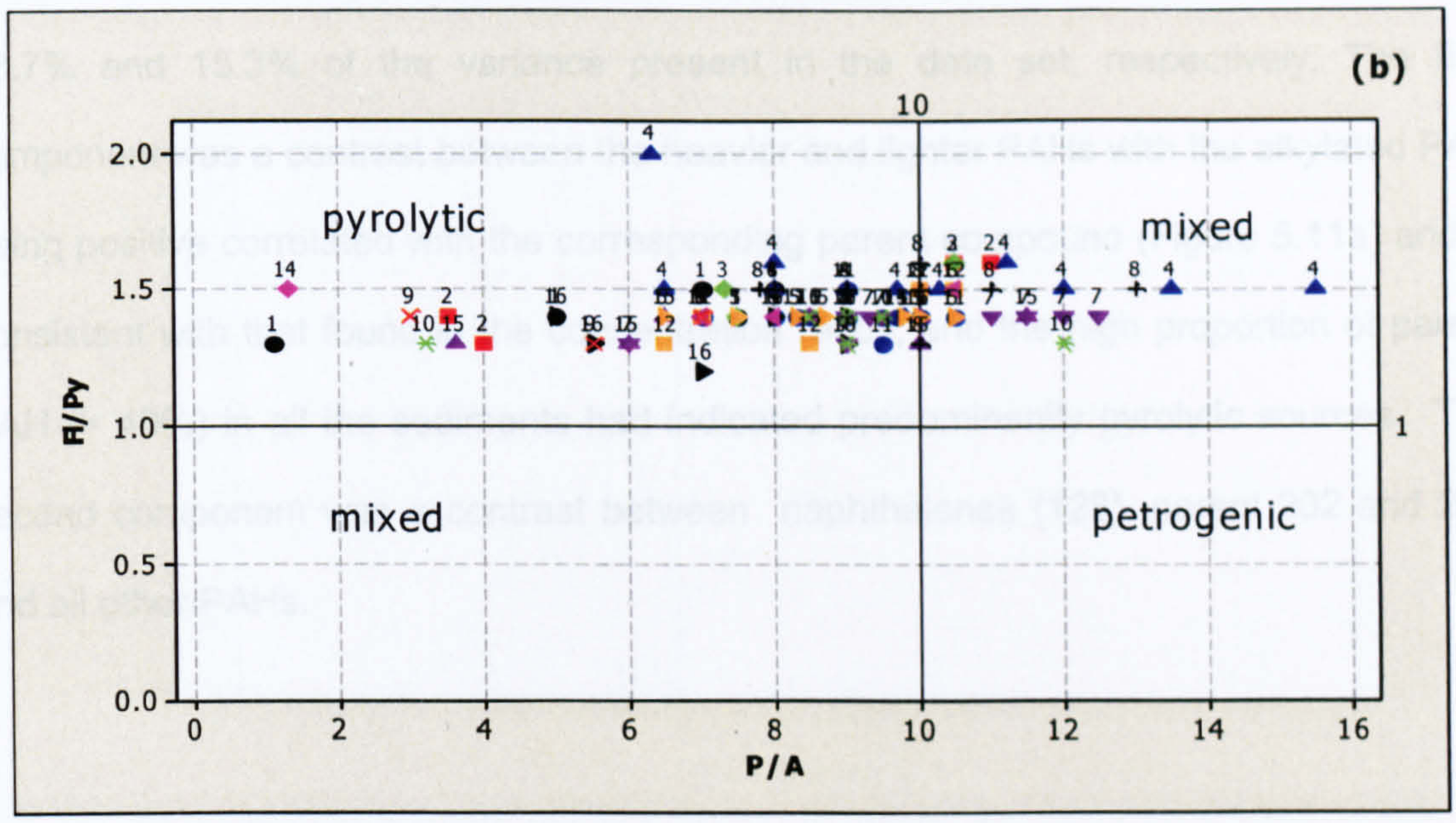

Figure 5.10 PAH concentration ratios used to assess the sources of PAHs in the Fladen Ground sediments collected in 2001. The Zones identified by high fluoranthene/pyrene (Fl/Py) ratios and low phenanthrene/anthracene (P/A) ratios and high Fl/Py and low methylphenanthrene/phenanthrene (MP/P) ratios were characteristic of pyrolytic PAHs. (a) Plot of Fl/Py ratios against P/A ratios. (b) Plot of Fl/Py ratios against MP/P ratios.

Further statistical analysis was done to looked at the parent and branched (alkylated) PAH distributions. Principal Component Analysis (PCA) was used to examine spatial differences in the PAH profiles along the Zones. The results were simplified by summarising the multivariate data set using relatively few components. Clustering only occurs if samples have similar properties and does not include any information on the group membership (*e.g* location of the sample). PAHs the same distance from centre and with the same direction are positvely correlated, those in opposite directions are negatively correlated, and those perpendicular are not correlated. Specifically, PCA was applied to the parent and alkylated concentrations normalised to the total PAH concentration (proportion of total concentration). Minitab 14 was used for the analysis. The results of the analysis were viewed by plotting the principal components (PC1 and PC2) with the greatest variance against one another. PC1 and PC2 accounted for 33.7% and 15.3% of the variance present in the data set, respectively. The first component was a contrast between the heavier and lighter PAHs with the alkylated PAH being positive correlated with the corresponding parent compound (Figure 5.11a) and is consistent with that found in the concentration ratios, and the high proportion of parent PAH (> 40%) in all the sediments had indicated predominantly pyrolytic sources. The second component was a contrast between naphthalenes (128), parent 202 and 252 and all other PAHs.

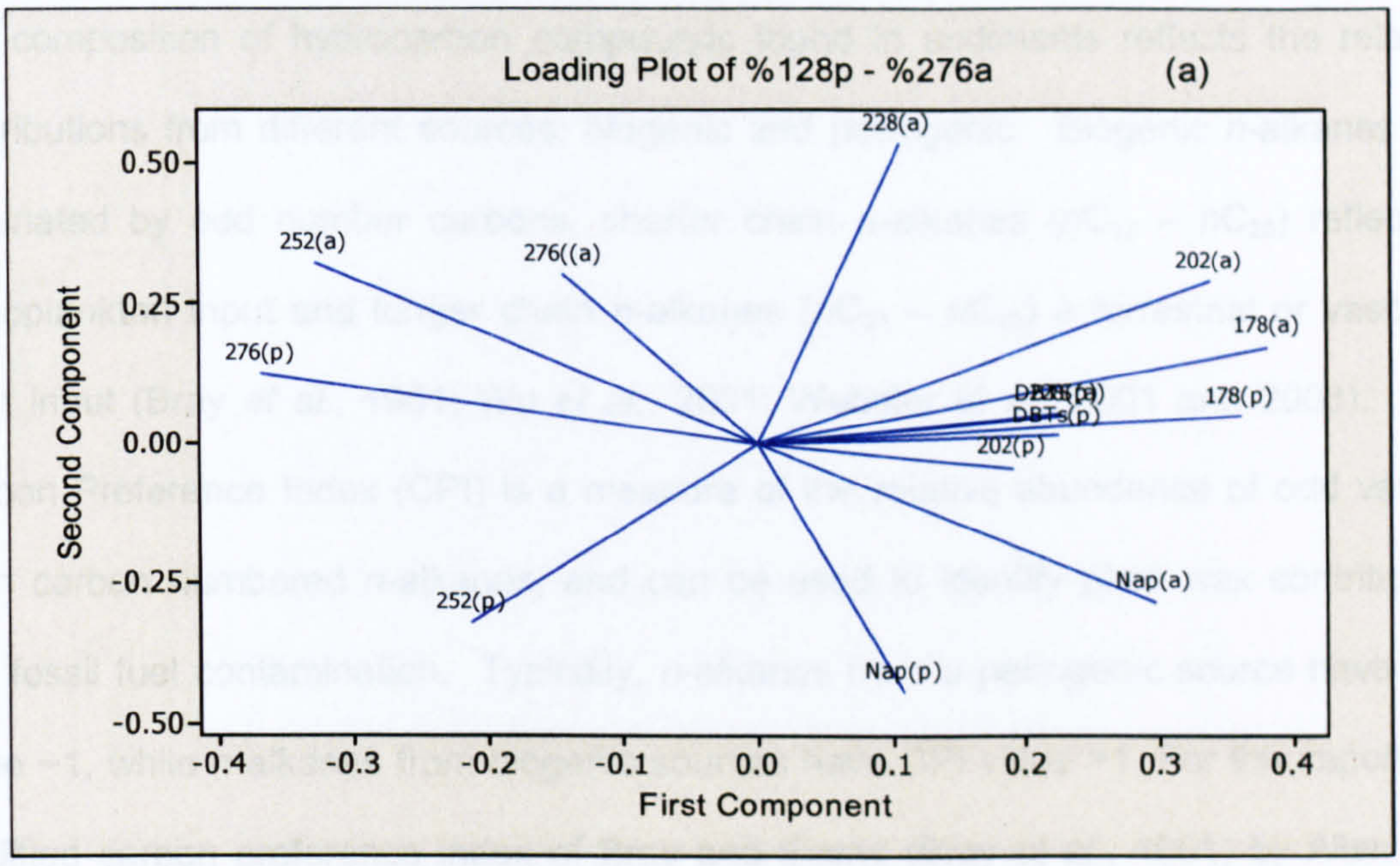

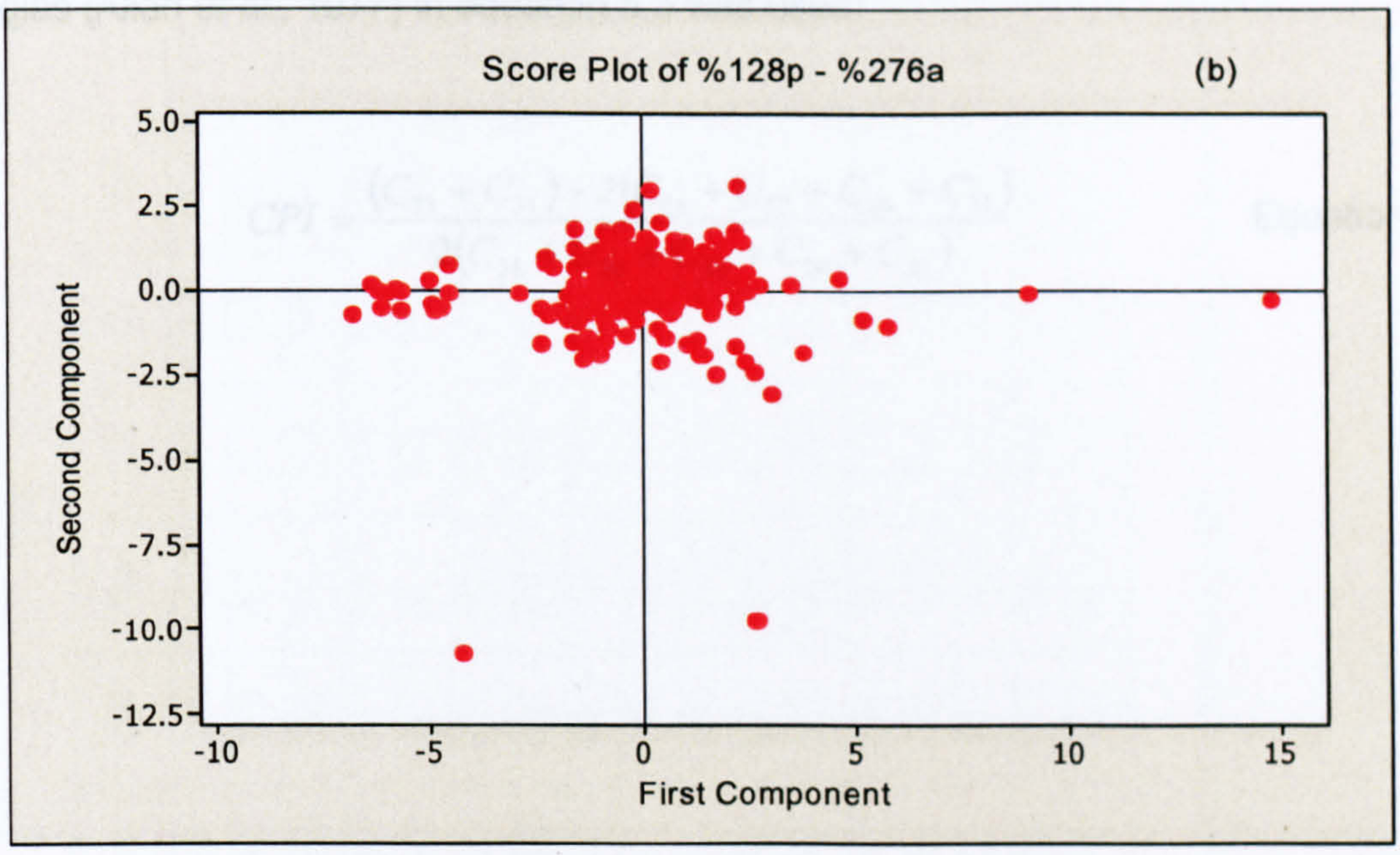

Figure 5.11 Principal component analysis of the survey by ring group parents and alkylated. (a) Loading plot of %128-%276, showing the lighter PAH compounds with a negative first component, and the 5- and 6-ring with a positive first component. (b) Score plot showing samples in the right half of the graph were mainly from Zones 1, 2, 8, 12, 13, 14 and 16. These samples contained a higher proportion of the lighter PAHs, indicative of greater petrogenic input.

5.3.g Aliphatic Hydrocarbons Analysis

The composition of hydrocarbon compounds found in sediments reflects the relative contributions from different sources: biogenic and petrogenic. Biogenic *n*-alkanes are dominated by odd number carbons, shorter chain *n*-alkanes (nC_{12} – nC_{25}) reflecting phytoplankton input and longer chain *n*-alkanes (nC_{21} – nC_{33}) a terrestrial or vascular plant input (Bray *et al.*, 1961; Wu *et al.*, 2001; Webster *et al.*, 2001 and 2003). The Carbon Preference Index (CPI) is a measure of the relative abundance of odd versus even carbon numbered *n*-alkanes, and can be used to identify plant wax contribution and fossil fuel contamination. Typically, *n*-alkanes from a petrogenic source have CPI value ~1, while *n*-alkanes from biogenic sources have CPI value >1. For this report the modified carbon preference index of Bray and Evans (Bray *et al.*, 1961) by Allan and Douglas (Allan *et al.*, 1977) in equation 5.3 was used:

$$CPI = \frac{(C_{23} + C_{33}) + 2(C_{25} + C_{27} + C_{29} + C_{31})}{2(C_{24} + C_{26} + C_{28} + C_{30} + C_{32})} \qquad \text{Equation 5.3}$$

Table 5.12 Summary of the total *n*-alkane concentration nC_{12} - nC_{33} (µg kg^{-1} dry weight).

Zones	Number of samples	Data								Normalised Data							
		Min	Mean	Med	Max	SD	CV	Var	SE	Min	Mean	Med	Max	SD	CV	Var	SE
1	20	24.6	59.9	53.8	118.5	28.9	48.2	833.7	6.5	29.9	111.8	79.0	404.0	89.5	80.1	8007.7	20.0
2	20	24.8	96.8	73.4	293.7	71.3	73.7	5083.7	15.9	65.0	136.7	91.5	569.3	135.0	98.7	18221.0	30.2
3	20	57.7	115.5	104.6	213.0	39.8	34.5	1586.2	8.9	78.4	119.0	115.2	269.1	41.2	34.6	1697.5	9.2
4	13	78.5	129.8	113.1	317.3	61.6	47.4	3789.0	17.1	70.3	145.4	120.8	247.3	59.5	40.9	3544.1	16.5
5	10	23.7	64.7	63.0	91.4	18.2	28.1	330.8	5.8	43.7	95.6	92.6	139.6	31.6	33.1	999.6	10.0
6	9	53.5	100.8	97.1	177.6	37.4	37.1	1401.7	12.5	49.6	125.9	106.6	330.2	82.7	65.7	6845.2	27.6
7	18	37.4	100.5	88.1	223.2	46.4	46.1	2152.4	10.9	35.6	92.7	77.3	195.3	43.4	46.8	1882.1	10.2
8	10	59.9	206.8	143.5	490.6	156.5	75.7	24493.6	49.5	61.8	256.7	196.4	609.2	176.0	68.5	30962.0	55.6
9	18	37.2	61.0	60.6	120.6	18.7	30.7	350.2	4.4	54.4	103.3	95.9	180.7	35.8	34.7	1283.5	8.4
10	11	61.4	105.4	106.7	168.9	29.3	27.8	861.2	8.8	59.2	134.9	102.2	401.4	99.5	73.7	9891.7	30.0
11	17	79.3	118.6	107.7	259.8	42.8	36.1	1829.2	10.4	53.8	92.7	84.6	171.3	32.2	34.7	1035.3	7.8
12	9	40.3	78.6	69.8	147.7	34.2	43.6	1172.1	11.4	63.4	103.0	104.8	163.6	33.4	32.4	1113.4	11.1
13	20	30.1	55.4	44.8	180.1	34.2	61.7	1169.1	7.6	36.3	85.8	62.4	311.7	62.8	73.2	3940.7	14.0
14	14	45.6	86.4	78.8	162.1	34.9	40.4	1220.9	9.3	37.2	89.5	81.2	170.0	38.0	42.5	1447.0	10.2
15	20	45.1	89.4	86.7	145.7	25.7	28.8	663.0	5.8	42.3	76.1	70.1	121.8	24.3	32.0	590.9	5.4
16	13	60.0	106.7	111.4	158.4	32.0	29.9	1021.1	8.9	61.8	121.8	121.9	229.5	43.1	35.4	1861.2	12.0
Total	242	23.7	97.2	N/A	490.6	44.5	44.3	2887.5	3.7	35.6	115.7	N/A	609.2	63.5	52.4	5685.4	5.0

Min = Minimum; Med = Median; Max = Maximum; SD = Standard Deviation; CV = Coefficient of Variance; Var = Variance; SE = Standard Error of the mean.

The total *n*-alkane concentrations ($nC_{12} - nC_{33}$) ranged from 23.7 µg kg^{-1} dry weight in a samples in Zone 5 to 490.6 µg kg^{-1} dry weight in a sample in Zone 8 (Table 5.11 and Appendix 4). The Zone mean total *n*-alkane concentration ranged 55.4 µg kg^{-1} dry weight (SE = 7.6, *n* = 20) in Zone 13 to 206 µg kg^{-1} dry weight (SE = 49.5 µg kg^{-1} dry weight, *n* = 10) in Zone 8. The mean total *n*-alkane concentration for the whole far field area was 97.2 µg kg^{-1} dry weight (SE = 11.7 µg kg^{-1} dry weight, *n* = 242). The CPI value ranged from 0.7 in samples in Zones 5, 8 and 15 to 4.5 in a sample in Zone 13 (mean = 1.4, SE = 0.1 and *n* = 242) (Table 5.12).

Table 5.13 Summary of the Carbon preference index (CPI).

Zones	No. of samples	min	mean	med	max	SD	CV	Var	SE
1	20	0.8	1.6	1.2	3.8	0.9	22.4	0.8	0.4
2	20	0.8	1.9	1.2	4.3	1.2	22.4	1.4	0.4
3	20	0.8	1.4	1.2	2.7	0.6	22.4	0.4	0.3
4	13	0.8	1.3	1.2	2.0	0.4	27.7	0.2	0.4
5	10	0.7	1.2	1.0	2.0	0.5	31.6	0.3	0.4
6	9	0.8	1.5	1.4	2.7	0.6	33.3	0.4	0.5
7	18	0.8	1.3	1.2	2.0	0.4	23.6	0.2	0.3
8	10	0.7	1.2	1.1	2.1	0.4	31.6	0.2	0.4
9	18	0.8	1.2	1.1	2.0	0.4	23.6	0.2	0.3
10	11	0.8	1.2	1.1	2.0	0.4	30.2	0.2	0.4
11	17	0.8	1.3	1.2	2.0	0.4	24.3	0.2	0.3
12	9	0.8	1.2	1.1	2.0	0.3	33.3	0.1	0.4
13	20	0.8	1.6	1.2	4.5	1.0	22.4	1.0	0.4
14	14	0.8	1.4	1.2	2.0	0.5	26.7	0.3	0.4
15	20	0.7	1.4	1.2	3.0	0.6	22.4	0.4	0.3
16	13	0.8	1.3	1.2	2.0	0.4	27.7	0.2	0.4
Total	242	0.7	1.3	N/A	4.5	0.7	24.4	0.5	0.1

Min = Minimum; Med = Median; Max = Maximum; SD = Standard Deviation; CV = Coefficient of Variance; Var = Sample Variance; SE = Standard Error of the mean.

Table 5.12 shows Zones with higher mean total *n*-alkanes concentration (>100 µg kg^{-1} dry weight) had multiple oil wells (Zones 4, 6, 8, 10, 11 and 16) and/or fine sediment and organic carbon content (Zones 3, 7 and 11). These Zones are situated closely together on the central and top right corner of the Fladen Ground with the exception of Zone 16. These Zones also had higher concentrations of Forties crude, diesel oil equivalents, and total PAH concentrations.

The odd carbon-number compounds in the range of $nC_{25} - nC_{33}$ predominate, and nC_{29} and nC_{33} are the major (C_{max}) component in most samples. This distribution pattern is indicative of a prominent terrigenous input derived from higher plant waxes (Brassell *et al.*, 1978). However, since the plant wax is more resistance to biodegradation, their proportion may represent to a certain extent an overestimate of the terrigenous influx in the sampling area as a result of evaporation, dispersion, dilution, and degradation (Dutta and Harayama, 2000).

From Figure 5.12 it can be seen that higher concentrations of *n*-alkane were found in the north east of the Fladen Ground (Zones 4, 7 and 8). Also these Zones had the three highest total PAH concentrations (Table 5.7) and were in the mixed zone of the PAH concentration ratios of Fl/Py against P/A (P/A >10; Figure 5.10b). Zone 4 had the highest mean diesel oil equivalent value and a mean Forties crude value lower than the stratified mean, whilst Zones 7 and 8 had oil equivalents values greater than the stratified mean for diesel. For the Forties crude oil Zone 8 had oil equivalent value less than stratified mean value whilst Zone 7 mean value was greater than the stratified mean (Tables 5.5 and 5.6). In addition Zone 7 had a higher percentage of organic carbon and proportion of fine material (< 63 µm fraction) (Tables 5.1 and 5.2). Therefore, the accumulation of *n*-alkanes may be due to a higher input of hydrocarbon due to the oil installations in Zones 4 and 8, and fine sediment materials and higher

organic carbon content for Zone 7. Another possible explanation for the higher concentrations in these Zones could be due to circulation pattern in the Fladen Ground.

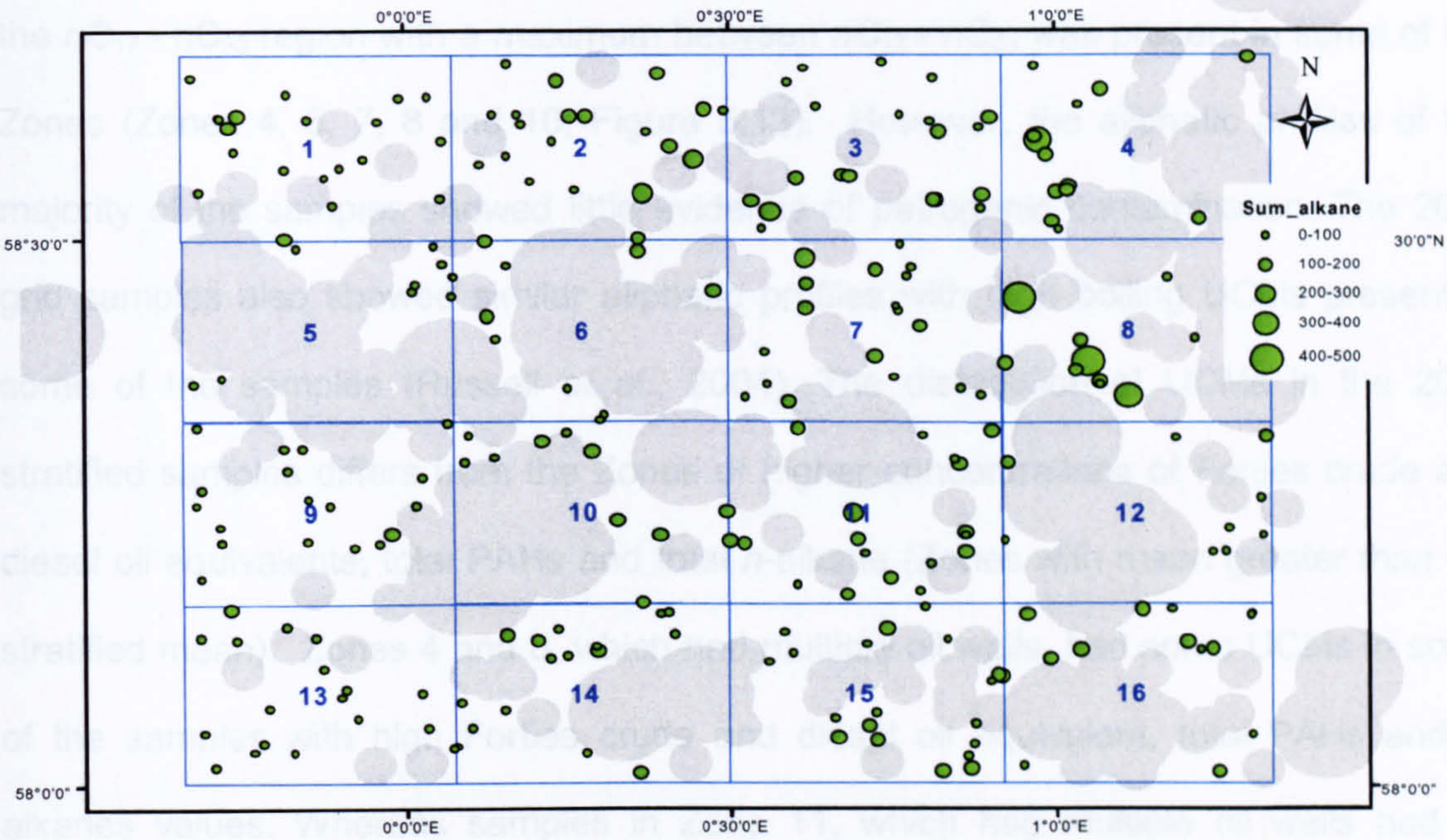

Figure 5.12 Spatial distribution of total *n*-alkane concentration (nC_{12} - nC_{33}) (µg kg^{-1} dry weight), showing higher concentrations of samples in Zones with multiple oil wells or platform, and/or higher organic carbon content and proportion of the < 63 µm particle size. Large grey circles are < 5km radius of multiple oil wells and small grey circles are < 2km radius of a single oil well. Green circles are proportional to concentrations.

Non-biodegraded crude oils contain a range of *n*-alkanes, which decrease in concentration with increasing carbon number, and show no odd carbon predominance. After exposure, the oil gradually degrades (weathers) with the lighter *n*-alkanes being lost first, through biodegradation, evaporation or dissolution into the water column. Eventually almost all *n*-alkanes will be lost and only a hump will be observed in the GC-FID chromatogram (Webster *et al.*, 2000 and 2001). This is known as an unresolved complex mixture (UCM) and comprises of a mixture of alicyclic compounds (Gough and Rowland, 1990; Killops and Al-Juboori, 1990) and has a well-known linkage to degraded

or weathered petroleum residues (Venkatesan *et al.*, 1980; Readman *et al.*, 1987). However, some UCM distributions, mainly in the lower molecular weight range, can be attributed to bacterial degradation of natural organic matter such as algae *detritus* (Venkatesan and Kaplan, 1982). A high boiling unresolved complex mixture (UCM) in the nC_{17} - nC_{33} region with a maximum between nC_{27} - nC_{33} was present in some of the Zones (Zones 4, 6, 7, 8 and 10; Figure 5.13). However, the aliphatic profiles of the majority of the samples showed little evidence of petrogenic contamination. The 2001 grid samples also showed similar aliphatic profiles with high boiling UCMs present in some of the samples (Russell *et al.*, 2004). The distribution of UCMs in the 2001 stratified samples differs from the Zones of higher concentrations of Forties crude and diesel oil equivalents, total PAHs and total *n*-alkane (Zones with mean greater than the stratified mean). Zones 4 and 8, which had multiple oil wells, had some UCMs in some of the samples with high Forties crude and diesel oil equivalent, total PAHs and *n*-alkanes values. Whereas samples in Zone 11, which had multiple oil wells had no visible UCMs in samples with high Forties crude and diesel oil equivalent, total PAHs and *n*-alkanes values. As the values of TOC and particle size of the samples with UCMs are not different from the samples without UCMs, then the conclusion must be that there was a higher petrogenic input to these areas (Zones 4 and 8) than the rest of the Fladen Ground.

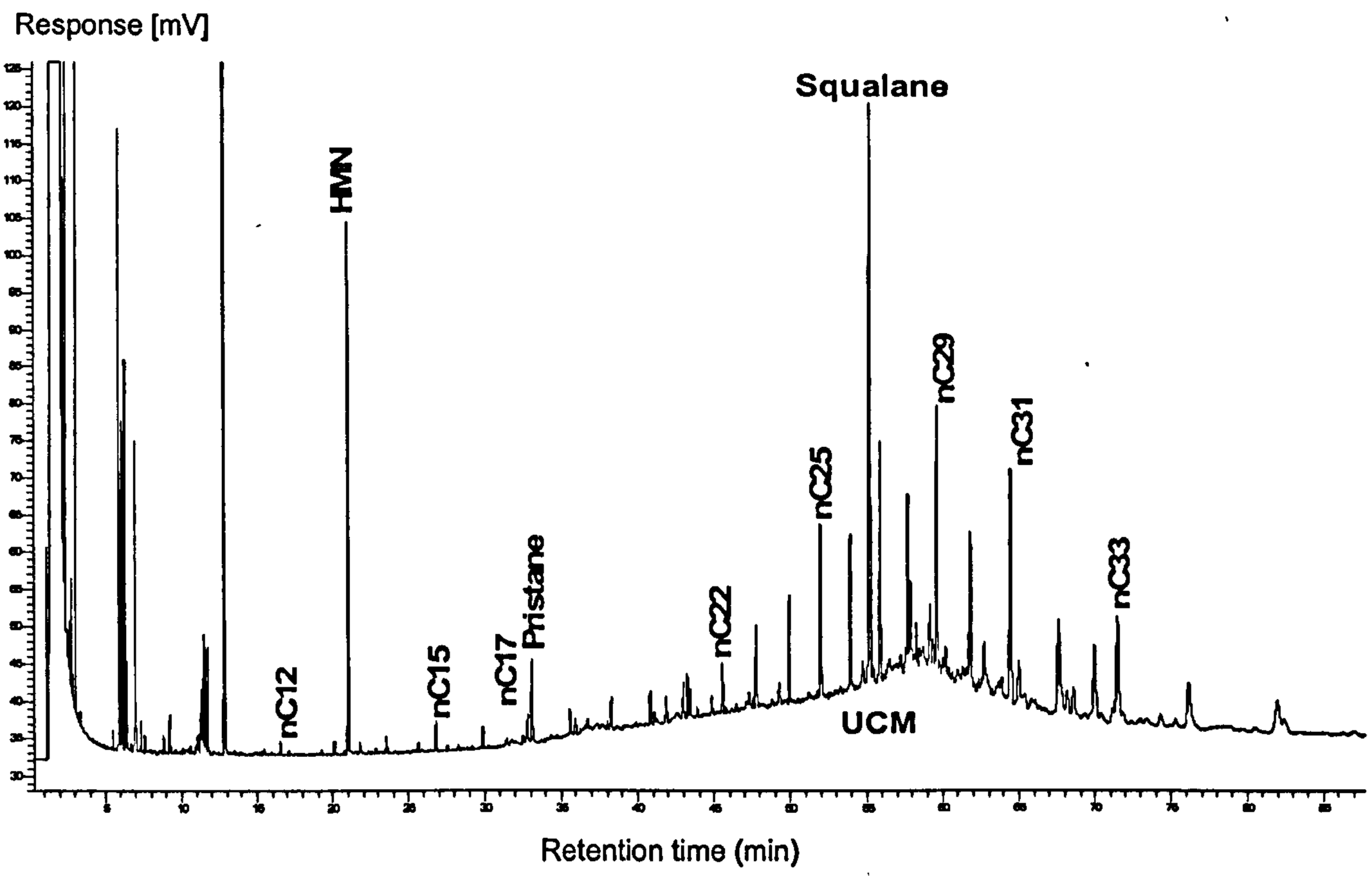

Figure 5.13 Chromatograms of aliphatic hydrocarbon profiles of typical sediment sample (Zone 4). Note the bimodal unresolved complex mixture that suggests petrogenic contamination. The internal standards were squalane and heptamethylnonane (HMN). Squalane was used for quantification.

5.3.h Geochemical Biomarkers Analysis

Crude oils give a characteristic geochemical biomarker profile, which can be used to identify oil contamination. Identification of petrogenic sources of PAHs using PAH concentration ratios alone can be difficult, due to weathering or bacterial oxidation which alters the PAH and the *n*-alkanes profile of crude oil (Venkatesan *et al.*, 1990; Webster *et al.*, 2003). The geochemical biomarker profiles of crude oil are unaffected by weathering or bacterial oxidation. The double peaks in the *m/z* 191 mass chromatogram (triterpane profile) are due to the 22S and 22R diastereoisomers of each of the C_{31}-C_{35} homohopanes and are characteristic of all crude oils (Figures 5.14a and b). These doublets decrease in size with increasing carbon number. North Sea and Middle

Eastern oils can be identified from their triterpane profiles. North Sea oil (Figure 5.14b) contains a characteristic triterpane, bisnorhopane (two less methyl groups than hopane), and C_{29} hopane in lower abundance compared to the C_{30} hopane. Middle Eastern oil does not contain bisnorhopane and the ratio of C_{29} hopane to hopane is higher than found in North Sea oils (Webster *et al.*, 2001).

The aliphatic fraction of the sediments identified as having petrogenic contamination (Figure 5.13) from the GC-FID aliphatic profiles were further analysed by GC-MS for geochemical biomarkers (triterpanes and steranes). All the samples analysed contained a high proportion of the natural triterpanes such as diploptene and the natural homohopane diastereoisomers 22R, 17α, 21β-homohopane, with diploptene dominating the profiles (Figure 5.14a). In addition, the triterpane profiles also showed low levels of crude oil contamination (Figure 5.14a). There was a small bisnorhopane peak indicating the presence of North Sea oil. However, the proportion of the bisnorhopane to norhopane was smaller than normal North Sea oil (Figure 5.14), and similar to Middle Eastern oil. Therefore, the geochemical biomarker profiles indicated that most sediment samples had been exposed to both North Sea and Middle Eastern crude oils. The presence of the Middle Eastern oil could be as a result of shipping activities as it is used in bunker fuel.

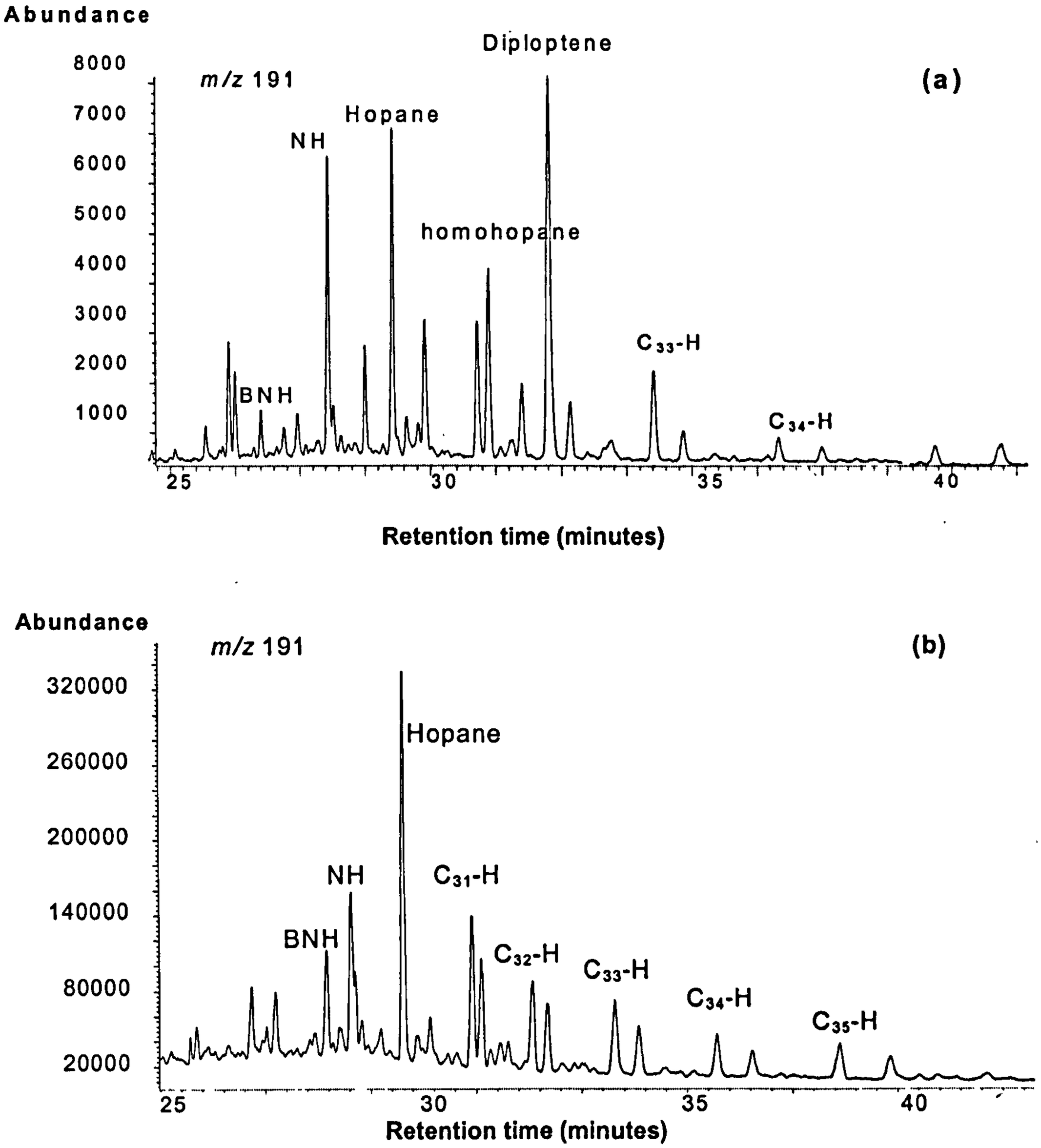

Figure 5.14 (a) Triterpane profile of a typical sediment collected from the Fladen Ground in the 2001 stratified survey. The largest peak in the chromatogram was due to the naturally occurring triterpene diploptene. Homohopane doublet peaks indicate there was petrogenic contamination. The high ratio of C_{29} hopane and the small bisnorhopane (BNH) peak indicate the contaminations was due to a combination of North Sea and Middle Eastern crude oils. (b) Triterpane profile of Gulfaks crude oil containing C_{29} hopane (NH), hopane and the doublet peaks due to the C_{31} – C_{35} homohopane diasteroisomers (C_{31}-H to C_{35}-H), the North sea oil specific marker bisnorhopane(BNH) can also be seen.

5.4 CONCLUSIONS

The total PAH concentrations (2- to 6-ring parent and alkylated PAHs including the 16 US EPA PAHs) in sediments were relatively low (Table 5.14). Also the level of the ten PAH individual concentrations were relatively lower in comparison with the OSPAR background assessment concentrations (BACs) for the northern North Sea. The PAHs input were generally higher in the north of the survey area, and lower in the south of the survey area, in particularly, southern end of the survey area. The PAH distribution profile and concentration ratios indicated a predominantly pyrolytic input, being dominated by the heavier, more persistent, 5- and 6-ring compounds, and with a high proportion of the parent PAH. Also the distribution of the mean PAHs showed a significant correlation between the sediment organic content and particle size, suggesting the importance of particulate organic coatings in PAH sorption. Estimates of 'total hydrocarbon' concentrations expressed as 'oil' equivalents of crude (Forties crude) or diesel oil were relatively low (Table 5.14).

The *n*-alkane profiles of a number of the sediments contained small, high boiling point UCMs, indicative of limited petrogenic input from weathered oil. The geochemical biomarker profiles of the sediments containing UCMs showed a small bisnorhopane peak and a high proportion of norhopane to hopane, indicating that there was contamination from both Middle Eastern and North Sea oils, and therefore not solely as a result of any oil exploration activity in the area. The most likely source of petrogenic contamination was from shipping activity.

Temporal changes in the distribution and composition of hydrocarbon in the Fladen Ground will be assessed using the 2001 stratified random survey and the data obtained from the 1989 and 2001 conventional grid surveys in the next chapter. In addition, there is comparison of the stratified random and conventional grid regimes.

Table 5.14 Summary of the overall particle size analysis (PSA), total organic carbon (TOC), oil equivalent concentrations of diesel and Forties crude oil, total polycyclic aromatic hydrocarbon concentration and total *n*-alkane concentration (nC_{12}-nC_{33}). All concentrations are in dry weight.

	Min	Mean	Max	SD	CV	Var	SE
PSA (%)	25.1	67.6	89.0	10.9	17.3	152.5	0.8
TOC (%)	0.09	0.91	1.89	0.20	23.35	0.04	0.01
Diesel ($\mu g\ g^{-1}$)	1.6	5.1	14.4	1.5	29.0	2.9	0.1
Forties crude ($\mu g\ g^{-1}$)	4.0	13.8	41.2	4.6	34.1	24.5	0.3
Total PAH ($\mu g\ kg^{-1}$)	29.0	108.2	404.7	34.9	31.3	1595.6	2.7
Total *n*-alkane ($\mu g\ kg^{-1}$)	23.7	97.2	490.6	44.5	44.3	2887.5	3.7

Min = Minimum; Max = Maximum; SD = Standard Deviation; CV = Coefficient of Variance; Var = Variance; SE = Standard Error of the mean

CHAPTER SIX

INVESTIGATION OF TEMPORAL TRENDS IN THE FLADEN GROUND AND COMPARISON OF GRID AND STRATIFIED RANDOM SAMPLING REGIMES

6.1 BACKGROUND

In 1989, part of the Fladen Ground was surveyed to monitor the impact of cutting discharges (Walsham *et al.*, 2002). Sampling followed a systematic, or grid, design, with sediments collected at 3 km intervals along five transects spaced 5 km apart. The grid design was chosen to give good spatial coverage of the survey area. The survey was repeated in 2001 to assess any changes in hydrocarbon concentrations and composition following the cessation of cutting oil based muds discharges in the 1990s (Figure 2.2). A second survey of the Fladen Ground was conducted in 2001, using the random stratified sampling design (Figure 2.5). This considered a much wider area than the grid survey and focussed on hydrocarbon concentrations and composition in the far-field.

To investigate for temporal trends, of data between the 1989 grid, 2001 grid and 2001 stratified random surveys, only the far field Day Grab samples from the 1989 and 2001 grid surveys were used. Forty samples of the 1989 and 2000 grid surveys could be classified as common areas with the stratified Zones of 5, 6, 10, 11, 12 and 16, shown in Figure 5.1. In 2001 all samples were analysed for PAHs, however in 1989 only 25 were analysed for PAHs. Therefore 40 of the 2001 grid samples and only 6 of the 25 samples analysed for PAHs in the 1989 grid survey could be used in the comparison of the PAH temporal trend.

The aim of this chapter is to assess any changes in distribution of hydrocarbon concentrations and composition 1989-2001 in the Fladen Ground, especially, after the cessation of the oil based cutting mud in the late 1990s. In addition to allow the comparison of conventional grid and the new stratified random sampling regimes.

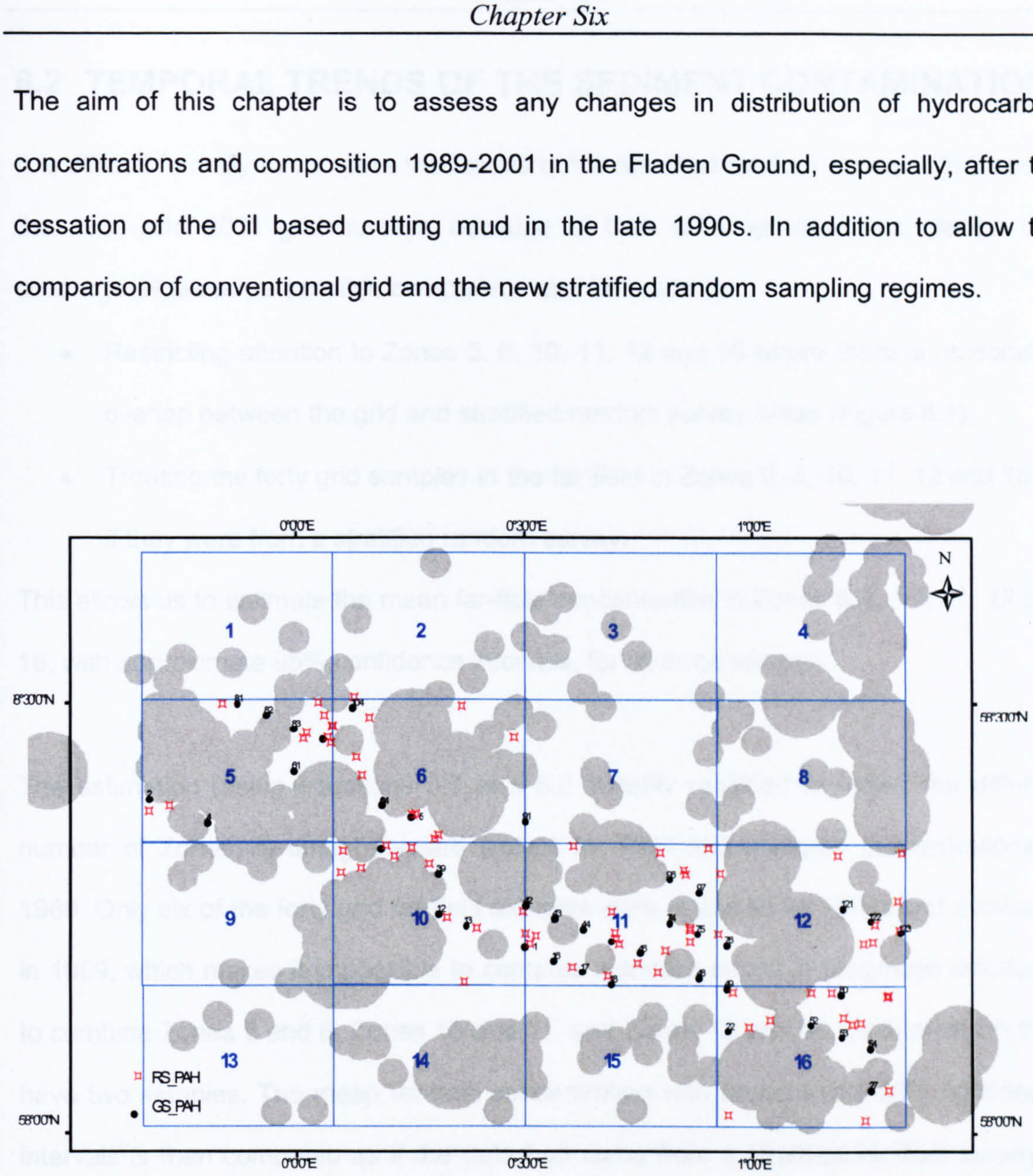

Figure 6.1 Location of Common site of the grid sampling (GS; 1989 and 2001) and the 2001 stratified random sampling (RS), indicating the Zones and oil platforms. Grey circles are near field sites (big circles are multiple oil wells and small circles are single oil well). Black dots are grid samples site with labelled number and red stars are the stratified random sites. Note only samples from the far field areas are used in comparisons.

6.2 TEMPORAL TRENDS OF THE SEDIMENT CONTAMINATION

It is difficult formally to compare the results of the stratified random survey with those of the 1989 and 2001 grid surveys because of their differing objectives, design and coverage. However, a sensible comparison can be made by:

- Restricting attention to Zones 5, 6, 10, 11, 12 and 16 where there is reasonable overlap between the grid and stratified random survey areas (Figure 6.1)
- Treating the forty grid samples in the far-field in Zones 5, 6, 10, 11, 12 and 16 as if they were from a stratified random survey.

This allows us to estimate the mean far-field concentration in Zones 5, 6, 10, 11, 12 and 16, with approximate 95% confidence intervals, for all three surveys.

The estimation (using equations 5.1 and 5.2 suitably modified to reflect the different number of Zones) is straightforward except for PAH and *n*-alkane concentrations in 1989. Only six of the forty grid far-field samples were analysed for PAHs and *n*-alkanes in 1989, which makes it impossible to compute standard errors. A pragmatic solution is to combine Zones 5 and 6, Zones 10 and 11, and Zones 12 and 16, each of which then have two samples. The mean far-field concentration with approximate 95% confidence intervals is then computed as if the data had come from a stratified random survey of these three larger Zones.

The means and 95% confidence intervals are shown below (Figures 6.2 and 6.3).

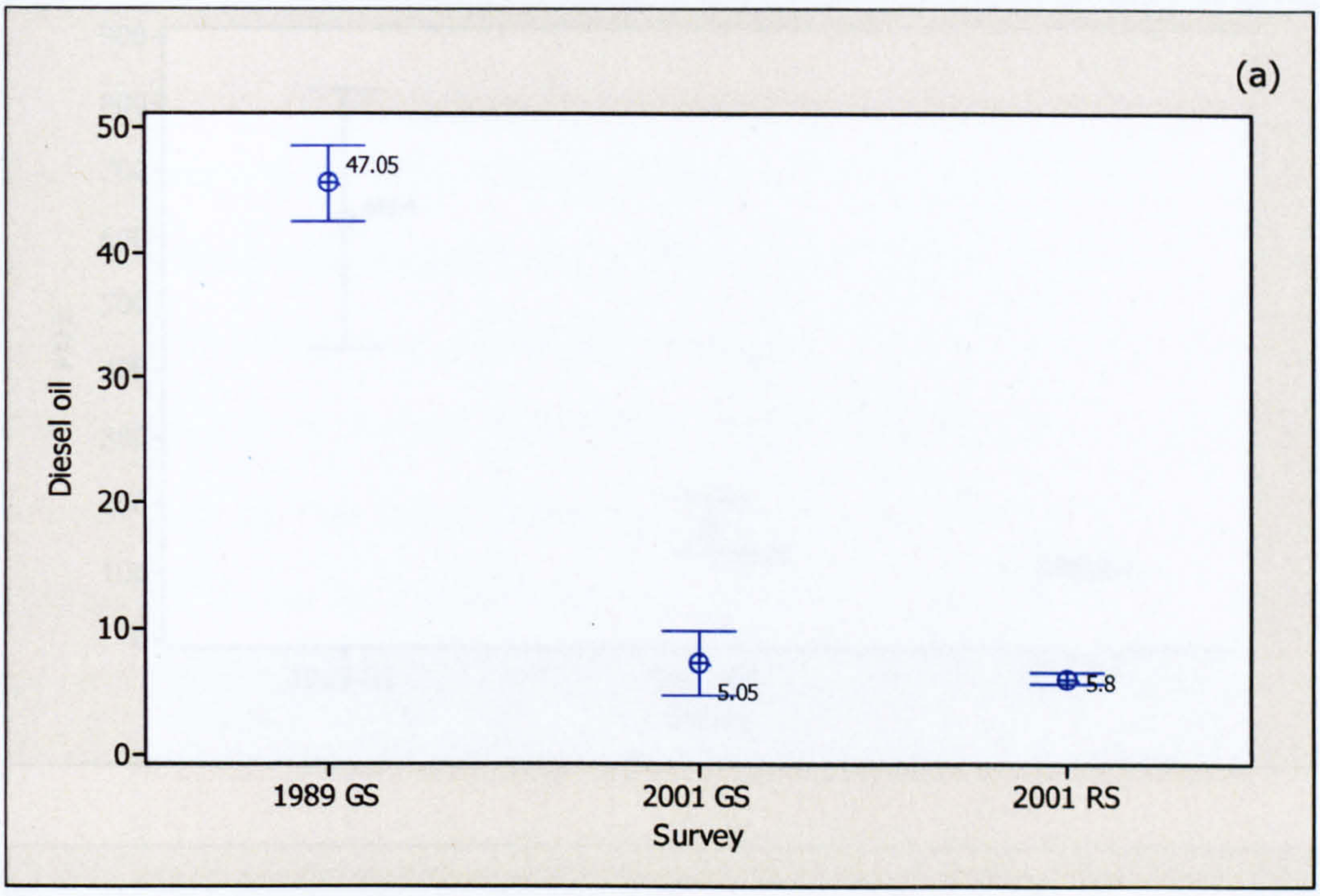

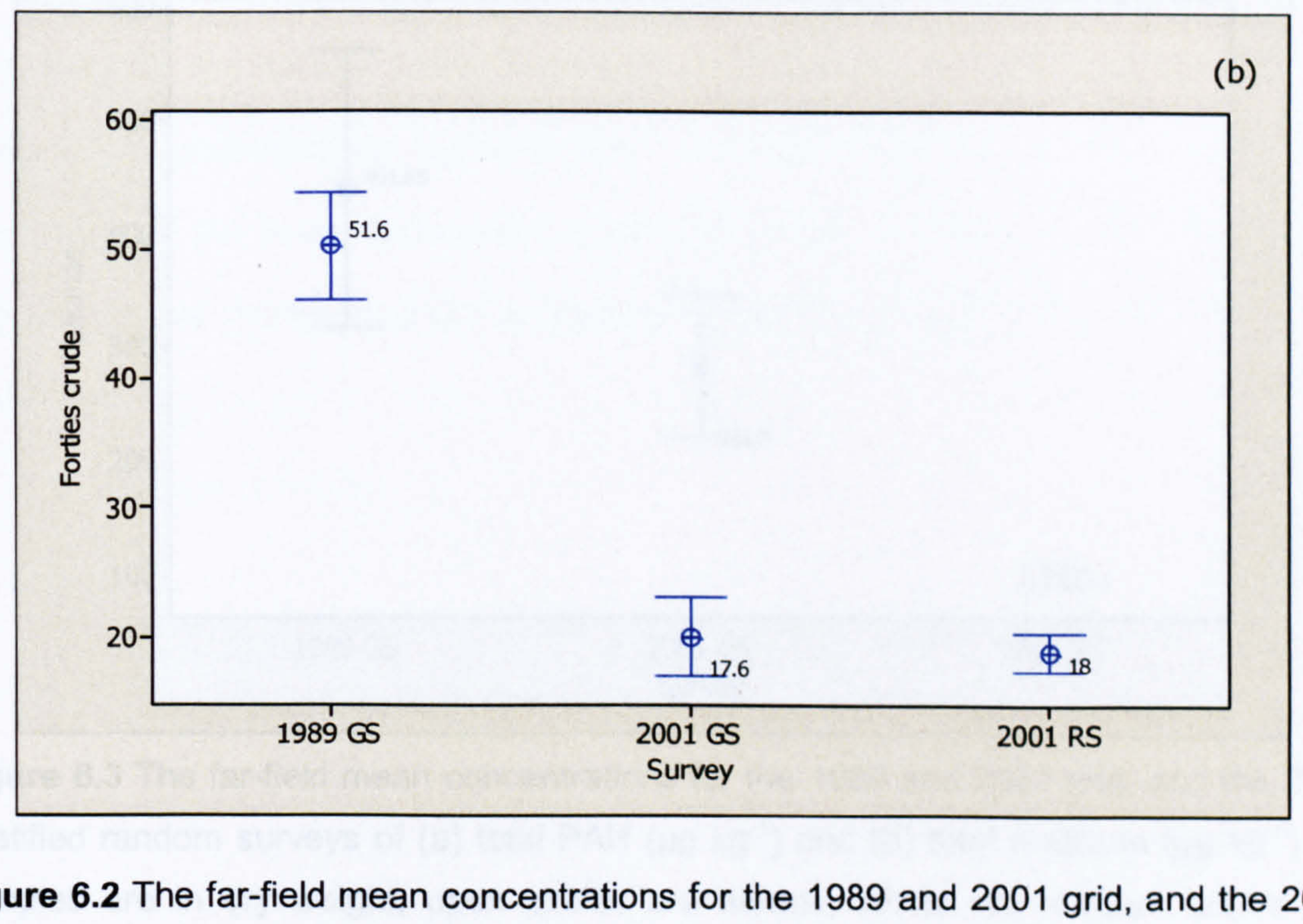

Figure 6.2 The far-field mean concentrations for the 1989 and 2001 grid, and the 2001 stratified random surveys of (a) Forties crude oil equivalent (μg g^{-1}), (b) diesel oil equivalent (μg g^{-1}). All samples are in dry weight, open circles are means, labels are median values and vertical lines are the 95% confidence intervals.

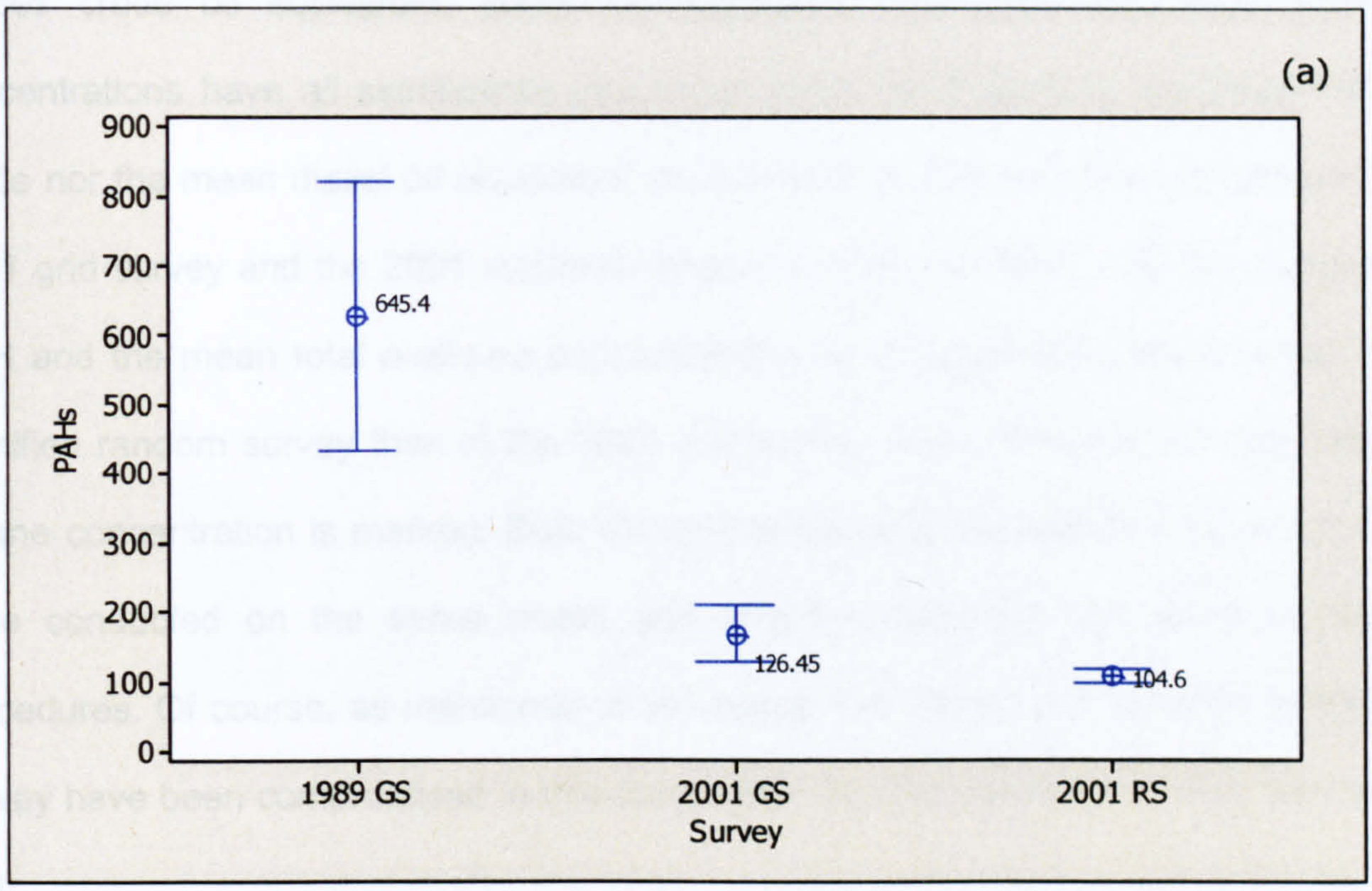

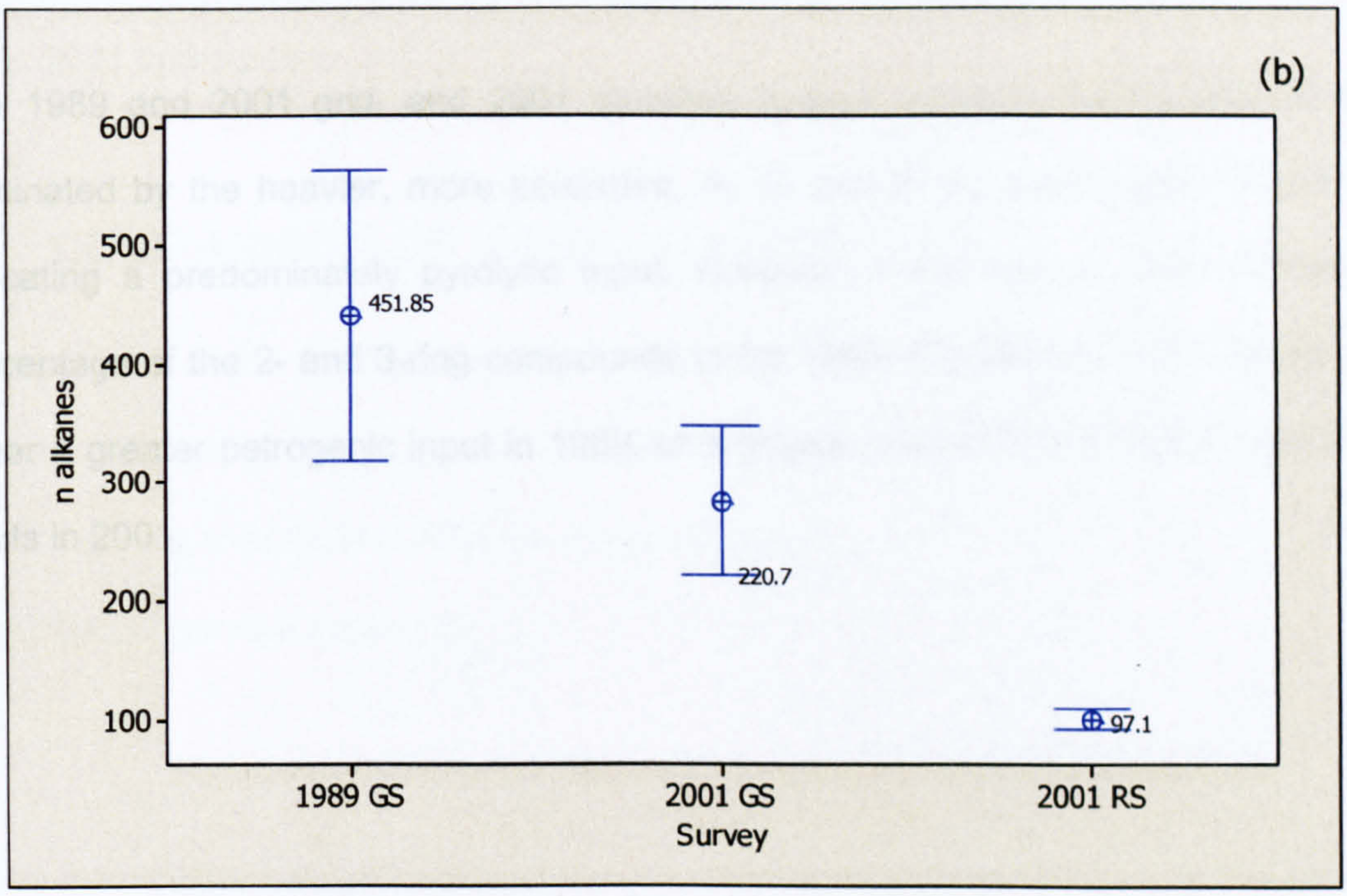

Figure 6.3 The far-field mean concentrations for the 1989 and 2001 grid, and the 2001 stratified random surveys of (a) total PAH (μg kg^{-1}) and (b) total *n*-alkane (μg kg^{-1}). All samples are in dry weight, open circles are means, labels are median values and vertical lines are the 95% confidence intervals.

Forties crude oil equivalent, diesel oil equivalent, total PAH and total *n*-alkane concentrations have all significantly decreased since 1989. Neither the mean Forties crude nor the mean diesel oil equivalent concentrations differ significantly between the 2001 grid survey and the 2001 stratified random survey. However, both the mean total PAH and the mean total *n*-alkane concentrations were significantly lower in the 2001 stratified random survey than in the 2001 grid survey. The difference in mean total *n*-alkane concentration is marked. Both the grid survey and the stratified random survey were conducted on the same cruise and analysed following the same accredited procedures. Of course, as mentioned at the outset, the design and purpose of the grid survey have been compromised in this comparison by only using the far-field part of the grid.

The 1989 and 2001 grid, and 2001 stratified random surveys, PAH profile of were dominated by the heavier, more persistent, 4-, 5- and 6-ring compounds (Figure 6.4) indicating a predominately pyrolytic input. However, there was a slight increase in percentage of the 2- and 3-ring compounds in the 1989 compared to 2001. Suggesting either a greater petrogenic input in 1989, or a greater degradation of the 2- and 3-ring PAHs in 2001.

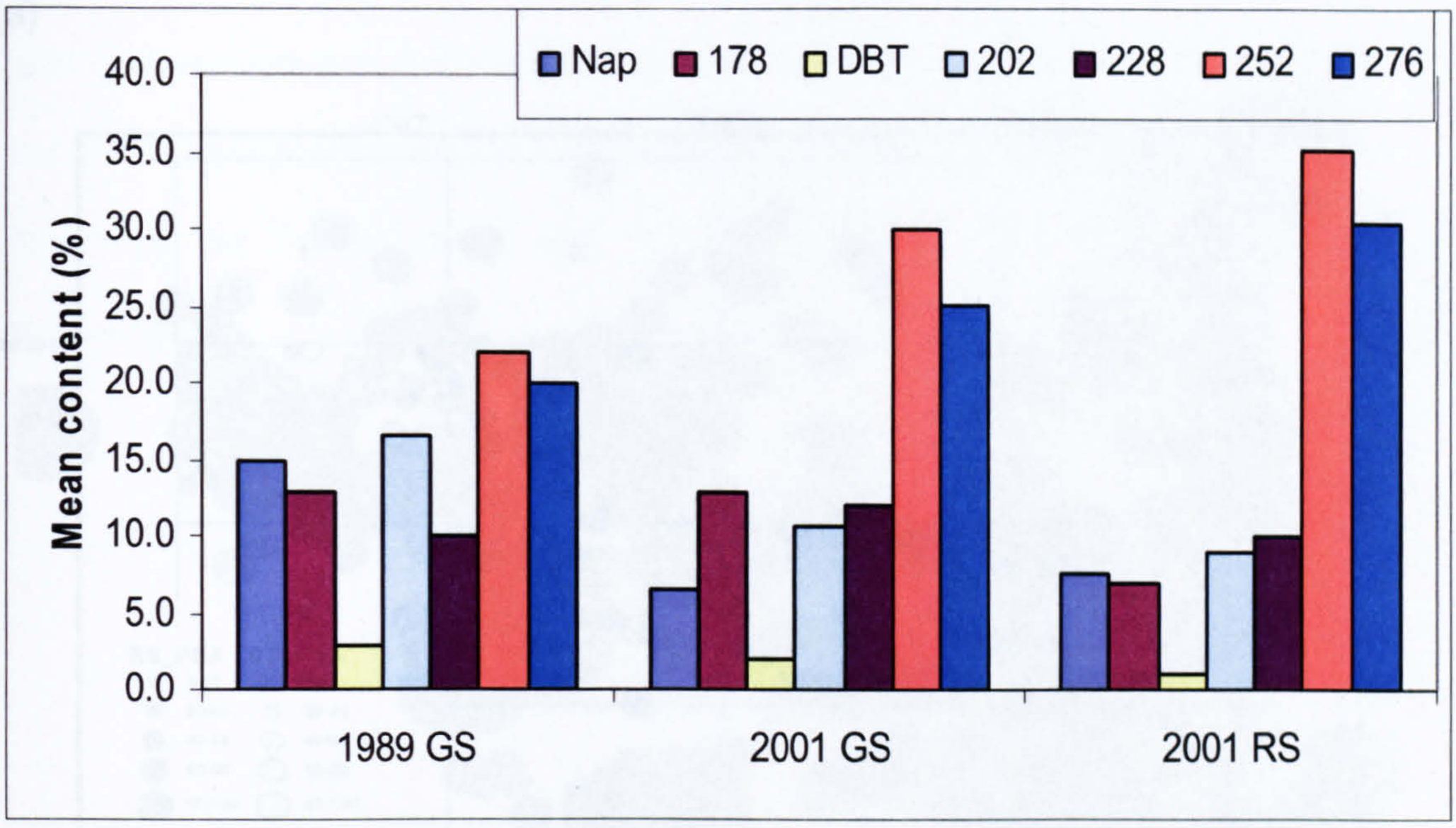

Figure 6.4 PAH profile for the common areas for the 2001 stratified random and the 1989, 2001 grid surveys.

6.3 COMPARISON OF SAMPLING SURVEYS

In comparison of the 2001 grid and 2001 random stratified sampling (Appendix 5), there were no significant differences ($p > 0.05$; ANOVA) in spatial distribution in both the percentage organic carbon (TOC) and percentage of < 63 μm fraction of the particle size (PSA) (Figures 6.5a and b).

(a)

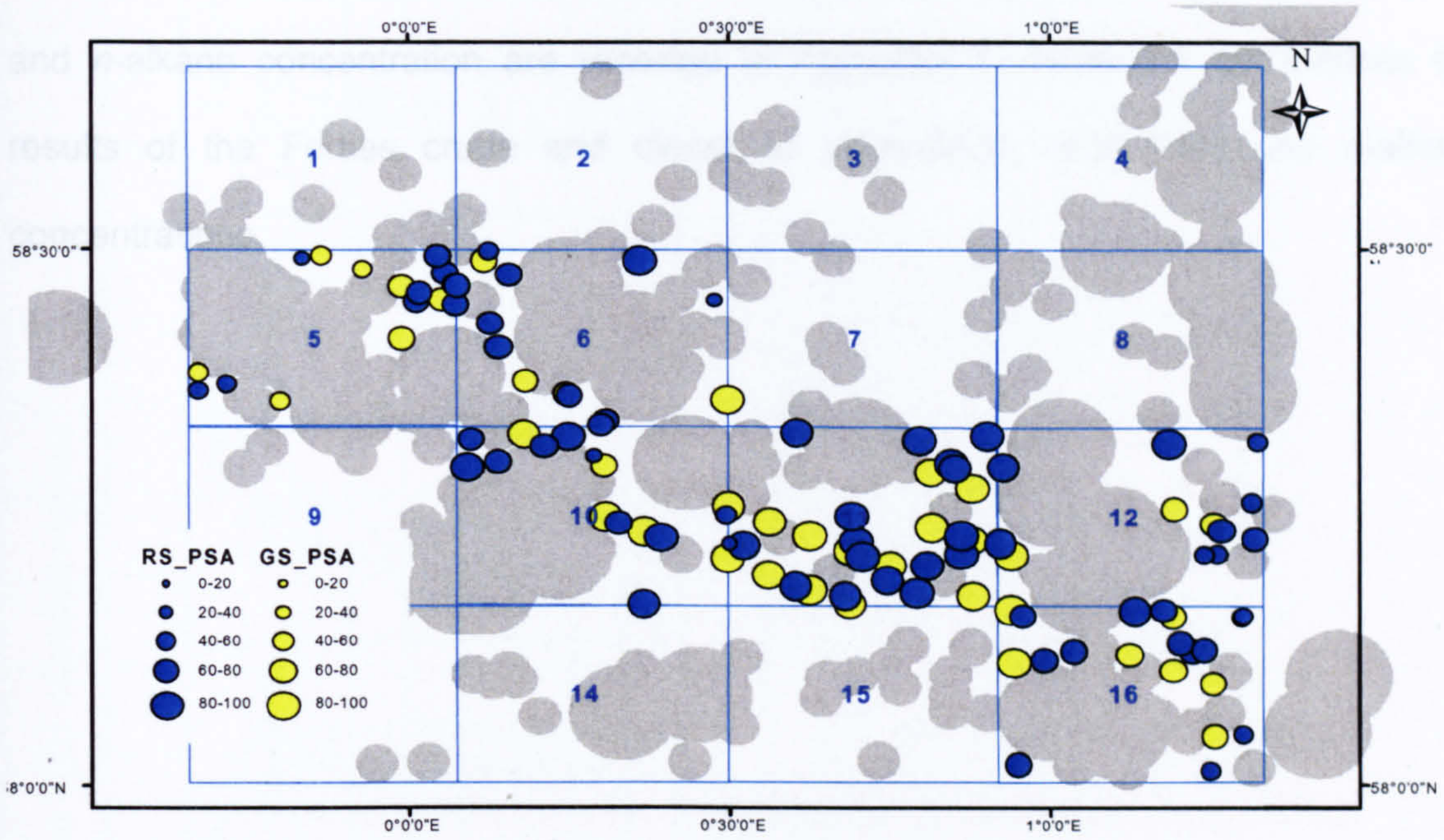

(b)

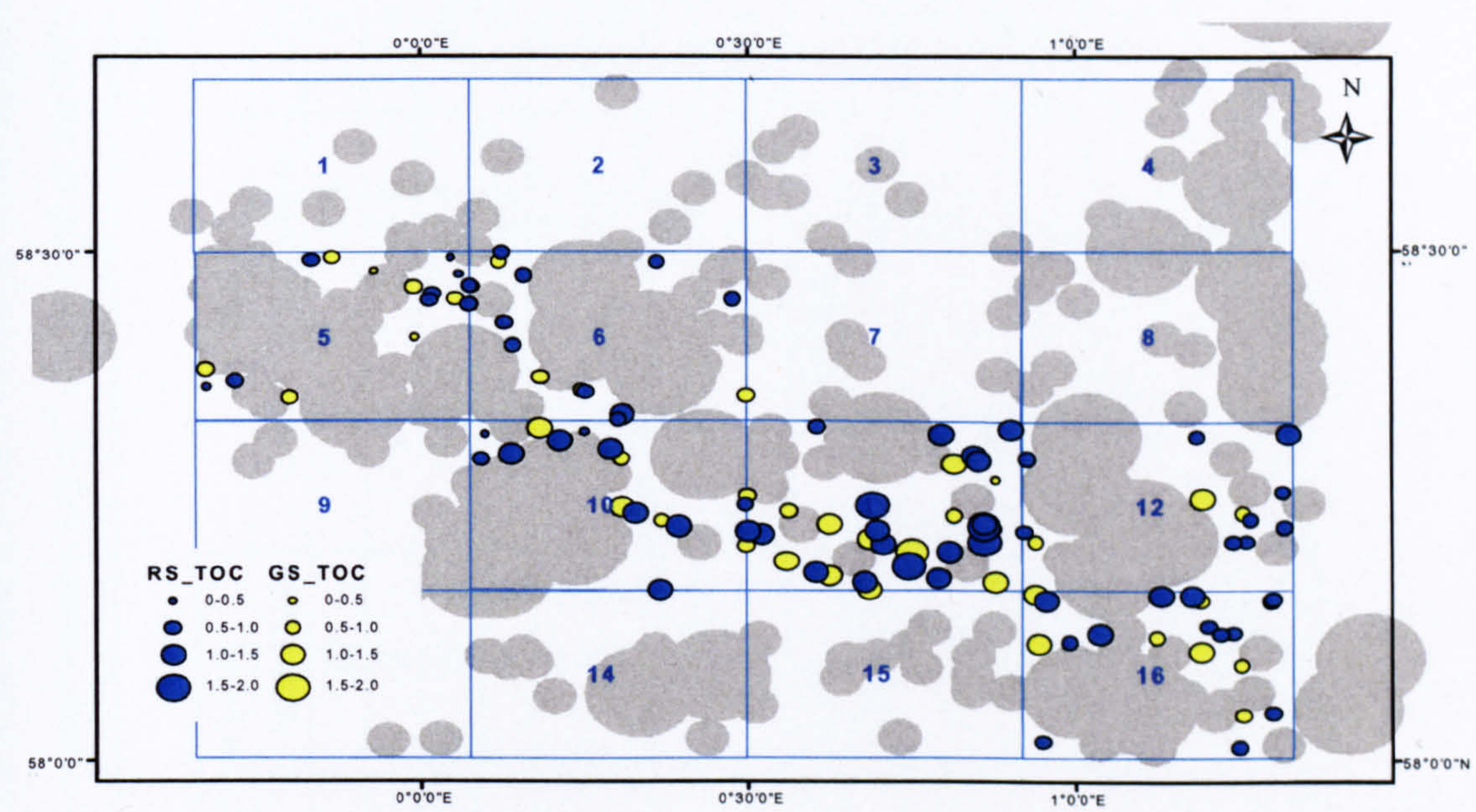

Figure 6.5 Spatial distribution of (a) PSA of < 63 μm (%) (b) TOC (%). Large grey circles are < 5km radius of multiple oil wells and small grey circles are < 2km radius of a single oil well. Yellow and blue circles are proportional to percentage content in the grid and stratified sampling surveys. Note there were no differences between the 2001 grid (GS) and 2001 stratified random (RS) surveys.

The Forties crude and diesel oil equivalent concentrations for the common areas of the 2001 grid and random stratified surveys are reported in Appendix 6 and the total PAH and *n*-alkane concentration are reported in Appendix 7. Table 6.1 summarises the results of the Forties crude and diesel oil equivalents, total PAH and *n*-alkane concentrations.

Table 6.1 Summary of the mean and standard deviation of the Zones for Forties crude and diesel oil equivalent (μg g^{-1} dry weight), total PAH and total *n*-alkane concentrations (μg kg^{-1} dry weight) of the 2001 grid and 2001 stratified surveys.

Mean										
Zones	No. of samples		Forties		Diesel		Total PAH		Total *n*-alkane	
	Grid	Stratified	Grid	Stratified	Grid	Stratified	Grid	Stratified	Grid	Stratified
5	7	10	12.2	14.5	5.6	7.0	88.0	131.4	144.8	64.7
6	4	9	16.0	18.2	4.1	5.2	101.2	87.0	193.8	100.2
10	6	11	16.9	20.6	24.9	6.3	128.7	101.2	308.9	107.5
11	12	17	24.0	22.2	5.9	6.5	266.6	134.4	439.0	118.6
12	4	9	20.6	17.1	5.1	5.0	168.8	85.2	211.2	79.0
16	7	13	18.5	17.5	5.6	5.3	145.7	86.6	225.5	106.7
Total	40	69	20.0	18.7	7.2	6.0	167.2	107.0	283.3	99.2
Standard Deviation										
Zones	No. of samples		Forties		Diesel		Total PAH		Total *n*-alkane	
	Grid	Stratified	Grid	Stratified	Grid	Stratified	Grid	Stratified	Grid	Stratified
5	7	10	3.3	3.7	5.2	1.8	25.2	52.5	65.5	18.19
6	4	9	0.6	4.1	0.2	1.2	14.3	23.4	38.8	37.4
10	6	11	9.1	8.7	17.2	2.5	98.4	26.6	189.9	29.5
11	12	17	11.8	5.3	1.7	1.4	178.6	23.9	255.7	42.8
12	4	9	2.3	4.9	0.4	1.2	49.4	31.5	63.8	34.2
16	7	13	10.3	6.2	2.0	1.7	82.8	38.5	113.2	32.0
Total	40	69	9.5	5.5	7.8	1.6	128.5	31.4	197.7	33.5

The boxplots of Forties crude and diesel oil equivalents shows no significant differences in the mean concentrations of the 2001 grid and 2001 stratified random surveys (Figures 6.2a and b). However, there was significant difference in the mean of the total PAH and total *n*-alkane concentrations, for the 2001 grid and 2001 stratified random surveys (Figures 6.3a and b). Figure 6.6 shows spatial distribution of total PAH and *n*-alkane concentrations in the common areas of the stratified random and grid surveys, all the samples in the stratified random survey had concentrations below 200 μg kg^{-1} dry weight for the total PAH and *n*-alkane concentrations. However, in the grid survey considerable amount of sediments samples had concentration above 200 μg kg^{-1} dry weight for both total PAH and *n*-alkane, especially in Zone 11, where some samples had concentrations above 400 μg kg^{-1} dry weight for both total PAH and *n*-alkane. Sample from this Zone had to be re analysed to find out, if there was any lost in hydrocarbon due to storage, the result shows no lost due to storage. Therefore, the conclusion is that there was a higher input of hydrocarbon in that particular site.

(a)

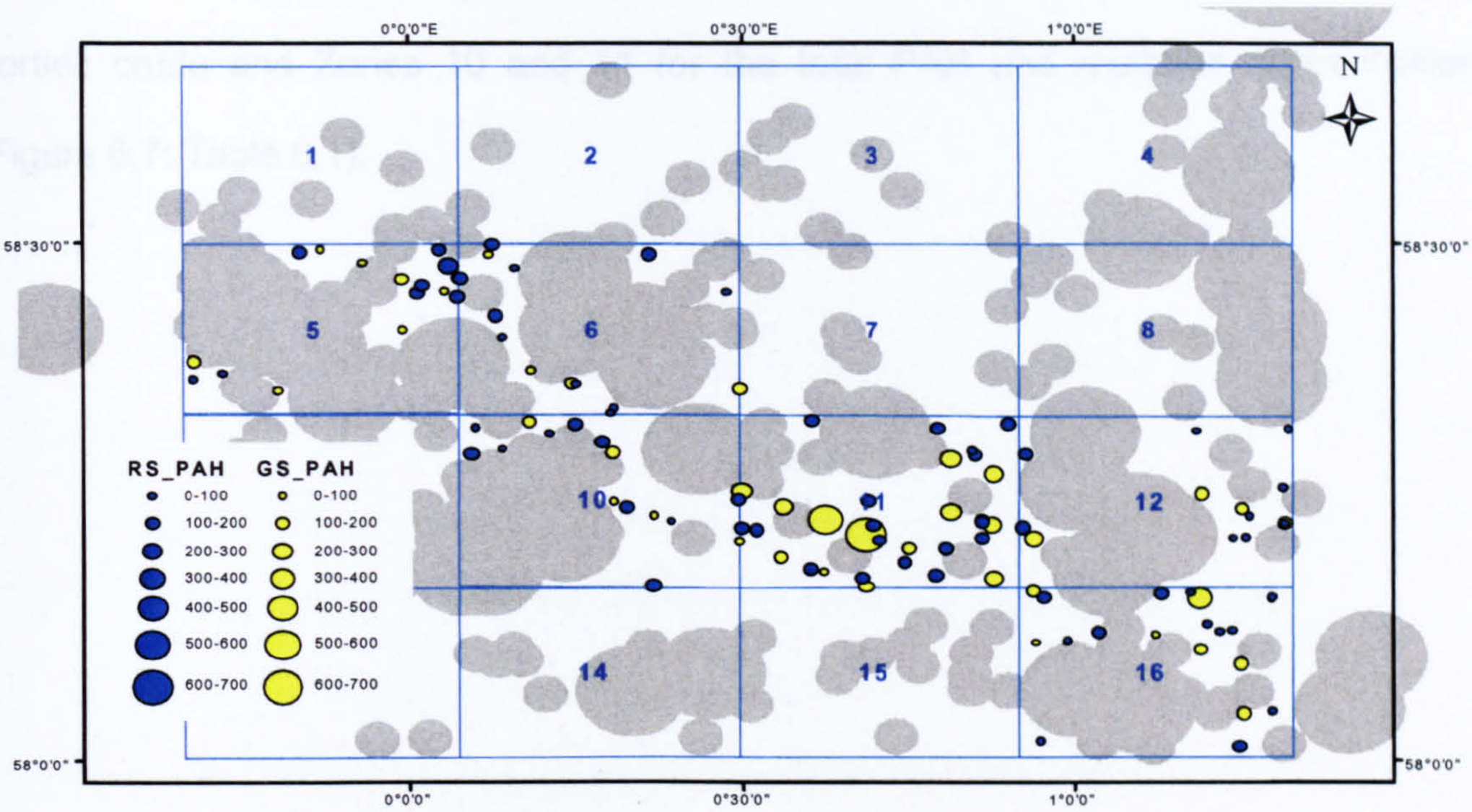

(b)

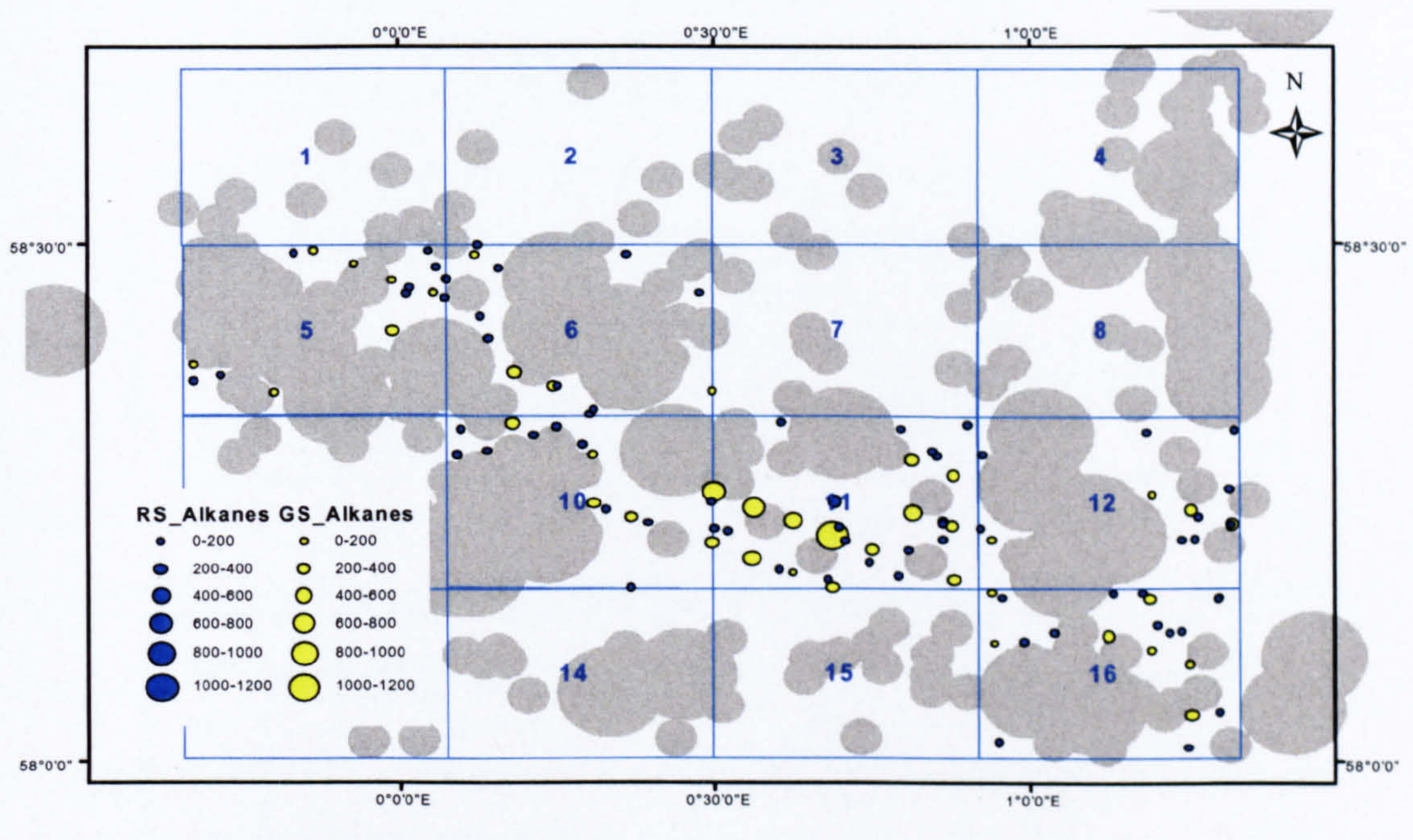

Figure 6.6 Spatial distributions in μg kg^{-1} dry weight of (a) total PAH and (b) total *n*-alkane (nC_{12} - nC_{33}) comparing the 2001 grid (GS) and 2001 stratified (RS) surveys. Large grey circles are < 5km radius of multiple oil wells and small grey circles are < 2km radius of a single oil well. Yellow and blue circles are proportional to concentrations in the grid and stratified sampling surveys. Note the significant difference between the grid and stratified surveys in Zone 11 ($p > 0.05$; ANOVA).

For precision of the two sampling regimes, the standard deviation was plotted against the Zones, and significant variation was observed in Zone 10 for the diesel, Zone 11 for Forties crude and Zones 10 and 11 for the total PAH and *n*-alkane concentrations (Figure 6.7; Table 6.1).

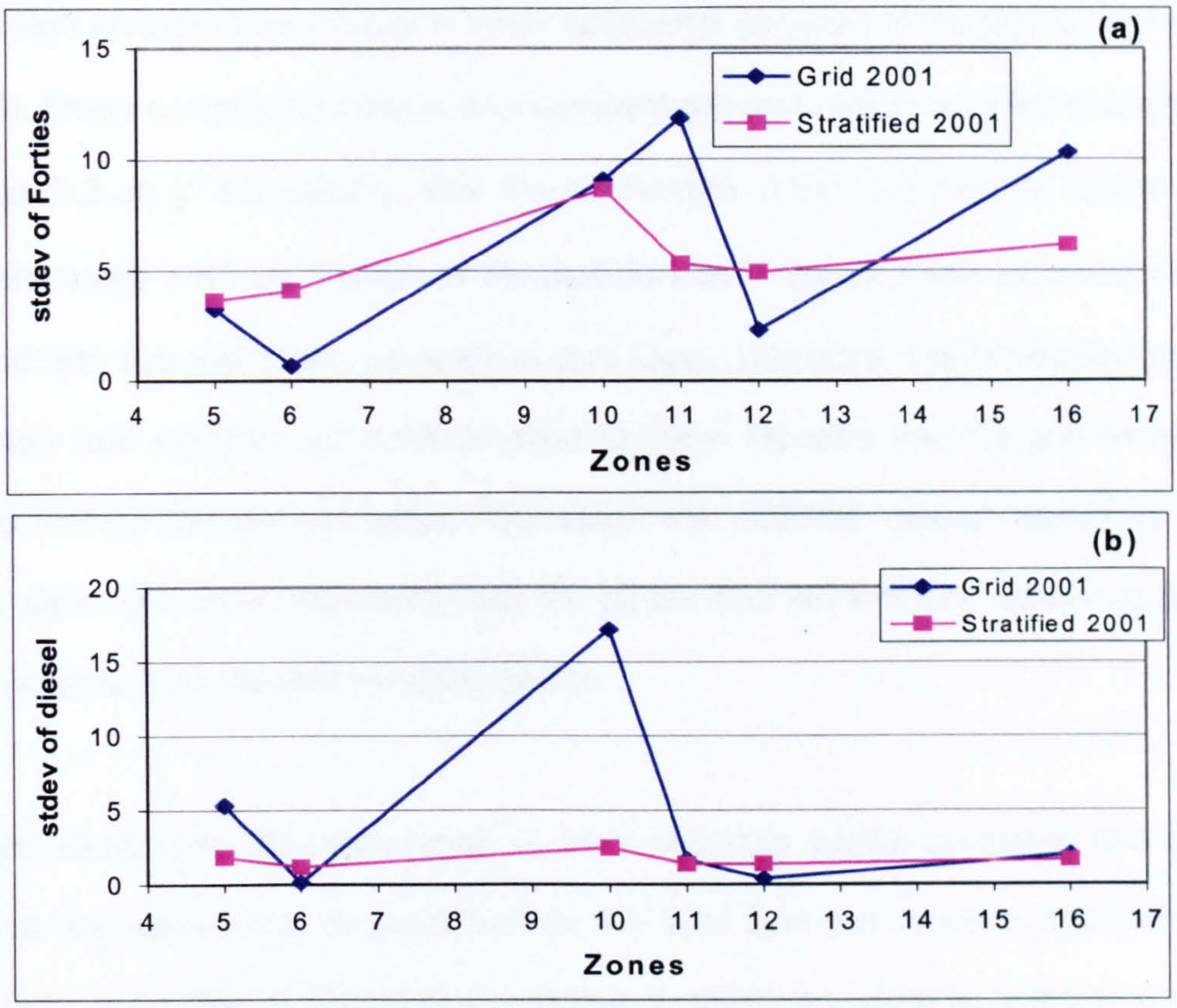

Figure 6.7 Variation of the sample population over the Zones shown within grid and stratified sampling, (a) Forties, (b) diesel, (c) PAHs and (d) *n*-alkanes.

The high variations in Zone 11 for the Forties crude, total PAH and *n*-alkanes may be due to high concentrations value in three sediments samples of the grid survey (43, 44 and 45). These samples had diesel oil equivalent concentrations close to the overall grid average (7.2 μg g^{-1} dry weight). Also the percentage of the total organic carbon (TOC) and percentage > 63 μm fraction of the particle size (PSA) of these sediments are not different with the rest of the samples in that Zone. Therefore, the conclusion must be that there was a higher hydrocarbon input to these samples and the grid design was able to identify the hotspot areas. Therefore, the stratified random sampling design clearly gave less mean concentrations for all the four parameters, achieving a much lower variance than the grid sampling design.

The grid design has the advantages of more complete spatial coverage, and is more practical and convenient to implement in the field than the random stratified design (especially when little or no previous information exists on which to optimise a random stratified design). The grid design also has the advantage of being able to identify hotspots, as observed. Perhaps more importantly, it would be possible to estimate the probability of detecting hotspots of particular sizes. Because sampling in a grid design is inherently biased, it is possible to overestimate or underestimate a population characteristic aligned with the grid as observed in the analyses. The grid design often requires statistical analysis that is based on assumptions that are difficult to substantiate. The stratified design can be cost and time effective, and can produce estimates with increased precision and lower variance (Figure 6.7) compare to the grid design. However, optimal design of stratified sampling programmes requires reliable prior knowledge of the population in order to effectively define the Zones and to allocate the most appropriate sample numbers to Zones.

The increase in precision, or alternatively reductions in time and cost, obtainable through stratified random sampling, depends on the quality of the information used to set up the design. Any possible increases in precision are particularly dependent on strength of the correlation of the auxiliary stratification variable with the variable observed in the study. In this study, stratification was primarily made on arbitrary geographical grounds (defining sampling Zones). As a secondary step, samples were confined to far-field areas. This secondary step was based upon the concept that concentrations of the variables of interest (primarily hydrocarbons) might well be greater close to discharges from oil installations. This is undoubtedly true, in that many surveys have shown accumulation of cuttings and associated hydrocarbons close to oil installations and that the main area of interest was the potential contamination of the seabed out with the immediate surroundings of installations. However, there may be some scope for reconsideration of the criteria used to define near and far field sites.

A potentially more powerful form of stratification might be designed around the relationships between chemical contaminants and supporting variables such as particle size, organic carbon and water depth. However, while these approaches may be statistically attractive, designs which require the collection of defined numbers of samples of particular particle size (for example) could present significant practical difficulties in the field.

6.3.a Sample size

The following table (Table 6.2) illustrates how the precision (expressed as the % coefficient of variation) of estimates of mean concentration depends on the total sample size (*n*) based on the variability observed in the 2001 stratified random survey.

Table 6.2 Summary of the precision of the estimation of mean concentration on the total sample size, express as the % coefficient of variable.

n	% coefficient of variation			
	Forties crude	Diesel	Total PAH	Total *n*-alkane
16	8	8	10	15
32	6	5	7	10
48	5	4	6	9
100	3	3	4	6
242	2	2	2	4

The choice of sample size will depend on the objectives of the survey. But to illustrate, consider a long-term surveillance monitoring programme to detect a 100% increase in hydrocarbon concentrations (should it occur). Sixteen samples per year would estimate the mean concentration of all four types of hydrocarbons with a coefficient of variation of 15% or better. And this would allow us to detect a 100% increase in concentration over ten or twenty years if the between-year coefficient of variation is 12% or 24% respectively (Nicholson *et al.*, 1997). (The between-year coefficient of variation is a measure of random fluctuations in mean concentrations from year to year due e.g. to fluctuating environmental conditions. It is difficult to estimate without a long time series, but UK National Marine Monitoring Programme data suggest that the between-year coefficient of variation for total PAH concentrations is typically somewhere between 10 and 30%).

Small sample sizes would necessitate some revision of the stratification to ensure sufficient samples within each stratum to estimate variances, standard errors etc. In the illustration above, an obvious change would be to combine the sixteen strata into four larger strata, i.e. Zones 1, 2, 5, 6, Zones 3, 4, 7, 8, Zones 9, 10, 13, 14, and Zones 11, 12, 15, 16.

6.3.b Sample allocation

In the 2001 stratified random survey, the number of samples in each Zone was chosen by *proportional allocation*, with the number of samples proportional to the available far-field area. However, there are other criteria that can be used to allocate numbers of samples to strata. In particular, knowing the variation in concentration between samples within Zones means that the number of samples can be chosen by *optimal allocation*. This allocation gives more samples to Zones with high variability and maximises the precision of the estimate of mean concentration for the whole far-field given a fixed total sample size *n*. If σ_h is the standard deviation in concentration between samples in Zone h, A_h is the far field area in Zone h, then the optimal allocation is

$$n_h = \frac{nA_h\sigma_h}{\sum_{k=1}^{16} A_k\sigma_k} \qquad \text{Equation 6.1}$$

Optimal allocations for estimating the mean concentrations of Forties crude, diesel, total PAH, and total *n*-alkanes, assuming a total fixed samples size of 242, are shown in Table 6.3. They suggest increasing the numbers of samples in Zones 4 and 8 and reducing the numbers of samples in Zones 13 and 15.

Note that strict adherence to optimal allocation can lead to problems for two reasons. First, the estimates of variability are themselves subject to error and will be inflated in some Zones just by chance. Second, when the total sample size is relatively small, the optimal allocation can give only one or two samples in some Zones, which makes it difficult to estimate levels of variability in these Zones.

Table 6.3 Optimum allocation of samples between strata/Zones to provide estimates of the population mean or total with the lowest variance for PAH, Forties crude, diesel and *n*-alkane analyses, assuming a fixed total number of samples (242). The numbers of samples for each of the variables are assessed individually, and are combined (averaged) to give an optimal number per Zone, treating all variables as of equal weight/importance.

Zones	Proportional allocation as performed	Optimum allocations (equation 4)				
		PAH	Forties	diesel	*n*-alkanes	Average
1	20	11	16	24	13	17
2	20	17	19	27	31	22
3	20	22	11	14	18	19
4	13	38	21	31	22	29
5	10	14	7	11	4	10
6	9	6	8	7	7	8
7	18	26	25	14	20	18
8	10	28	21	25	45	25
9	18	9	13	11	7	13
10	11	7	18	15	6	14
11	17	12	19	15	16	14
12	9	8	10	7	7	9
13	20	7	7	6	15	10
14	14	12	13	10	10	10
15	20	12	17	12	11	12
16	13	14	17	14	9	13
Total sample size	242	242	242	242	242	242

6.4 CONCLUSIONS

This study has highlighted the benefits and limitations of both sampling regimes in the oil and gas exploration and production areas. The grid design has the benefits of more spatial coverage, and is more practical and convenient to implement in the field than the stratified random design. The grid design was also able to identify hotspots, and, perhaps more importantly, it would be possible to estimate the probability of detecting hotspots of particular sizes. But because sampling in a grid design is inherently biased, it has the disadvantage that it is possible to overestimate or underestimate a population characteristic aligned with the grid. Also the grid design often requires statistical analysis

that is based on assumptions that are difficult to substantiate, and also missing stations arising, for example, from bad weather at sea or being located in near field areas are difficult to accommodate in the statistical analysis.

The stratified sampling design gave much more reliable mean concentrations for all the four parameters, achieving a much lower variance than the grid sampling design. The stratified design is cost and time effective, and produces estimates with increased precision (lower variance) compared to the grid sampling design. The increase in precision, or alternatively reductions in variance, time and cost, obtainable through stratified random sampling, depends on the quality of the information used to set up the design. Any possible increases in precision are particularly dependent on strength of the correlation of the auxiliary stratification variable with the variable observed in the study.

Spatial analysis will be applied in studying the pattern on spatial structure features of the hydrocarbon contaminated sediments in the Fladen Ground, using the stratified random surveys in chapter 7.

CHAPTER SEVEN

SPATIAL ANALYSIS FOR QUALITY ASSESSMENT OF THE HYDROCARBONS

7.1 INTRODUCTION

Geographical distribution of the concentration and composition of hydrocarbons is an important element of an assessment of the quality of the marine environment. A number of mathematical methods are available for carrying out such study using data obtained through sampling and chemical determination of hydrocarbons. Among the methods, spatial structure analysis has been widely identified as a useful tool in illustrating the spatial patterns of the variables (Wang and Qi, 1998). It is also an important basis for a number of other spatial analysis procedures, such as kriging analysis. Descriptive statistics and histograms (Figure 7.1) will not give information on the spatial patterns of the hydrocarbons (Caeiro *et al.*, 2003). One can fit trend surfaces to spatial data of ever increasing order, and eventually analysis by ANOVA at some specified level of significance, trend surfaces of increased order will not provide a statistically significant improvement in the fit to the data. The weights and neighbourhood of trend is dependent upon the variogram of the data. The degree of spatial continuity of the data (regionalized variables) is given by the variogram. In this chapter, spatial analysis was applied to the pattern of spatial structure features of the hydrocarbon contamination in sediments from the Fladen Ground. The aim of this chapter is to explore patterns in the structural analysis of the hydrocarbons contamination measured in the Fladen ground.

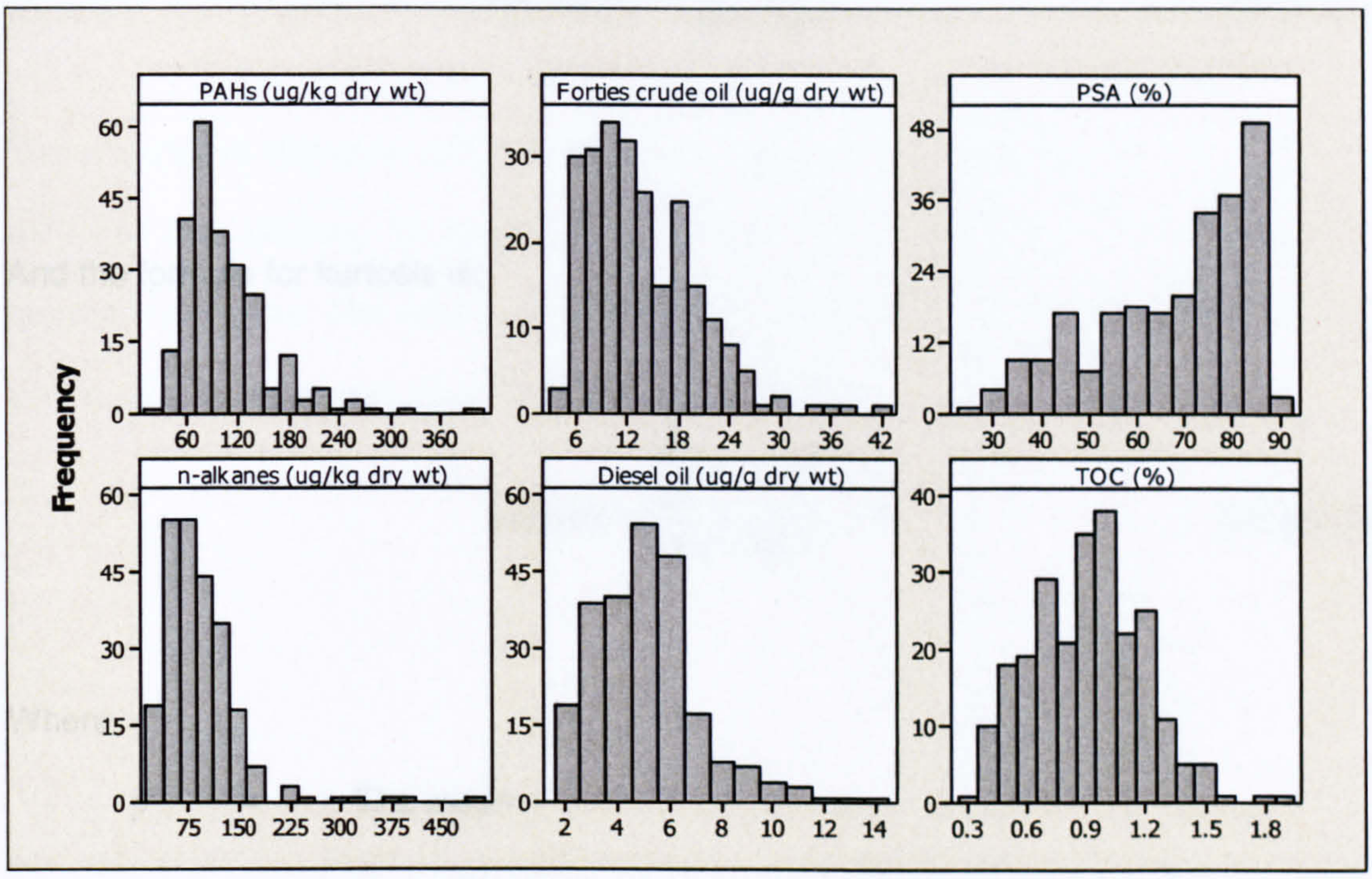

Figure 7.1 Histogram of the parameters measured for the whole Fladen Ground.

7.1.a Statistical Distributions

Statistical parameters describe the shape of a random variable's probability density function (PDF). The Skewness is a measure of the degree of asymmetry of a distribution. A distribution, or data set, is symmetric if it looks the same to the left and right of the center point. Kurtosis is a measure of the degree of peakedness of a distribution. A distribution with a high peak (> 0) is termed *leptokurtic*, a flat-topped curve (< 0) is termed *platykurtic*, and the normal distribution (kurtosis = 0) is *mesokurtic*.

For univariate data, the formula for skewness is:

$$skewness = \frac{\sum_{i=1}^{N}(y_i - \bar{y})^3}{(N-1)s^3} \qquad \text{Equation 7.1}$$

And the formula for kurtosis is;

$$kurtosis = \frac{\sum_{i=1}^{N}(y_i - \bar{y})^4}{(N-1)s^4} - 3 \qquad \text{Equation 7.2}$$

Where

$\bar{y}$ = The mean

y_i = The y^{th} sample

s = The standard deviation

N = The number of samples.

The calculated values of the skewness (Table 7.1) and kurtosis (Table 7.2) shows that the bulk sediment characteristics (i.e. organic carbon content and particle size) are normally distributed (Figure 7.1) with a low coefficient of variance (see section 5.3.d). However, the PAHs and *n*-alkanes concentrations (Figure 7.1), showed a sharp peak (Table 7.2), highly skewed to the right (Table 7.1), weak continuity and a large coefficient of variance (see sections 5.3.f and 5.3.i). Similar results were observed in the distributions of Forties crude oil equivalents and of diesel oil equivalents, but with less marked peaks. The highly

skewed results show that there are *outlier* values, which may cause erratic and unstable estimates of the variance.

The descriptive statistics and histograms do not incorporate the spatial locations of the data into their defining computations, as shown above. The variogram is a quantitative descriptive statistic that can give graphical representation and characterise the spatial continuity (i.e. roughness) of data (Christakov, 2001).

Table 7.1 Skewness of the TOC, PSA, diesel, Forties crude, PAHs and *n*-alkanes for each of the Zones and the Overall sediment samples for the stratified random sampling in the Fladen Ground.

Zones	No of samples	TOC	PSA	Diesel	Forties	PAHs	*n*-alkanes
1	20	0.31	0.30	1.60	1.34	0.39	0.65
2	20	0.44	-1.30	0.77	0.86	0.50	1.30
3	20	0.21	-0.79	0.62	0.20	1.45	0.62
4	13	-0.11	-0.60	0.26	0.19	0.80	2.67
5	10	-0.39	-1.13	-0.34	0.35	2.17	-0.95
6	9	-0.40	-2.35	-0.32	-0.30	0.61	0.98
7	18	0.82	-0.20	0..00	1.36	0.47	1.24
8	10	-0.58	-0.56	2.60	1.93	1.73	0.97
9	18	0.55	0.21	0.19	0.26	-0.13	1.83
10	11	-0.55	-0.71	1.26	1.29	-0.13	0.46
11	17	1.01	0.30	0.83	1.15	0.45	2.37
12	9	0.73	-0.12	0.37	0.40	0.88	1.30
13	20	0.29	-0.11	0.40	0.85	0.18	2.87
14	14	0.90	-1.45	0.23	1.76	2.48	0.89
15	20	0.33	-0.16	0.25	0.86	0.50	0.21
16	13	0.26	-0.11	1.83	1.75	1.0	0.03
Total	242	0.34	-0.71	1.08	1.10	1.85	2.89

Table 7.2 Kurtosis of the TOC, PSA, diesel, Forties crude, PAHs and *n*-alkanes for each of the Zones and the Overall sediment samples for the stratified random sampling in the Fladen Ground.

Zones	No of samples	TOC	PSA	Diesel	Forties	PAHs	*n*-alkanes
1	20	-0.44	0.54	3.72	1.66	-0.53	-0.66
2	20	2.01	1.81	0.01	0.09	-0.24	1.69
3	20	-0.50	0.34	0.24	-0.63	3.49	0.17
4	13	-1.00	-1.77	-0.64	-0.96	1.72	8.12
5	10	-2.04	-0.18	-1.22	-1.01	5.58	2.65
6	9	1.03	6.50	-1.30	-1.43	-0.36	1.20
7	18	-0.42	-0.93	0.70	3.84	-0.10	1.45
8	10	-0.45	-0.25	7.22	3.69	3.50	-0.70
9	18	0.81	-1.63	-0.48	-0.35	-0.57	5.63
10	11	-0.67	-1.62	2.90	2.69	0.22	0.84
11	17	0.72	1.61	1.50	1.65	-0.01	7.41
12	9	-0.36	-0.95	-1.72	-1.65	0.63	1.09
13	20	-1.12	-0.54	-0.41	0.89	-0.13	9.53
14	14	0.42	1.33	-0.03	3.87	6.97	0.22
15	20	-0.21	-1.21	0.21	0.09	-0.49	0.01
16	13	-1.58	-1.40	5.64	4.49	0.11	-0.86
Total	242	0.12	-0.59	2.17	1.71	5.66	13.60

7.2 DATA ACQUISITION AND ANALYTICAL METHOD

7.2.a Data Acquirement

The 2001 Fladen Ground stratified random sampling survey data were used. Data were analysed using the SURFER® Golden software version 8 for the experimental variance and theoretical variogram using the linear model. MINITAB® software version 14 was used create contour maps (Kriging analysis).

7.2.b Analytical Method

The variogram characterizes the spatial continuity or roughness of a data set (Webster and Oliver, 2001). In kriging, a variogram is first constructed using a spatial set of data e.g. the sediment data from the Fladen Ground. A variogram has two parts: an experimentally-derived component data and a theoretical (model) component (Houlding, 2000). An experimental variogram is constructed by first calculating the variance of each point in the data set with respect to each of the other points. The experimental variogram consists of the plotted variances versus the distance between each data point at the site. The model variogram is curved line through the experimental variogram points. The model represents a simple mathematical function modeling the trend in the points of the experimental variogram (Chiles and Delfiner, 1999). The variogram applied in kriging can be used to calculate the expected error of the estimation at each target interpolation point since the estimation error is a function of the distance to surrounding data points. The mathematical definition of variogram is (the average squared difference of values separated approximately by lag distance (h):

$$\gamma(\Delta x, \Delta y) = \frac{1}{2}\varepsilon\left[\{Z(x+\Delta x, y+\Delta y) - Z(x,y)\}^2\right] \qquad \text{Equation 7.3}$$

Where

$Z(x,y)$ = value of the variable at location (x,y)

x = Longitude

y = Latitude

ε = the statistical expectation operator.

There are also theoretical variograms which model the structure of the underlying correlation between data points:

Exponential Model

$$\gamma(h) = c_o + c\left(1 - e^{-\left(\frac{h}{a}\right)}\right) \qquad \text{Equation 7.4}$$

Spherical Model

$$\gamma(h) = c_o + c\left[\frac{3}{2}\frac{h}{a} - \frac{1}{2}\frac{h^3}{a^3}\right] \qquad \text{Equation 7.5}$$

Linear Model

$$\gamma(h) = c_o + bh \qquad \text{Equation 7.6}$$

Where,

c_o = the nuggets

c = the sill

a = the range of the variogram model

h = lag distance

b = the slope.

Three parameters define the variogram:

Nugget (c_o): represents unresolved, sub-grid scale variation or measurement error and is seen on the variogram as the intercept of the variogram.

Range (a): The scalar that controls the degree of correlation between data points, usually represented by as a distance.

Sill (c): the value of the variance as the lag (h) goes to infinity; it is equal to the total variance of the data set.

The relationship between the variogram and covariance is:

1. Correlation is zero when the variogram value approaches the sill
2. The correlation is positive when the variogram value is less than the sill
3. The correlation is negative when the variogram exceeds the sill.

7.2.c Variogram Behaviour

The primary variogram behaviours are as follows:

⇒ *Randomness or lack of spatial correlation*: The variations have no spatial correlation, and these random variations are the results of deterministic process. The processes are highly non-linear and chaotic leading to variations that have no spatial correlation structure. Typically, only a small portion of the variability is explained by random behaviour. This type of variogram behaviour is called *nugget effect.*

⇒ *Sediment trends*: All environmental processes impart a trend in the distribution of physical properties, e.g., particle size. Such trends can cause the variogram to show a negative correlation at large distances. In fine/coarse sediments, the sediments size is negatively correlated with the availability of the hydrocarbons

due to their hydrophobic and stable chemical properties. The large negative correlation can cause the variance to increase beyond the sill variance.

⇒ *Areal trends*: These have an influence on the vertical variogram, i.e., the vertical variogram will not encounter the full variability of the sediments property being considered. There will be a positive correlation below the sill variance for large distances in the vertical direction. This type of behaviour is called *zonal anisotropy*.

7.3 RESULTS AND DICUSSION

The experimental variograms obtained from the Fladen ground data are shown in Figures 7.2 – 7.4. As illustrated in Figures 7.2 and 7.4, the sediments experimental variograms shows a well defined structure with variogram increasing with lag distance for TOC, PSA, and Forties crude and diesel oil equivalents and total PAHs concentrations. But in the total *n*-alkane concentrations there was lack of spatial correlation structure (Figure 7.4b). Nugget effects were observed in all the variogram of the PSA, TOC, Forties crude and diesel oil equivalents, total PAHs and total *n*-alkane concentrations. There were trends in the results of the PSA, TOC, Forties crude and diesel oil equivalent, and as well as the total PAH concentrations. The existence of a trend was suggested by lack of attainment of a sill in the variogram. As the distances between data pairs increase, the differences between data values also systematically increase. Therefore the experimental variogram does not have a sill value (it is infinite); they cannot be used in simulation algorithms such as sequential Gaussian simulation (exponential and spherical models).

The linear model of the variograms was chosen as the theoretical variogram, because a linear model gives the best results when using a real experimental data which contain experimental errors (Glover *et al.*, 2004). In this model, the data do not support any

evidence for a sill or range but rather appear to have increasing variance as the lag distance increases. This is a key sign that the proper choice for a particular data set is the linear model. The linear model is concerned with the slope and intercept of the experimental variogram (Equation 7.6). The slope (b) is nothing more than the ratio of the sill (c) to the range (a).

The slope of the linear model of the parameters measured were 2.5 for the PSA and 0.1 for TOC, 12.3 for the oil equivalents of Forties crude and 2.1 for the oil equivalents of diesel. The total PAH concentrations has slope of 742.0 and 0 for and total *n*-alkane concentrations. There was no correlation between the variogram and the covariance for the total *n*-alkane concentration, because the value of the slope was 0, this shows that the variogram was equal to the nugget for the total *n*-alkane concentrations.

(a)

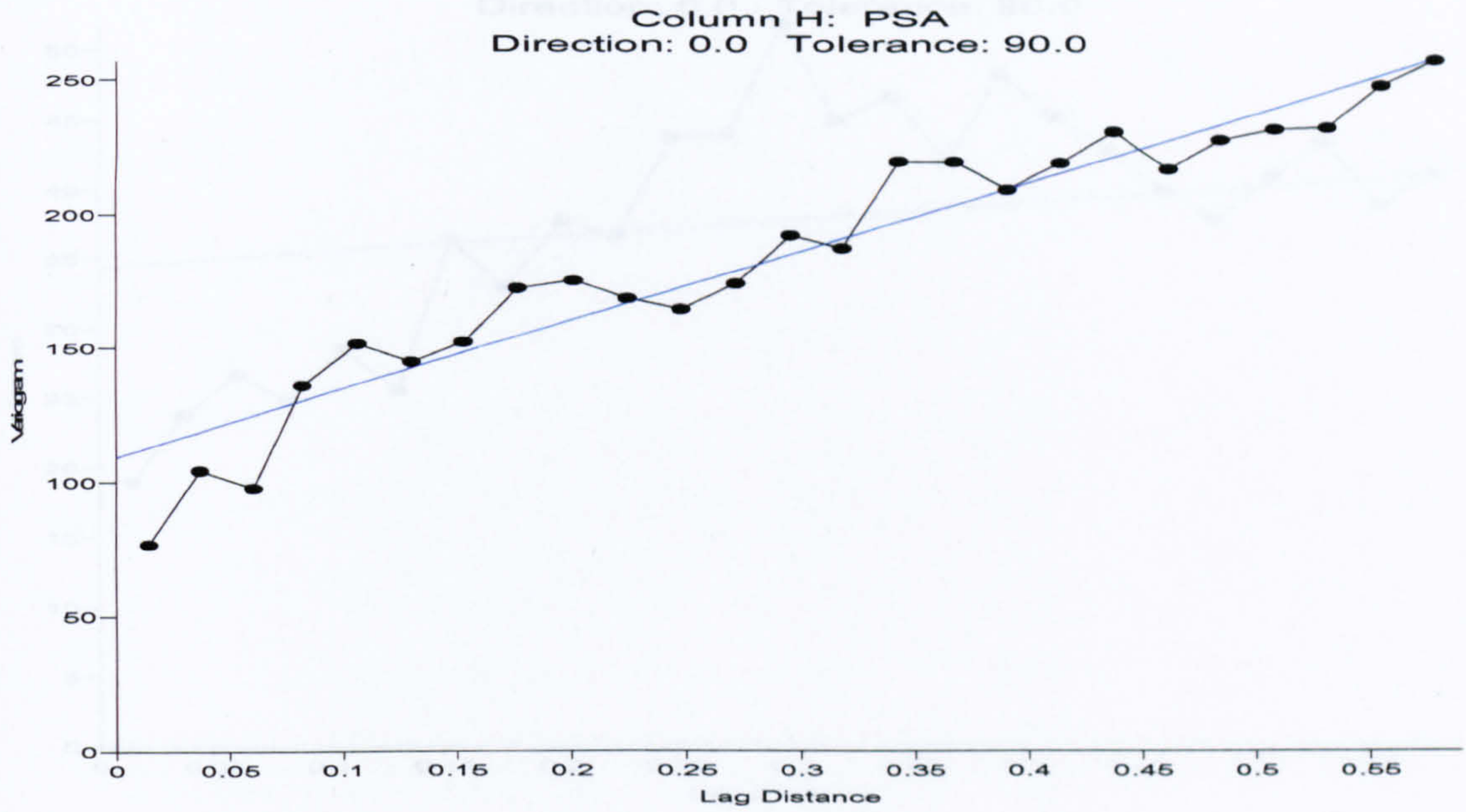

(b)

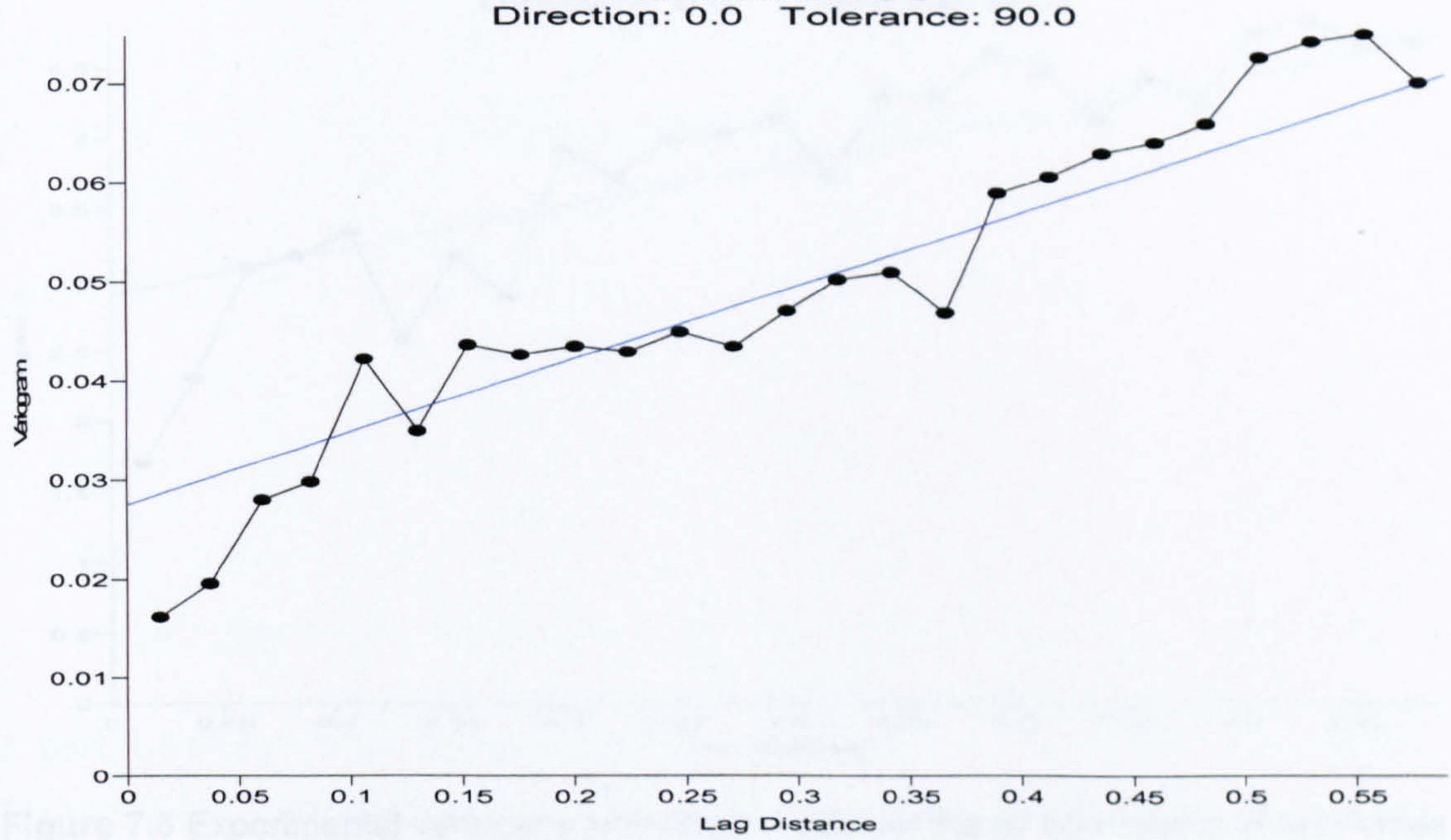

Figure 7.2 Experimental variogram with linear model for (a) PSA (b) TOC, at direction 0.0^0 and tolerance 90.0^0

(a)

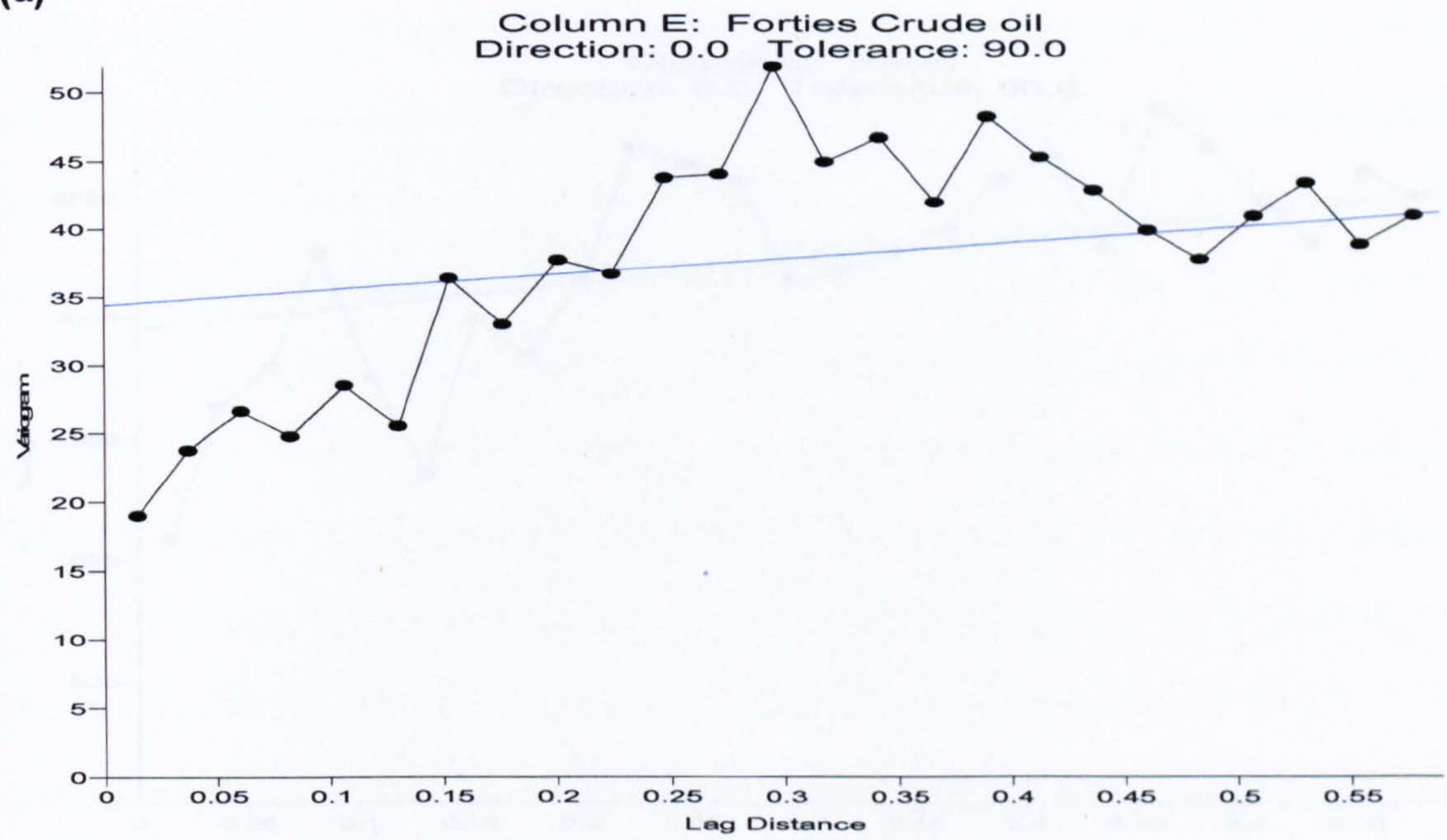

(b)

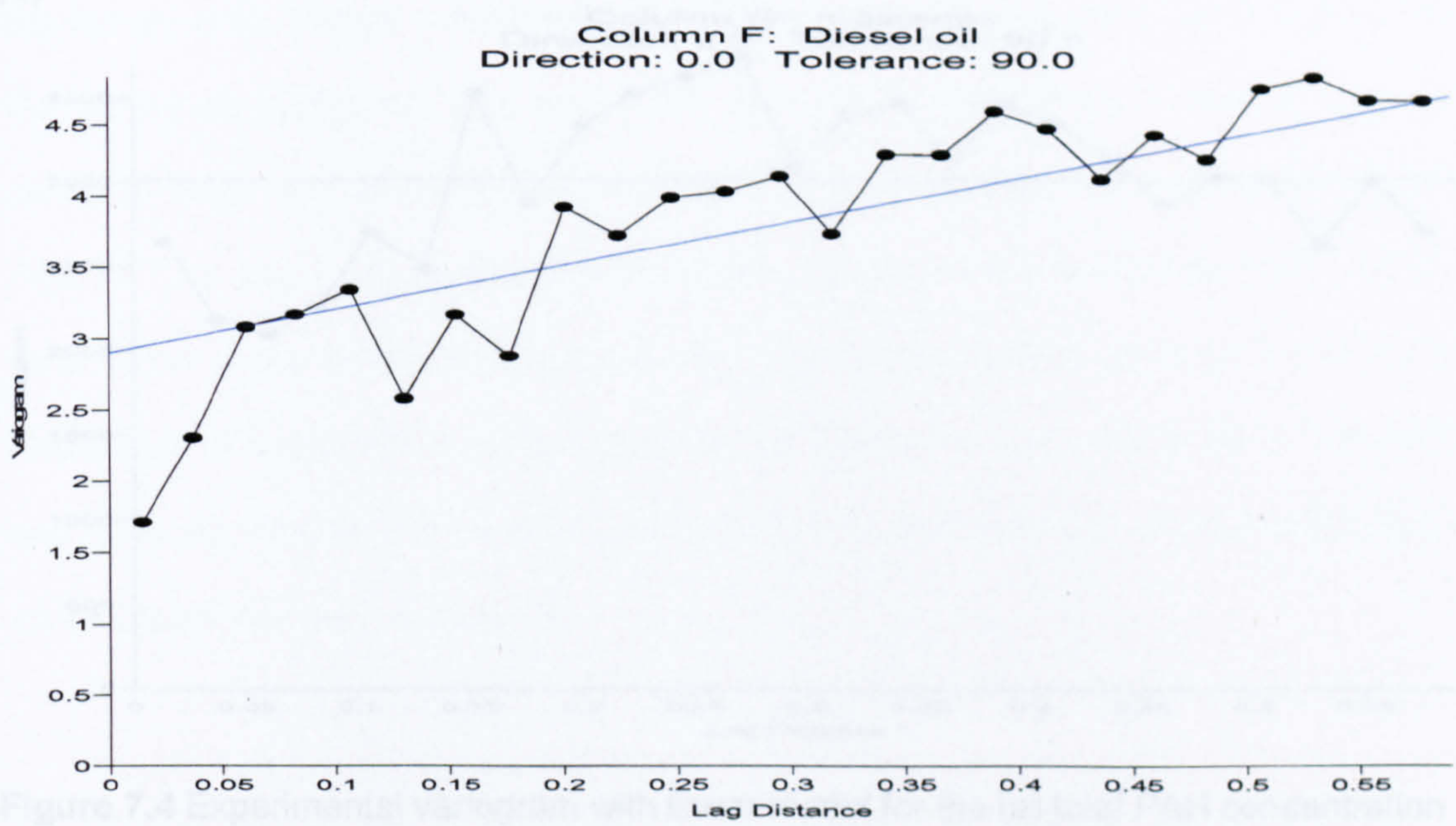

Figure 7.3 Experimental variogram with linear model for the oil equivalents of (a) Forties crude (b) diesel, at direction 0.0^0 and tolerance 90.0^0.

(a)

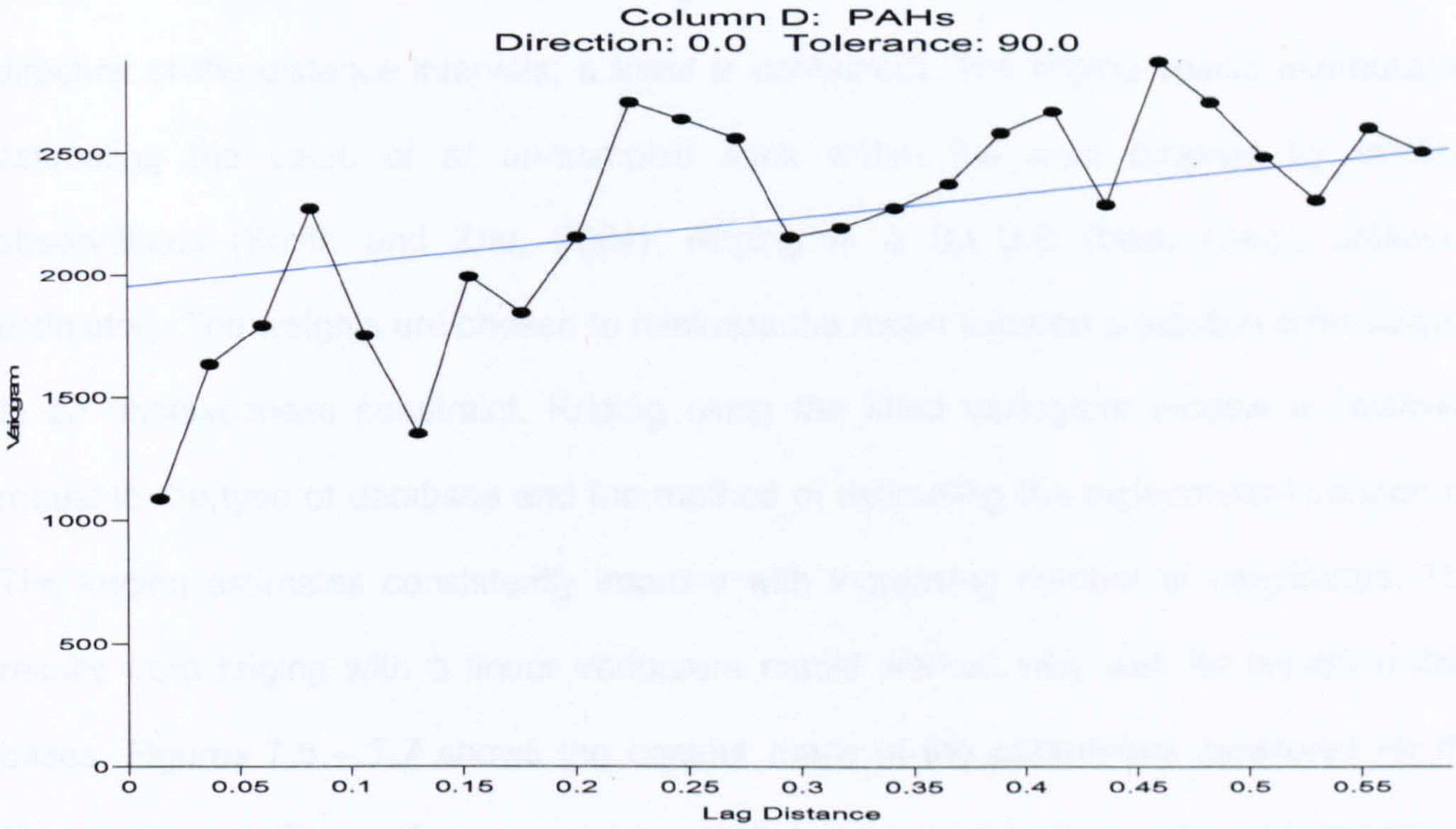

(b)

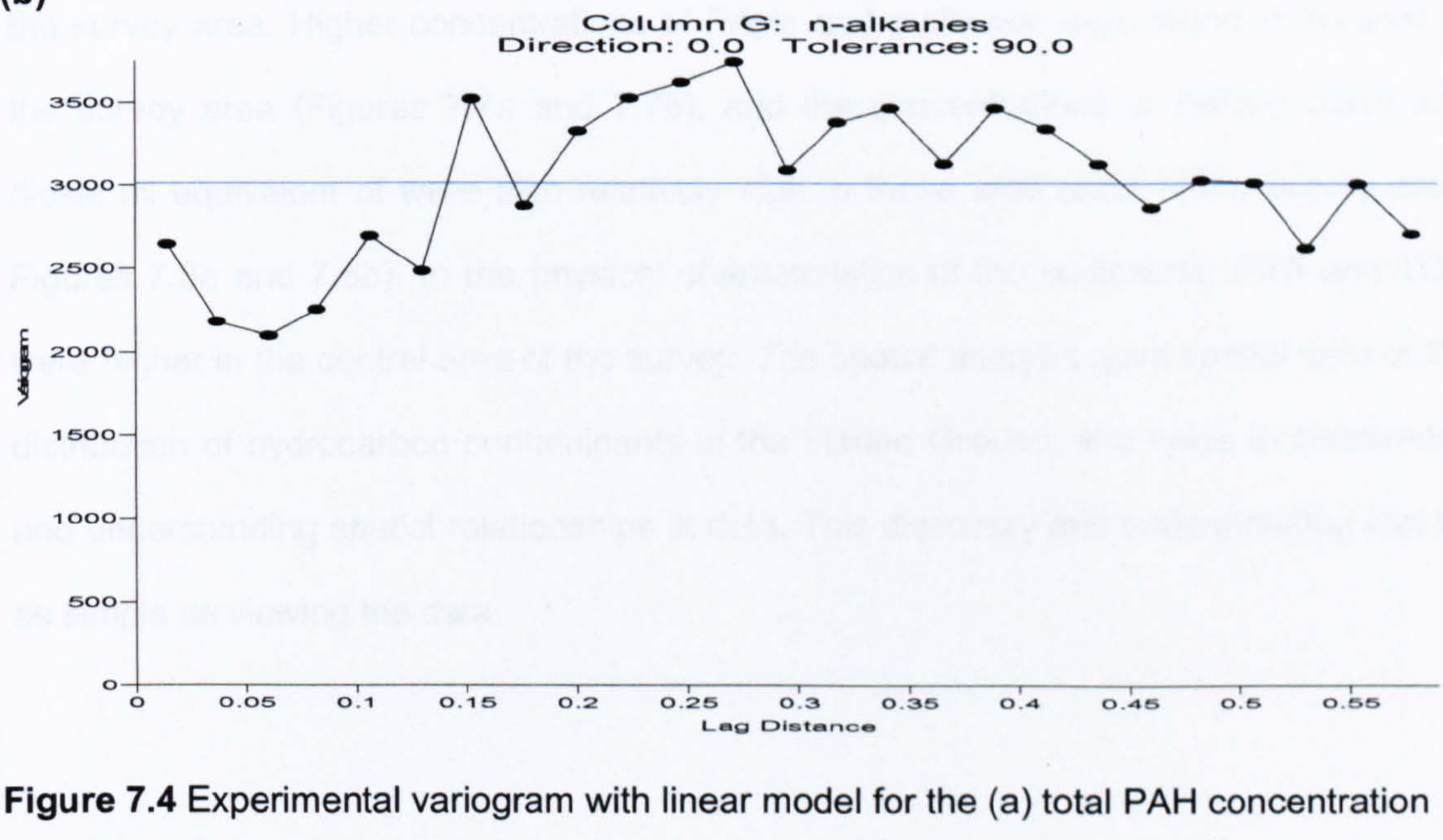

Figure 7.4 Experimental variogram with linear model for the (a) total PAH concentration (b) total *n*-alkane concentration crude, at direction 0.0^0 and tolerance 90.0^0.

The contour maps were computed using the universal kriging spatial interpolation (used under anisotropic conditions, when variogram is a function of both the distance and the direction of the distance intervals; a trend is contained). The kriging spatial interpolation estimating the value of at un-sampled sites within the area covered by existing observations (Smith and Zhu, 2004), Kriging is a B.L.U.E (best, linear, unbiased estimator). The weights are chosen to minimize the mean squared prediction error subject to an unbiasedness constraint. Kriging using the fitted variogram models is relatively robust to the type of database and the method of estimating the experimental variogram. The kriging estimates consistently improve with increasing number of neighbours. The results from kriging with a linear variogram model worked very well for elevation data bases. Figures 7.5 – 7.7 shows the contour maps of the parameters measured for the Fladen Ground. The contour maps show similar patterns of hydrocarbon contaminants in the survey area. Higher concentrations of PAHs and *n*-alkanes were found in the east of the survey area (Figures 7.7a and 7.7b), and the concentrations of Forties crude and diesel oil equivalent of were also relatively high in these area (east of the survey area; Figures 7.6a and 7.6b). In the physical characteristics of the sediments, PSA and TOC were higher in the central area of the survey. The spatial analysis gave spatial view of the distribution of hydrocarbon contaminants in the Fladen Ground, and helps in discovering and understanding spatial relationships in data. This discovery and understanding can be as simple as viewing the data.

(a)

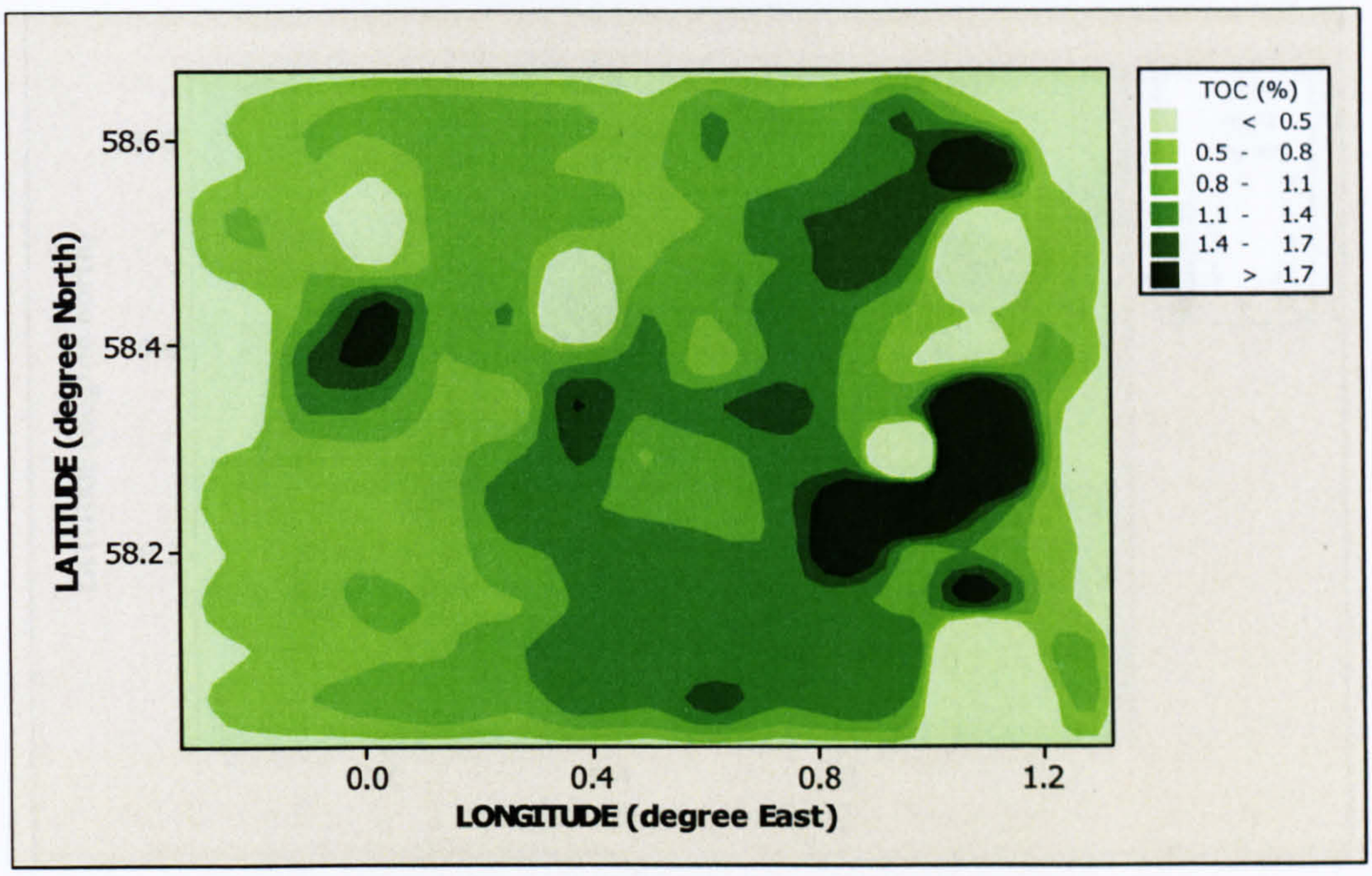

(b)

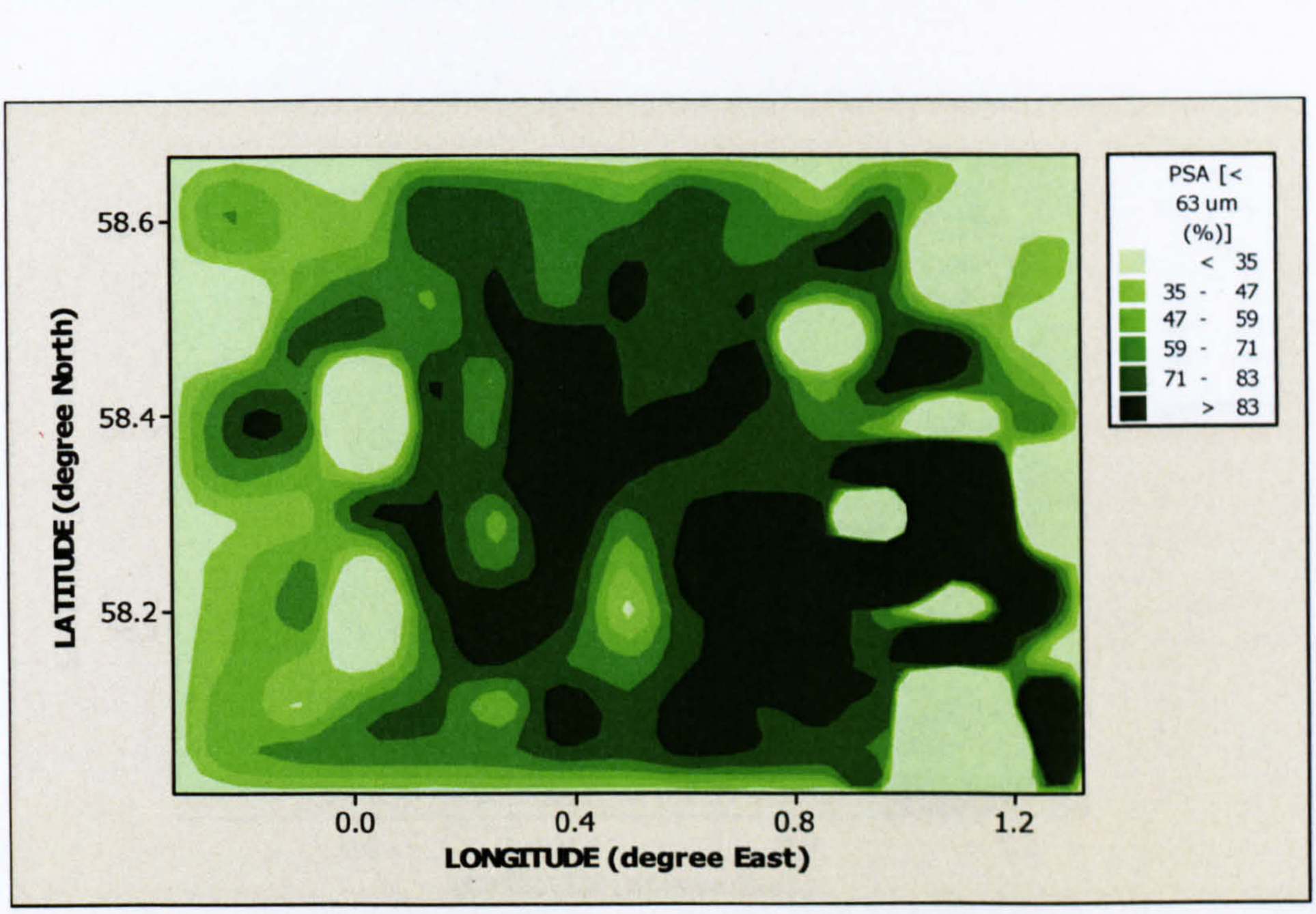

Figure 7.5 Contour maps showing the distribution pattern of (a) TOC (%) and (b) PSA (< 63 μm (%))

(a)

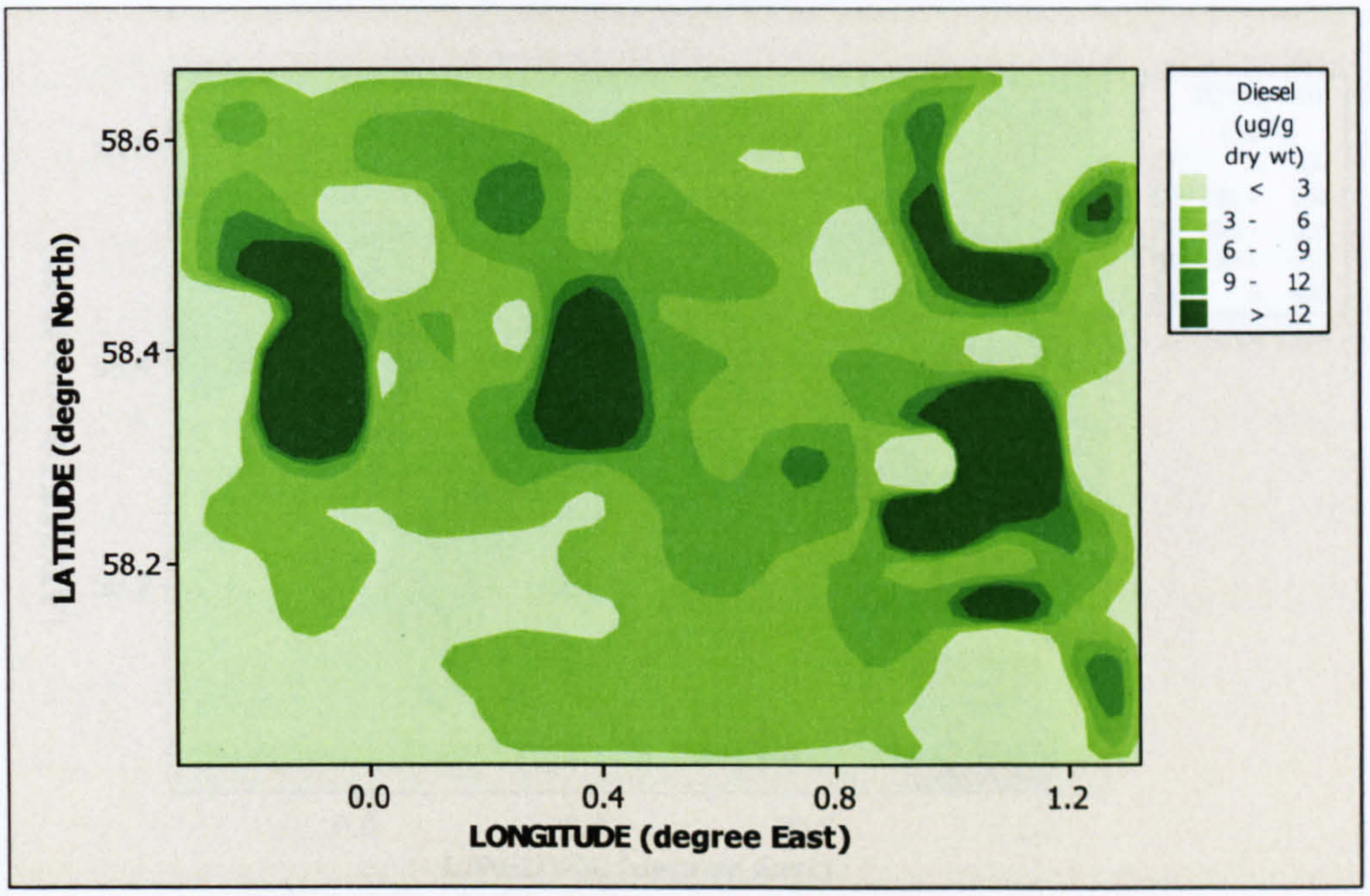

(b)

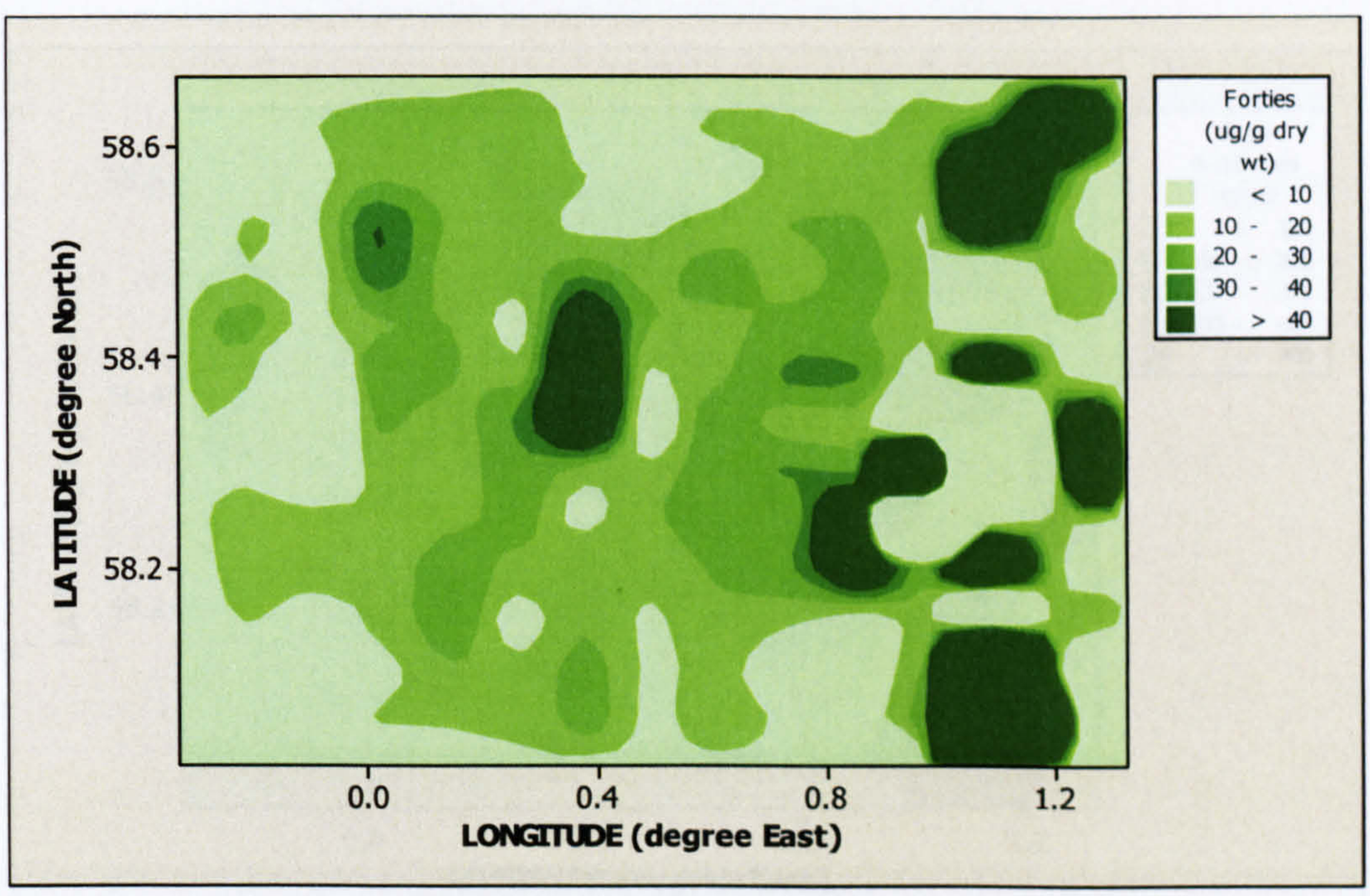

Figure 7.6 Contour maps showing the distribution pattern of the oil equivalent of (a) diesel oil (b) Forties crude. All concentrations are in μg g^{-1} dry weight.

(a)

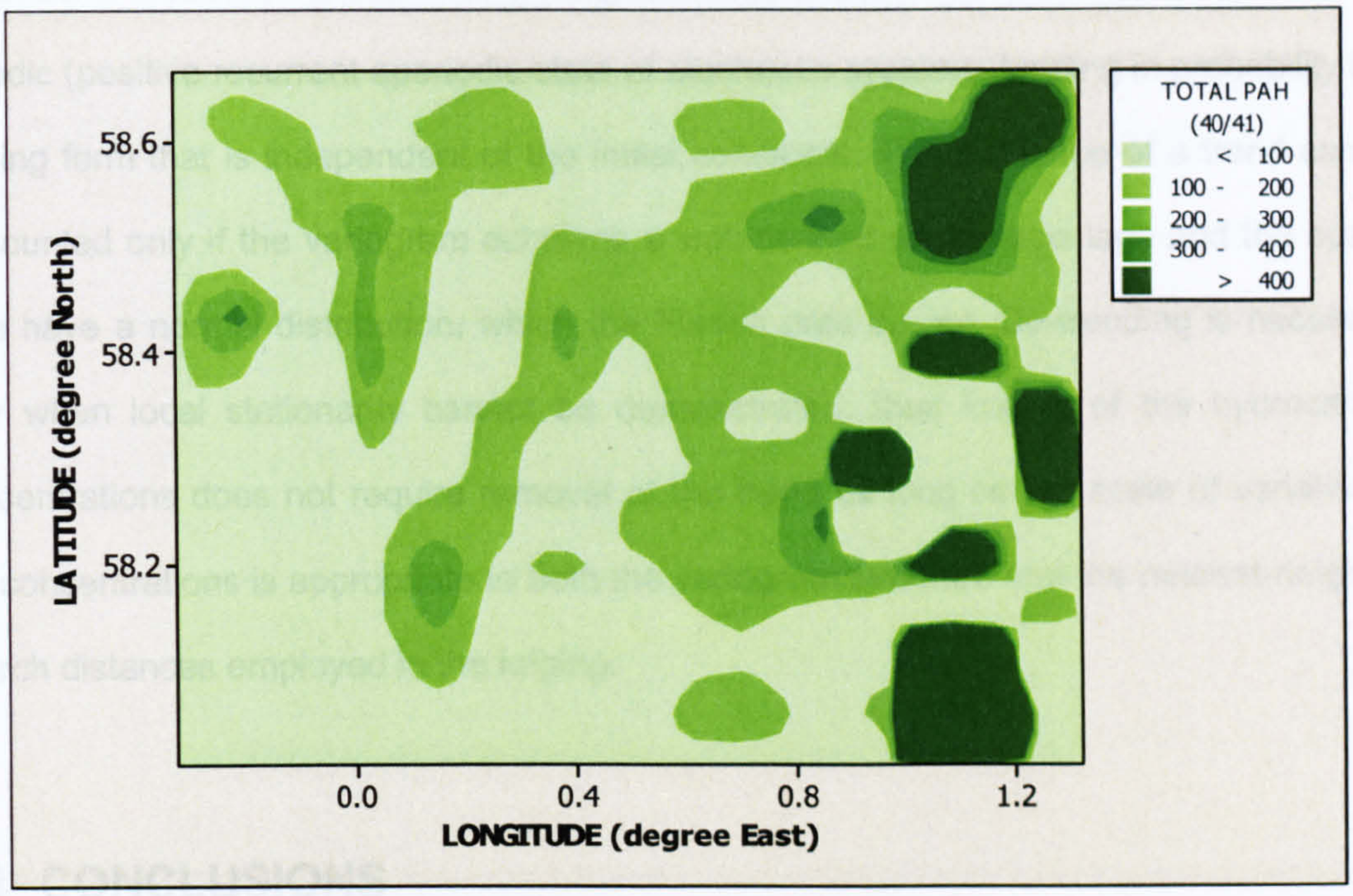

(b)

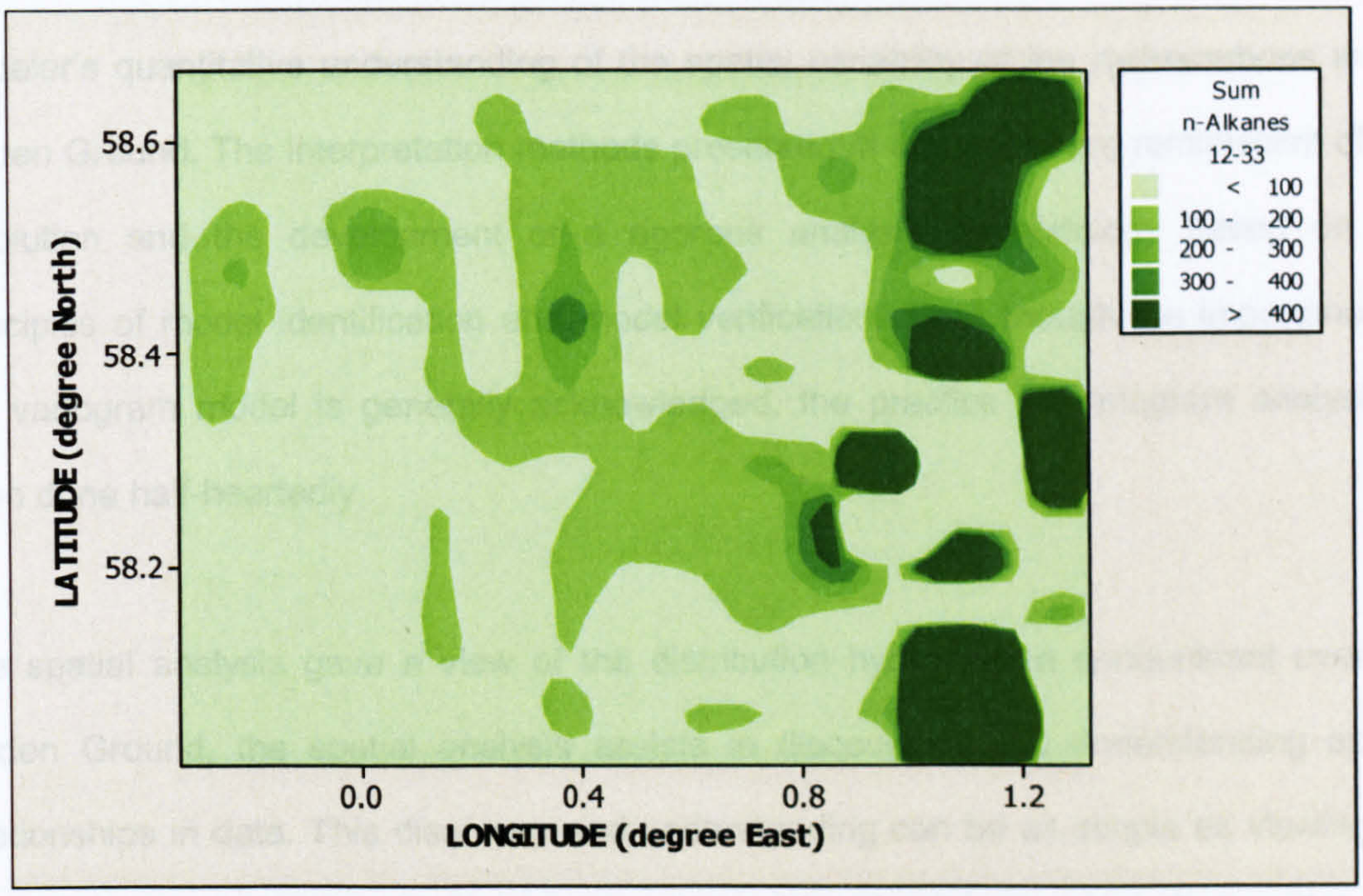

Figure 7.7 Contour maps showing the distribution pattern of (a) total PAH concentration and (b) total *n*-alkane concentration. All concentrations are in μg kg^{-1} dry weight.

The existence of a trend in the variogram and spatial pattern in the contour maps of the parameters measured shows that the regionalized variable were non-stationary and non-ergodic (positive recurrent aperiodic state of stochastic systems: tending in probability to a limiting form that is independent of the initial condition). The existence of a trend can be discounted only if the variogram achieves a well-defined sill at large lags and the spatial data have a normal distribution, which the Fladen data do not. De-trending is necessary only when local stationarity cannot be demonstrated; thus kriging of the hydrocarbon concentrations does not require removal of the trend as long as the scale of variation of the concentrations is appropriate to both the variogram structure and the nearest-neighbor search distances employed in the kriging.

7.4 CONCLUSIONS

Spatial interpolation is important in environmental studies. The variogram represents the modeler's quantitative understanding of the spatial variability of the hydrocarbons in the Fladen Ground. The interpretation methods presented in this paper are reminiscent of the revolution and the development of a rigorous analysis methodology based on the principles of model identification and model verification. Even though the importance of the variogram model is generally acknowledged, the practice of variogram analysis is often done half-heartedly.

The spatial analysis gave a view of the distribution hydrocarbon contaminant over the Fladen Ground, the spatial analysis assists in discovering and understanding spatial relationships in data. This discovery and understanding can be as simple as viewing the data. The spatial analysis can be able to perform other functions such as finding distance, assigning proximity, calculating density, creating contours, and deriving slope. Therefore

spatial interpolation is a valuable way to illustrate the accumulation of hydrocarbons in environment (sediments).

CHAPTER EIGHT

A FIELD STUDY TO INVESTIGATE COMPOSITE RANDOM SAMPLING

8.1 INTRODUCTION

Based on the outcome of the stratified random sampling design used in the Fladen Ground, a field study was designed based around the relationships between chemical contaminants and supporting variables such as particle size, organic carbon and water depth. The original intention had been to carry out a field study in the deltaic region of river Niger, in southern Nigeria. However, conditions in Nigeria at the time prevented this from being done. Instead, areas of the Firth of Forth (Figure 8.1) and Firth of Clyde (Figure 8.2) were selected, based on their sediment characteristics and water depth. The areas were offshore of the estuarine areas, with an average water depth of 80 and 45 meters, in the outer parts of the Firths of Clyde and Forth, respectively. Both chosen sites were offshore and subject to general shipping traffic and were expected to have similar sediment compositions. Composite random sampling design was used. Initial samples were collected using random sampling design and analysed, and then the samples were divided into a mixture of sub-samples. The number of samples in each area was chosen by *optimal allocation*, with the number of samples collected, based on the area and 5% standard deviation of the mean of the water depth, i.e. 25 samples were collected in areas roughly equal to the areas of near and far fields in each of the Fladen Ground Zones (456.01 km^2). The aim of the work is to estimate a within–stratum mean value for each of the chosen measurement parameters. The objective is to determine

experimentally whether this can be done with more thorough coverage (better representation), better precision and less variance at lower analytical cost, by using composite random sampling.

8.1.a Sampling Design

Composite sampling involves physical combination of homogenised samples to form a set of new samples (i.e., composite samples). The chemical analyses are then performed on the aliquots of the composite samples. Because the compositing physically averages the individual samples, averaging the analytical results of the smaller number of composite samples can produced an estimated mean that is more precise than, or at least as precise as, one based on many more individual sample results.

Composite sampling will generally be an appropriate strategy when all of the following conditions hold:

⇒ The anticipated concentrations for most composites will exceed detection limits

⇒ The process of compositing will not affect the sample integrity

⇒ Analytical costs are high relative to costs associated with sampling

⇒ There are no practical difficulties that impede the selection of multiple samples of units, where each sample is selected according to a given statistical design

⇒ There are no practical difficulties in undertaking the necessary compositing.

The main benefit of composite sampling is that it may achieve better precision of an estimated mean at less cost, and data analysis is usually straightforward. The limitation of composite sampling is that it yields a reduced amount of information on variability; for

example composite sampling loses information on individual samples and on spatial (or temporal) patterns.

8.1.b Sampling Areas

The Firth of Forth (Figure 8.1) is the estuary or firth of the River Forth, where it flows into the North Sea between Fife to the north, and West Lothian, the City of Edinburgh, and East Lothian to the south. A large number of towns line the shores, as well as the petrochemical complexes at Grangemouth and Burntisland, the commercial docks at Leith, oilrig construction yards at Dalgety Bay and Methil and the naval dockyard at Rosyth, with numerous other industrial areas including the areas around the Forth bridges. The Firth is important for nature conservation. The Firth of Forth Islands SPA (Special Protection Area) is host to over 90,000 breeding seabirds every year. There is a bird observatory on the Isle of May.

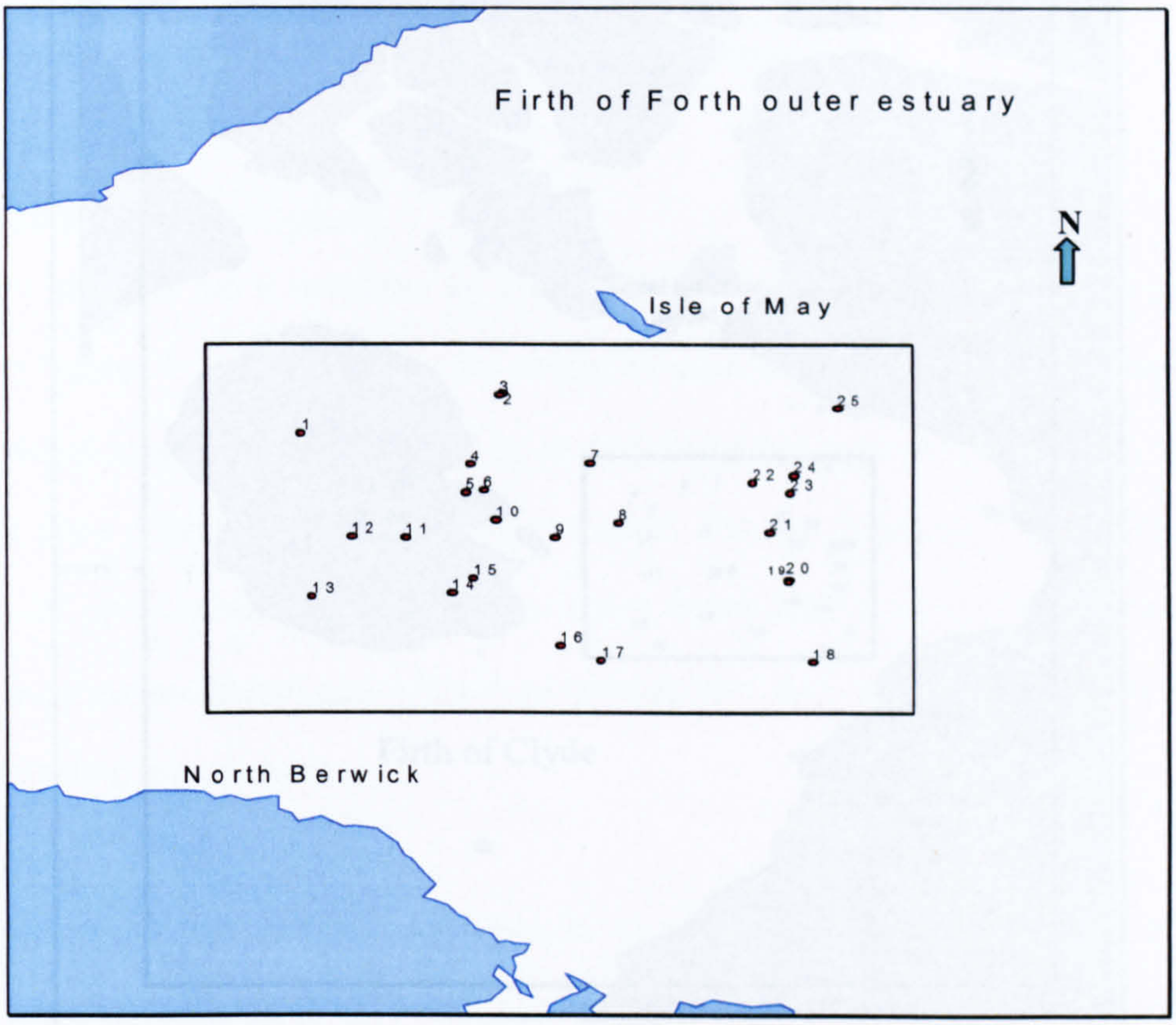

Figure 8.1 Map of the Firth of Forth showing location of the sampling area.

The Firth of Clyde (Figure 8.2) on the west coast of Scotland serves a greater human population than any other Scottish coast water area. Inputs of waste and domestic and industrial effluent are correspondingly large. The primary sources of hydrocarbon contamination include effluent from military (e.g. Holy Loch), domestic, municipal and industrial facilities.

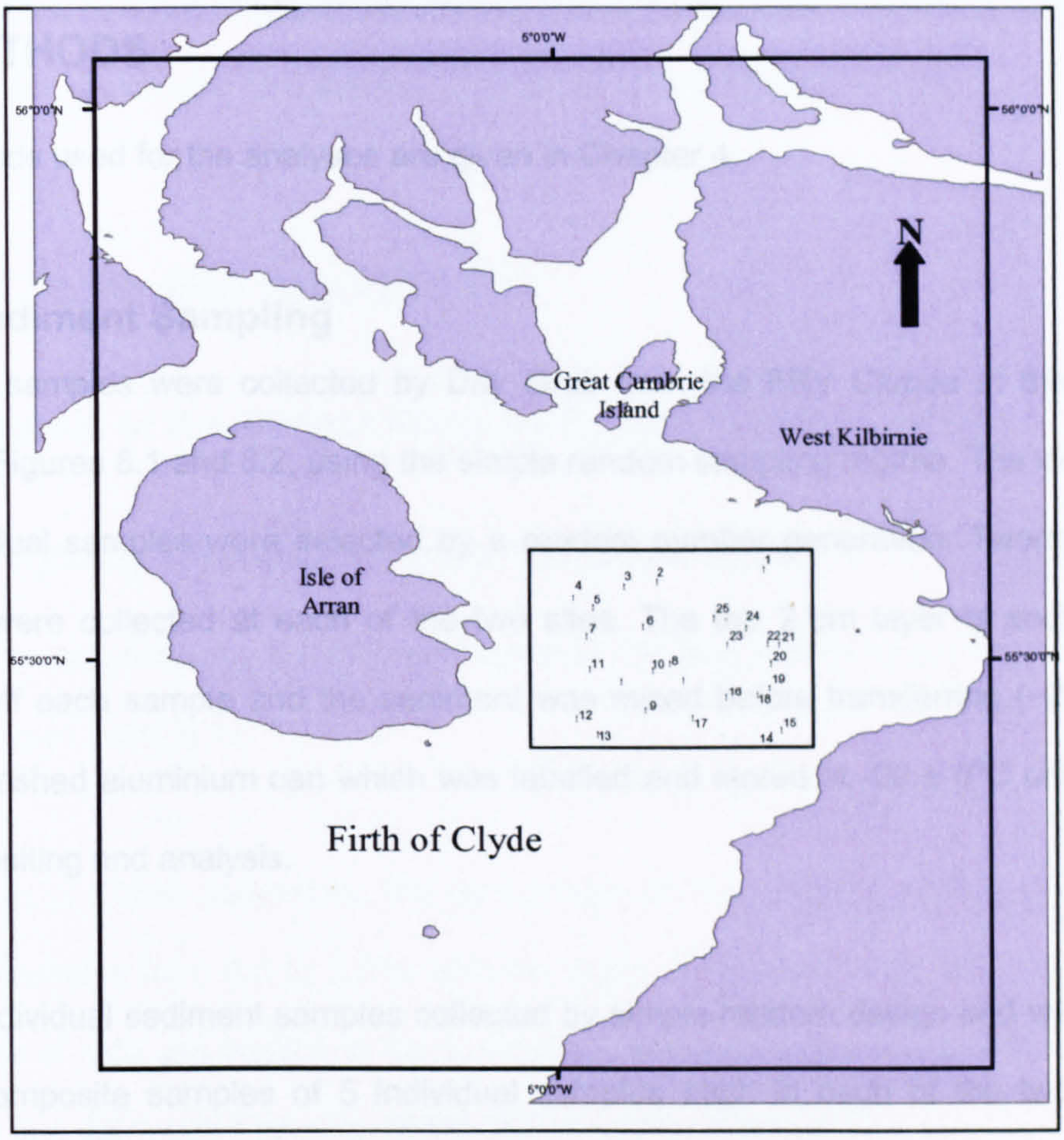

Figure 8.2 Map of the Firth of Clyde showing location of the sampling area

8.2 METHODS

The methods used for the analyses are given in Chapter 4.

8.2.a Sediment Sampling

Sediment samples were collected by Day Grab from the FRV *Clupea* at the locations shown in Figures 8.1 and 8.2, using the simple random sampling regime. The locations for the individual samples were selected by a random number generation. Twenty five (25) samples were collected at each of the two sites. The top 2 cm layer of sediment was scraped off each sample and the sediment was mixed before transferring (~200 g) to a solvent washed aluminium can which was labelled and stored at -20 ± 5°C until required for compositing and analysis.

The 25 individual sediment samples collected by simple random design and were used to form 5 composite samples of 5 individual samples each in each of the two sampling areas. All the individual (simple random sampling) and the composite random sampling sediments samples were analysed for particle size (PS), total organic carbon (TOC), ultra-violet fluorescence (UVF) oil equivalent concentrations, PAHs, *n*-alkanes, steranes and triterpanes, as described in Chapter 4. Full details of the sampling locations are given in Appendix 8.

8.2.b Statistical Analyses

Data were analysed using the MINITAB® software version 14. Analysis of variance (ANOVA) at significance level of 5% was used to detect significant differences among the means of TOC%, and PSA, and the oil equivalents of the Forties crude and diesel, PAHs

and *n*-alkanes concentrations of the Zones. Spearman's Rank correlation was used to determine non-parametric correlations among the parameters measured.

8.3 RESULTS AND DISCUSSION

8.3.a Results of the Simple Random Sampling (SRS) Design

8.3.a.i Physical Characteristics of the Sediments

Physical characteristics of the sediment samples are tabulated in Appendices 9 – 12 and summarized in Table 8.1.

In the Firth of Clyde sediments, the percentage of total organic carbon (TOC) varied between samples from 0.3 to 2.0%; and the mean TOC was 1.41% (SE = 0.09%). The percentage of < 63 μm fraction in the sediment (PSA) varied between samples from 22.7 to 99.7%; and the mean PSA was 86.6% (SE = 4.27%) (Table 8.1).

Percentage total organic carbon (TOC) in the Firth of Forth sediments varied between samples from 0.4 to 4.2%; and the mean TOC was 1.02% (SE = 0.15%). The PSA varied between samples from 18.7 to 61.5%; mean PSA was 41.2% (SE = 2.63%; Table 8.1). The Firth of Clyde sediments had higher percentage of the fine material and the organic content than the Firth of Forth, as expected by their difference in water depth. In general, TOC tends to be higher in the deep sediments.

Table 8.1 Summary of the individual simple random sampling (SRS) design of the TOC; < 63 μm fraction (PSA), diesel and Forties oil equivalent concentrations, total PAH and total *n*-alkane concentrations. Concentrations are on a dry weight basis.

Variables	Stations	Min	Mean	Med	Max	SD	SE	CV
TOC (%)	Clyde	0.3	1.4	1.5	2.0	0.43	0.09	30.4
	Forth	0.4	1.0	0.7	4.2	0.75	0.15	73.8
PSA (%)	Clyde	22.7	86.6	95.9	99.7	21.34	4.27	24.6
	Forth	18.7	41.2	38.1	61.5	13.17	2.63	32.0
Diesel ($\mu g\ g^{-1}$)	Clyde	8.1	63.2	59.5	120.9	34.99	7.00	55.4
	Forth	7.8	27.6	19.2	72.6	17.69	3.54	64.2
Forties ($\mu g\ g^{-1}$)	Clyde	47.8	404.1	385.1	791.7	222.10	44.40	55.0
	Forth	47.1	161.8	116.3	351.5	100.10	20.00	61.9
Total PAH ($\mu g\ kg^{-1}$)	Clyde	116.0	1858.0	1871.0	3405.0	979.00	196.00	52.7
	Forth	173.8	532.4	454.1	1200.0	294.40	58.90	55.3
n-Alkanes ($\mu g\ kg^{-1}$)	Clyde	63.8	489.6	487.6	1238.1	242.00	48.40	49.4
	Forth	49.8	349.1	322.2	743.1	169.40	33.90	48.5

Min = Minimum; Med = Median; Max = Maximum; SD = Standard Deviation;
CV = Coefficient of Variation; Var = Sample Variance; SE = Standard Error of the mean.

TOC and PSA in the Firth of Clyde measurements were positively correlated with each other and with the corresponding total PAH and total *n*-alkane concentrations (Table 8.2a). However, there were no correlation between the oil equivalent concentrations and TOC, the corresponding total PAH and total *n*-alkane concentrations. TOC and PSA in the Firth of Forth measurements were positively correlated with each other and with the corresponding oil equivalent, total PAH and total *n*-alkane concentrations (Table 8.3a). To investigate differences in hydrocarbon concentrations that are **not** due to the physical characteristics of the sediment, it is necessary to normalise the concentrations to e.g.

TOC. Note that, even having normalised to TOC, the oil equivalent, total PAH and total *n*-alkane concentrations are still positively correlated in the Firth of Forth (Table 8.3b), whilst in the Forth of Clyde there was no correlation between the oil equivalent, and total PAH and total *n*-alkane (Table 8.2b). This just means that, even having accounted for the physical characteristics of the sediment in the Firth of Forth, samples with higher oil equivalent concentrations also tended to have higher total PAH and total *n*-alkane concentrations.

Table 8.2 Spearman's Rank correlation coefficients of the 25 sediment samples from the Firth of Clyde (a) Raw data, (b) Data normalised to total organic carbon (TOC). Values greater than 0.40 or less than - 0.40 are significant at the 5% level or better.

(a)

	TOC	PSA	Forties	Diesel	PAHs	*n*-Alkane
TOC	-	0.76	0.42	0.44	0.91	0.73
PSA	0.76	-	0.53	0.56	0.73	0.64
Forties	0.42	0.53	-	0.98	0.31	0.42
Diesel	0.44	0.56	0.98	-	0.32	0.46
PAHs	0.91	0.73	0.31	0.32	-	0.85
n-Alkane	0.73	0.64	0.42	0.46	0.85	-

(b)

	PSA	Forties	Diesel	PAHs	*n*-Alkane
PSA	-	0.35	0.40	0.61	0.47
Forties	0.35	-	0.99	0.01	0.34
Diesel	0.40	0.99	-	0.03	0.37
PAHs	0.61	0.03	0.03	-	0.64
n-Alkane	0.47	0.34	0.37	0.64	-

Table 8.3 Spearman's Rank correlation coefficient of the Firth of Forth (a) Raw data, (b) Normalised data to sediment total organic carbon (TOC). Values greater than 0.40 or less than - 0.40 are 5% significant to 25 sediment samples.

(a)

	TOC	PSA	Forties	Diesel	PAHs	*n*-Alkane
TOC	-	0.87	0.74	0.80	0.80	0.71
PSA	0.87	-	0.61	0.63	0.66	0.59
Forties	0.74	0.61	-	0.97	0.84	0.85
Diesel	0.80	0.63	0.97	-	0.87	0.88
PAHs	0.80	0.66	0.84	0.87	-	0.96
n-Alkane	0.71	0.59	0.85	0.88	0.96	-

(b)

	PSA	Forties	Diesel	PAHs	*n*-Alkane
PSA	-	0.10	0.07	-0.01	-0.32
Forties	0.10	-	0.98	0.67	0.56
Diesel	0.07	0.98	-	0.60	0.72
PAHs	-0.01	0.67	0.60	-	0.86
n-Alkane	-0.32	0.56	0.72	0.86	-

8.3.a.ii UVF Analysis

The diesel oil equivalent concentrations in the Firth of Clyde sediments varied between samples from 8.1 to 120.9 μg g^{-1} dry weight; with a mean concentration of 27.6 μg g^{-1} dry weight (SE = 7.0 μg g^{-1} dry weight). The Forties crude oil equivalent concentrations varied between samples from 47.8 to 791.7 μg g^{-1} dry weight; with a mean concentration of 404.1 μg g^{-1} dry weight (SE = 44.4 μg g^{-1} dry weight; Table 8.1).

The diesel equivalent concentrations in the Firth of Forth sediments varied from 7.8 to 72.6 μg g^{-1} dry weight; mean diesel oil concentration was 27.6 μg g^{-1} dry weight (SE = 3.5 μg g^{-1} dry weight). The Forties crude oil equivalent concentrations varied between samples from 47.1 to 351.5 μg g^{-1} dry weight; and mean Forties crude oil concentration was 161.8 μg g^{-1} dry weight (SE = 20.0 μg g^{-1} dry weight).

As observed in the sediment characteristics (section 8.3.a.i), the concentrations of Forties crude and diesel oil equivalents were generally higher in the Firth of Clyde sediments than in the Firth of Forth.

8.3.a.iii PAHs Analysis

The total PAH concentrations (2- to 6-ring parent and alkylated, including the 16 US EPA PAHs) in the Firth of Clyde sediments varied between samples from 116.0 to 3405 μg kg^{-1} dry weight; the mean total PAH concentration was 1858.0 μg kg^{-1} dry weight (SE = 196.0 μg kg^{-1} dry weight).

The total PAH concentration in the Firth of Forth sediments varied between samples from 173.8 to 1200.1 μg kg^{-1} dry weight with a mean total PAH concentration of 532.4 μg kg^{-1} dry weight (SE = 58.9 μg kg^{-1} dry weight) (Table 8.1).

Sources of the PAHs

The proportion of parent PAHs was lower than that of the alkylated PAHs in all the sediments of the two sites (i.e. Firth of Clyde and Firth of Forth), values less or greater than 40% are associated with petrogenic and pyrolytic sources, respectively. The

proportion varied from 39.9 to 44.4% (mean = 42.6%, SE = 0.2%) for the Clyde sediments, whilst for the Firth of Forth it varied from 32.2 to 41.6% (mean = 35.2%, SE = 0.5%; Table 8.1). Petrogenic sources are dominated by 2- and 3-ring alkylated PAHs, whereas pyrolytic sources are characterized by heavier, parent PAHs. The PAH distribution profile for both the Firth of Clyde and Firth of Forth were found to be dominated by the heavier, more persistent, 4- to 5-ring compounds (Figure 8.3), indicative of predominately pyrolytic sources. However, the lower proportion of parent PAHs in the Forth of Forth (< 40%) compared to the Clyde (> 40%) may indicate that there is a greater petrogenic input in the Firth of Forth. The Firth of Forth also has a slightly higher percentage of 2 and 3-ring PAHs than the Firth of Clyde. However, there were no significant differences between the proportions of the parent PAH for the Firth of Clyde and Firth of Forth sediments ($p > 0.05$; ANOVA).

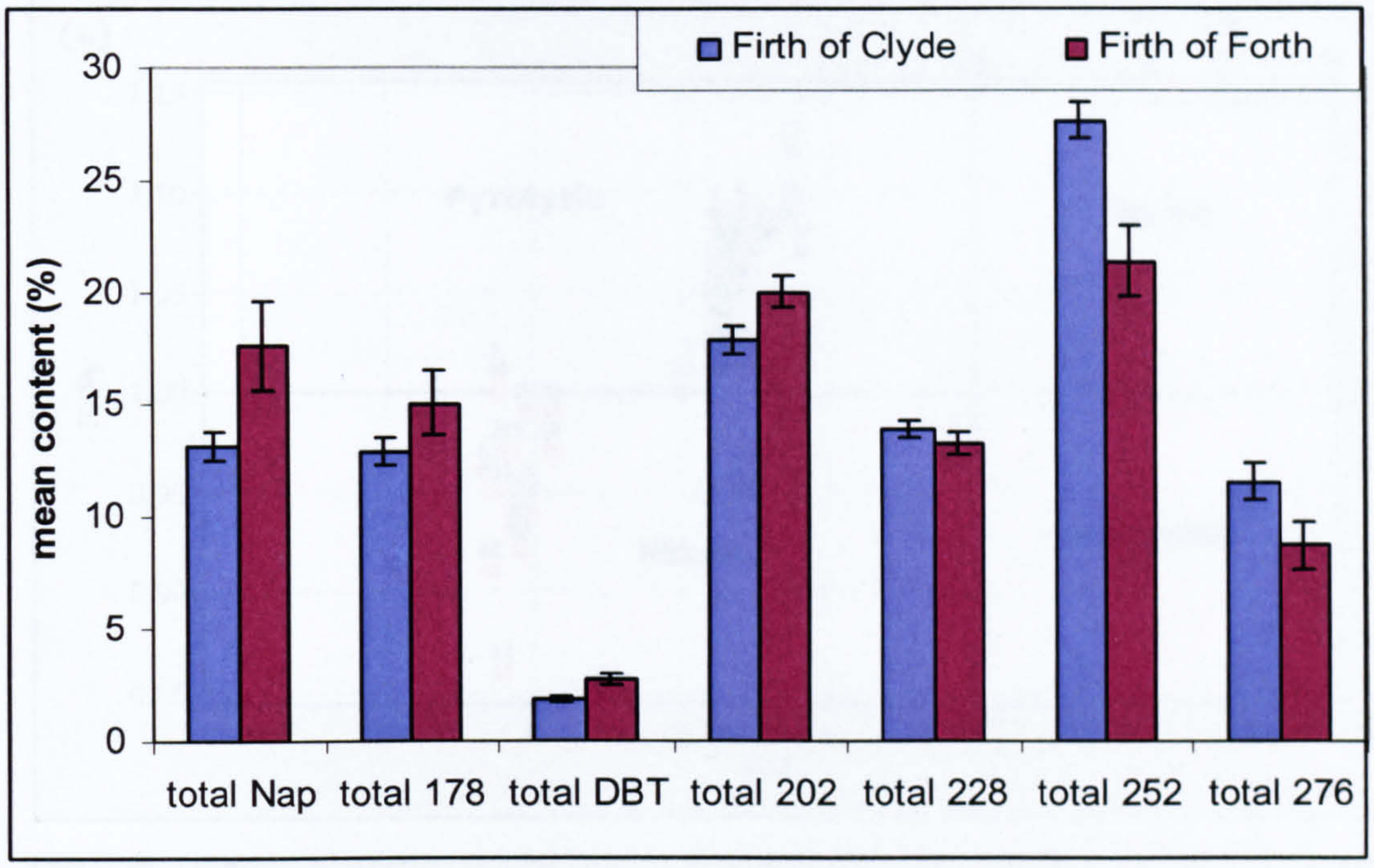

Figure 8.3 PAH profile of the Firth of Clyde and Firth of Forth.

Total naphthalenes (parent and C_1-C_4); total 178, phenanthrene/anthracene (parent and C_1-C_3); total DBT, dibenzothiophenes (parent and C_1-C_3); total 202, fluoranthene/pyrene (parent and C_1-C_3); total 228, benzanthracene/benzophenthrenes/chrysene/triphenylenes (parent and C_1-C_2); total 252, benzofluoranthene/benzopyrene/perylene and total 276, indenopyrene/benzoperylene (parent and C_1-C_2).

PAH concentration ratios were used in distinguishing PAHs sources as described in section 5.3.h. It was observed (Figures 8.4a and b) that all the Firth of Clyde sediment samples had concentration ratios of P/A and MP/P below 10 and 2, respectively, and 24 of the samples had Fl/Py ratio greater than 1. These suggest that PAHs are of a predominately pyrolytic origin in the Firth of Clyde.

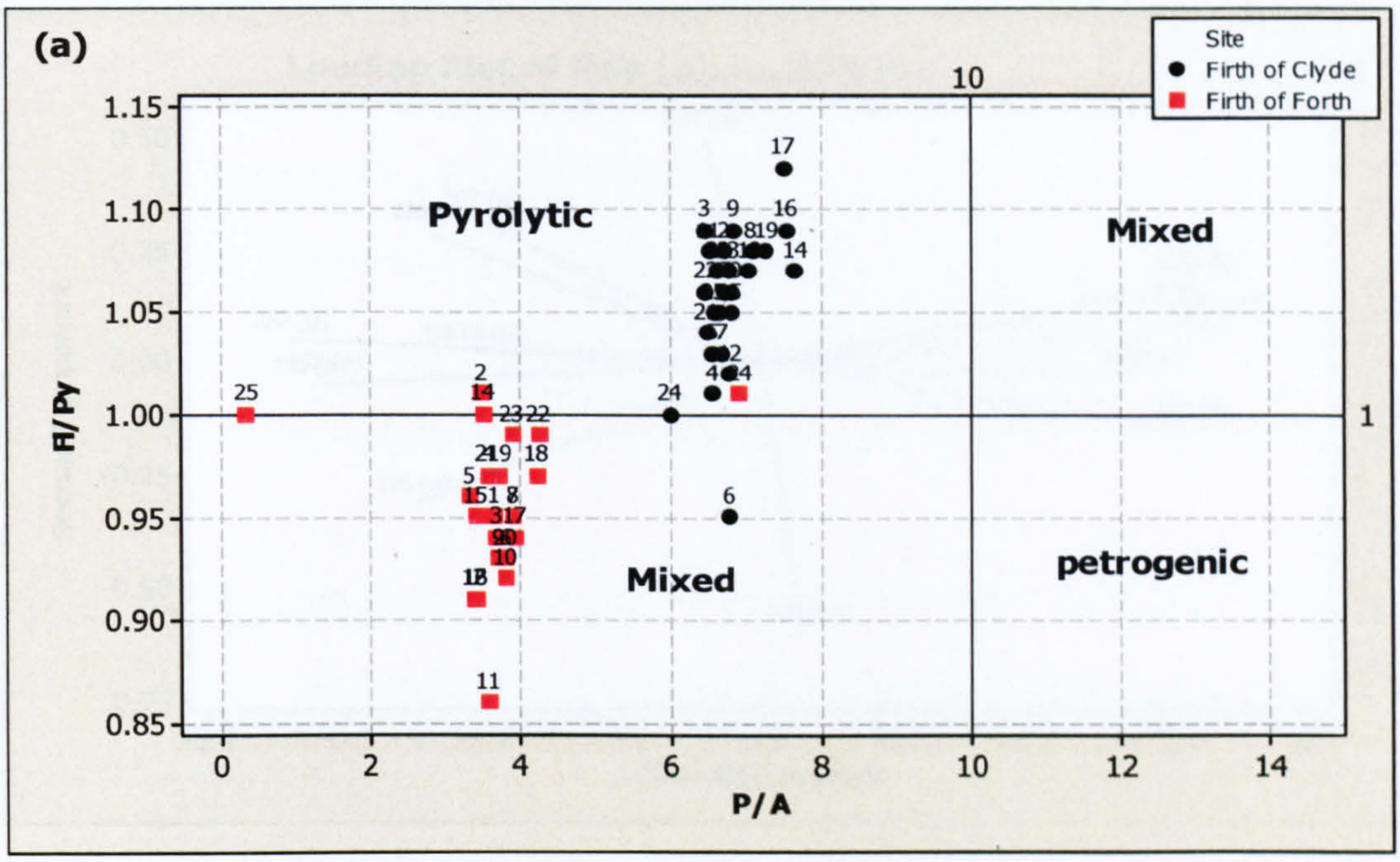

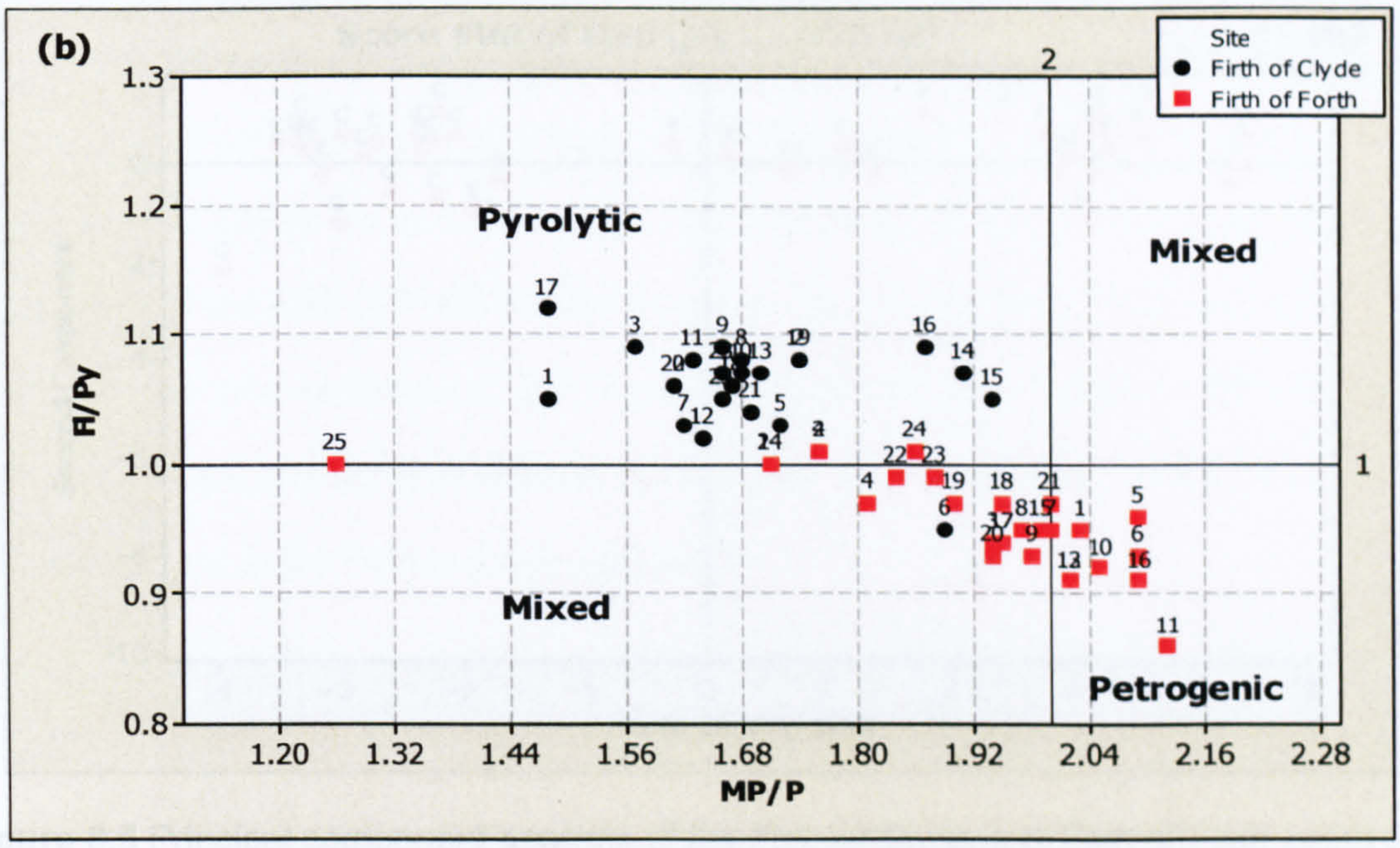

Figure 8.4 PAH concentration ratios used to assess the sources of PAHs. The Zones identified by high fluoranthene/pyrene (Fl/Py) ratios and low phenanthrene/anthracene (P/A) ratios and high Fl/Py and low methylphenanthrene/phenanthrene (MP/P) ratios were characteristic of pyrolytic PAHs. (a) Plot of Fl/Py ratios against P/A ratios. (b) Plot of Fl/Py ratios against MP/P ratios. Black dots represent Firth of Clyde sediments and red squares represent Firth of Forth sediments.

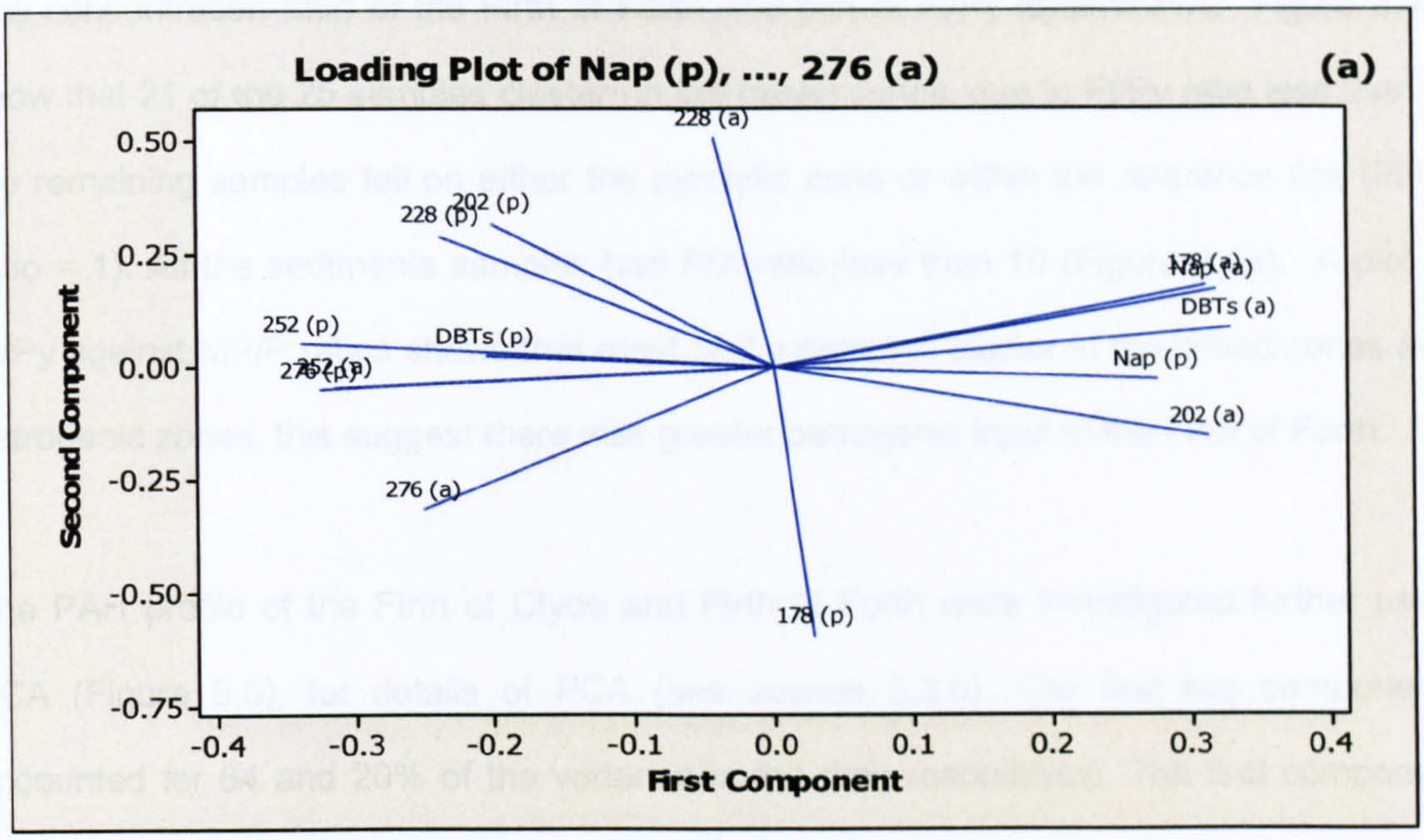

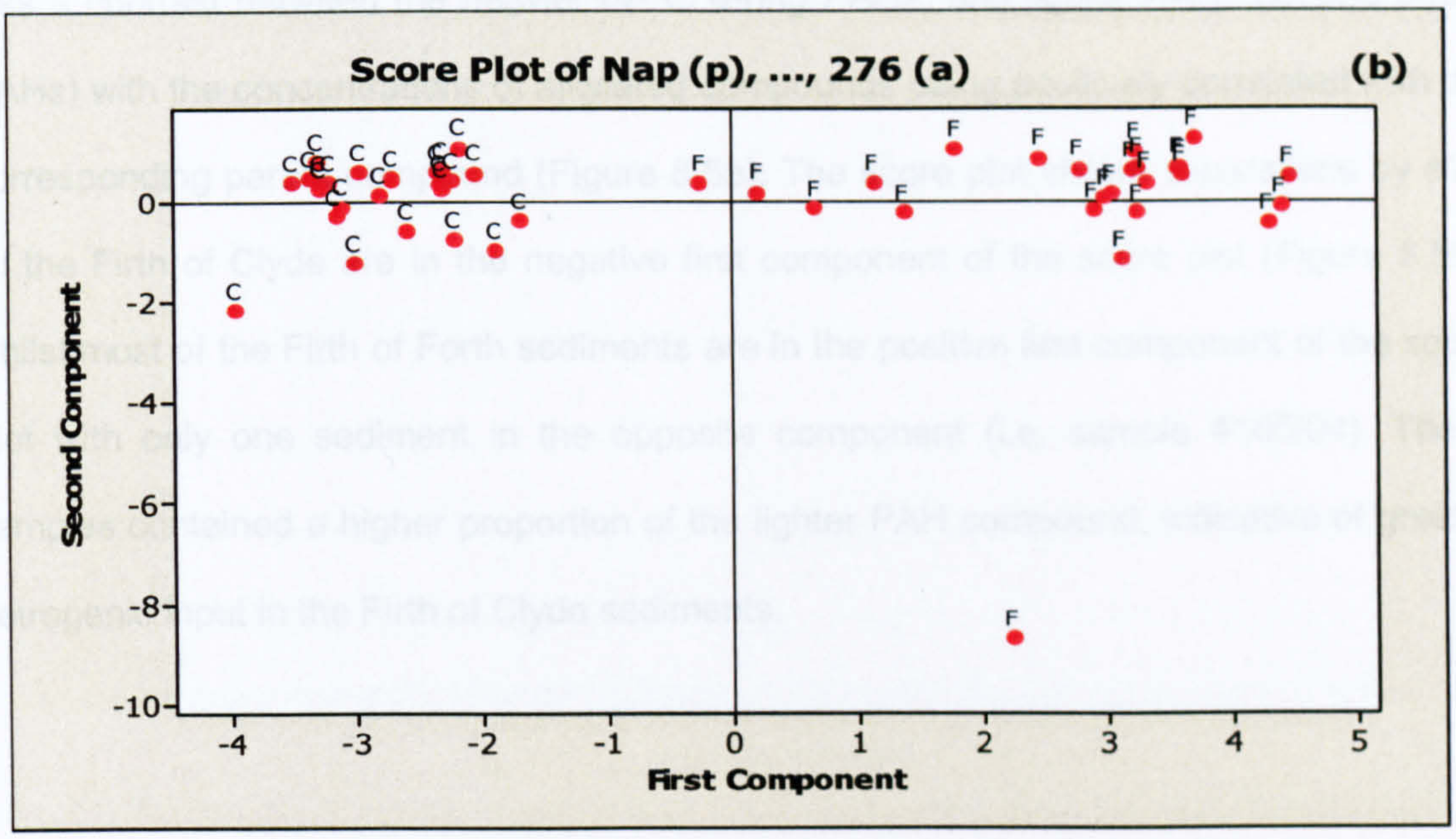

Figure 8.5 Principal component analysis of the Firth of Clyde and Firth of Forth using ring group, parent and alkylated compounds. (a) Loading plot, showing the lighter PAH compounds with a positive first component, and the heavier, more persistent, compounds with negative first components. (b) Samples in the left half of the graph were all from Firth of Clyde and samples from the right half of the graph were from the Firth of Forth and contained a higher proportion of the lighter PAHs, indicative of greater petrogenic input. C and F symbolize Firth of Clyde and Firth of Forth sediments, respectively.

The concentration ratio of the Firth of Forth (the plot of Fl/Py against P/A; Figure 8.4b) show that 21 of the 25 samples cluster on the mixed zones, due to Fl/Py ratio less than 1, the remaining samples fell on either the pyrolytic zone or within the reference line (Fl/Py ratio = 1). All the sediments samples had P/A ratio less than 10 (Figure 8.4a). A plot of Fl/Py against MP/P ratios shows that most of the samples cluster in the mixed zones and petrogenic zones, this suggest there was greater petrogenic input in the Firth of Forth.

The PAH profile of the Firth of Clyde and Firth of Forth were investigated further using PCA (Figure 8.5), for details of PCA (see section 5.3.h). The first two components accounted for 64 and 20% of the variance in the data respectively. The first component was a contrast between the heavier (4- to 6-ring PAHs) and lighter PAHs (2- and 3-ring PAHs) with the concentrations of alkylated compounds being positively correlated with the corresponding parent compound (Figure 8.5a). The score plot shows separations by site, all the Firth of Clyde are in the negative first component of the score plot (Figure 8.5b), whilst most of the Firth of Forth sediments are in the positive first component of the score plot with only one sediment in the opposite component (i.e. sample 4165/04). These samples contained a higher proportion of the lighter PAH compound, indicative of greater petrogenic input in the Firth of Clyde sediments.

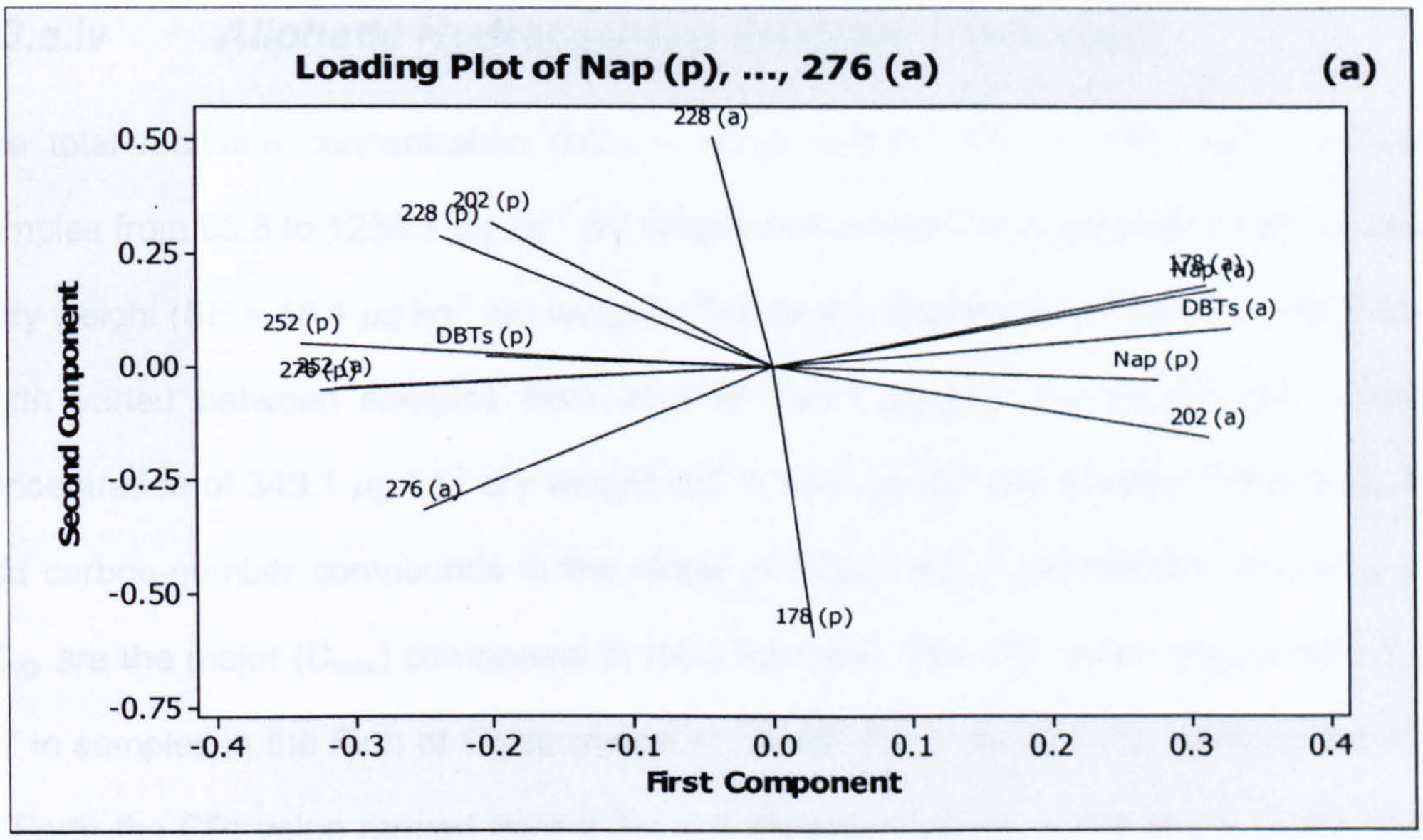

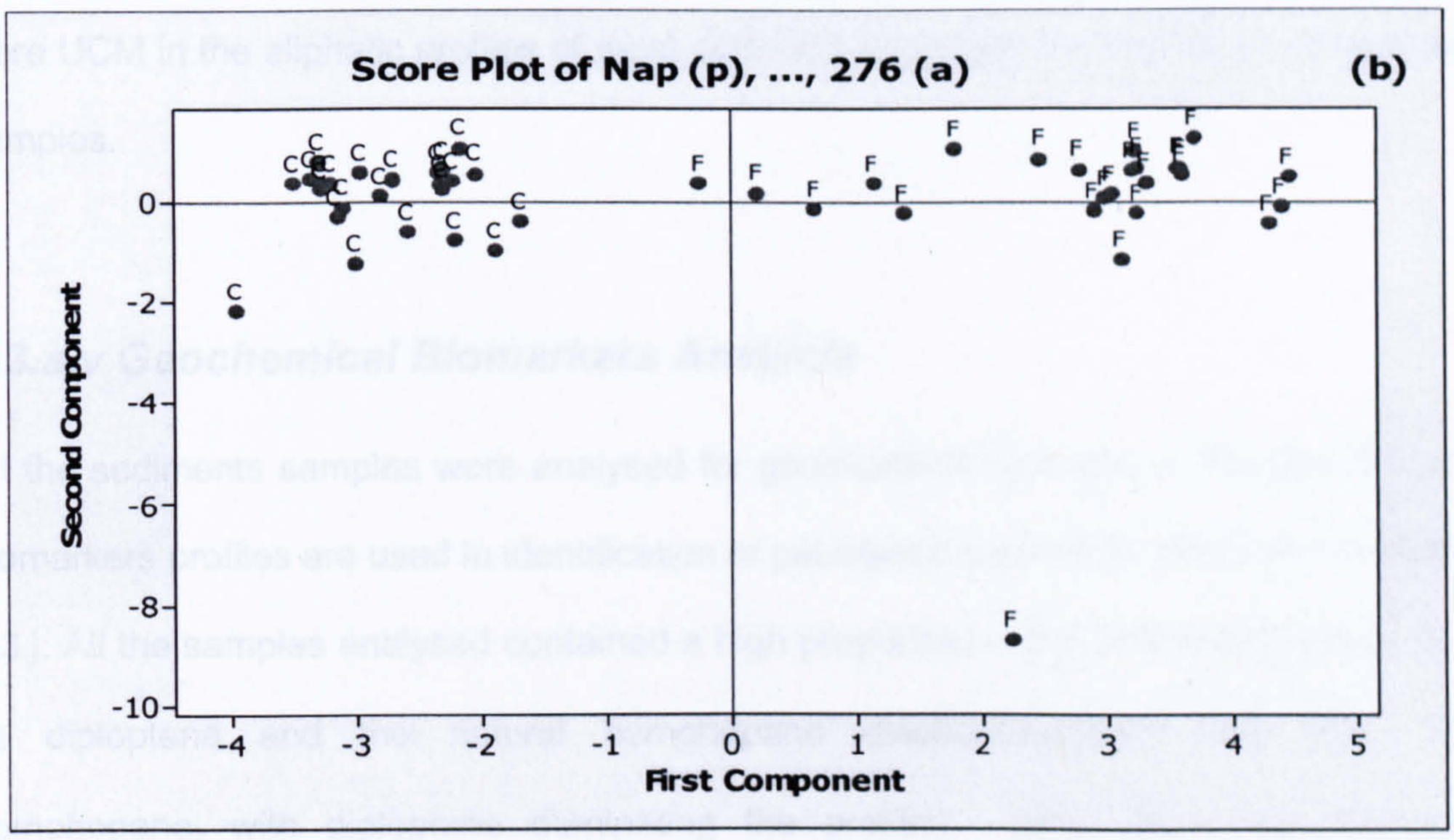

Figure 8.5 Principal component analysis of the Firth of Clyde and Firth of Forth using ring group, parent and alkylated compounds. (a) Loading plot, showing the lighter PAH compounds with a positive first component, and the heavier, more persistent, compounds with negative first components. (b) Samples in the left half of the graph were all from Firth of Clyde and samples from the right half of the graph were from the Firth of Forth and contained a higher proportion of the lighter PAHs, indicative of greater petrogenic input. C and F symbolize Firth of Clyde and Firth of Forth sediments, respectively.

8.3.a.iv Aliphatic Hydrocarbons Analysis (n-alkanes)

The total *n*-alkane concentration (nC_{12} – nC_{33}) in the Firth of Clyde varied between samples from 63.8 to 1238.1 μg kg^{-1} dry weight with a mean concentration of 489.6 μg kg^{-1} dry weight (SE = 48.4 μg kg^{-1} dry weight). The total *n*-alkane concentration in the Firth of Forth varied between samples from 49.8 to 743.1 μg kg^{-1} dry weight with a mean concentration of 349.1 μg kg^{-1} dry weight (SE = 33.9 μg kg^{-1} dry weight) (Table 8.1). The odd carbon-number compounds in the range of nC_{25} – nC_{33} predominate, and nC_{29} and nC_{33} are the major (C_{max}) component in most samples. The CPI value ranged from 1.1 – 2.7 in samples in the Firth of Clyde (mean = 1.8, SE = 0.1 and n = 25), whilst in the Firth of Forth the CPI value ranged from 2.3 – 4.2 (mean = 3.0, SE = 0.1 and n = 25). There were UCM in the aliphatic profiles of most sediment especially the Firth of Forth sediment samples.

8.3.a.v Geochemical Biomarkers Analysis

All the sediments samples were analysed for geochemical biomarkers. The geochemical biomarkers profiles are used in identification of petrogenic sources as described in section 5.3.j. All the samples analysed contained a high proportion of the natural triterpanes such as diploptene and the natural homohopane diastereoisomers 22R, 17α, 21β-homohopane, with diploptene dominating the profiles. Also there were presence homohopane doublets, indicative of the Gulfaks crude oil.

8.3.b Results of the Composite Random Sampling (CRS) Design

The composition of the composite samples for the Clyde and Firth of Forth are given in Table 8.4. 5 ± 0.1 g of each of the freeze dried sediment samples were mixed for TOC

and PSA analysis, whilst for the fluorescence, PAHs, aliphatic analysis and geochemical biomarker determination, 40 ± 1.0 g of each of the sediment samples were mixed together. Four replicates samples were analysed for the TOC and PSA analyses, whilst two replicate samples were analysed for oil equivalents of Forties and diesel oils, total PAH and total *n*-alkane concentration. The data are tabulated in Appendices 11-13 and summarised in Tables 8.5. In particular, the summary tables give mean values with standard errors for the Firth of Clyde and Firth of Forth composite sediments.

Table 8.4 Compositions of the composite samples,

	Composite sample	Samples Identification				
Firth of Clyde	731/05	4110/04	4114/04	4116/04	4127/04	4131/04
	732/05	4109/04	4113/04	4120/04	4125/04	4128/04
	733/05	4111/04	4123/04	4124/04	4129/04	4132/04
	734/05	4108/04	4117/04	4118/04	4126/04	4130/04
	735/05	4112/04	4115/04	4119/04	4121/04	4122/04
Firth of Forth	736/05	4149/04	4151/04	4155/04	4156/04	4166/04
	737/05	4143/04	4146/04	4153/04	4161/04	4162/04
	738/05	4145/04	4154/04	4159/04	4164/04	4165/04
	739/05	4147/04	4152/04	4157/04	4163/04	4167/04
	740/05	4144/04	4148/04	4150/04	4158/04	4160/04

Percentage TOC varied from composite sample between 1.3 to 1.5%, and the mean was 1.4% (SE = 0.02%; Table 8.5), and the percentage of < 63 μm of the PSA varied from composite sample between 85.8 to 91.7%; mean PSA was 89.0% (SE = 2.14%; Table 8.5) for the Firth of Clyde sediments. The percentage TOC varied between composite samples from 0.8 to 0.9%; mean TOC was 0.9% (SE = 0.01%; Table 8.5), and the percentage of < 63 μm of the PSA varied between composite sample from 38.8 to 44.4%; mean PSA value was 41.3% (SE = 0.89%; Table 8.5).

Table 8.5 Summary of the TOC, PSA, oil equivalents of Forties and diesel, total PAH and total *n*-alkane concentrations for the composite random sampling for Firth of Clyde and Firth of Forth. All concentrations are in dry weight.

Variables	Sampling	Min	Mean	Median	Max	SD	SE	CV (%)
TOC (%)	Clyde	1.3	1.4	1.4	1.5	0.05	0.02	3.5
	Forth	0.8	0.9	0.8	0.9	0.03	0.01	3.7
PSA (%)	Clyde	85.8	89.0	88.9	91.7	2.41	1.08	2.7
	Forth	38.8	41.3	40.8	44.3	2.00	0.89	4.8
Diesel ($\mu g\ g^{-1}$)	Clyde	59.5	69.5	73.4	75.0	6.98	3.12	10.0
	Forth	21.4	23.7	22.7	27.5	2.50	1.12	10.6
Forties ($\mu g\ g^{-1}$)	Clyde	375.3	472.3	500.8	524.2	63.20	28.30	13.4
	Forth	132.4	156.5	162.7	177.1	17.47	7.81	11.2
Total PAH ($\mu g\ kg^{-1}$)	Clyde	1331.0	1745.0	1811.0	2071.0	270.00	121.00	15.5
	Forth	395.7	511.6	530.0	603.3	83.60	37.40	16.4
n-alkanes ($\mu g\ kg^{-1}$)	Clyde	485.8	576.9	566.8	636.9	63.10	28.20	10.9
	Forth	256.0	297.5	284.1	379.6	49.50	22.20	16.7

Min = Minimum; Med = Median; Max = Maximum; SD = Standard Deviation;
CV = Coefficient of Variation; SE = Standard Error of the mean.

The Firth of Clyde sediments Forties crude oil equivalent concentrations varied for composite samples between 375.3 and 524.2 $\mu g\ g^{-1}$ dry weight with a mean concentration of 472.2 $\mu g\ g^{-1}$ dry weight (SE = 63.2 $\mu g\ g^{-1}$ dry weight; Table 8.5), and the diesel oil equivalent concentration varied from a composite sample from 59.5 to 75.0 $\mu g\ g^{-1}$ dry weight with a mean concentration of 69.5 $\mu g\ g^{-1}$ dry weight (SE = 6.98 $\mu g\ g^{-1}$ dry weight; Table 8.5).

The Firth of Forth sediment Forties crude oil equivalent concentrations varied between composite samples from 132.4 to 177.1 $\mu g\ g^{-1}$ dry weight, mean value was 156.5 $\mu g\ g^{-1}$ dry weight (SE = 7.8 $\mu g\ g^{-1}$ dry weight; Table 8.5), and the diesel oil equivalent

concentration varied from a composite sample between 21.4 to 27.5 μg g^{-1} dry weight; mean value was 23.7 μg g^{-1} dry weight (SE = 2.5 μg g^{-1} dry weight; Table 8.5).

The total PAH concentration, which is the sum of the parent and alkylated 2- to 6-ring including the 16 US EPA PAHs, varied in the Firth of Clyde composite samples between 1331.0 to 2071.0 μg kg^{-1} dry weight; mean total PAH concentration was 1745.0 μg kg^{-1} dry weight (SE = 121.0 μg kg^{-1} dry weight; Table 8.5), and the Firth of Forth had total PAH concentration varied from a composite sample between 395.7 to 603.3 μg kg^{-1} dry weight; mean total PAH concentration was 511.6 μg kg^{-1} dry weight (SE = 37.4 μg kg^{-1} dry weight; Table 8.5).

The total *n*-alkane concentration (nC_{12} – nC_{33}) varied from a composite sample between 485.8 to 636.9 μg kg^{-1} dry weight; mean total *n*-alkane concentration was 576.9 μg kg^{-1} dry weight (SE = 63.1 μg kg^{-1} dry weight; Table 8.5) for the Firth of Clyde sediments, whilst for the Firth of Forth sediments, the total *n*-alkane concentration varied from a composite sample between 256.0 to 379.0 μg kg^{-1} dry weight; mean total *n*-alkane concentration was 297.5 μg kg^{-1} dry weight (SE = 16.7 μg kg^{-1} dry weight; Table 8.5).

Table 8.6 Summary of the individual simple random sampling (SRS) and composite random sampling (CRS) designs of the TOC; < 63 μm fraction (PSA), diesel and Forties oil equivalent concentrations, total PAH and total *n*-alkane concentrations. Concentrations are on a dry weight basis.

Variables	Stations	Simple Random Sample (SRS)		Composite Random Samples (CRS)	
		Mean	SE	Mean	SE
TOC (%)	Clyde	1.4	0.09	1.4	0.02
	Forth	1.0	0.15	0.9	0.01
PSA (%)	Clyde	86.6	4.27	89.0	1.08
	Forth	41.2	2.63	41.3	0.89
Diesel ($\mu g\ g^{-1}$)	Clyde	63.2	7.00	69.5	3.12
	Forth	27.6	3.54	23.7	1.12
Forties ($\mu g\ g^{-1}$)	Clyde	404.1	44.40	472.3	28.30
	Forth	161.8	20.00	156.5	7.81
Total PAH ($\mu g\ kg^{-1}$)	Clyde	1858.0	196.00	1745.0	121.00
	Forth	532.4	58.90	511.6	37.40
Total *n*-Alkane ($\mu g\ kg^{-1}$)	Clyde	489.6	48.40	576.9	28.20
	Forth	349.1	33.90	297.5	22.20

SE = Standard Error of the mean.

In principle, the average of the composite random sampling sediment samples should be equal to the average of the individual (simple random sampling) sediment samples, i.e. with zero systematic error. **In all the parameters measured, there were no significant differences between the mean values of the composite random sampling and the simple random sampling ($p > 0.05$; ANOVA) for both the Firth of Clyde and Firth of Forth sediments** (Table 8.6). The 95% confidence interval for all the parameters in the

Firth of Clyde and Firth of Forth shows no significant differences (Figure 8.6) between the composite random sampling and the random sampling.

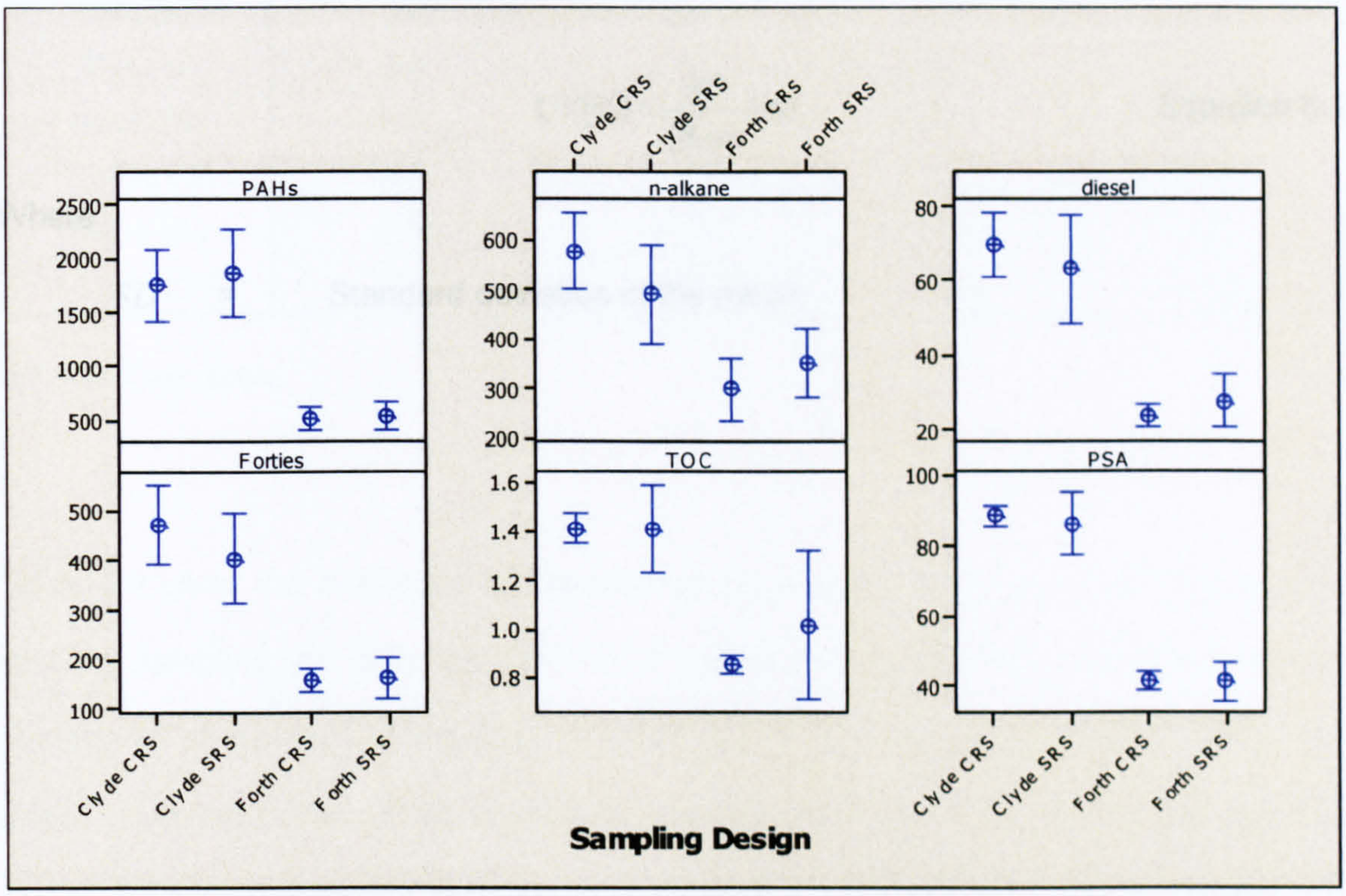

Figure 8.6 The 95% confidence interval for the means of TOC (%), PSA (%), diesel (μg g^{-1} dry weight), Forties (μg g^{-1} dry weight), total PAH concentrations (μg kg^{-1} dry weight), and total *n*-alkane concentrations (μg kg^{-1} dry weight). CRS represent composite random sampling and SRS is simple random sampling.

Further statistical analysis based on the precision of each analytical method was used to determined if the differences between the mean variance of the two sampling regime are within the analytical precision of each analysis. The coefficients of variance between the sampling regimes were calculated using the following formula:

$$CV(\%) = \frac{SD}{Mean} 100 \qquad \text{Equation 8.1}$$

Where

SD = Standard deviation of the mean,

Table 8.7 Precisions of the UKAS accredited analyses, calculated analyses and the coefficients of variance of the two sampling for the Firth of Clyde and Firth of Forth.

Analytical Method	UKAS Analytical Precision %	Calculated Precision of replicate analyses %	Coefficient of Variance %	
			Firth of Clyde	Firth of Forth
CHN (%)	2.5	0.8	0.21	1.64
PSA (%)	2.5	1.6	1.88	0.15
Diesel (%)	N/A	8.6	6.78	10.67
Forties (%)	N/A	10.4	11.01	2.36
PAHs (%)	< 10	9.8	4.44	2.82
n-alkanes (%)	N/A	10.6	11.58	11.29

N/A = Not applicable.

Table 8.6 gives the coefficient of variance of the composite random sampling and the random sampling for both the Firth of Clyde and Firth of Forth sediments. All the coefficients of variance of the Firth of Clyde and Firth of Forth samples are below the stated precision of the UKAS accredited methods (i.e. CHN, PSA and PAHs analysis). The coefficients of variance were also compared with the calculated precisions of replicate analyses. The calculated precisions are the precisions of the four replicate samples (Section 4.13.a). The coefficients of variance for the parameters measured were also lower or slightly higher than the calculated precisions (Table 8.6).

Comparisons of the distribution of the total PAH concentration shows that there were no significant differences in the PAH profiles (PAH composition) of the composite random sampling and the random sampling for both Firth of Clyde and Firth of Forth sediments ($p > 0.05$; ANOVA: Figures 8.7). Also the geochemical biomarkers profiles shows no significant differences in the statistics of the abundance of the steranes and triterpane

profile between the composite random sampling and the random sampling for both the Firth of Clyde and Firth of Forth ($p > 0.05$; ANOVA).

Therefore, in all the parameters measured, there was no significant difference in the mean values of the composite random sampling sediments and the random sampling sediments for both the Firth of Clyde and Firth of Forth. Also the composite random sampling gave mean values with less variance at lower cost and in less time.

(a)

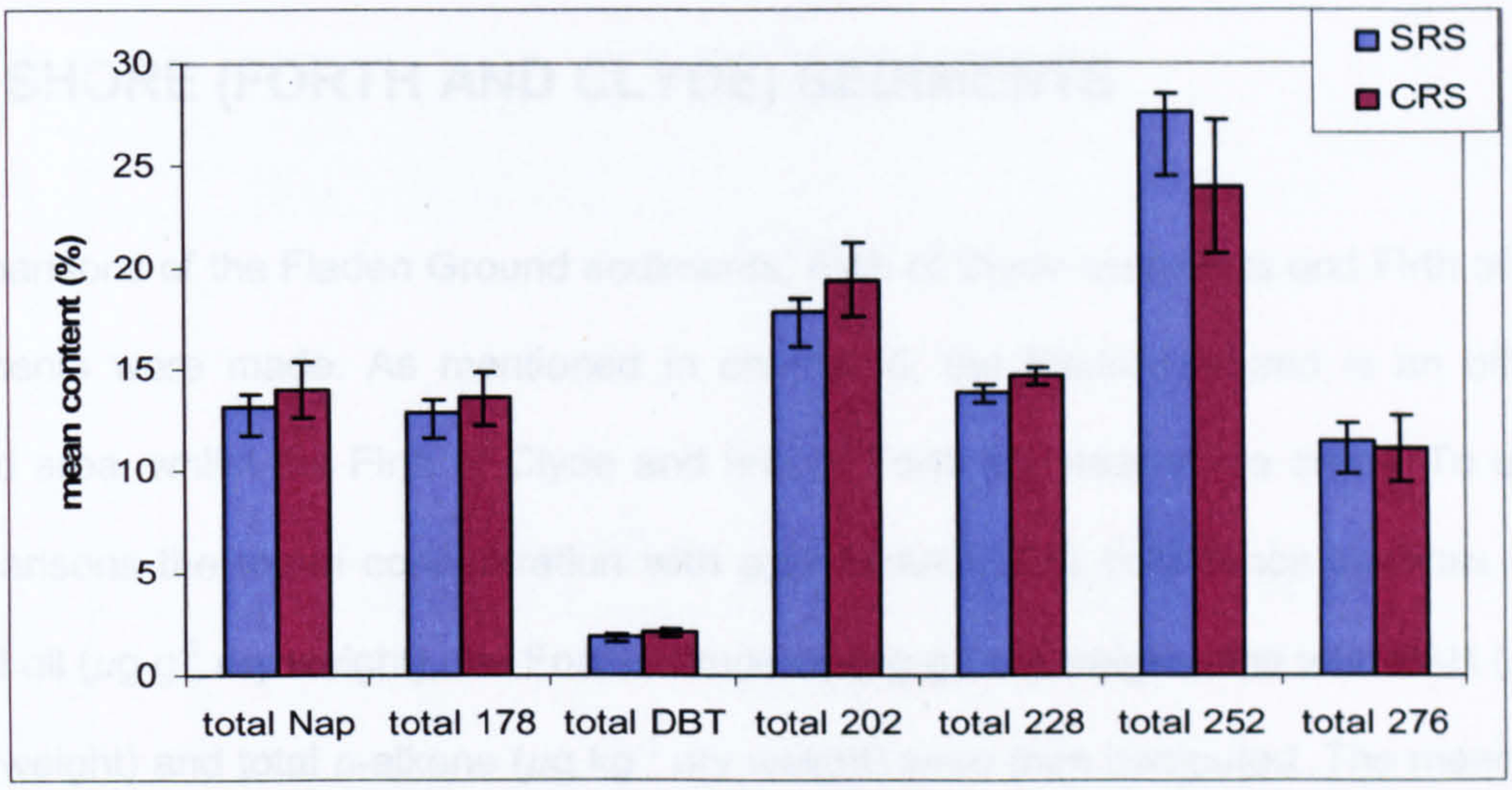

(b)

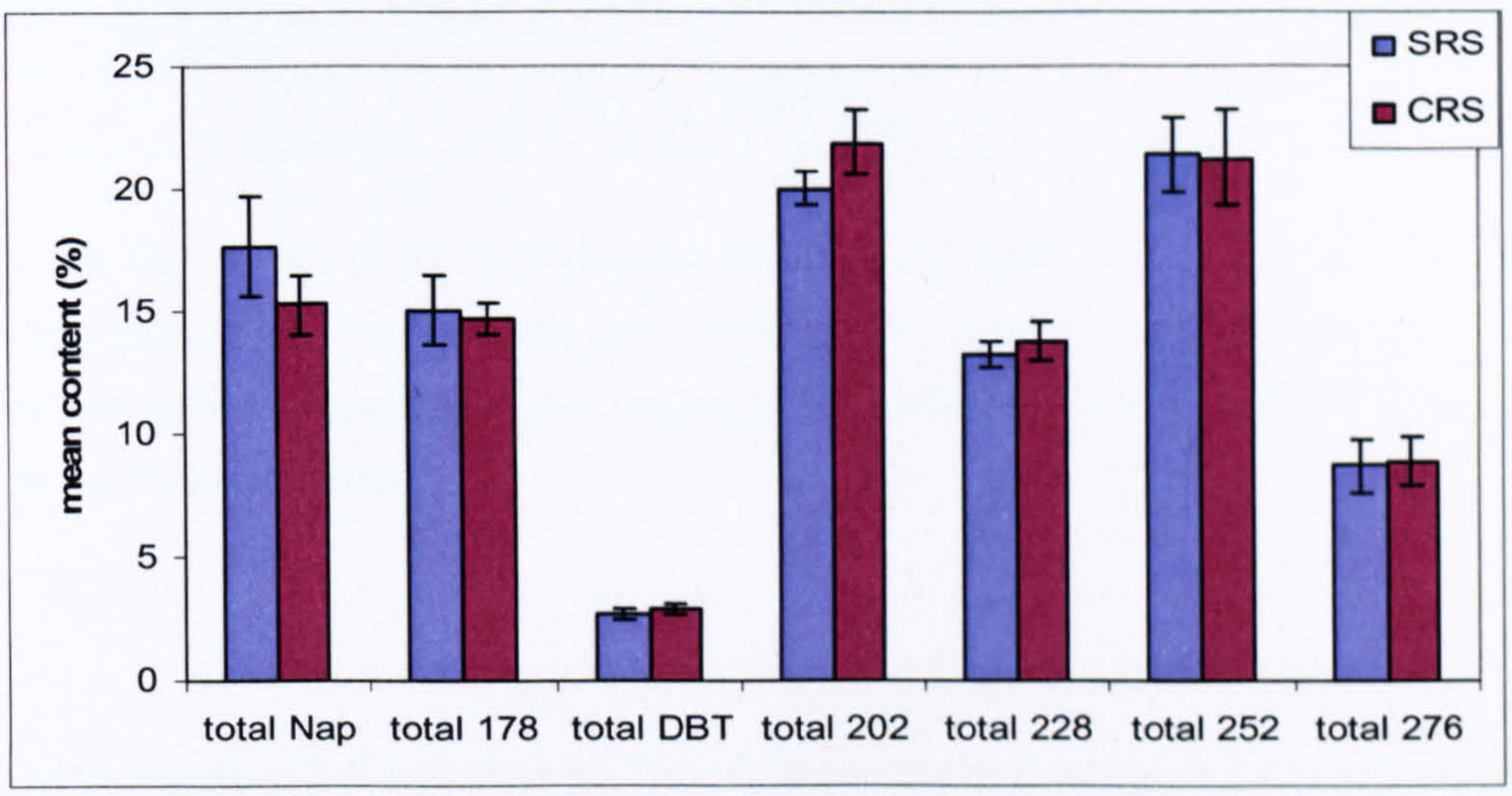

Figure 8.7 Profiles of total PAH concentration by ring classes (a) Firth of Clyde (b) Firth of Forth, showing the similarities in the distributions of the composite random sampling (CRS) and the simple random sampling (SRS) of the two survey areas. Error bars represents the standard deviation of the mean.

Total naphthalenes (parent and C_1-C_4); total 178, phenanthrene/anthracene (parent and C_1-C_3); total DBT, dibenzothiophenes (parent and C_1-C_3); total 202, fluoranthene/pyrene (parent and C_1-C_3); total 228, benzanthracene/benzophenthrenes/chrysene/triphenylenes (parent and C_1-C_2); total 252, benzofluoranthene/benzopyrene/perylene and total 276, indenopyrene/benzoperylene (parent and C_1-C_2).

8.4 COMPARISON OF THE OFFSHORE (FLADEN) AND NEAR-SHORE (FORTH AND CLYDE) SEDIMENTS

Comparisons of the Fladen Ground sediments, Firth of Clyde sediments and Firth of Forth sediments were made. As mentioned in chapter 5, the Fladen Ground is an offshore oilfield area, whilst the Firth of Clyde and firth of Forth are near-shore areas. To enable comparisons the mean concentration with approximate 95% confidence intervals of the diesel oil (μg g^{-1} dry weight), the Forties crude oil (μg g^{-1} dry weight), the total PAH (μg kg^{-1} dry weight) and total *n*-alkane (μg kg^{-1} dry weight) were then computed. The means and 95% confidence intervals are shown below (Figure 8.8).

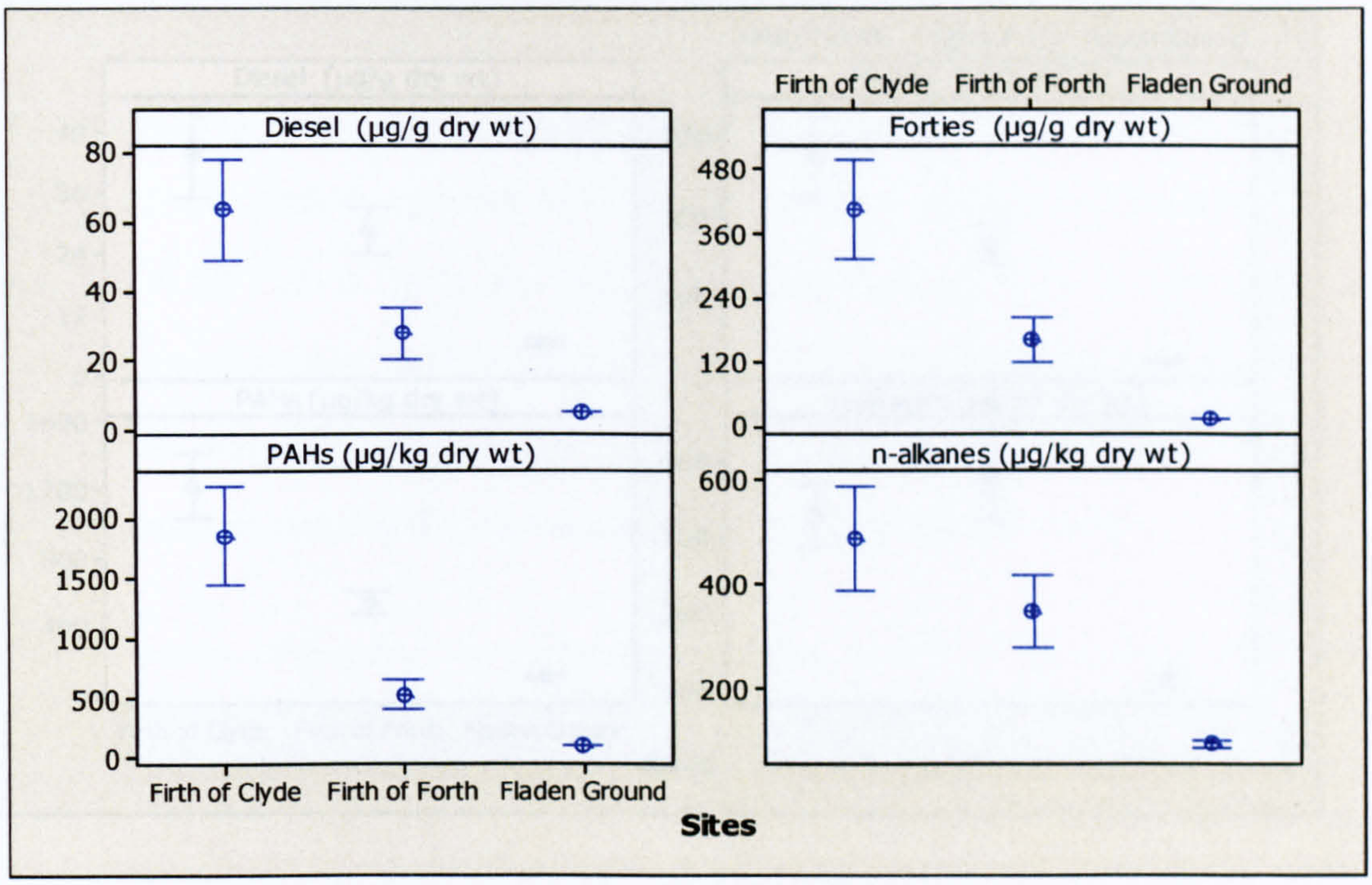

Figure 8.8 The mean concentrations for the Firth of Clyde, Firth of Forth and Fladen Ground surveys of the Forties crude and diesel oil equivalent, total PAH and total *n*-alkane concentration. All samples are in dry weight, open circles are means and vertical lines are the 95% confidence intervals.

There were significant differences in hydrocarbon concentrations in the three areas. The concentrations of hydrocarbons in the Fladen Ground sediments were significantly lower than in either the Firth of Clyde or Firth of Forth sediments. The concentrations were normalized to TOC to remove any effects caused by the organic carbon content in the sediment. Even having normalized the concentrations of the hydrocarbon to TOC, still there were significant differences in the normalized data (Figure 8.9) of the Fladen Ground and the Firth of Clyde and Firth of Forth.

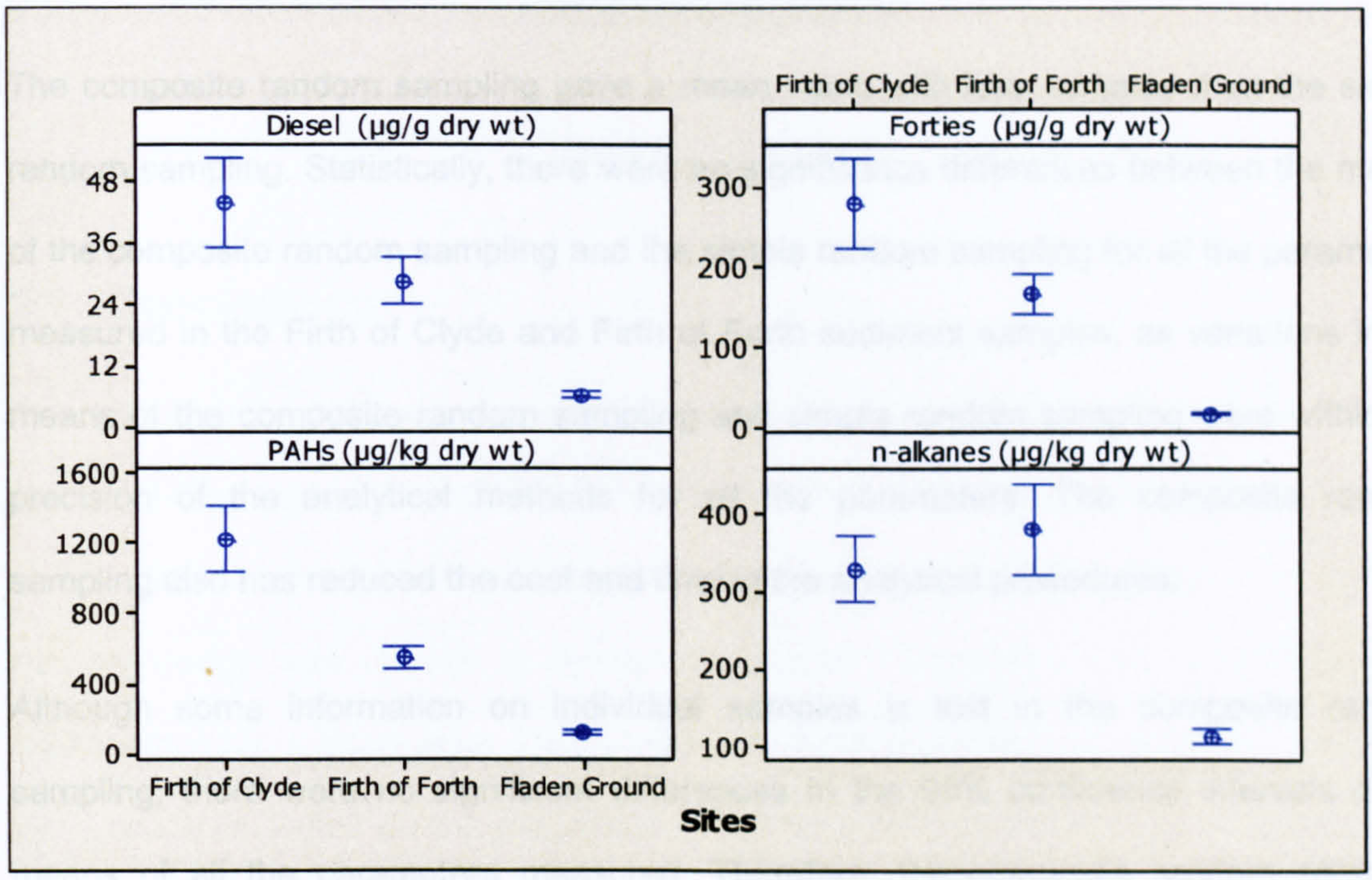

Figure 8.9 The mean concentrations normalized to TOC for the Firth of Clyde, Firth of Forth and Fladen Ground surveys of the Forties crude and diesel oil equivalent, total PAH and total *n*-alkane concentration. All samples are in dry weight, open circles are means and vertical lines are the 95% confidence intervals.

The low concentrations of hydrocarbons in the Fladen Ground may be attributed to one main source of the contaminant (also might be others such as atmospheric) i.e., activities of the oil and gas industry. In the estuary, however, the legacy of riverine inputs and direct discharges from past industrial and transport activities and, at some restricted localities, the inputs of dredged material and sewage sludge dumping operations will all have contributed to the estuary high hydrocarbons concentrations.

8.5 CONCLUSIONS

The composite random sampling gave a mean value with less variance than the simple random sampling. Statistically, there were no significance differences between the means of the composite random sampling and the simple random sampling for all the parameters measured in the Firth of Clyde and Firth of Forth sediment samples, as variations in the means of the composite random sampling and simple random sampling were within the precision of the analytical methods for all the parameters. The composite random sampling also has reduced the cost and time in the analytical procedures.

Although some information on individual samples is lost in the composite random sampling, there were no significant differences in the 95% confidence intervals of the means of all the parameters measured. Therefore, the composite random sampling, coupled with the stratified sampling, will achieve better representation better precision of an estimated mean, at less cost, and data analysis is usually easy.

CHAPTER NINE

CONCLUSIONS

9.1 Conclusions

The aim of this work was to design a robust spatial sampling strategy that will give representative information on contamination of sediments since one-off sampling can clearly give results that are unrepresentative of the site being studied. The stratified random design was chosen to assess the spatial composition and concentrations of hydrocarbons in a study area. Zones were constructed equally and numbers of samples were allocated based on the proportion of the far field area in the Zone. Near field are areas < 5 km from multiple oil wells or < 2 km from a single well, whilst far field are areas > 5 km from multiple oil wells or > 2 km from a single oil well. A total of 16 Zones was then defined using prior information on the spatial variation in the physical and chemical characteristic of the sediments in the field area. In addition to providing data to allow the comparison of conventional grid and the new stratified random sampling regimes, this research work has also provided important data on composition and concentrations of hydrocarbons in sediments of the chosen area. The Fladen Ground has been the focus of offshore oil and gas production over the past 30-40 years and is a key fishing area in the northern North Sea.

This study has highlighted the benefits and limitations of both sampling regimes in the oil and gas exploration and production areas. The grid design has the benefits of more spatial coverage, and is more practical and convenient to implement in the field than the random stratified design. The grid design was also able to identify hotspots, and, perhaps

more importantly, it would be possible to estimate the probability of detecting hotspots of particular sizes. Because sampling in a grid design is inherently biased, it has the disadvantage that it is possible to overestimate or underestimate a population characteristic aligned with the grid. The grid design often requires statistical analysis that is based on assumptions that are difficult to substantiate, and also missing stations arising, for example, from bad weather at sea or being located in near field areas are difficult to accommodate in the statistical analysis.

The samples from the study area had to be analysed using a range of measurement methods to provide the data to assess the sampling regimes. Two hundred and forty two (242) sediments samples were analysed for particle size (PSA), total organic carbon (TOC), oil equivalents of the Forties crude and diesel oils, total polycyclic aromatic hydrocarbon (PAH) concentrations, total *n*-alkane concentrations and geochemical biomarkers. Measurement techniques used included laser granulometry employing a Malvern Mastersizer E Particle Size Analyser (PSA), whilst TOC was determined using Perkin Elmer CHN elementary analyser following acid treatment. Fluorescence analysis using ultraviolet visible absorption and fluorescence spectroscopy (UVF) was utilised for the oil equivalents of the Forties crude and diesel oil. Gas chromatography using mass specific detection (GC-MS) was utilised for PAHs and geochemical biomarkers and gas chromatography with flame ionisation detector (GC-FID) was used for the more general aliphatic hydrocarbon analysis (*n*-alkanes).

The total PAH concentrations (2- to 6-ring parent and alkylated PAHs including the 16 US EPA PAHs) in sediments were relatively low (e.g. 108.2 μg kg^{-1} dry weight). Also, the concentrations of the ten individual PAH (naphthalene, phenanthrene, anthracene, fluoranthene, pyrene, benz[a]anthracene, chrysene, benzo[a]pyrene, benzoperylene and

indenopyrene) were relatively low in comparison with the OSPAR background assessment concentrations (BACs). The total PAH concentrations of sediments samples collected from the 2001 stratified survey were lower than in sediments samples collected from the 2001 grid survey, and considerably lower compared with the sediments samples collected in 1989 grid survey. The PAH distribution profile in the Fladen Ground indicated potential source dependence, as the levels were generally higher in the Zones of higher percentage < 63 μm particle sizes fractions and organic carbon content. Suggesting the importance of particulate organic coating in PAH sorption, consistent with the commonly accepted hydrophobic partition theory. In addition, non-point sources, in particular pyrolytic, were dominant sources in the area. PAH distribution and concentration ratios indicated a predominantly pyrolytic input, being dominated by the heavier, more persistent, 5- and 6-ring compounds, and with a high proportion of the parent PAH. However, the 1989 sediments had a higher proportion of the 2- and 3-ring compound compared to the 2001 grid and stratified sediments, suggesting that there was greater petrogenic input in 1989.

The *n*-alkane profiles of a number of the 2001 stratified sediments contained, small, high boiling point UCMs, similar to the 2001 grid sediments, indicative of limited petrogenic input from weathered oil. The geochemical biomarker profiles of the 2001 stratified sediments (containing UCMs) contained a small bisnorhopane peak and a high proportion of norhopane to hopane, indicating that there was contamination from both Middle Eastern and North Sea oils.

There were no significant differences in the overall mean between the Forties crude and diesel oil equivalents and total PAH concentration in the 2001 stratified random sediments compared to the 2001 grid sediment. However, there was a significant difference in the

total *n*-alkane concentrations; the 2001 grid total *n*-alkane concentrations were higher than the 2001 total *n*-alkane concentrations. Significant differences was observed within the mean of some Zones for Diesel in Zone 10, Forties in Zone 11 and total PAH concentrations in Zone 11. In comparison of the temporal trend between 1989 - 2001, there were significant differences in the hydrocarbon composition and concentrations following the cessation of discharges of cuttings in the Fladen Ground in the late1990s. The reduction was also due to tighter control of discharges of produced water and amount of flaring at the flarestacks. There were reduction of more than 60% in Forties crude, in Diesel oil, total PAHs and total *n*-alkane concentrations in the 2001 sampling surveys compared to the 1989 survey.

The stratified random sampling design gave much more reliable mean concentrations for all the four parameters, achieving a much lower variance than the grid sampling design. The stratified random design is cost and time effective, and produces estimates with increased precision (lower variance) compared to the grid sampling design. The increase in precision, or alternatively reductions in variance, time and cost, obtainable through stratified random sampling, depends on the quality of the information used to set up the design. Any possible increases in precision are particularly dependent on strength of the correlation of the auxiliary stratification variable with the variable observed in the study.

For optimum allocations of samples among Zones, the optimisation process allocates more samples to those variable/Zone combinations that show relatively high variance, and lower numbers of samples to those where the variance is relatively low. In general, there tends to be a degree of covariance between the numbers of samples allocated to each variable. For example, the numbers allocated to Zones 4 and 8 are mainly high in

comparison to those allocated to Zones 6 and 12. This suggests some similarity in the distribution of variance between Zones for all the variables measured.

In the spatial analysis of the Fladen Ground data, a nuggets effects were observed in the variograms for all parameters The variograms indicated trends in the PSA, TOC, total PAH concentrations and in the forties crude oil equivalent and diesel oil equivalents because of the lack of attainment of a sill in the variograms for these variables. The spatial analysis gave an Ariel view of the hydrocarbon contamination in the Fladen Ground, and assisted in discovering and understanding of the spatial relationships in the data. This discovery and understanding can be as simple as viewing the data in the more convenient and readily appreciated form. The spatial analysis can perform other functions such as finding distance, assigning proximity, calculating density, creating contours, and deriving slopes. Therefore spatial interpolation is a useful way to explore the accumulation of hydrocarbons in the environment (sediments).

A field study was designed, based on the outcome of the stratified random sampling design, to investigate a composite random sampling design, and to estimate a within–stratum mean value for each of the chosen measurement parameters with more thorough coverage (better representation), better precision and less variance at lower analytical cost in the near-shore environment (Firth of Clyde and Firth of Forth). The study showed that the composite random sampling gave a mean value with less variance than the simple random sampling. Statistically, there were no significance differences between the means of the composite random sampling and of the simple random sampling for all the parameters measured in the Firth of Clyde and Firth of Forth sediment samples, as variations in the means of the composite random sampling and simple random sampling

were within the precision of the analytical methods for all the parameters. The composite random sampling also reduced the cost and time in the analytical procedures.

Although, the information on individual samples was lost in the composite random sampling, there were no significant differences in the 95% confidence intervals between the means of all the parameters measured. Therefore, the composite random sampling, couple with the stratified sampling, will achieve better representation, and better precision of estimated means at less cost, and data analysis is usually easy.

9.2 Recommendations

Clearly, any recommendations for future survey design depend on the objectives of the survey. The 2001 stratified random survey has shown that far-field concentrations in the Fladen Ground are much lower than in 1989 and that the concentrations of the ten individual PAHs for which Background Concentrations have been established are all near background. This suggests that any future decreases in hydrocarbon concentrations in the far-field will be small and that there is little point in investing heavily in trying to detect such changes in the far-field. Future monitoring of the far-field in the Fladen Ground would therefore be for surveillance purposes; i.e. to detect any increases in hydrocarbon concentrations.

Grid surveys or stratified random surveys

In principal, grid surveys (with a random starting point) and stratified random surveys both can provide unbiased estimates of mean hydrocarbon concentrations (Cochran, 1977). Further, given the same sample size, grid surveys are often more precise than stratified

random surveys in practice (Cochran, 1977), although it is harder to estimate the precision of a grid survey. However, grid surveys are not well suited to irregular survey areas such as the Fladen far-field. It is also much easier to adapt a stratified random survey to deal with missing values arising from bad weather etc. A stratified composite random survey is therefore recommended for future surveys of the hydrocarbon contaminants.

Sample size

The choice of sample size will depend on the objectives of the survey. But to illustrate, consider a long-term surveillance monitoring programme to detect a 100% increase in hydrocarbon concentrations (should it occur). Sixteen samples per year would estimate the mean concentration of all four types of hydrocarbons with a coefficient of variation of 15% or better (base on the Fladen data). And this would allow us to detect a 100% increase in concentration over ten or twenty years if the between-year coefficient of variation is 12% or 24% respectively (Nicholson *et al.*, 1997). (The between-year coefficient of variation is a measure of random fluctuations in mean concentrations from year to year due e.g. to fluctuating environmental conditions. It is difficult to estimate without a long time series, but UK National Marine Monitoring Programme data suggest that the between-year coefficient of variation for total PAH concentrations is typically somewhere between 10 and 30%).

Small sample sizes would necessitate some revision of the stratification to ensure sufficient samples within each stratum to estimate variances, standard errors etc. In the illustration above, an obvious change would be to combine the sixteen strata into four larger strata, i.e. Zones 1, 2, 5, 6, Zones 3, 4, 7, 8, Zones 9, 10, 13, 14, and Zones 11, 12, 15, 16.

Sample allocation

In the 2001 stratified random survey, the number of samples in each Zone was chosen by *proportional allocation*, with the number of samples proportional to the available far-field area. However, there are other criteria that can be used to allocate numbers of samples to strata. In particular, knowing the variation in concentration between samples within Zones means that the number of samples can be chosen by *optimal allocation*. This allocation gives more samples to Zones with high variability and maximises the precision of the estimate of mean concentration for the whole far-field, given a fixed total sample size *n*. If σ_h is the standard deviation in concentration between samples in Zone *h*, then the optimal allocation is

$$n_h = \frac{nA_h\sigma_h}{\sum_{k=1}^{16} A_k\sigma_k} \qquad \text{Equation 9.1}$$

Optimal allocations for estimating the mean concentrations of Forties crude, diesel, total PAH, and total *n*-alkanes, assuming a total fixed samples size of 242, can be triple using the stratified composite random sampling, so that less samples will be analysed.

Note that strict adherence to optimal allocation can lead to problems for two reasons. First, the estimates of variability are themselves subject to error and will be inflated in some Zones just by chance. Second, when the total sample size is relatively small, the optimal allocation can give only one or two samples in some Zones, which makes it difficult to estimate levels of variability in these Zones.

CHAPTER TEN

REFERENCES

Ahn, Y., Sanseverino, J. and Saylor, G.S. (1999) Analyses of polycyclic aromatic hydrocarbon degrading bacteria isolated from contaminated soils. *Biodegradation*, **10**, 149-157.

Allan, J. and Douglas, A.G. (1977) Variations in the content and distribution of *n*-alkanes in a series of Carboniferous vitrinites and sporinits of bituminous rank. *Geochimica Cosmochimica Acta,* **41**, 1223-1230.

Appel, J., Bockhron, H. and Frenklach, M. (2000) Kinetic modelling of soot formation with detailed chemistry and physics: Laminar premixed flames of C_2 Hydrocarbon. *Combustion and Flame,* **121**, 122-136.

Bailey, N., Chapman, C., Kinnear, J., Bora, D. and Weetman, A. (1993) Estimation of Nephrons stock biomass on the Fladen Ground by TV Survey, ICES CM 1993/R:34.

Basford, D.J. and Eleftherious, A. (1989) The macrobenthic in fauna of the offshore northern North Sea. *Journal Marine Biology Association*, UK, **69**, 123-143.

Baumard, P, Budzinski, H, Garrigues, P, Dizer, and Hansen, P.D. (1999) Polycyclic aromatic hydrocarbons in recent sediments and mussels (*mytilus edilis*) from the Western Baltic Sea: occurrence, bioavailabilty and seasonal variations. *Marine Environmental Research,* **47**, 17-47.

Baumard, P., Budzinski, H. and Garrigues, P. (1998) Polycyclic aromatic hydrocarbons in sediments and mussels of the western Mediterranean Sea. *Environmental Toxicology Chemistry,* **17**, 768-776.

Baumard, P., Budzinski, H., Garrigues, P., Narbonne, J.F., Burgeot, T., Michel, X. and Bellocq, J. (1999a) Polycyclic aromatic hydrocarbons (PAH) burden of mussels (*Mytilus* sp.) in different marine environments in relation with PAH contamination, and bioavailability. *Marine Environment Research,* **47**, 415-439.

Baumard, P., Budzinski, H., Garrigues, P., Sorbe, J.C., Burgeot, T. and Bellocq, J. (1998b) Concentrations of PAHs in various marine organisms in relation to those in sediments and to trophic level. *Marine Pollution Bulletin,* **36**, 951-960.

Baumard, P., Budzinski, H., Michon, Q., Garrigues, P., Burgeot, T. and Bellocq, J. (1998a) Origin and bioavailability of PAHs in the Mediterranean Sea from mussel and sediment records. Estuarine, *Coastal and Shelf Science,* **47**, 77-90.

Bauschlichers Jr., C.W. and Ricca, A. (2000) Mechanisms for polycyclic aromatic hydrocarbon (PAH) *growth. Chemical Physics Letters*, **326**, 283-287.

Berthou, F. and Vignier, V. (1986). Analysis and fate of dibenzothiophene derivatives in the marine environment. *International Journal of Environmental Analytical Chemistry,* **27**, 81-96.

Bittner, J.D. and Howard, J.B. (1981) Composition profiles and reaction mechanism in near sooting premixed benzene / oxygen / argon flame. *Eighteenth Symposium (international) on Combustion [proceedings].* The Combustion Institute, Pittsburgh. 1105-1116.

Boese, B.L.,Lamberson, J.O., Swartz, R.S., Ozretich, R. and Cole, R. (2000) Phtoinduced toxicity of PAHs and alkylated PAHs to a marine infauna amphipod *(Rhepoxynius abronius). Archive of Environmental Contamination Toxicology*, **34**, 235-240.

Bongiovanni, R., Borgarello, E. and Pelizzetti, E. (1989). Oil spills ion the aquatic environment: the chemistry and photochemistry at water/oil interface. *Chimica Industriale (Milan)*, **71**, 12-17.

Brakstad, F. and grahl-Nielsen, O. (1988) Identification of weathered oils. *Marine Pollution Bulletin*, **19**, 319-324.

Brandsma, M.G. and Smith, J.P. (1996) Dispersion modeling perspectives on the environmental fate of produced water discharges. In: M. Reed and S. Johnson, Eds., Produced water: Rnvironmental Issue and Mitigation Technologies. Plenum, New York. 215-224.

Brassell, S.C., Eglinton, G., Maxwell, J.R. and Philp, R.P. (1978) Natural background of alkanes in aquatic environment, In: Hutzinger, O., Van Levyveld, I.H. and Zoeteman, B.J., (Eds.), Aquatic pollutants:transformation and biological effects. Pergamon, Oxford, UK, 69-86.

Bray, E.E and Evans, E.D. (1961) Distributions of *n*-paraffins as a clue to the recognition of source beds. *Geochimica Cosmochimica Acta,* **22**, 2-15.

Broman, D, Naf, C Axelman, J, Bandh, C Pettersen, H, Johnstone, R and Wallberg, P. (1996) Significance of bacteria in marine waters for the distribution of hydrophobic organic contaminants. *Environmental Science and Technology,* **30**, 1238-1241.

Budzinski, H., Jones, I., Bellock, J., Pié rald, C. and Garrigues, P. (1997) Evaluation of sediment contamination by polycyclic aromatic hydrocarbons in the Gironde estuary . *Marine Chemistry,* **58**, 85-97.

Budzinski, H.T., Nadalig, T., Raymond, N., Matuzahroh, N. and Gilwicz, M. (2000) Evidence of two metabolic pathways for degradation of 2-methylphenanthrene by *Sphingomanas sp.* Strain (2MPHII). *Environmental Toxicology Chemistry*, **19**, 2672-2677.

Butler, J.D. and Crossley, F. (1981) Reactivity of polycyclic aromatic hydrocarbons adsorbed on soot particles. *Atmosphere Environment* **15**, 91-94.

Caeiro, S., Painho, M., Goovaerts, P., Costa, H. and Sousa, S. (2003) Spatial sampling design for sediment in estuaries. *Environmental Modelling and Software*, **18**, 853-859.

Campbell, I.D and Dwek R.A. (1984) 'Fluorescence' Biological Sectroscopy. Benjamin, 91-212

Cereceda-Balic, E., Kleist, E., Prast, H., Schlimper, H., Engel, H.E. and Gunther, K. (2002) Description and evaluation of sampling system for long-time monitoring of PAHs wet deposition. *Chemosphere,* **49**, 331-340.

Cerniglia, C.E and Heitkamp, M.A. (1989) In microbial degradation of PAH in aquatic environment, ed. U. Vanarasi, 41-68. CRC press, Boca Raton, FL.

Cerniglia, C.E. (1993) Biodegradation of polycyclic aromatic hydrocarbons. *Current Opinion of Biotechnology.* **4**, 331-338.

Cerniglia, C.E., Sutherland, J.B. and Croe, S.A. (1992) Fungal metabolism of aromatic hydrocarbons. In: Winkelmann, G., Ed., Microbial Degradation of Natural Products. Weinheim, New York. 193-217.

Chiles, J. and Delfiner, P. (1999) Geostatistics: Modelling Spatial Uncertainty, John Wiley and Sons, New York, ISBN: 0471083151, 695.

Christakos, G. (2001) Modern Spatiotemporal Geostatistics, Oxford University Press; ISBN: 0970331703, 442.

Clarke, W. A. V and Hosking, P.L. (1986) Statistical methods for geographers. John Wiley & Sons, Inc., 513.

Cochran, W.G. (1977). Sampling techniques, 3rd edition. John Wiley & Sons New York: 413.

Cretney, W.J., Crawford, W., Masson, D. and Hamilton, T. (2003) Physical oceanographic and geological setting of a possible offshore oil and gas industry in the Queen Charlotte Basin. http://www.pac.dfo-mpo.gc.ca/sci/psarc/ (accessed 14/5/2005)

Darling, P.S. (1988) A study of the chemical dispersibility of fresh and weathered crude oil. Proc. 11th Artic and Marine Oil Spill Program Technical Seminar. *Environment Canada.* Ottawa, Ontario, Canada. 481-499.

David, B. and Boule, P. (1993) Phototransformation of hydrophobic pollutants in aqueous medium. I. –PAH adsorbed to silica. *Chemosphere,* **26**, 1671-1630.

de Maagd, P.G.-J., ten Hulscher D.Th.E.M., Van den Heuvel H., Opperhuizen, A. and Sun, D.T.H.M.. (1998) Physicochemical properties of polycyclic aromatic hydrocarbons: aqueous solubilties, n-octanol/water portion coefficients, Henry's law constants. *Environmental Toxicological Chemistry*, **14**, 767-773.

DTI. 2001. Department of Trade and Industry Brown Book (2001) The Stationary Office, Norwich. http://www.dbd-data.co.uk/bb2001/book.htm (accessed 15/6/2003)

DTI. 2004. Department of Trade and Industry Brown Book (2004) The Stationary Office, Norwich. http://www.og.dti.gov.uk/information/bb_updates/chapters/Table3_3.htm (accessed 30/11/2004)

DTI. 2004. Department of Trade and Industry Brown Book (2004a) The Stationary Office, Norwich. http://www.og.dti.gov.uk/information/bb_updates/chapters/Table3_2.htm (accessed 30/11/2004)

DTI. 2004. Department of Trade and Industry Brown Book (2004b) The Stationary Office, Norwich. http://www.dti.gov.uk/energy/inform/energy_indicators/internet_04_e10.3wp.xls (accessed 30/11/2004)

DTI. 2004. Department of Trade and Industry Brown Book (2004c) The Stationary Office, Norwich. http://www.og.dti.gov.uk/information/bb_updates/chapters/Table3_1.htm (accessed 30/11/2004)

Dutta, T.K. and Harayama, S. (2000) Fate of crude oil by the the combination of photooxidation and biodegradation. *Environmental Science Technology*, **34**, 1500-1505.

Dyreborg, S., Arvin, E., Broholm, K. and Christensen, J. (1996) Biodegradation of thiphene, benzothiophene, and benzofuran with eight different primary substrates. *Environmental Toxicology Chemistry,* **15**, 2290-2292.

Ehrhardt, M.G. and Burns, K.A. (1990) Petroleum-derived dissolved organic compounds concentrated from inshore waters in Bermuda. *Journal of Experiment Marine Biological Ecology.* **37**, 53-64.

Ehrhardt, M.G., Burns, K.A. and Bicego, M.C. (1992) Sunlight-induced compositional alterations in the seawater soluble fraction of crude oil. *Marine Chemistry* **37**, 53-64.

EPA Region III (U.S. Environmental Protection Agency, Region III). (2000) Risk-based Concentration Table, EPA Region III, philadelphia, PA.
http://www.epa.gov/reg3hwmd/riskmenu.htm (accessed 12/5/2003).

Ferdendes, M.B., Sicre, M.-A., Boireau, A. and Tronszynski, J. (1997) Polyaromatic hydrocarbon (PAH) distributions in the Seine River and its estuary. *Marine Pollution Bulletin,* **34**, 857-867.

Fernández, P., Vilanova, R. and Grimalt, J.O. (1996) PAH distributions in sediments from high mountain lakes. *Polycyclic Aromatic Compounds*, **9**, 121-128.

Gabriel, K.R (1978) A simple method of multiple comparisons of means. *Journal of American statistic Association*, **73**, 724-729.

Glover, D.M., Jenskins, W.J. and Doney, S.C. (2004) Model, Data Analysis and Numerical Techniques for geochemistry. Department of Marine chemistry and geochemistry. Woods Hole Oceanographic Institutte. http://w3eos.whoi.edu/12.747/chaps/chap02/chapter04.pdf (accessed 14/8/05).

Gobas, F.A.P.C., Purdy, R., Granville, G., Cowan, E-E., Gannon, J., Lewis, M., Socha, A. and Chapman, P.M. (2001) A proposal for hazard identification of organic chemical based on inherent toxicity, *SETAC Globe*, **2**, 33-34.

Gorman, A.A. (1992) The bimolecular reactivity of singlet molecular oxygen. *Advance Photochemistry,* **17**, 217-237.

Gough, M.A. and Rowland, J. (1990) Characterisation of unresolved complex mixtures of hydrocarbons in petroleum. *Nature,* **344**, 648-650.

Gowland, B.T.G., McIntosh, A.D., Davies, I.M., Moffat, C.F. and Webster, L., (2002) Implications from a field study regarding the relationship between polycyclic aromatic hydrocarbons and glutathione S-transferase activity in mussels. *Marine Environmental Research,* **54**, 231-235.

Grimmer, G (1983) Environmental Carcinogens: Polycyclic Aromatic Hydrocarbons. CRC Press, Boca Raton, FL.

Gschwend, P.M. and Hites, R.A. (1981) Fluxes of polycyclic aromatic hydrocarbon to marine and lacustrine sediments in the north-eastern United State. *Geochimica et Cosmochimica Acta,* **45**, 2359-2367.

Gustafsson, O., Haghesta, F., Chan, C., Macfarlane, J. and Gschwend, P.M. (1997) Quantification of the dilute sedimentary soot phase: implications for PAH speciation and bioavailability. *Environmental Science and Technology,* **31**,203-209.

Haining, R. (1990) Spatial data analysis in the social and environmental sciences. Cambridge University Press. 483.

Harvey. G.R. (1995) Petroleum hydrocarbon oxidation products in marine atmosphere. *Marine pollution Bulletin,* **30**, 425-426.

Hashimoto, T., Tahara, S., Takaoka, S., Tori, M. and Asakawa, Y. (1994) Structures of binaphthyl and three novel benzophenone derivatives with plant-growth inhibitory activity from the fungus *Daldinia concentrica. Physical and Pharmaceutical Bulletin*, **42**,1528-1530.

Houlding, S. (2000) Practical Geostatistics – Modeling and Spatial Analysis, Springer – verlag, New York, 160.

Hunt, C.D. (1986) Fate and bioaccumullation of soil-associated low-level naturally occuring radiativity following disposal into a marine ecosystem. Final report to office of radiation

programs, U.S. Environmental Protection Agency, Washington, DC. Marine Ecosystems Research Laboratory, Graduate School of Oceanography, University of Rhode Island, Narragansett, RI.

IARC. (1987) IARC monographs on the evaluation of carcinogenic risk of chemicals to humans: Overall evaluation of carcinogenicity. An updating of IARC monographs volume **1-42** supply 7. *International Agency for Research on Cancer*, Lyon, France.

Jacquot, F., Guiliano, M., Doumenq, P., Munoz, D. and Mille, G. (1996) *In vitro* photo-oxidation of crude oil maltene fractions: evolution of fossil biomarkers and polycyclic aromatic hydrocarbons. *Chemosphere,* **33**, 671-681.

Jassby, A.D., Cole, B.E. and Cloern, J.E. (1997) The Design of Sampling transects for characterising Water Quality in Estuaries. *Estuarine, Coastal and Shelf Science*, **45**, 285-302.

Jiang, C., Alexander, R., Kagi, R.I. and Murray, A.P. (2000) Origin of perylene in ancient sediments and its geological significance. *Organic Geochemistry*, **31**, 1545-1559.

Juhasz, L. and Naidu, R. (2000) Bioremediation of high molecular weight polycyclic aromatic hydrocarbons: a review of the microbial degradation of benzo[*a*]pyrene. *International Biodeterioration and Biodegradation*, **45**, 57-88.

Karickhoff, S.W., Brown, D.S. and Scott, T.A. (1979) Sorption of hydrophobic pollutants on natural sediment, *Water Research,* **13**, 241-248.

Karman, C.C., Johnsen, S., Schobben, H.P.M. and Scholten, M.C. Th. (1996) Ecotoxicology risk of produced water discharged from oil production platforms in the Statfjord and Gullsfahs Field. Pages 127-134 **In**: M.Reed and S. Johnsen, Eds., Produced water 2. *Environmental Issues and Mitigation Technologies*. Plenum Press, New York.

Kerr, J.M., Melton, H.R., McMillen, S.J., Magaw, R.I. and Naughton, G. (1999). Polyaromatic hydrocarbon content in crude oils around the world. **SPE 52724.** Paper

presented at the 1999 SPE/EPA Exploration and Production Environmental Conference, Austin, TX. *Society of Petroleum Engineers*, Richardson, TX. 10.

Killops, S.D. and Al-Juboor, M., (1990). Characterisation of the unresolved complex mixture (UCM) in gas chromatograms of biodegraded petroleums. *Organic Geochemistry*, **15**, 147-160.

Kropp, K.G., Goncalves, J.A., Anderson, J.T. and Fedorak, P.M. (1994) Bacterial transformations of benzothiophene and methylbenzotrhiophene. *Environmental Science and Technology*, **28**, 1348-1356.

Krylov, K.G., Huang, X.-D., Zeiler, L.F., Dixon, D.G. and Greenberg, B.M. (1997) Mechanistic quantitative structure-activity relationship model for photoinduced toxicity of polycyclic aromatic hydrocarbons: I. Physical model based on chemical kinetics in two-comartment system. *Environmental Toxicology Chemistry*, **16**, 2283-2295

LaFlamme, R.E. and Hites, R.A. (1978) The global distribution of polycyclic aromatic hydrocarbons in recent sediments. *Geochimica et Cosmochimica Acta*, **42**, 289-303.

Lake, J. L., Norwood, C. and Dimock, C. (1979) Origins of polycyclic aromatic hydrocarbons in estuarine sediments. *Geochimica et Cosmochemica Acta*, **43**, 1847-1854.

Law, R.J., Kelly, C., Baker, K., Jones, J., Mcintosh, A.D., and Moffat, C.F. (2002) Toxic equivalency factors for PAH and their applicability in shellfish pollution monitoring studies. *Journal of Environmental Monitoring*, **4**, 383-388.

Li, A., Razak, I.A., Ni, F., Gin, M.F. and Christensen, E.R. (1998) Polycyclic aromatic hydrocarbons in the sediments of the Milwaukee Harbour estuary, Wisconsin, USA. *Water, Air and Soil Pollution*, **101**,417-434.

Long, E.R., Macdonald, D., Smith, S.L and Carlder, F.D. (1995) Incidence of adverse biological effects within ranges of chemical concentrations in marine estuarine sediments, *Environmental Management*, **19**, 81-97.

Mackay, D., Shiu,W.Y., and Ma, K.C. (1992) Illustrated Handbook of Physical-chemical Properties and environmental Fate for Organic Chemicals. Polynuclear Aromatic Hydrocarbons, Polychlorinated Dioxins, and Dibenzofurans. Lewis Publishers, Chelsea, MI.

Mathey, A., Van Roy, W., Van Vaeck, L., Eckhardt, G. and Steglich, W. (1994) *In situ* analysis of a new perylene quinone in lichens by fourier-transform laser microprobe mass spectroscopy with external source. *Rapid Communications in Mass Spectrometry*. **8**, 46-52.

Mayer, L.M. (1999) Extent coverage of mineral surfaces by organic matter in marine sediments. *Geochimica et Cosmochimica Acta*, **63**, 207-215.

McDonald, B.G. and Chapman, P.M. (2002) PAH phototoxicity-an ecologically irrelevant phenomenon? *Marine Pollution Bulletin*, **44**, 1321-1326.

McElroy, A.E, Farrington, J.W and Teal, J.M. (1989) Bioavailability of polycyclic aromatic hydrocarbons in the aquatic environment: In metabolism of polycyclic aromatic hydrocarbons in the aquatic environment, ed. U. Varanasi, 1-40, CRC press, Boca Raton, FL.

McGroddy, S.E., and Farrington, J.W. (1995) Sediment porewater partitioning of polycyclic aromatic hydrocarbons in three cores from boston harbour, Massachussetts. *Environmental Science and Technology*, **30**, 172-177.

McGroddy, S.T. (1993) Sediment-porewater partitioning of PAHs and PCBs in Boston Harbour. Mass., *Ph.D*. Umass, Boston. MA.

Meador, J.P., Stein, J.E,., Reichert, W.L and Varanasi, U. (1995). Bioaccumulation of polycyclic aromatic hydrocarbons by marine organisms. *Reviews of Environmental Contamination and Toxicol*ogy, **143**, 79-165.

Mearns, J.C., Wood, S.G, Hasset, J.J and Banwaff, W.L. (1980) Sorption of Polynuclear aromatic hydrocarbons by sediments and soils, *Environmental Science and Technology*, **14**, 1524-1528.

Mekenyan, O.G., Ankley, G.T., Veith, G.D. and Call, D.J. (1994) QSARs for phototoxicity. I. Acute lethality of polycyclic aromatic hydrocarbons to *Dophnia magma*. *Chemosphere*, **28**, 567-582.

Mill, T., Mabey, W.R., Lan, B.Y. and Baraze, A. (1981) Photolysis of polycyclic aromatic hydrocaebons in water. *Chemosphere,* **10**, 1281-1290.

Miller, J.A. and Melius, C.F, (1992) Kinetics and thermodynamic issues in the flame formation of aromatic compounds in flame of aliphatic fuels. *Combustion and Flame,* **91**, 21-39.

MLA SOP 0110. Freeze-dried operations.

MLA SOP 0170. Removal of Carbonate from Sediments prior to the Determination of Organic Carbon

MLA SOP 840. Automated particle size determination of sediments.

MLA SOP 885. Determination of total organic carbon and nitrogen in sediments.

MLA SOP 1310. Quality control procedures.

MLA SOP 1600. Extraction of sediment for fluorescence and hydrocarbon analysis.

MLA SOP 1605. Preparation of standard solutions of PAHs.

MLA SOP 1610. Analysis of aliphatic hydrocarbon by GC-FID.

MLA SOP 1625. Analysis of PAHs by GC-MS.

Moffat, C.F., McIntosh, A.D., Webster, L., Shepherd, N.J., Dalgarno, E.J., Brown, N.A. and Moore, D.C. (1998) Determination and environmental asssment of hydrocarbons in fish, shellfish and sediments following an oil spill at the Captain Field. *Fisheries Research Services (FRS) Internal Report* No. **9/98**.

Moriarty, N.W., Brown, N.J. and Frenklach, M. (1999) Hydrogem migration in the phenylen-2-yl radical. *Journal of Physical Chemistry*, **103**, 7127-7135.

Neff, J.M. (1979) Polycyclic aromatic hydrocarbons in the aquatic environment. Sources, fate and biological effects, Applied Science Publishers. Barking, Essex, England, 262.

Neff, J.M. (1990) Composition and fate of petroleum and spill-treating agents in marine environment. **In**: J.R., Geraci and D.J. St. Aubin, Eds., Sea mammals and oil: confronting the risks. Academic Press, San Diego, 1-33.

Neff, J.M. (2002) Bioaccumulation in marine organisms: Effect of contaminants from oil well produced water. Elsevier Science Ltd. Oxford, UK. 242-245.

Nicodem, D.E., Fernandes, M.C.Z., Guedes, C.L.B. and Correa, R.J. (1997) Photochemical processes and environmental impact of petroleum spills. *Biogeochemical*, **39**, 121-138.

Nicholson MD, Fryer RJ, Ross CA (1997). Designing monitoring programmes for detecting temporal trends in contaminants in fish and shellfish. *Marine Pollution Bulletin*, **34**, 821-826.

Nieuwenhuize, J., Maas, Y., Middleburg, J.J. (1994) Rapid analysis of organic carbon and nitrogen in particulate material. *Marine Chemistry*, **45**, 217-224.

NOAA. (1988) A summary of selected data on chemical contaminants in sediments collected during 1984, 1985 and 1987. *National Oceanic and Atmospheric Administration*, Washington D.C.

OSPAR (1997) Background / Reference Concentrations for Contaminants in seawater, biota and sediment. OSPAR Commission. London.

OSPAR Commission. (2002) Polycyclic aromatic hydrocarbons, OSPAR Priority Substances, OSPAR Commission, London.

OSPAR (2005) Background Concentrations for Contaminants in seawater, biota and sediment. OSPAR Commission. **ASMO 2005**, London.

Patin, S. (1999) Environmental impact of offshore oil and gas industry. Eco-Monitoring Publishing, East Newport, NY, 425.

Pelletier, E., Burgess, R.M. Ho, K.T., Kuhn, A., McKinney, R.A and Ryba, S.A. (1997) Phototoxicity of individual polycyclic aromatic hydrocarbons and petroleum to marine invertebrate larvae and juveniles. *Environmental Toxicological Chemistry*, **16**, 2190-2199.

Pothuluri, J.V. and Cerniglia, C.E. (1994) Microbial metabolism of polycyclic aromatic hydrocarbons. **In**: Chaudhry, G.R., Ed., Biological degradation and bioremediation of toxic chemicals. Diascorides Press, Portland, OR. 92-124.

Ravelet, C., Krivobok, S., Sage, L., and Steiman, R. (2000) Biodegradation of pyrene by sediment fungi. *Chemosphere,* **40**, 557-563.

Readman, J.W, Mantoura, R.F.C and Rhead, M.M. (1987) A record of polycyclic aromatic hydrocarbon (PAH) pollution obtained from accreting sediments of the Tamar estuary, UK: evidence for non-equilibrium behaviour of PAH. *The Science of the Total Environment,* **66**, 73-94.

Readman, J.W., Mantoura, R.F.C. and Rhead, M.M. (1984) The physical-chemical speciation of polycyclic aromatic hydrocarbons (PAHs) in aquatic systems. *Fersenius Z. Analytical Chemistry,* **319**, 126-131.

Robertson, A. (1998) Petroleum hydrocarbons in AMAP Assessment Report: *Artic Pollution Issue*, 661-716. *Artic Monitoring and Assessment Programme (AMAP)* Oslo, Norway.

Rochkind-Dunbisky, M.C., Sayler, G.S. and Backburn, J.W. (1987) Microbial decomposition of chlorinated aromatic hydrocarbons. Marcel Decker, New York. 48-65.

Russell, M., Webster, L., Walsham, P., Parker, G., McIntosh, A.D., Dalgarno, E.J., McIntosh, A.D. and Moffat, C.F. (2005) The effect of oil exploration and production in the Fladen Ground: Composition and concentration of hydrocarbons in sediment samples collected during 2001 and their comparison with sediment samples collected in 1989. *Marine Pollution Bulletin*. **50**, 638-651.

Saminov, M.V., Saminova, T.N, Carroll, J, Matishov, G.G Dahle, S and Kristoffer, N. (2000) Polycyclic aromatic hydrocarbons (PAHs) in sediment of the White Sea, Russia. *Marine Pollution Bulletin, **40***, 809-818.

Schwarzenbach, R.P, Gschwend, P.M and Imboden, D.M (1993) Environmental organic chemistry. John Wiley and Sons, New York.

Silliman, J.E., Meyers, P.A. and Eadie, B.J. (1998) Perylene: an indicator of alteration processes or precursor materials? *Organic Geochemistry*, **29**, 1738-1744.

Skoog, D.A., West, D.M. and Holler, F.J. (1997) Fundamentals of Analytical Chemistry, 7th Edition, Saunders College Publishing (Harcout College Publishers, London.

Smith, J.N. and Levy, E.M. (1990) Geochronology of polycyclic aromatic hydrocarbons contamination in sediments of the Saguenay Fjord. *Environmental Science and Technology*, **24**, 847-879.

Smith, R.L. and Zhu, Z. (2004) Asymptotic theory for kriging with estimated parameters and its application to network design. http://www.stat.unc.edu/postscript/rs/supp5.pdf (accessed 14/9/2005).

Soclo, H.H., Garrigue, P. and Ewald, M. (1986) Analyse quantitative des hydrocrabures aromatiques polycucliques dans les sédiments récents par chromatographie en phase liquide détection spectrofluorimétrique. *Analysis*, **14**, 344-350.

Strømgren, T., Sørstrøm, S.E., Schou, L., Kaarstad, I., Aunaas, T., Brasksad, O.G. and Johnsen, Ø. (1995) Acute toxic effects of produced water in relation to chemical composition and dispersion. *Marine Environmental Reaserch*, **40**, 147-169.

Sutherland, J.B. (1992) Detoxification of polycyclic aromatic hydrocarbons by fungi. *Journal of Industrial Microbiology*, **9**, 62-63.

Sutherland, J.B., Rafii, F., Khan, A.A. and Cerniglia, C.E. (1995) Mechanisms of polycyclic aromatic hydrocarbon degradation. **In**: Microbial transformation and degradation of toxic organic chemicals. Wiley-Liss Publishers, NY. 269-306.

Syndes, L.K., Hemmingsen, T.H., Skare, S., Hansen, S.H., Falk-Petersen, I.-B., Lønning, S. and Østgaard, K. (1985) Seasonal variations in weathering and toxicity of crude oil on water under artic conditions. *Environmental Science and Technology*, **19**, 1076-1081.

Taylor, J.R. (1997) An introduction to error analysis. 2nd ed. Sausalito, CA: University Science Books.

Thominette, F. and Vedu, J. (1984) Photo-Oxidative behaviour of crude oils relative to sea pollution. Part II. Photo-induced phase separation. *Marine Chemistry*, **15**, 105-115.

Tissot, B.P. and Welte, D.H., (1984) Petroleum formation and occurrence. Springer-Verlag, Berlin.

Tolosa, I., de Mora, S., Sheikholeslami, M.R., Villeneuve, J-P., Bartocci, J. and Cattini, C. (2004) Aliphatic and aromatic hydrocarbons in coastal Caspian Sea sediments. *Marine Pollution Bulletin*, **48**, 44-60.

Topping, G., Davies, J.M., Mackie, P.R. and Moffat, C.F. (1997) The impact of the *Braer* spill on commercial fish and shellfish. **In**: The impact of an oil spill in turbulent waters: The *Braer* (Davies, J.M and Topping, G. Eds), The Stationary Office, Edinburgh, 121-143.

UKOOA (2000) Environmental Report.
http://www.ukooa.co.uk/issues/2000report/enviro00_emissions.htm#water (accessed 15/4/2004)

UNEP/IOC/IAEA. (1992) Determination of petroleum hydrocarbons in sediments. Reference Methods for Marine Pollution Studies No. 20, UNEP, Nairobi, Kenya, 75.

Valerio, F. and Lazzarotto, A. (1985) Photochemical degradation of polycyclic aromatic hydrocarbons (PAH) in real and laboratory conditions. *International Journal of Environmental Analytical Chemistry,* **23**, 135-151.

Varanasi, U., Reichert, W.L., Stein, J.E., Brown, D.W. and Sanborn, H.R (1985) Bioavailabilty and biotransformation of aromatic hydrocarbons in benthic organism exposed to sediment from an Urban estuary, *Environmental Science and Technology,* **19**, 836-841.

Van den Hout, K.D. (Ed.). (1993) The impact of atmospheric deposition of non-acidifying pollutants on the quality of European forest soils and the North East. Main report of the ESQUAD project. Report by Delft Hydraulics, RIVM, DLO and IMW-TNO; IMW-TNO report nr **R93/329**, Delft, 143.

Veith, G.D., Mekenyan, O.G., Ankley, G.T. and Call, D.J. (1995) QSAR of subtituent effects on the photoinduced acute toxicity of PAHs. *Chemosphere*, **30**, 2129-2142.

Venkatesan, M.I., Brenar, N.S., Tuth, E., Bonilla, J. and Kaplan, I.R. (1980) Hydrocarbons in age – dated sediments cores from two basins in the southern California Bight. *Geochimica Cosmochimica Acta,* **44**, 789-802.

Venkatesan, M.I. and Kaplan, I.R. (1982) Distribution and transport of hydrocarbons in surface sediments of Alaskan outer continental shelf. *Geochimica Cosmochimica Acta,* **46**, 2135-2149.

Venkatesan, M.I., Ruth, E., and Kaplan, I.R. (1990) Triterpenols from sediments of Santa Monica Basin, Southern California Bight, USA. *Organic Geochemistry*, **16**, 1015-1024.

Walch, S.P. (1995) Characterisation of the minimum energy paths for the ring closures reactions of C_4H_3 with acetylene. *Journal of Chemical Physics*, **103**, 8544-8547.

Walsham, P., Webster, L., McIntosh, A.D., Fryer, R.J., Mackie, P.R., and Moore, D.C. (2002) The effect of oil exploration and production in the Fladen Ground: Composition and concentration of hydrocarbons in sediment samples collected during 1989. *Fisheries Research Services (FRS) Internal Report* No. **13/02.**

Wakeham, S.G., Schaffner, C. and Giger, W. (1980) Polycyclic aromatic hydrocarbons in recent lake sediments –II. Compounds derived from biogenic precusors during early diagenesis. *Ceochimica et Cosmochimica Acta*, **44**, 415-429.

Wang, H. and Frenklach, M. (1994) Calculations of rates coefficients for the chemically activated reactions with vinylic and aromatic radicals. *Journal of Physical Chemistry*, **98**, 11465-11489.

Wang, H. and Frenklach, M. (1997) A detailed kinetic modelling study of aromatics formation in laminar premixed actylene and ethylene flame. *Combustion and Flame*, **110**, 173-221.

Wang, X.J. and Qi, F. (1998) The effects of sampling design on spatial structure analysis of contaminated soil. *The Science of the Total Environment*, **224**, 29 -41 .

Wang, Z. and Fingas, M.F. (2003) Development of oil hydrocarbon fingerprinting and identification techniques. Marine *Pollution Bulletin*, **47**, 423-452.

Webster, L., Angus, L., Topping, G., Dalgarno, E.J. and Moffat, C.F. (1997a) Long term monitoring of polycyclic aromatic hydrocarbons in mussels (*Mytilus edulis*) following the *Braer* oil spill. *Analyst*, **122**, 1491-1495.

Webster, L., McIntosh, A.D., Moffat, C.F., Dalgarno, E.J., Brown, N.A. and Fryer, R.J. (2000) Analysis of sediment from Shetland Island voes for polycyclic aromatic hydrocarbons, sterenes and tritepene. *Journal of Environmental Monitoring*, **2**, 29-38.

Webster, L., Fryer, R.J., Dalgarno, E.J., Megginson, C. and Moffat, C.F (2001). The polycyclic aromatic hydrocarbon composition of sediments from voes and coastal areas in the Shetland and Orkney Islands. *Journal of Environmental Monitoring*, **3**, 591-601.

Webster, L., Mackie, P.R., Hird, S. J., Munro, N.A and Moffat, C.F. (1997) Development of analytical methods for determination opf synthetic mud base fluids in marine sediments. *Analyst*, **122**, 1485-1490.

Webster, L., Twigg, M., Megginson, C., Moffat, C, Walsham, P and Parker, G. (2003) Aliphatic hydrocarbons and polycyclic aromatic hydrocarbons (PAHs) in sediment collected from the 110miles hole and along a transent from 58°58.32'N 1°10.38'W to the inner Moray Firth, Scotland. *Journal Environmental Monitoring*, **5**, 395-403.

Webster, R. (1999) Sampling, Estimating and Understanding Soil Pollution. Ed. Gómez-Hernández, J., Soares, A., Froidevaux, R., *GeoEnvII 98 – Geostatistics for Environmental Applications*. Qualitative Geology and Geostatistics. Kluwer Academic Publishers. 25-37.

Webster, R. and Oliver, M.A. (2001) Geostatistics for Environmental Scientists, John Wiley and Sons Ltd., Chichester, England, 271.

Weilműnster, P., Keller, A. and Homann, K, -H. (1999) Large molecules, radicals, ions, and small soot particles in fuel-rich hydrocarbon flames: Part I: positive ions of polycyclic aromatic hydrocarbons (PAH) in low-pressure premixed flames of acetylene and oxygen. *Combustion and Flame,* **116**, 62-83.

White K.L. (1986) An overview of immunotoxicolgy and carcinogenic polycyclic aromatic hydrocarbons, *Environmental Carcinology Review,* **2**, 163-202.

Whittle K.J., Anderson, D.A., Mackie, P.R., Moffat, C.F., Shepherd, N.J. and McVicar, A.H. (1997) The impact of the *Braer* oil on caged salmon. **In**: The impact of an oil spill in turbulent waters: The *Braer* (Davies, J.M. and Topping, G. Eds), The Stationary Office, Edinburgh, 144-160.

Wills, J. and Sakhalina, V. (2000) A survey of offshore oilfield drilling wastes and disposal techniques to reduce the ecological impact of sea dumping. http://www.offshore-environment.com/producedwaters.html (accessed 15/4/2004).

Wilson, S.C. and Jones, K.C. (1993) Bioremediation of soil contaminated with polynuclear aromatic hydrocarbons (PAHs): a review. *Environmental Pollution*, **81**, 229-249.

Wu, Y., Zhang, J., Mi, T. and Li, B. (2001) Occurrence of *n*-alkanes and polycyclic aromatic hydrocarbons in the core sediments of the yellow Sea. *Marine Chemistry,* **76**, 1-15.

Xu-cheng, W., Zhang, Y and Chen, R.F. (2001) The distribution and partitioning of polycyclic aromatic hydrocarbons (PAHs) in different size fractions in sediments from Boston Harbour, *United states Maritime Pollution Bulletin*, vol. **42**, no. **11**, 1139-1149.

Zhou, J. L. and Maskaouli, K. (2003) The distribution of polycyclic aromatic hydrocarbons in water and surface sediments from Daya Bay, China. *Environmental Pollution*, **121**, 269-281.

The development and application of a statistical sampling regime for determining hydrocarbon distributions in marine sediment

FISHERIES RESEARCH SERVICES

Abdulwaheed S. Ahmed[a, b], Lynda Webster[a], Ian M. Davies[a], Marie Russell[a], Pam Walsham[a], Gill Packer[a], Rob J. Fryer[a], Colin F. Moffat[a] and Pat Pollard[b].
[a] Fisheries Research Services (FRS) Marine Laboratory, 375 Victoria Road, Aberdeen AB11 9DB, Scotland.
[b] School of Life Sciences, The Robert Gordon University, St Andrew Street, Aberdeen AB25 1HG, Scotland.

INTRODUCTION

The North Sea has been the focus of offshore oil and gas production over the past 35 - years and, as a result of this, hydrocarbons have been discharged to the area during ling (*via* cuttings contaminated with oil-based drill muds), production (*via* produced er discharges) and *via* incomplete combustion during flaring operations. The Fladen und in the North Sea, is a potentially accumulative area due to the fine muddy iments (Fig. 1), and low water current velocities. In addition, the area is one of the t heavily fished areas of the North Sea. A stratified random sampling design was lied to the Fladen Ground in 2001 to estimate hydrocarbon concentrations in far field iments. Sixteen zones were constructed of equal size and near (< 5 km from a tiple oil wells and < 2 km from single oil well) and far (> 5 km from a multiple oil wells >2 km from single oil well) field areas defined (Fig. 2). The number of samples that e collected per zone was based upon the proportion of far field area. All samples e screened for aromatic hydrocarbons by ultraviolet fluorescence (UVF). In addition, ples were analysed for polycyclic aromatic hydrocarbons (PAH) by gas matography-mass spectrometry (GC-MS).

gure 1 The generalised pattern of rth Sea currents in relation to Fladen Ground.

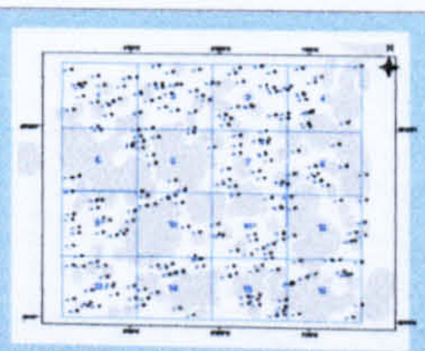

Figure 2 Location of the stratified random sampling sites, indicating the Zones and oil platforms. Grey circles are near field sites (big circle are multiple oil wells and small circles are single well).

METHOD

mpling

hundred and forty two (242) sediment samples were collected by Day Grab, from FRV *Scotia* in 2001.

rticle size and CHN analyses

particle size (PS) of the sediment samples (freeze-dried) was determined by laser nulometry employing a Malvern Mastersizer E Partcle Size Analyzer. The total anic carbon (TOC) was determined on freeze-dried, ground sediment, following acid itment to remove carbonate, using a Perkin Elmer CHN elemental analyzer.

raction of sediments for fluorescence and hydrocarbon analysis

ch sediment sample was thoroughly mixed and an aliquot removed for the ermination of the water content. Two aliphatic standards and six deuterated PAH ndards were added to a second aliquot and the hydrocarbons were extracted by ication with dichloromethane (DCM)/methanol. The DCM was isolated and dried over SO_4. The DCM fraction was made to a known volume (100 ml), and an aliquot (10 removed for UVF analysis. The remaining extract was solvent exchanged to *iso*-ane, reduced in volume and the aliphatic and aromatic hydrocarbons separated by atic high performance liquid chromatography (HPLC). The aliphatic hydrocarbons e analysed by gas chromatography with flame ionization detection (GC-FID) and the matic hydrocarbons by GC-MS. Geochemical biomarker compositions (steranes and erpanes) were also determined by GC-MS.

H, PS and TOC methods are accredited at FRS to international standard ISO 17025.

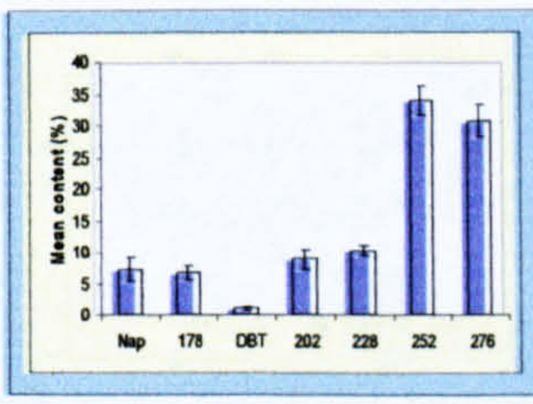

Figure 5 PAH profile for the Fladen Ground, represented by ring classes. Note the predominance of the 4- to 6-ring (%202 - %276) PAHs, which indicates a more pyrolytic input. Error bars represent standard deviation of the mean.

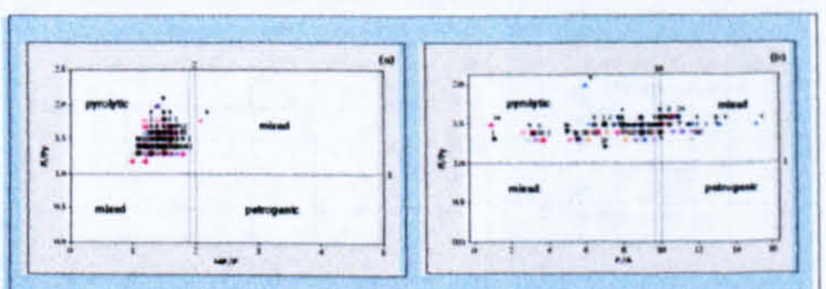

Figure 4 PAH concentration ratios used to assess the sources of PAHs in the Fladen Ground sediments collected in 2001. The zones identified by high fluoranthene/pyrene (Fl/Py) ratios and low phenanthrene/anthracene (P/A) ratios and high Fl/Py and low methylphenanthrene/phenanthrene (MP/P) ratios were characteristic of pyrolytic PAHs. (a) Plot of Fl/Py ratios against MP/P ratios. (b) Plot of Fl/Py ratios against P/A ratios.

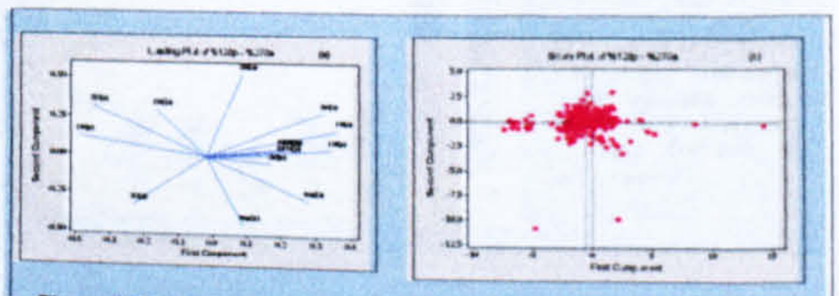

Figure 5 Principal component analysis of the 2001 stratified random survey including ring group parent and alkylated compounds. (a) Loading plot of %128-%276, showing the lighter PAH compounds with a positive first component, and the 5- and 6-ring with a negative first component. (b) Score plot showing no obvious separation by Zones.

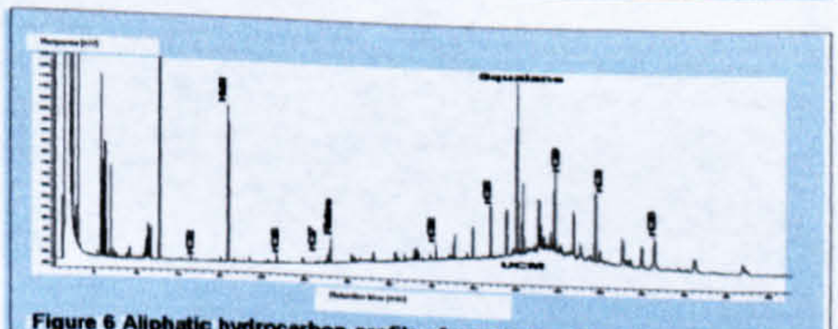

Figure 6 Aliphatic hydrocarbon profile of a typical sediment sample (Zone 4). Note the small high boiling unresolved complex mixture that suggests petrogenic contamination.

ble 1 Summary of TOC, PSA, UV fluorescence, total *n*-alkane (nC_{15}-nC_{33}) and total PAH (2- to 6- ring, parent and branched) data. All concentrations are on a dry ight basis.

ne numbers	No. of samples	TOC (%)		PSA (% < 63 µm)		Forties equivalents (µg g^{-1})		Diesel equivalents (µg g^{-1})		Total PAH (µg kg^{-1})		Total *n*-alkane (µg kg^{-1})		CPI	
		Mean	SE	Mean	S E	Mean	SE	Mean	SE	Mean	SE	Mean	SE	Mean	SE
1	20	0.64	0.04	48.9	2.6	9.7	0.8	5.0	0.4	96.9	4.2	59.9	6.5	1.6	0.4
2	20	0.90	0.03	73.1	2.2	12.1	1.0	6.2	0.5	94.6	6.8	96.8	15.9	1.9	0.4
3	20	0.98	0.05	68.6	3.0	8.7	0.6	4.5	0.2	104.0	8.5	115.5	8.9	1.4	0.3
4	13	0.97	0.10	63.2	5.7	13.1	1.7	7.0	0.8	206.6	23.0	129.8	17.1	1.3	0.4
5	10	0.71	0.07	64.1	4.2	14.5	1.2	7.0	0.6	133.9	16.6	64.7	5.8	1.2	0.4
6	9	0.89	0.06	73.9	3.6	18.2	1.4	5.2	0.4	89.1	7.8	100.8	12.5	1.5	0.5
7	18	1.10	0.04	79.6	1.2	19.5	1.4	5.8	0.3	154.6	11.1	100.5	10.9	1.3	0.3
8	10	0.80	0.05	59.3	4.6	12.4	2.4	6.6	0.9	147.1	23.8	206.8	49.5	1.2	0.4
9	18	0.62	0.04	51.4	3.2	10.2	0.8	3.3	0.2	61.7	4.2	61.0	4.4	1.2	0.3
10	11	0.93	0.09	64.8	7.5	21.0	2.7	6.1	0.8	107.0	8.2	105.4	8.8	1.2	0.4
11	17	1.31	0.06	86.7	0.4	22.2	1.3	6.5	0.3	137.2	5.8	118.6	10.4	1.3	0.3
12	9	0.76	0.05	67.9	5.2	17.0	1.6	5.0	0.4	87.0	10.5	78.6	11.4	1.2	0.4
13	20	0.69	0.03	58.0	1.5	7.4	0.4	2.2	0.1	53.9	2.8	55.4	7.6	1.6	0.4
14	14	0.98	0.03	75.5	2.3	14.0	1.2	4.6	0.3	81.6	8.7	86.4	9.3	1.4	0.4
15	20	1.19	0.03	82.3	0.8	13.0	0.9	4.0	0.2	95.5	5.0	89.4	5.8	1.4	0.3
16	13	0.91	0.06	65.5	3.0	17.5	1.7	5.3	0.5	88.1	10.7	106.7	8.9	1.3	0.4
Total	242	0.91	0.01	67.6	0.8	13.8	0.3	5.1	0.1	108.2	2.7	97.2	3.7	1.3	0.1

= Standard Error of the mean; CPI = Carbon Preference Index

RESULTS

The mean values with standard errors for the far field area in each Zone, and for the total survey area are presented in Table 1. TOC and PSA measurements were positively correlated with each other and with corresponding diesel and Forties oil equivalent, total PAH and *n*-alkane.

Total Hydrocarbon

Estimates of 'total hydrocarbon' concentrations are expressed as 'oil' equivalents. Concentrations around 50 µg g^{-1} dry weight are typical of those found in areas remote from oil and gas activity. Concentrations in offshore sediments above this background value are generally associated with offshore oil exploration and production activity. The Forties crude oil equivalent concentrations were all below 50 µg g^{-1} dry weight (Table 1); the mean concentration for the whole far field was 13.8 µg g^{-1} dry weight. The diesel equivalent mean concentration was 5.1 µg g^{-1} dry weight.

Polycyclic aromatic hydrocarbons (PAHs)

The mean total PAH concentrations (2- to 6-ring parent and alkylated) varied from 61.7 to 206.6 µg kg^{-1} dry weight, with an overall mean concentration of 108.2 µg kg^{-1} dry weight. OSPAR Background Concentrations (BCs) are typical concentrations found in sediments in uncontaminated parts of the OSPAR area (north-east Atlantic), and have been established for ten PAHs. Observed concentrations are said to be 'near background' if the mean concentration is statistically significantly below the corresponding Background Assessment Concentration (BAC). The observed mean concentrations of the ten PAHs in Fladen Ground sediments were all below the OSPAR BACs at the 5% significance level.

PAH Sources

The mean PAH percentage profile for the 16 Zones showed a similar pattern, being dominated by the heavier 4- to 6-ring compounds (Fig. 3), with a high proportion of the parent PAHs. Plotting the fluoranthene/pyrene (Fl/Py) ratios against either the phenanthrene/anthracene (P/A) or methylphenanthrene/phenanthrene (MP/P) ratios gives a pyrolytic (high Fl/Py and low P/A or MP/P) and a petrogenic (low Fl/Py and high P/A or MP/P) zone, the remaining may be indicative of mixed sources of PAHs (Fig. 4). The ratio plots showed most of the samples falling within the pyrolytic zone in the Fl/P vs. MP/P plot (Fig. 4a). The Fl/Py vs. P/A plot is more dispersed (Fig. 4b; the high P/A ratios (>10) suggest a possible petrogenic input).

The PAH profiles of the sediments were investigated further using principal component analysis (Minitab 14). The parent and alkylated concentrations were normalised to the total PAH concentration. The first two components only accounted for 34 and 15% of the variance in the data respectively. The first component was a contrast between the heavier (5- and 6-ring PAHs) and lighter PAHs (2- to 4-ring PAHs), with the alkylated PAHs being positively correlated with the corresponding parent compounds (Fig 5a). The score plot showed no obvious separation by Zone (Fig. 5b). These results are consistent with the PAH profiles, which show little difference in PAH composition between Zones, and may indicate a broadly common source of PAHs to sediments throughout the Fladen area.

Aliphatic hydrocarbon

The carbon preference index (CPI) of the *n*-alkanes (Table 1) indicated that the predominant input of hydrocarbons to the Fladen was biogenic (CPI >1). A small high boiling unresolved complex mixture (UCM) was present in some of the Zones (such as Zone 4, 6, 7, 8 and 10; Fig. 6), indicative of a limited petrogenic input from highly weathered oil. Geochemical biomarker (triterpane) profiles indicated all sediments had low levels of crude oil contamination, and are exposed to both North Sea and Middle Eastern crude oils (Fig. 7).

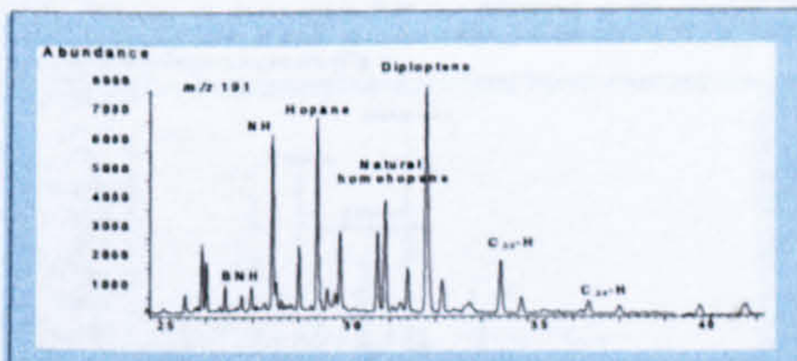

Figure 7 Triterpane profile of a typical sediment collected from the Fladen Ground in the 2001 stratified random survey. The largest peak in the chromatogram was due to diploptene, a naturally occurring triterpene. Homohopane doublet peaks indicate there was petrogenic contamination. The high ratio of C_{35} hopane and the small bisnorhopane (BNH) peak indicate that the contamination was due to a combination of North Sea and Middle Eastern crude oils.

CONCLUSIONS

The physical characteristics of the sediment were positively correlated with each other and with the corresponding diesel and Forties oil equivalent, total PAH and *n*-alkane concentrations. The mean concentrations of all the parameter measured varied widely between the Zones. The overall mean Forties crude and diesel oil equivalents were 13.8 and 5.1 µg g^{-1} dry weight, respectively. PAH concentrations (µg kg^{-1} dry weight) were all below the OSPAR BACs. PAHs percentage profiles are similar in the 16 Zones and were of a predominately pyrolytic origin. There was limited petrogenic input from both North Sea and Middle Eastern crude oils. The CPIs indicated a predominantly biogenic inputs. In general, there was a low level of hydrocarbon contamination in the sediments of the Fladen Ground. Therefore, based on the analytical data, there is minimal environmental impact from hydrocarbons in the Fladen Ground.

This project was funded by United Kingdom Offshore Operators Association (UKOOA)

STRIBUTION OF HYDROCARBONS IN THE FLADEN GROUND

ES CM 2005/S:40

FISHERIES RESEARCH SERVICES

hwaheed S. Ahmed[a, b] , Lynda Webster[a], Ian M. Davies[a], Pat Pollard[b], Marie Russell[a] and Colin F. Moffat[a].
eries Research Services (FRS) Marine Laboratory, 375 Victoria Road, Aberdeen AB11 9DB, Scotland.
ool of Life Sciences, The Robert Gordon University, St Andrew Street, Aberdeen AB25 1HG, Scotland.

INTRODUCTION

orth Sea has been the focus of offshore oil and gas production over the past 35 - ars and, as a result of this, hydrocarbons have been discharged to the area during g (*via* cuttings contaminated with oil-based drill muds), production (*via* produced discharges) and *via* incomplete combustion during flaring operations. The Fladen nd in the North Sea, is a potentially accumulative area due to the fine muddy ents (Fig. 1), and low water current velocities. In addition, the area is one of the heavily fished areas of the North Sea. A stratified random sampling design was d to estimate hydrocarbon concentrations in far field sediments. Sixteen zones constructed of equal size and near (< 5 km from a multiple oil wells and < 2 km from oil well) and far (> 5 km from a multiple oil wells and >2 km from single oil well) areas defined (Fig. 2). All samples were screened for aromatic hydrocarbons by olet fluorescence (UVF). In addition, samples were analysed for polycyclic atic hydrocarbons (PAHs) by gas chromatography-mass spectrometry (GC-MS).

re 1 The generalised pattern of Sea currents in relation to laden Ground.

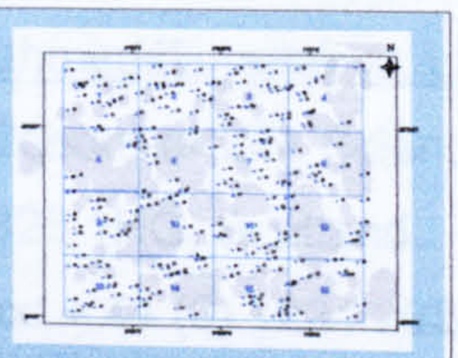

Figure 2 Location of the stratified random sampling sites, indicating the Zones and oil platforms. Grey circles are near field sites (big circle are multiple oil wells and small circles are single well).

METHOD

pling
hundred and forty two (242) sediment samples were collected by Day Grab, from RV *Scotia* in 2001.

cle size and CHN analyses
article size (PS) of the sediment samples (freeze-dried) was determined by laser ilometry employing a Malvern Mastersizer E Partcle Size Analyzer. The total ic carbon (TOC) was determined on freeze-dried, ground sediment, following acid ment to remove carbonate, using a Perkin Elmer CHN elemental analyzer.

ction of sediments for fluorescence and hydrocarbon analysis
sediment sample was thoroughly mixed and an aliquot removed for the mination of the water content. Two aliphatic standards and six deuterated PAH dards were added to a second aliquot and the hydrocarbons were extracted by ation with dichloromethane (DCM)/methanol. The DCM was isolated and dried over SO_4. The DCM fraction was made to a known volume (100 ml), and an aliquot (10 moved for UVF analysis. The remaining extract was solvent exchanged to *iso*-ne, reduced in volume and the aliphatic and aromatic hydrocarbons separated by atic high performance liquid chromatography (HPLC). The aliphatic hydrocarbons analysed by gas chromatography with flame ionization detection (GC-FID) and the atic hydrocarbons by GC-MS. Geochemical biomarker compositions (steranes and panes) were also determined by GC-MS.

PS and TOC methods are accredited at FRS to international standard ISO 17025.

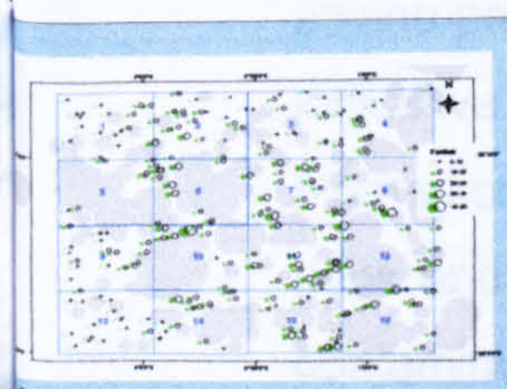

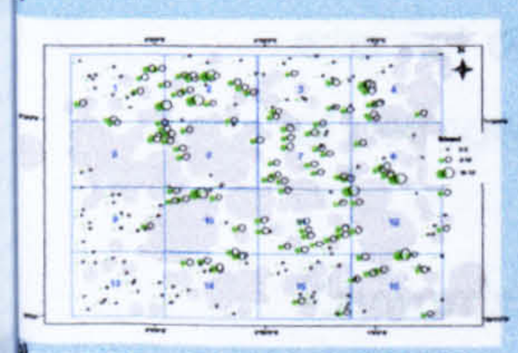

Figure 3 Spatial distribution of the Fladen Ground sediments collected in the 2001 stratified random survey.
(a) Forties oil equivalent concentrations (µg g^{-1} dry weight).
(b) Diesel oil equivalent concentrations (µg g^{-1} dry weight).
Large grey circles are < 5 km radius of multiple oil wells and small grey circles are < 2 km radius of a single well. Green circles are proportional to concentrations of Forties or diesel oil equivalents.

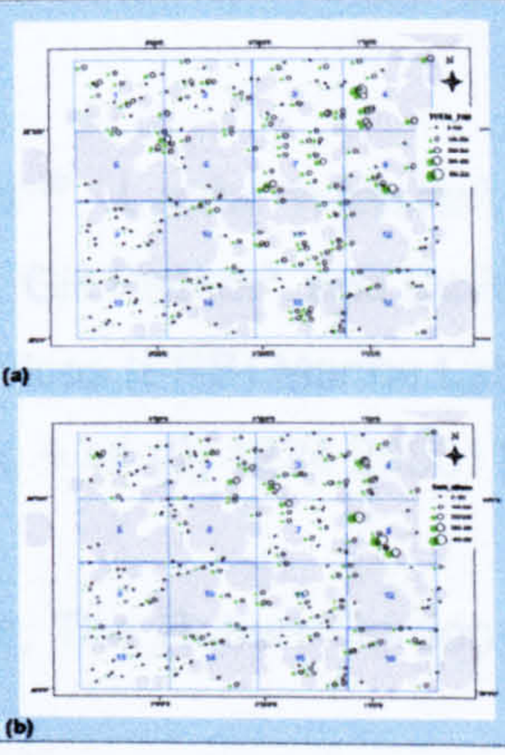

Figure 4 Spatial distribution of the Fladen Ground sediments collected in the 2001 stratified random survey.
(a) Total PAH concentration (µg kg^{-1} dry weight).
(b) Total *n*-alkane concentration (µg kg^{-1} dry weight).
Samples close to oil platform have an high total PAH and total *n*-alkane concentrations.
Large grey circles are < 5 km radius of multiple oil wells and small grey circles are < 2 km radius of a single well. Green circles are proportional to concentrations.

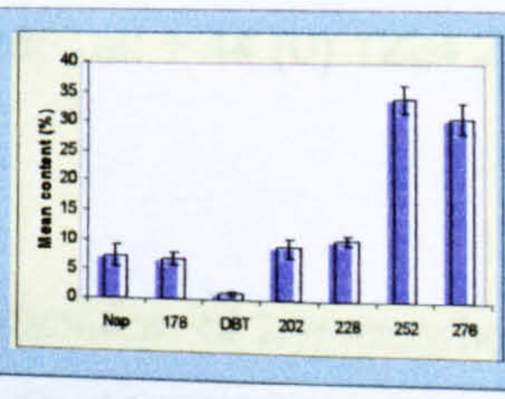

Figure 5 PAH profile for the Fladen Ground, represented by ring classes. Note the predominance of the 4- to 6-ring (%202 - %276) PAHs, which indicates a more pyrolytic input. Error bars represent standard deviation of the mean.

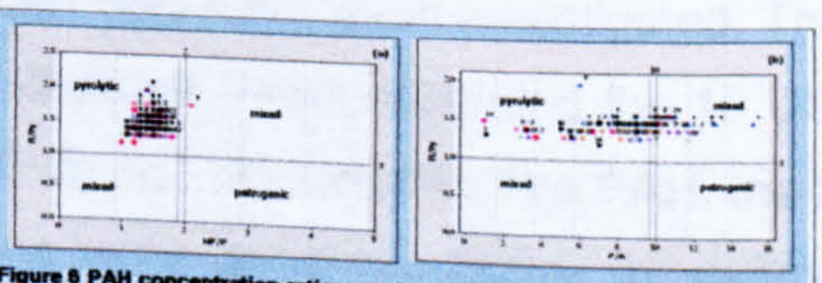

Figure 6 PAH concentration ratios used to assess the sources of PAHs in the Fladen Ground sediments collected during the 2001 stratified random survey. The zones identified by high fluoranthene/pyrene (Fl/Py) ratios and low phenanthrene/anthracene (P/A) ratios and high Fl/Py and low methylphenanthrene/phenanthrene (MP/P) ratio were characteristic of pyrolytic PAHs. (a) Plot of Fl/Py ratios against MP/P ratio. (b) Plot of Fl/Py ratios against P/A ratio.

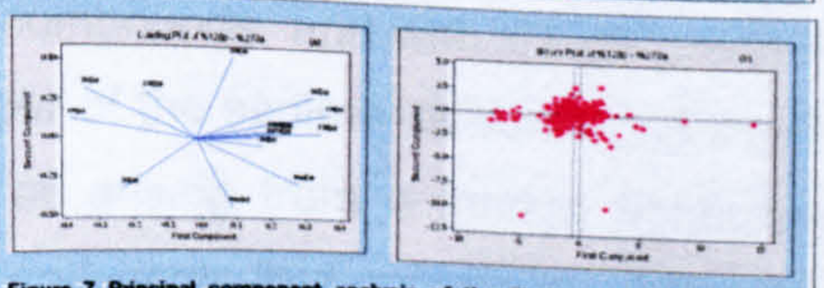

Figure 7 Principal component analysis of the Fladen Ground sediments collected during the 2001 stratified random survey, including ring group parents and alkylated compounds. (a) Loading plot of %128-%276, showing the lighter PAH compounds with a positive first component, and the 5- and 6-ring with a negative first component. (b) Score plot showing samples in the right half of the graph contained a higher proportion of the lighter PAHs, indicative of greater petrogenic input.

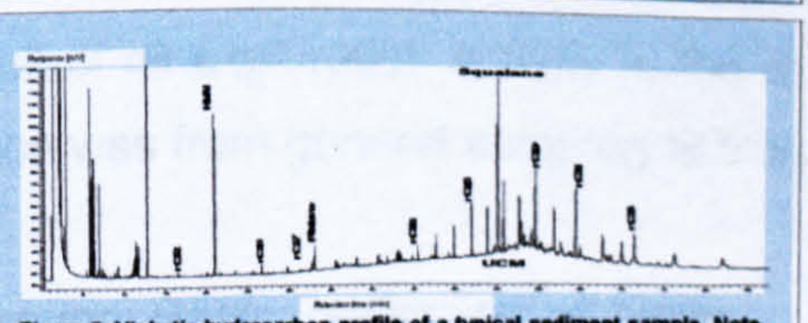

Figure 8 Aliphatic hydrocarbon profile of a typical sediment sample. Note the small high boiling unresolved complex mixture that is indicative of petrogenic contamination.

RESULTS

The spatial distribution of the hydrocarbons are shown in Figures 3 and 4. Percentage TOC and PSA measurements were positively correlated with each other and with corresponding diesel and Forties oil equivalent, total PAH and *n*-alkane concentrations.

Total Hydrocarbon
Estimates of 'total hydrocarbon' concentrations are expressed as 'oil' equivalents. Concentrations around 50 µg g^{-1} dry weight are typical of those found in areas remote from oil and gas activity. Concentrations in offshore sediments above this background value are generally associated with offshore oil exploration and production activity. The Forties crude oil equivalent concentrations were all below 50 µg g^{-1} dry weight (Fig. 3a); the Forties concentrations varied from 4.0 to 41.2 µg g^{-1} dry weight; the overall mean Forties concentration was 13.8 µg g^{-1} dry weight (SE = 0.3 µg g^{-1} dry weight) . The diesel oil equivalent concentration varied from 1.6 to 14.4 µg g^{-1} dry weight; the overall mean diesel concentration was 5.1 µg g^{-1} dry weight (SE = 0.1 µg g^{-1} dry weight) (Fig. 3b).

Polycyclic aromatic hydrocarbons (PAHs)
The total PAH concentrations (2- to 6-ring parent and alkylated) varied from 29.0 to 404.7 µg kg^{-1} dry weight (Fig. 4a); the mean total PAH concentration was 108.2 µg kg^{-1} dry weight (SE = 2.7 µg kg^{-1} dry weight). OSPAR Background Concentrations (BCs) are typical concentrations found in sediments in uncontaminated parts of the OSPAR area (north-east Atlantic), and have been established for ten PAHs. Observed concentrations are said to be 'near background' if the mean concentration is statistically significantly below the corresponding Background Assessment Concentration (BAC). The observed mean concentrations of the ten PAHs in Fladen Ground sediments were all below the OSPAR BACs at the 5% significance level.

PAH Sources
The mean PAH percentage profile for the Fladen Ground was dominated by the heavier 4- to 6-ring compounds (Fig. 5), with a high proportion of the parent PAHs. Plotting the fluoranthene/pyrene (Fl/Py) ratios against either the phenanthrene/anthracene (P/A) or methylphenanthrene/phenanthrene (MP/P) ratios gives a pyrolytic (high Fl/Py and low P/A or MP/P) zone, and a petrogenic (low Fl/Py and high P/A or MP/P) zone, the remaining may be indicative of mixed sources of PAHs (Fig. 4). The ratio plots showed most of the samples falling within the pyrolytic zone in the Fl/P vs. MP/P plot (Fig. 6a). The Fl/Py vs. P/A plot is more dispersed (Fig. 6b; the high P/A ratios (>10) suggest a possible petrogenic input).

The PAH profiles of the sediments were investigated further using principal component analysis (Minitab 14). The parent and alkylated concentrations were normalised to the total PAH concentration. The first two components only accounted for 34 and 15% of the variance in the data respectively. The first component was a contrast between the heavier (5- and 6-ring PAHs) and lighter PAHs (2- to 4-ring PAHs), with the alkylated PAHs being positively correlated with the corresponding parent compounds (Fig 7a). The score plot showed no obvious separation by Zone (Fig. 7b). These results are consistent with the PAH profiles, which show little difference in PAH composition between Zones, and may indicate a broadly common source of PAHs to sediments throughout the Fladen area.

Aliphatic hydrocarbons
The total *n*-alkane concentrations varied from 23.7 to 490.6 µg kg^{-1} dry weight (Fig. 4b); the overall mean concentration was 97.2 µg kg^{-1} dry weight (SE = 3.7 µg kg^{-1} dry weight), the carbon preference index (CPI) of the *n*-alkanes indicated that the predominant input of hydrocarbons to the Fladen was biogenic (CPI >1). A small high boiling unresolved complex mixture (UCM) was present in some of the Zones (such as Zone 4, 6, 7, 8 and 10; Fig. 8), indicative of a limited petrogenic input from highly weathered oil. Geochemical biomarker (triterpane) profiles indicated all sediments had low levels of crude oil contamination, and are exposed to both North Sea and Middle Eastern crude oils (Fig. 9).

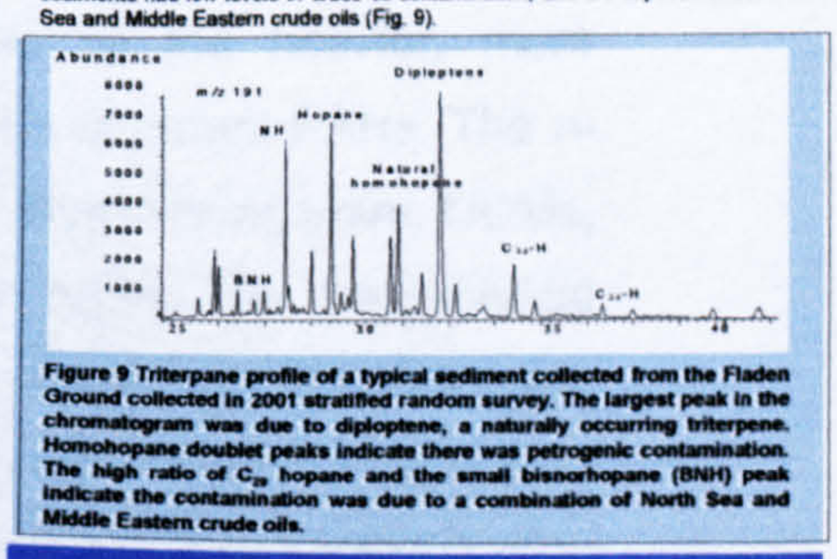

Figure 9 Triterpane profile of a typical sediment collected from the Fladen Ground collected in 2001 stratified random survey. The largest peak in the chromatogram was due to diploptene, a naturally occurring triterpene. Homohopane doublet peaks indicate there was petrogenic contamination. The high ratio of C_{29} hopane and the small bisnorhopane (BNH) peak indicate the contamination was due to a combination of North Sea and Middle Eastern crude oils.

CONCLUSIONS

The physical characteristics of the sediment samples were positively correlated with each other and with the corresponding diesel and Forties oil equivalent, total PAH and *n*-alkane concentrations. The mean concentrations of all the parameters measured varied widely between the Zones. The overall mean Forties crude and diesel oil equivalents were 13.8 and 5.1 µg g^{-1} dry weight, respectively. PAH concentrations (µg kg^{-1} dry weight) were all below the OSPAR BACs. PAH percentage profiles are similar in the 16 Zones and were of a predominately pyrolytic origin. There was a limited petrogenic input from both North Sea and Middle Eastern crude oils. The CPIs indicated a predominantly biogenic input. In general, there was a low level of hydrocarbon contamination in the sediments of the far field Fladen Ground. Therefore, based on the analytical data, there is limited environmental impact from the hydrocarbons in the Fladen Ground

This project was funded by United Kingdom Offshore Operators Association (UKOOA)

The distribution and composition of hydrocarbons in sediments from the Fladen Ground, North Sea, an area of oil production

Abdulwaheed S. Ahmed*[ab], Lynda Webster[a], Pat Pollard[b], Ian M. Davies[a], Marie Russell[a], Pam Walsham[a], Gill Packer[a], and Colin F. Moffat[a] .

[a] Fisheries Research Services (FRS) Marine Laboratory, 375 Victoria Road, Aberdeen AB11 9DB, Scotland. Fax: + 44 (0) 1224 295511; Tel: + 44 (0) 1224 876544; E-mail: a.ahmed@marlab.ac.uk

[b] School of Life Sciences, The Robert Gordon University, St Andrew Street, Aberdeen AB25 1HG, Scotland.
Fax: + 44 (0) 1224 262828; Tel: + 44 (0) 1224 262800; E-mail: p.pollard@rgu.ac.uk

Abstract

The distribution and composition of hydrocarbons in sediment from the Fladen Ground oilfield in the northern North Sea have been investigated. The total PAH concentrations (2- to 6-ring parent and alkylated PAHs, including the 16 US EPA PAHs) in sediments were relatively low (< 100 μg kg^{-1} dry weight). The PAH, the Forties crude and diesel oil equivalents concentrations were generally higher in sediment of fine grain size and higher organic carbon concentration. PAH distributions and concentration ratios indicated a predominantly pyrolytic input, being dominated by the heavier, more persistent, 5- and 6-ring compounds, and with a high proportion of parent PAHs. The *n*-alkane profiles of a number of the sediments contained small, high boiling point, UCMs, indicative of weathered oil arising from a limited petrogenic input. The geochemical biomarker profiles of the sediments that contained UCMs showed a small bisnorhopane peak and a high proportion of norhopane relative to hopane, indicating that there was contamination from both Middle Eastern and North Sea oils. Therefore contamination was not directly as a result of oil exploration activity in the area. The most likely source of petrogenic contamination was from general shipping activity.

Keywords: The Fladen Ground; PAHs; *n*-alkanes; oil fields.

Description and evaluation of a sampling system for monitoring of hydrocarbons in sediments

Abdulwaheed S. Ahmed*[ab], Lynda Webster[a], Pat Pollard[b], Ian M. Davies[a] and Colin F. Moffat[a].

[a] Fisheries Research Services (FRS) Marine Laboratory, 375 Victoria Road, Aberdeen AB11 9DB, Scotland. Fax: + 44 (0) 1224 295511; Tel: + 44 (0) 1224 876544; E-mail: a.ahmed@marlab.ac.uk

[b] School of Life Sciences, The Robert Gordon University, St Andrew Street, Aberdeen AB25 1HG, Scotland. Fax: + 44 (0) 1224 262828; Tel: + 44 (0) 1224 262800; E-mail: p.pollard@rgu.ac.uk

Abstract

A composite random sampling design was used to estimate the concentrations of hydrocarbon contaminants in two near shore areas of Scotland. The aim of this work is to estimate a mean value for each of the chosen measurement parameters, and to determine experimentally whether this can be done with more thorough coverage (better representation), better precision and less variance at lower analytical cost through a composite random sampling scheme rather than a simple random sampling scheme. Initial samples were collected using simple random sampling design and analysed, and then the samples were divided into a series of composite sub-samples. Sediment samples were analysed for particle size distribution, total organic carbon (TOC) and UVF oil equivalent concentrations, polycyclic aromatic hydrocarbons (PAHs) and *n*-alkanes. This study demonstrated that the composite random sampling gave a mean value with less variance than the simple random sampling, at significantly reduced analytical effort (and cost). Statistically, there were no significance differences between the means of the two sampling design for all the parameters measured.

Keywords: Composite random sampling, Simple random sampling, PAHs, Firth of Clyde, Firth of Forth.

Hydrocarbons in sediments in the Fladen Ground: a Comparison of Grid and Stratified Random Sampling Regimes

Abdulwaheed S. Ahmed*[ab], Lynda Webster[a], Pat Pollard[b], Ian M. Davies[a], Colin F. Moffat[a].

[a] Fisheries Research Services (FRS) Marine Laboratory, 375 Victoria Road, Aberdeen AB11 9DB, Scotland. Fax: + 44 (0) 1224 295511; Tel: + 44 (0) 1224 876544; E-mail: a.ahmed@marlab.ac.uk

[b] School of Life Sciences, The Robert Gordon University, St Andrew Street, Aberdeen AB25 1HG, Scotland. Fax: + 44 (0) 1224 262828; Tel: + 44 (0) 1224 262800; E-mail: p.pollard@rgu.ac.uk

Abstract

Contaminant inputs from hydrocarbons discharge, a major source of contamination to the Fladen Ground, have declined drastically during the last two decades as a result of improved treatment processes and better source control. To assess the contaminant temporal changes in the Fladen Ground sediments, a study was initiated in 2001, in which samples were collected using a stratified random sampling design and a conventional grid sampling design. Five Zones corresponding to the 1989 grid surveys. Samples were analyzed for particle size, total organic carbon (TOC) and UVF oil equivalents concentration, polycyclic aromatic hydrocarbons (PAHs) and *n*-alkanes. Sediment hydrocarbon concentrations decreases from 1989 - 2001 and were similar in the PAH distributions, concentrations ratios indicated a predominantly pyolytic input, being dominated by the heavier and more persistent 4- to 6-ring compound, and containing a high proportion of parent PAH, however, there was greater petrogenic inputs in the 1989 grid survey, due to a higher proportion of the 2- and 3-ring compounds compare to the 2001 stratified survey. The study further investigates the effect of interaction between the sampling designs and the spatial pattern of the contaminants. Statistically, there were no significant differences in the parameters measures between the two sampling regimes, however, the stratified random sampling gave less variance in all. The study also highlighted the benefit and limitations of each design.

Keywords: PAHs; Stratified random sampling; Grid sampling; Fladen Ground.